



UNIVERSITAT<sup>DE</sup>  
BARCELONA

# Mechanisms that regulate intracellular DNA entanglement

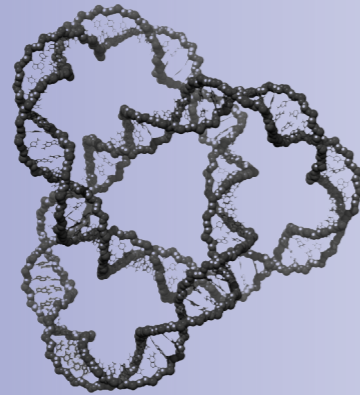
Silvia Dyson Coral



Aquesta tesi doctoral està subjecta a la llicència **Reconeixement 4.0. Espanya de Creative Commons.**

Esta tesis doctoral está sujeta a la licencia **Reconocimiento 4.0. España de Creative Commons.**

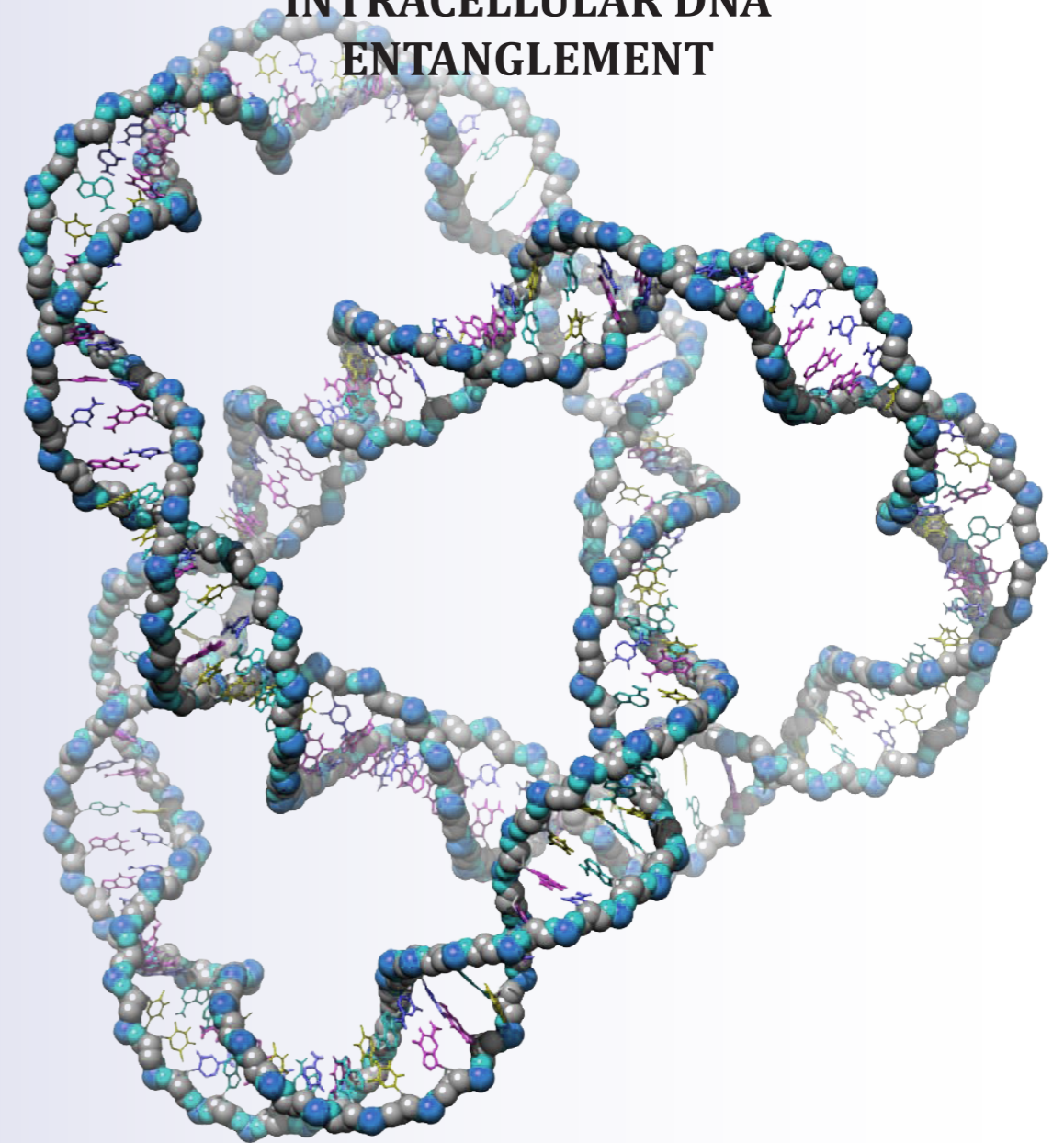
This doctoral thesis is licensed under the **Creative Commons Attribution 4.0. Spain License.**



DOCTORAL THESIS 2021

DOCTORAL THESIS 2021

**MECHANISMS THAT REGULATE  
INTRACELLULAR DNA  
ENTANGLEMENT**



Sílvia Dyson Coral

Sílvia Dyson Coral



UNIVERSITAT DE  
BARCELONA

**ibmb**  
INSTITUT DE BIOLOGÍA MOLECULAR DE BARCELONA





UNIVERSITAT DE  
BARCELONA

**DOCTORAL THESIS**

# **MECHANISMS THAT REGULATE INTRACELLULAR DNA ENTANGLEMENT**

Thesis submitted by Silvia Dyson Coral to qualify for the  
degree of PhD from the University of Barcelona

Genetics Program

This work has been carried out under the direction of Dr. Joaquim Roca Bosch  
Structural Biology Unit – Molecular Biology Institute of Barcelona (IBMB-CSIC)

Thesis director

A blue ink signature of Joaquim Roca Bosch, written in a cursive style.

Joaquim Roca Bosch

Thesis tutor

A blue ink signature of Montserrat Corominas Guiu, written in a cursive style.

Montserrat Corominas  
Guiu

Doctoral student

A blue ink signature of Silvia Dyson Coral, written in a cursive style.

Silvia Dyson Coral

Barcelona, September 2021





*“Nothing in life is to be feared,  
it is only to be understood.”*

Marie Curie



To my parents.



## **ACKNOWLEDGMENTS**

When arriving at the end of the journey to earn a PhD, it is inevitable to look back and reflect on the path that has been taken. From where I am standing now, all I can say is that it has not been easy but it was definitely worth it. The completion of the thesis has not been an individual achievement, I have relied on many people along the way without whom this project would not have been possible. I would like to dedicate these pages to thank the generous people who provided guidance and friendship.

I would like to take this opportunity to first and foremost express my deep sense of gratitude to Dr. Joaquim Roca for giving me the opportunity to carry out my PhD research in his lab. I have been extremely lucky to be able to work under his guidance and to have had the opportunity to learn from all his scientific knowledge. I should also like to acknowledge the assistance of my tutor Dr. Montserrat Corominas, for being available to help at all times.

It has been a genuine pleasure to carry out my PhD studies surrounded by a great group of scientists who made it easy to show up every day with a big smile. I would like to thank Toni, my predecessor, who not only has been the best mentor but also has become a great friend. Joanna that with her kindness and wise counsel, has been helping me throughout the PhD not only professionally but also personally. Belén, who has always been so caring towards me, thank you for always encouraging me. Ofelia, thank you for your continuous great advice and positive energy. Ricky, thank you for sharing all your experience to help me grow scientifically.

I should also like to thank all the talented scientists and staff that have crossed my path at the Scientific Park of Barcelona (PCB). Thank you for all the enriching conversations and for being a source of motivation.

I would also like to thank all the incredible people who have participated and accompanied me in my scientific training during my BSc and MSc. Especially I would like to mention Peter and Hima and all the other lab members I met at Westminster University where I carried out my final degree project, and my previous supervisor, Dr. Pooja Basnett, for always guiding me in the right direction.

I also want to share my absolute gratitude towards all my family for their constant love and support. To my Dad, whom I love and miss deeply, for always believing in me even when I didn't believe in myself. Thank you for being the best role model I could ever have. To my Mum, for always being there for me no matter what, and always lending me an ear when I need it the most. Thank you for encouraging me to move forward and for being an example of courage and strength. To my grandparents, who have been one

of the biggest sources of inspiration throughout my life. Finally, to my cousins, uncles and especially my aunts, Sally and Montse, for always being so loving and caring, I am so grateful.

I also want to mention my dear friends, who have accompanied me through all this project. My two best friends Annika and Marta and their families, who have been beside me for as long as I can even remember. Thank you for being there in all the highs and lows, I can't imagine a life without you. To Aina for always making me laugh and being an example of an empowered scientific woman. To my university classmates, especially, Clara, Blanca, Diego and Maria who have become lifelong friends. To Anna, my fellow scientist and friend, thank you for always encouraging me to follow my own path. Sarah and Ester, thank you for all the laughs and good memories. Finally, I would like to give a special thanks to Sara and Josep, who have lived with me for the past four years, thank you for becoming my second family and for helping me with the design of the cover page of this thesis.

I couldn't finish these acknowledgements without mentioning Mike and his family, Jeanne, Paul and Juliana, thank you for always having the doors of your home open to us, but especially thanks to Mike for all the language corrections and good advice.

After writing these words I can only feel lucky and grateful for having such great mentors, friends and family. Thank you all for being a part of my PhD journey and I can't wait to start the next step of my career surrounded by such amazing people.

---

# Synopsis

---





## SYNOPSIS

Topoisomerase II often produces DNA knots and catenates when its DNA strand passage activity equilibrates the topology of intracellular DNA. However, these DNA entanglements are detrimental for the normal development of genomic transactions such as replication and transcription. Fortunately, there is a mechanism actively removing these unwanted DNA entanglements *in vivo*. More specifically, previous studies performed in our laboratory uncovered that the *in vivo* correlation between knot formation and chromatin length linearly increased up until a length of 5 Kb (about 25 nucleosomes) but then reached a plateau in larger chromatin domains. This inflection is inconsistent with the expected increasing linear correlation between knot formation and chain length observed *in vitro* and *in silico*. In order to clarify which mechanism is actively minimizing the DNA entanglements in intracellular chromatin, three plausible mechanisms were proposed and tested in this thesis.

First, the possibility that *in vivo* DNA supercoiling could bias topoisomerase II activity towards untangling the genome was tested. Nevertheless, experimental results revealed the opposite effect. Accumulation of positive DNA supercoiling during transcription increases the DNA's knotting probability 25-fold.

Second, the assumption that topoisomerase II alone is capable of minimizing the overall DNA entanglement to values below the thermodynamic equilibrium was tested. The experimental results indicate that even though this ability is functioning *in vitro*, it does not minimize the overall entanglement of intracellular chromatin.

Finally, the possibility that the loop extrusion capacity of SMC (structural maintenance of chromosomes) complexes, such as condensin and cohesin could help to disentangle the genome was also tested. The loop extrusion process could tighten DNA entanglements towards the outside of the loops and consequently enforce their removal by topoisomerase II. These experiments uncovered that the activity of condensin, but not of cohesin, promotes the resolution of DNA knots formed within chromatin fibers both in interphase and mitosis. Moreover, inactivation of condensin restores the expected linear correlation between DNA knot formation and chromatin length. Condensin is very well known for its role during mitosis, however, its role during

## Synopsis

interphase remained mostly unknown. The results of this thesis suggest that condensin is able to extrude DNA loops in order to minimize DNA entanglements throughout the entire cell cycle. This critical role could explain why inactivation of condensin during interphase is followed by many genome dysfunctions.

---

# Index

---



**INDEX**

<b>SYNOPSIS</b> .....	<b>11</b>
<b>INTRODUCTION</b> .....	<b>19</b>
<b>1. DNA STRUCTURE</b> .....	<b>19</b>
<b>2. DNA TOPOLOGY</b> .....	<b>23</b>
2.1 DNA topology regulation .....	28
2.1.1 Chromatin structure .....	29
2.1.2 SMC complexes .....	31
2.1.3 DNA topoisomerases .....	33
2.1.4 Main functions of DNA topoisomerases .....	38
<b>3. WHAT IS A KNOT?</b> .....	<b>41</b>
3.1 How do DNA molecules become knotted? .....	43
3.2 How are DNA knots analyzed? .....	44
3.3 Factors determining DNA knotting probability .....	47
3.4 Why are DNA knots informative? .....	49
3.5 Occurrence of DNA knots in biological systems .....	51
3.5.1 Supercoiling as a way to reduce knotting .....	56
3.5.2 Intrinsic capacity of topoisomerase II to simplify DNA knots .....	57
3.5.3 Removal of DNA entanglements via loop extrusion .....	58
<b>OBJECTIVES</b> .....	<b>61</b>
<b>PUBLICATIONS</b> .....	<b>65</b>
<b>GENERAL DISCUSSION:</b> .....	<b>123</b>
1. DNA supercoiling markedly increases DNA knotting probability in chromatin .....	125
2. Transient DNA knotting is common during transcriptional supercoiling of DNA .....	127
3. Topoisomerase II activity alone does not minimize intracellular DNA knots .....	129
4. Condensin is required to minimize DNA knotting in chromatin .....	131
5. Condensin mediated knot minimization supports that its DNA loop extrusion activity performs in vivo .....	132
6. Opposite effects of condensin and cohesin .....	133
7. Condensin's loop extrusion activity might resolve sister chromatid interlinks .....	134
8. Short- and long-range DNA entanglements of intracellular chromatin .....	136
9. Relevance of condensin in interphase .....	137
10. An ancestral solution to the general problem of DNA entanglement .....	139
<b>CONCLUSIONS</b> .....	<b>143</b>
<b>REFERENCES</b> .....	<b>147</b>



---

# Introduction

---





## INTRODUCTION

### 1. DNA STRUCTURE

The distinctive DNA structure consists of two antiparallel polynucleotide chains that wind around each other to form a double helix. The pentose (2'-deoxyribose) and the phosphate group of each nucleotide make up the backbone of the chains, while the nitrogen bases are found in the center of the helix and hold the two chains together via hydrogen bonds. In the backbone of the molecule, each pentose forms a phosphodiester bond with the two adjacent phosphates, one through its 3' hydroxyl and the other through its 5' hydroxyl group. In the center of the molecule, the nitrogen bases are paired in a specific way: Adenine pairing with Thymine, (A = T) and Cytosine pairing with Guanine (C≡G) (Figure 1A) (Franklin & Gosling, 1953; Watson & Crick, 1953).

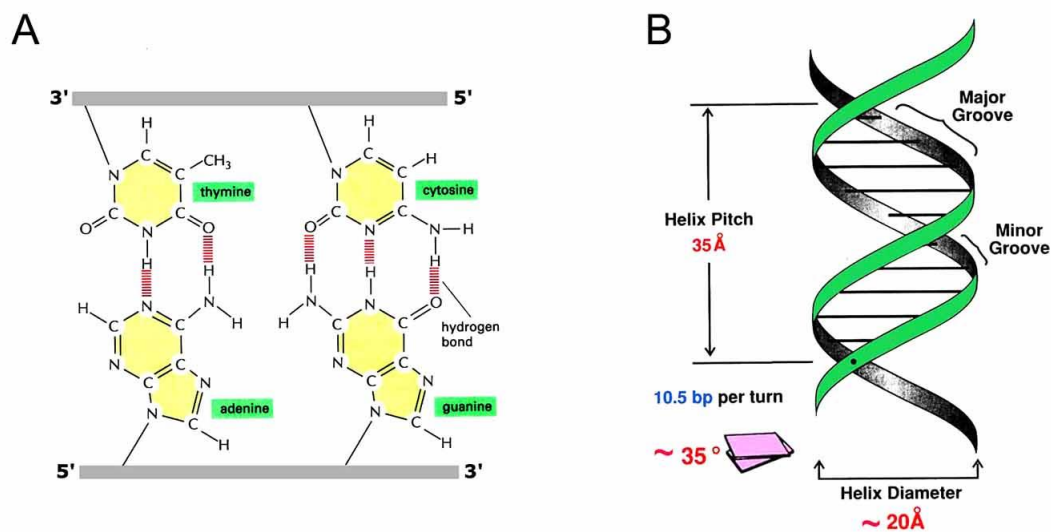


**Figure 1 – DNA structure** (A) Representation of the DNA's complementary base pairing, held together by hydrogen bonds. (B) Dimensions of the double-helical form of the DNA.

Due to the stacking of the DNA base pairs (bp), each base rotates about 35 degrees counterclockwise relative to the pair below. This rotation allows the assembly of a double helix that is dextrorotary or right-handed. In the canonical DNA model, known as the B form, each double helix turn includes approximately 10.5 bp within a length of 3.5 nm and a geometric diameter of approximately 2 nm (Figure 1B) (Lavelle, 2014; Travers & Muskhelishvili, 2015; Heinemann & Roske, 2020). However, since the double helix has

## Introduction

high helical or twisting flexibility (Figure 2A), these parameters fluctuate based on the DNA's thermodynamic state and vary according to the nucleotide sequence and the media surrounding the DNA (ionic force, pH, temperature) (A. Marko et al., 2011). For instance, at room temperature, torsional fluctuations between stacked base pairs can usually alter the angle of rotation between  $\pm 5$  and 7 degrees. Consequently, rather than having a fixed inter-base-pair helical twist of approximately 35 degrees, the actual value fluctuates between 28 and 40 degrees, and one third of the time it reaches values beyond these limits. These fluctuations occur simultaneously for all base pairs. Therefore, the rigid picture of DNA shown in text books is just depicting the archetypical configuration of the DNA structure. In reality, the double-helix is vastly more flexible and dynamic.

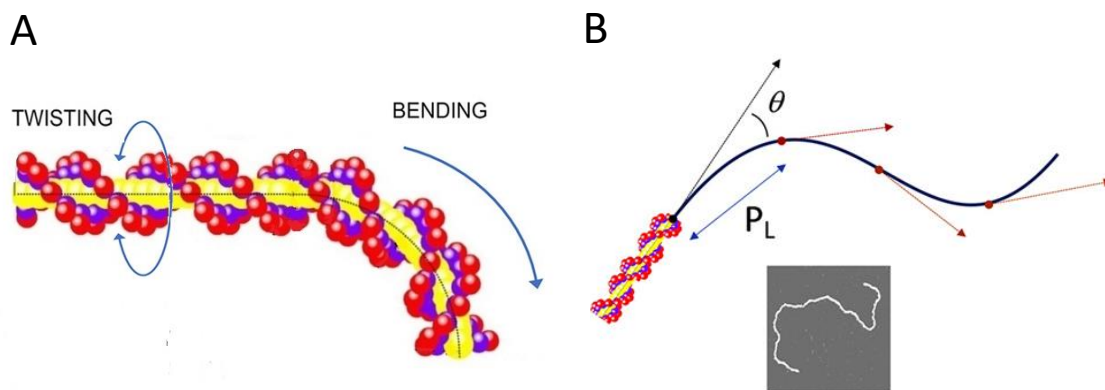


**Figure 2 – DNA Flexibility.** (A) Twisting and bending deformations of the DNA double helix. (B) The persistence length ( $P_L$ ) of a polymer (such as DNA) is measured by comparing the directions of the tangents originating from different points. The length where these directions stop correlating (i.e.,  $\theta \neq 0$ ) determines the  $P_L$ .

In addition to its high helical or twisting flexibility, the double helix can also undergo lateral bending, however, in a more rigid manner (Figure 2A). This bending rigidity is mainly a consequence of the repulsion between the negatively-charged adjacent phosphates present in the DNA backbone (Peters & Maher, 2010). However, whereas the DNA is quite stiff in short length scales (i.e., hundreds base pairs), the flexibility of the double helix is quite substantial when considering the full length of the DNA molecules which is usually extremely long, often expanding to millions of base pairs. Thus, the DNA behaves as a long flexible polymer, with a real contour length (end-to-

end distance) that is many orders of magnitude higher ( $\mu\text{m}$  to  $\text{cm}$ ) than its effective diameter ( $\text{nm}$ ).

The basic parameter quantifying the stiffness or bending flexibility of a long polymer is the persistence length ( $P_L$ ) (Figure 2B). To understand this complex concept, we imagine a long chord that is slightly flexible. When checking the flexibility of the chord in two close points the flexibility will be low, whereas if we check two points that are far apart the flexibility will be higher. In order to calculate this parameter, the correlation between the directions of the tangents originating from different points of the same cord is observed. The  $P_L$  is the length over which the directions of the tangents stop correlating. The  $P_L$  of double stranded DNA is  $50\text{nm}$ , which is roughly equal to  $150\text{ bp}$ . In the case of single stranded DNA the  $P_L$  is  $4\text{nm}$ , meaning that it is much more flexible (Klenin et al., 1988)

One consequence of the bending flexibility of long DNA molecules is that they can follow a 3D random path and occupy a space with a smaller radius than their own contour length (Bloom, 2008). This notion raises the question of how tight the DNA is packaged in the cell nucleus. In textbooks it is often said that genomic DNA undergoes a “drastic condensation”. But in fact, if we take the whole length of the human genome ( $2\text{ meters}$  of DNA) and allow it to fold spontaneously in free solution, the DNA will follow a random path that results in a conformation of only a few hundreds of micrometers in diameter (Post & Zimm, 1980). Therefore, packaging  $2\text{m}$  of DNA into a nucleus of a few micrometers in diameter is not as drastic as one could imagine (Figure 3). Another question that arises is how much free space is left in the nucleus after filling it with the entire DNA. However, considering the tiny diameter of the DNA, it turns out that  $2\text{m}$  of DNA will only occupy around the  $2\%$  of the nucleus interior volume, leaving plenty of room for other nuclear components (Lavelle, 2014). Therefore, DNA condensation is not so much a matter of packaging per se. Rather, DNA condensation is a matter of functional organization.

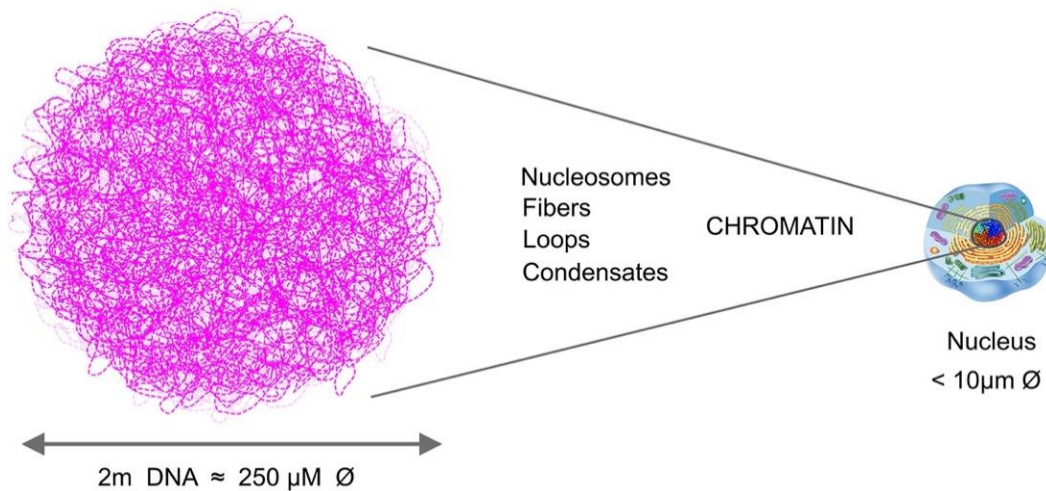


**Figure 3 – The DNA’s spatial path and packaging.** The DNA’s flexibility allows very long DNA molecules in free solution to fold into an intricate random path. For instance, 2m of DNA will spontaneously fold into a volume of about 250  $\mu$ m. Chromatin contributes in organizing rather than packaging the DNA inside the nucleus.

In eukaryotic cells, DNA is mainly organized by means of periodic wrapping around histone cores to form nucleosomes which interact with each other and other non-histone proteins to form chromatin fibers (Zhou & Bai, 2019). Such fibers are subsequently folded into loops through the action of SMCs (Structural Maintenance of Chromosomes) complexes, which are mainly represented by condensin and cohesin. By forming chromatin fibers and loops, cells are capable of organizing the DNA within the reduced nucleus space (Davidson & Peters, 2021). This allows the establishment of regions of greater and lesser accessibility which regulates the genetic activity; and also allows chromosomes to convert into individual entities that are easily segregable during cell division.

## 2. DNA TOPOLOGY

The double-helical structure of the DNA provides a great stability to the molecule, but at the same time it entails certain implications, such as the need to unwind the double helix to carry out many genomic transactions. Moreover, given that DNA molecules have a great length and are folded inside the nucleus, unwinding the double helix during DNA replication or transcription immediately provokes helical stress or tension. This helical tension cannot dissipate easily because there are few free ends that allow the DNA's free rotation. Additionally, in order to make up chromatin, the DNA associates with numerous proteins and macromolecular complexes which cause a huge rotational drag that delays the spinning of the DNA. Consequently, intracellular DNA behaves as a succession of closed topological domains which undergo different levels of helical stress (Mirkin, 2001). The double-helical topology of a closed DNA domain, such as a plasmid or a chromatin loop, can be described with 3 parameters: the linking number (Lk), the twist (Tw), and the writhe (Wr).

The Lk describes the number of times that two closed curves (i.e., DNA strands) intertwine with each other in a three-dimensional space (Figure 4A). The Lk is a topological invariant, which means it cannot be altered by any geometric deformation of the DNA (Marko & Siggia, 1995). Thus, the Lk can only be altered if one or both DNA strands are cut and rejoined again (Bates & Maxwell, 2005). The DNA's Lk equals  $N/h$ , where N is the total number of base pairs and h is the average number of base pairs required to complete a helical turn. As mentioned before the h value varies according to the environment (ionic force, pH, temperature), the nucleotide sequence and interactions with other molecules. When DNA adopts its minimum energy conformation (i.e., with no tension) in physiological conditions (0.2 M NaCl, pH 7, 37°C), h becomes  $h_0$  and is approximately 10.5 bp (Wang, 1979; Peck & Wang, 1981). However, due to the previously mentioned thermodynamic oscillations of the DNA, the h value fluctuates and, therefore, not all molecules will have an identical Lk value. Instead, DNA molecules present a Gaussian distribution of integer values of Lk centered in  $Lk_0$  (Lk in its minimum energy conformation). This thermodynamic distribution of Lk values leads to the

## Introduction

formation of a small ladder of topoisomers that can be observed when circular DNA molecules are electrophoresed in agarose gels (Figure 4B).

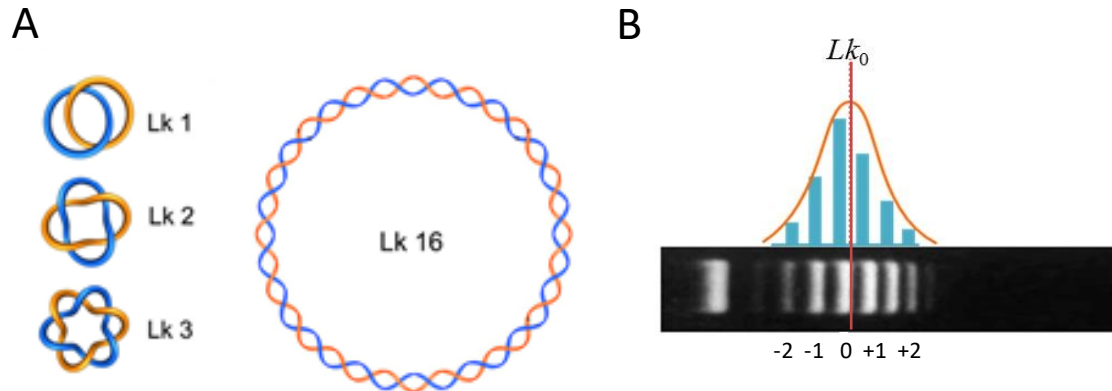


**Figure 4 – DNA Linking number (Lk)** (A) Depiction of the Lk values between two closed curves. (B) Lk values of a circular DNA forming a thermodynamic distribution in an agarose gel. The quantification of the intensities of the different Lk topoisomers form a Gaussian distribution centered in  $Lk_0$  (top).

In biological systems, the average Lk value of the DNA is generally lower than  $Lk_0$ . The difference between Lk and  $Lk_0$ , is called the linking number difference ( $\Delta Lk=Lk-Lk_0$ ). Moreover, the  $\Delta Lk$  value relative to  $Lk_0$  is called the superhelical density ( $\sigma$ ), such that  $\sigma=\Delta Lk/Lk_0$ . When  $\Delta Lk$  is negative ( $\sigma<0$ ) or positive ( $\sigma>0$ ), we say that DNA acquires negative or positive supercoiling, respectively. Such supercoiling can be constrained by proteins or other molecules, or it can be unconstrained and act as free supercoiling energy (helical tension). In eukaryotic and eubacterial cells,  $\sigma$  has a mean value of -0.05 and -0.06, respectively (Anderson & Bauer, 1978), which means that DNA molecules in vivo have a deficit of 5-6% in the Lk value relative to their  $Lk_0$  in vitro.

Although the DNA's Lk value cannot change unless the strands are cut and resealed, the Lk is the sum of two complex geometric parameters that can interconvert into each other through the deformation of the DNA: the Twist (Tw) and Writhe (Wr), such that  $Lk=Tw+Wr$  (White, 1969; Fuller, 1978).

The  $Tw$  measures how each individual strand of the DNA turns around another or, being more precise, around the central axis of the DNA helix (Figure 5) (Bates & Maxwell, 2005). The  $Wr$  measures the turns of the helix axis in space (i.e. non-planar deviations of the duplex) and it is calculated by averaging the number of (-) and (+) crossings of the DNA axis over itself in multiple spatial projections (Figure 5) (Fuller, 1971). Considering that  $Lk=Tw+Wr$ , any change of  $Lk$  translates into changes in  $Tw$  and  $Wr$  which means that:  $\Delta Lk=\Delta Tw+\Delta Wr$ . Conversely, when  $Lk$  is fixed,  $Tw$  and  $Wr$  deformations can compensate each other by altering the spatial geometry of the DNA (Figure 6A) (Roca, 2011a).

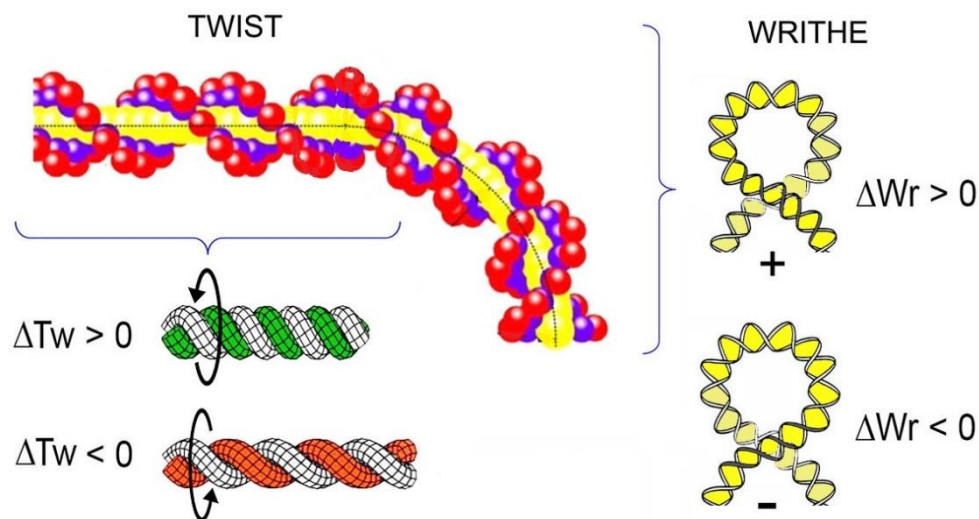


**Figure 5 - DNA twist ( $Tw$ ) and writhe ( $Wr$ ).** The  $Tw$  measures how individual DNA strands turn around the central axis of the duplex. Changes in the  $Tw$  value refer to unwinding ( $\Delta Tw < 0$ ) or overwinding ( $\Delta Tw > 0$ ) of the double helix. The  $Wr$  measures the turns of the double helix axis in space and its value correlates with the number of (-) and (+) crossings of the DNA axis over itself. Right-handed ( $\Delta Wr > 0$ ) and left-handed ( $\Delta Wr < 0$ ) turns determine the (+) or (-) sign of the crossings, as indicated.

Changes in the form of  $Tw$  imply unwinding or overwinding of the double helix, that is, an increase or decrease in the number of base pairs per turn. Thus, a negative  $\sigma$  involves a negative  $\Delta Tw$  (unwinding), whereas a positive  $\sigma$  involves a positive  $\Delta Tw$  (overwinding). Conversely, variations in the form of  $Wr$  are reflected in the spatial coiling of the DNA, which can lead to a solenoidal or to a plectonemic conformation (Figure 6B) (Bates & Maxwell, 2005). In the solenoidal conformation, DNA molecules form right-handed or left-handed supercoils, depending on whether  $\sigma$  is positive or negative, respectively. The

## Introduction

solenoidal fold is usually stabilized by proteins (for instance, with nucleosomes). In the plectonemic conformation, DNA folds by mutual interlacing of the two antiparallel sections of the duplex forming a super double helix. Depending on whether  $\sigma$  is positive or negative, this super double helix or plectoneme will be left-handed or right-handed, respectively (note that this is the opposite to a solenoid). In absence of proteins or other ligands, a DNA molecule with helical tension ( $\sigma \neq 0$ ) will spontaneously deform by Tw (30%) and Wr (70%) adopting a plectonemic configuration (Boles et al., 1990; Adrian et al., 1990).

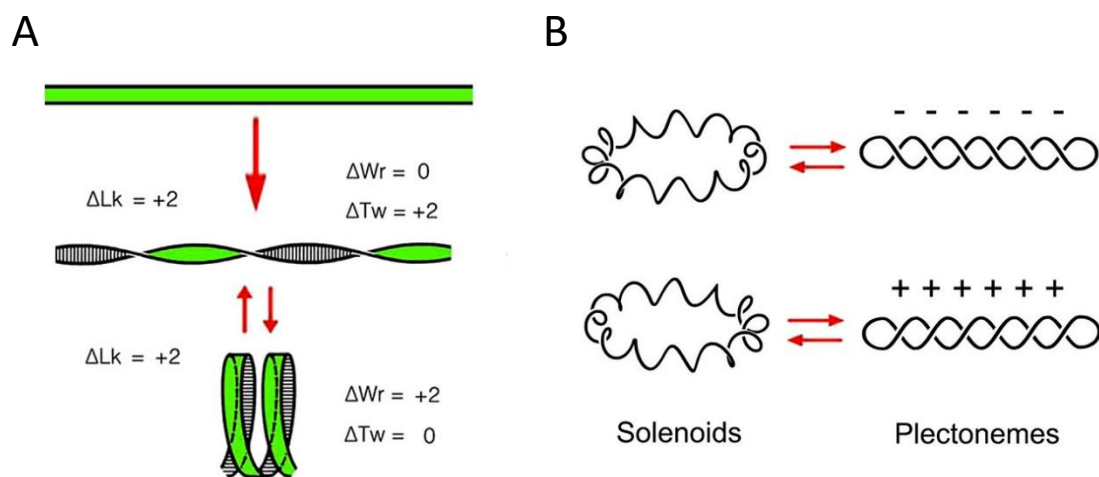


**Figure 6 - Tw and Wr conformations.** (A) Considering that  $Lk=Tw+Wr$ ,  $\Delta Tw$  and  $\Delta Wr$  deformations can interconvert into each other while the value of  $Lk$  is fixed. (B) Changes in  $Wr$  can produce solenoids (regular coils) or plectonemes (twisted loops).

The  $Wr$  value is the main determinant when it comes to the electrophoretic velocity of circular DNA molecules. As a circular DNA molecule becomes more positively or negatively supercoiled, it increases its absolute  $Wr$  (Vinograd et al., 1965; Gray et al., 1971). This means that the DNA becomes more compacted and consequently can move faster during electrophoresis. However, there is a limit of supercoiling compaction beyond which the velocity of DNA does not increase. This happens when supercoiled DNA adopts such a tight plectonemic conformation that the overall dimension (compaction) of the molecule no longer changes with further increases of its absolute  $Wr$ . This explains why in relaxed DNA, the equilibrium distribution of  $Lk$  topoisomers runs as a ladder of bands in an agarose gel (Figure 4B), but this ladder collapses in a



single band in the case of supercoiled DNA (Depew & Wang, 1975; Roca, 2009). Another problem regarding electrophoresis is that, since DNA mobility does not depend on the sign of  $Wr$ , we cannot tell whether the DNA sample is positively or negatively supercoiled.

Both problems can be solved by a two-dimensional (2D) gel electrophoresis, in which DNA runs in the presence of base-pair intercalators such as chloroquine (Figure 7). The intercalator unwinds the double helix and consequently reduces the  $Tw$  of the DNA. Since the  $Lk$  is fixed, this reduction of  $Tw$  becomes compensated by an increase of  $Wr$ . As a result, in the presence of an intercalator, negatively supercoiled DNA molecules (with negative  $Wr$ ) acquire a less negative  $Wr$  and run slower in an agarose gel (Hanai & Roca, 1999). Conversely, relaxed DNA molecules (i.e., with about zero  $Wr$ ) acquire positive  $Wr$  and run faster. Then, by using different concentrations of intercalator during the first and second gel dimensions, it is possible to resolve the ladders of  $Lk$  topoisomers that were completely collapsed due to the high level of compaction, and also distinguish positive from negatively supercoiled topoisomers (Roca, 2009).

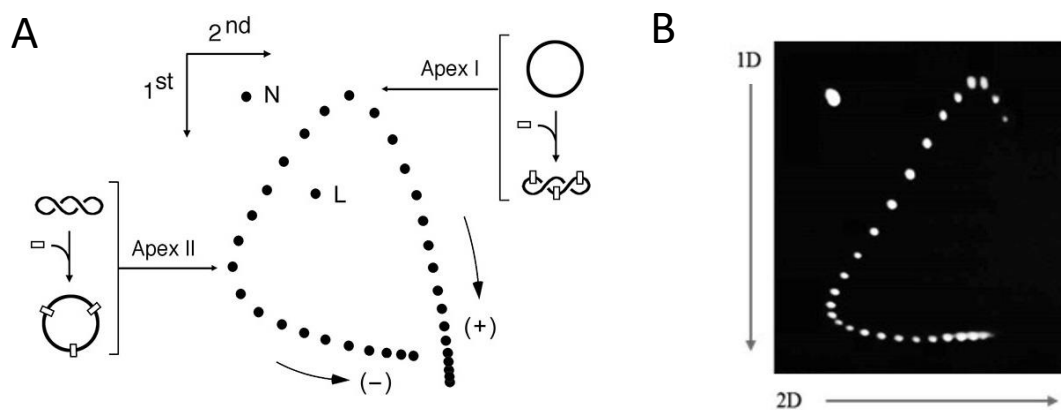


**Figure 7 – Separation of  $Lk$  topoisomers by a 2D electrophoresis.** (A) Schematic representation of the different  $Lk$  positions. Apex I indicates the topoisomer with the lowest  $Wr$  (less compaction and speed) during the first dimension. Upon increasing the concentration of intercalator (depicted as white rectangles) in the second dimension, the  $Wr$  value of the topoisomer found in Apex I increases and consequently has a higher speed during the second dimension, allowing it to separate from the nicked rings (N). Apex II indicates the topoisomer with the lowest  $Wr$  in the second dimension. This topoisomer was negatively supercoiled ( $Wr < 0$ ) in the first dimension, but upon binding with the intercalator, its  $Wr$  value increased to  $\approx 0$ . (L) indicates linearized rings. (B) 2D electrophoresis of a DNA plasmid.

In addition to the supercoiled DNA conformations that were previously mentioned, DNA molecules can also present knots and catenates (Valdes et al., 2018). In contrast to helical tension, which depends on the interlinking between the two strands of the double helix, knots and catenates reflect the intra- or inter-molecular interlinking of entire DNA molecules. As explained later, DNA knots and catenates occur frequently in biological systems and have to be removed to permit crucial processes, such as gene transcription and chromosome segregation.

### **2.1 DNA topology regulation**

The DNA topology, which includes the helical tension of the duplex (supercoiling) and the occurrence of knots and catenates, can be constrained or unconstrained (Roca, 2011).

The DNA topology is “constrained” when it is stabilized by external factors. For instance, the structural components of chromatin (i.e., nucleosomal fibers) which enforce the DNA to be folded in specific ways. Consequently, these DNA topology constrainters stabilize DNA deformations in the form of  $T_w$  and  $W_r$ . Likewise, other complexes (i.e., SMC complexes) appear to fold DNA into large loops and give a distinctive shape to interphase and mitotic chromosomes (J. Dixon et al., 2012).

Conversely, DNA topology is “unconstrained” when it is not stabilized, which results in the generation of topological stress. For instance, DNA tracking motors, such as RNA and DNA polymerases or DNA helicases, unwind the double helix and enforce the duplex to turn around its axis, which consequently generates helical tension (Giaever & Wang, 1988). In order to remove the DNA’s topological stress, nature has provided a family of enzymes called DNA topoisomerases, which transiently cut and reseal DNA strands to pass them through one another as if they were phantom chains (Wang, 1998). This mechanism allows DNA topoisomerases to modify the DNA’s topology by changing its  $L_k$  value.

### 2.1.1 Chromatin structure

The fundamental subunit of chromatin is the nucleosome, in which  $\approx 147$  bp of DNA wrap around eight histone proteins (also known as histone octamer) approximately 1.7 times in left-handed manner (Figure 8A) (Richmond et al., 1984; Luger et al., 1997). As a result, the nucleosome has a cylindrical shape of about 5 nm high and 11 nm wide. The deformation of the DNA around the histone octamer produces marked changes in  $Tw$  and  $Wr$ . The calculation of the nucleosomal  $Tw$  and  $Wr$  has been a matter of controversy for decades, due to contradicting results between data from crystal structures, biochemical and topological studies. This problem has recently been solved in our laboratory using a new experimental approach by obtaining measurements directly in native chromatin. We concluded that the DNA is deformed with approximately +0.2 units of  $Tw$  and -1.45 units of  $Wr$ , such that the  $\Delta Lk$  stabilized by each nucleosome is of -1.26 (Figure 8B) (Segura et al., 2018).

Nucleosomes are separated by linker DNA segments, of variable length (30 to 70 bp) depending on the organism and/or cell type. Consequently, an array of nucleosomes resembles a succession of beads on a string (Li & Zhu, 2015). Additionally, linker DNA segments and nucleosome free regions are occupied by other structural proteins and regulatory factors.

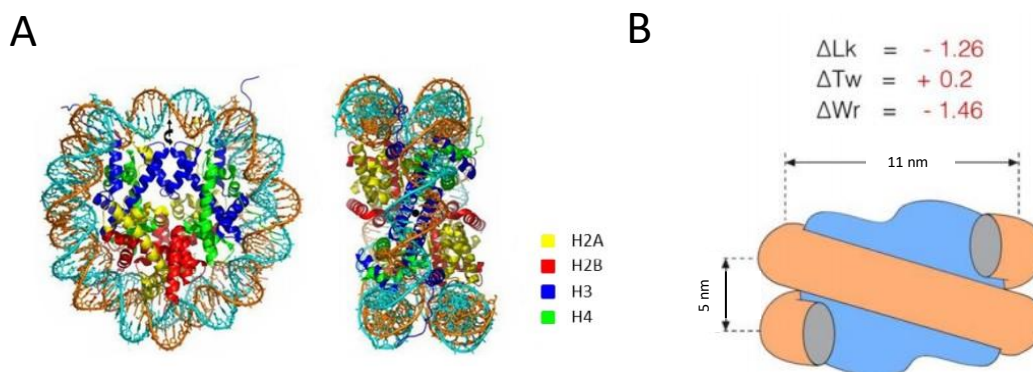


**Figure 8 – The nucleosome** (A) Crystallographic structure of the canonical nucleosome. 147 bp of DNA complete 1.7 turns around an octamer of histones H3, H4, H2A and H2B. (Adapted from Davey et al., 2002). (B)  $\Delta Lk$ ,  $\Delta Tw$  and  $\Delta Wr$  values that define the DNA topology in the nucleosome.

## Introduction

This first level of DNA folding is known as the basic nucleosomal fiber, it has a thickness of 10nm and it is very flexible. Most classic models propose that the 10nm nucleosome fiber folds into a structure of higher order known as the 30nm fiber (Figure 9A). Experiments based on electron microscopy and X-ray crystallography have led to different models which supported the 30nm fiber, such as the solenoidal model (Robinson et al., 2006) or the zig-zag pattern model (Song et al., 2014). Moreover, these 30 nm fibers were also proposed to further fold into helical superstructures (Belmont et al., 1989; Belmont & Bruce, 1994).

However, 30 nm fibers have never been observed in vivo. On the contrary, microscopy and staining techniques, such as FISH, provided images of irregular chromatin structures which had different dynamics and variable localization (Bronstein et al., 2009; Wiggins et al., 2010). More recently, high-resolution nanoscopy allowed the ultrastructure of individual chromatin fibers to be visualized in-vivo. In these images, chromatin fibers look like disordered granulated chains formed by nucleosome clusters (Figure 9B). Such granular chains have different sizes (5 to 24 nm in diameter) and nucleosome densities (Ou et al., 2017).

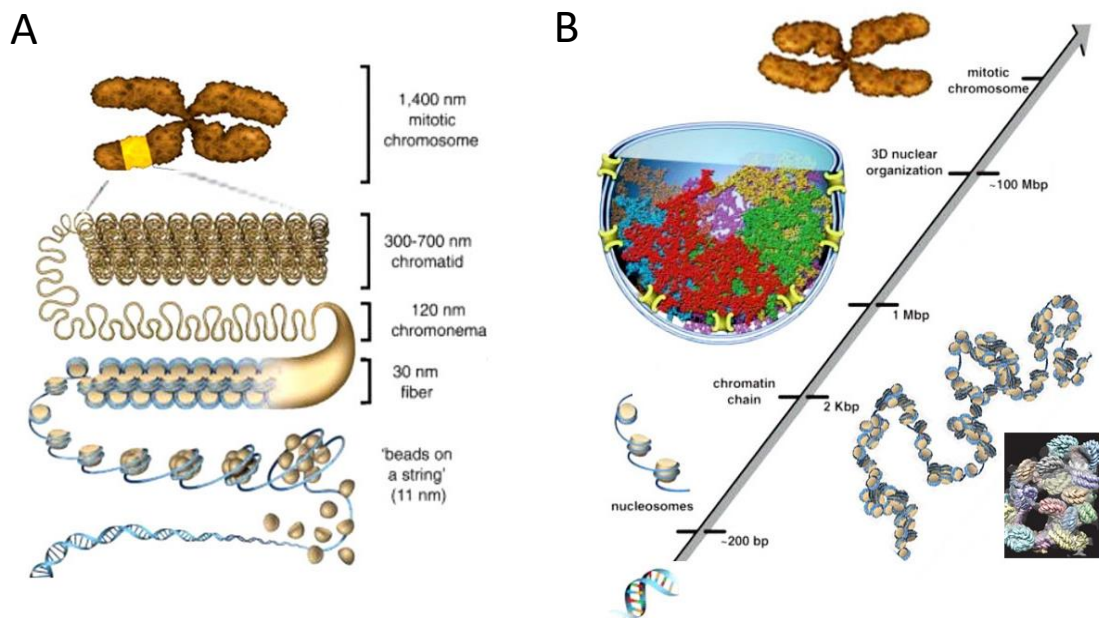


**Figure 9 – Chromatin folding** (A) The classic hierarchical chromatin folding model found in most text books. (B) Nanoscopy imaging reveals that chromatin fibers are disordered granulated chains formed by nucleosome clusters (Adapted from Ou et al., 2017).

In addition to the methods that visualize chromatin directly, other indirect techniques have been developed in the last couple decades to capture chromatin's 3D conformation such as 3C, 4C or Hi-C. These techniques quantitatively measure the frequencies of spatial contacts between different genomic sites and allow the generation of spatial organization models of chromatin (Dekker et al., 2002; Simonis et al., 2006; Lieberman-Aiden et al., 2009). Using the Hi-C technique, regions of around 0.1 to 1 mega-bases, where local chromatin interactions are more frequent than usual, are detected. These regions, which vary depending on the cell type and the stage of the cell cycle, were designated as topological associated domains (TADs) (J. Dixon et al., 2012). TADs have been proposed as the basic unit in the macro-organization of the genome and play a fundamental role in the coordination and regulation of gene expression (Jin et al., 2013).

### **2.1.2 SMC complexes**

SMC (structural maintenance of chromosomes) complexes, which include condensin, cohesin and the Smc5/6 complex, are major components of chromosomes in all living organisms, from bacteria to humans (Uhlmann, 2016). Typically, these complexes are found every 5-10 Kb along the DNA.

SMCs are ring-shaped complexes composed of a trimeric core formed by a heterodimer of Smc ATPases and a conserved kleisin, in addition to several other regulatory subunits (Figure 10A and 10B). SMCs bind to chromosomes by embracing one or more segments of DNA. This embracement is done through the opening and closure of distinct SMC compartments via ATP binding and hydrolysis (Hassler et al., 2018; Yatskevich et al., 2019).

SMCs have several essential and distinctive roles. Cohesin organizes chromatin into TADs during interphase and holds sister chromatids together from S-phase until metaphase (Onn et al., 2008; Nasmyth & Haering, 2009). Condensin plays a key role in the compaction and individualization of chromatids during cell divisions (Hirano, 2012a). Lastly, the Smc5/6 complex has been mainly implicated in DNA repair via homologous recombination (Aragón, 2018).

## Introduction

Recent single-molecule experiments have demonstrated that SMC complexes (mainly condensin and cohesin) are able to form DNA loops through a mechanism called loop extrusion (Ganji et al., 2018; Davidson et al., 2019; Kim et al., 2019). In this mechanism, a small DNA loop is threaded through the SMC ring and then pushed through the ring in an ATP-dependent manner. Consequently, the loop extends and DNA sequences that were far apart end up converging (Figure 10C) (Wang et al., 2015). This mechanism has never been visualized *in vivo*, however; many hypotheses have been proposed. In the case of cohesin, the loop extrusion mechanism is thought to be responsible for the formation of TADs (Sanborn et al., 2015; Fudenberg et al., 2016). In the case of condensin, the loop extrusion mechanism is thought to allow the condensation of mitotic chromosomes (Banigan et al., 2020).

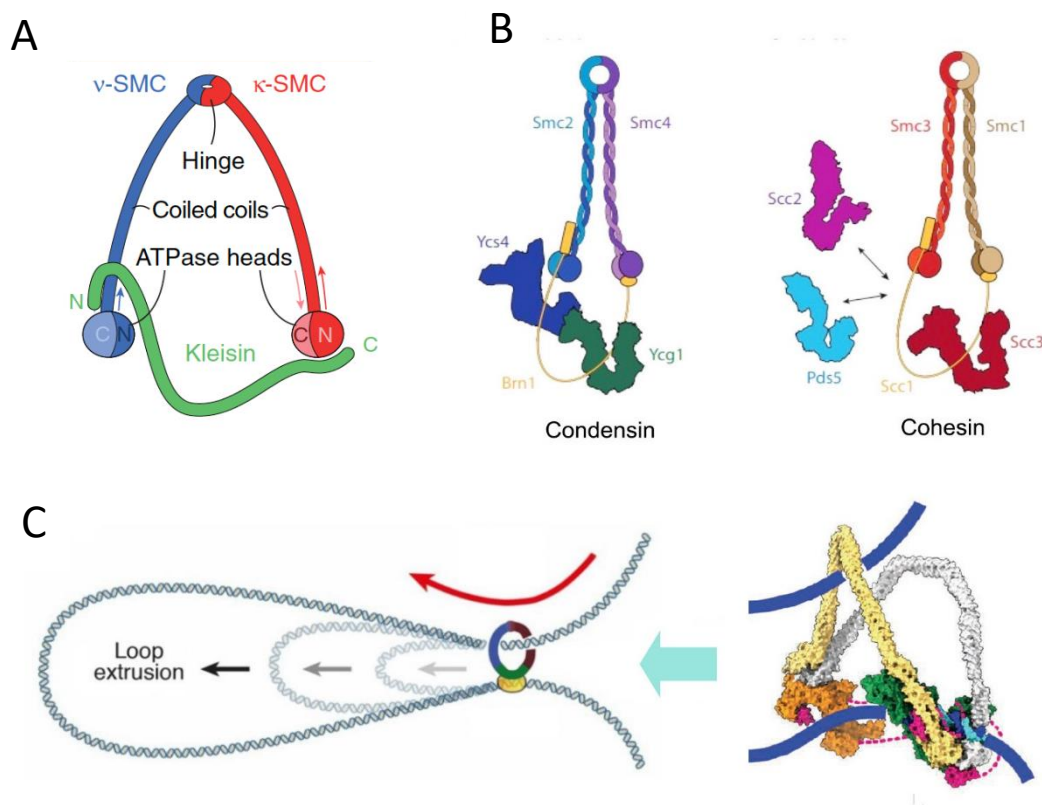


**Figure 10 – SMC (structural maintenance of chromosomes) complexes.** (A) Tripartite ring structure common in all SMC protein complexes. (B) Subunits that compose condensin and cohesin in *Saccharomyces cerevisiae*. (Adapted from Yatskevich et al., 2019) (C) The loop extrusion mechanism, where a small DNA loop is threaded through the SMC ring and then pushed in an ATP-dependent manner, allowing it to grow in size.

### 2.1.3 DNA topoisomerases

DNA Topoisomerases are a family of enzymes that transiently cleave DNA strands to change their topology. These enzymes are classified into two main types according to whether they cleave a single strand of DNA (type-1) or both strands (type-2). They are further divided into subfamilies according to their structure and mechanism. The main ones are Type-1A, Type-1B, Type-2A and Type-2B.

**Type-1A topoisomerases** are monomeric enzymes that only act on single stranded DNA, forming a covalent intermediate between a tyrosine of the active center of the enzyme and the 5'-phosphate end of the cleaved DNA. After the cleavage, they pass another single stranded DNA segment through the cut (Figure 11A). To perform this transport cycle, they do not consume any energetic cofactor, which means that they can only produce topological changes that are energetically favorable. With their mechanism, type-1A topoisomerases can perform catenation or decatenation and knotting or unknotting of single-stranded DNA molecules (Wang, 1996). However, type-1A topoisomerases are best known for their role in relaxing double-stranded DNA molecules that have negative helical tension ( $Lk < Lk_0$ ) and consequently present single stranded regions.

The best characterized enzyme of this subfamily is topoisomerase I present in *Escherichia coli* (*E. coli*) (Wang, 1971). It has a molecular weight of 97 kDa and its main function is to reduce the negative helical tension in bacterial chromosomes (Figure 11B). Another enzyme belonging to this subfamily is topoisomerase III, which is present in most bacteria and eukaryotic cells (Wallis et al., 1989). Although it is structurally very similar to *E. coli*'s topoisomerase I, its DNA relaxing activity is weak and mainly disentangles single-stranded DNA regions generated during recombination or replication (Kim & Wang, 1992).

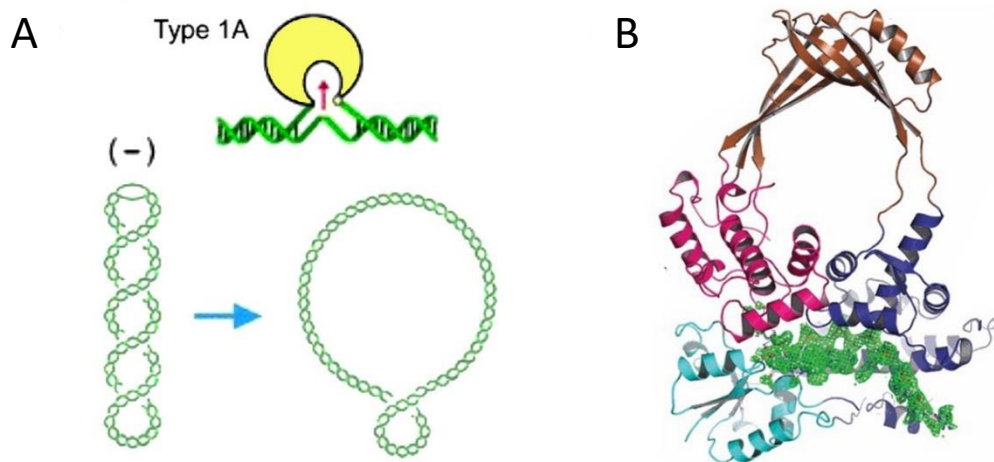


**Figure 11 – Type-1A topoisomerases.** (A) Type-1A topoisomerases relax (-) supercoiling by transiently cleaving single-stranded DNA regions and allowing the passage of the complementary DNA strand through the cut. Single-stranded regions frequently occur when DNA is unwound by (-) torsional stress. The torsional stress is reduced by successive reaction cycles, for as long as the enzyme can find single-stranded DNA. (B) Structure of *E. coli* DNA topoisomerase I. The bound DNA is shown in green.

**Type-1B topoisomerases** are monomeric enzymes that act on double-stranded DNA and cleave one of the two strands, in other words, they produce a transitory nick. The covalent intermediary during strand cleavage occurs between a tyrosine of the active site of the enzyme and the 3'-phosphate group of the cleaved DNA. The enzyme then allows the 5'-end to rotate freely around the uncleaved strand and, following one or several rotations, the enzyme re-seals the DNA double helix (Figure 12A) (McCoubrey & Champoux, 1986). Similar to type-1A topoisomerases, type-1B do not consume any energetic cofactor and consequently can only produce topological changes that are energetically favorable. Through their mechanism, type-1B topoisomerases completely relax positive and negative DNA helical tension (Figure 12A). Thus, they produce Lk distributions centered in  $Lk_0$  (Champoux, 1990).

The most representative enzyme of this group is topoisomerase I, present in all eukaryotic cells. Its molecular weight varies from 95 and 135 kDa depending on the organism (Figure 12B) (Eng et al., 1989; R. Lynn et al., 1989). Another well-characterized enzyme of this group is Vaccinia virus's topoisomerase I (Shuman & Moss, 1987), which contains the minimum domain necessary for its relaxing activity (32 kDa).



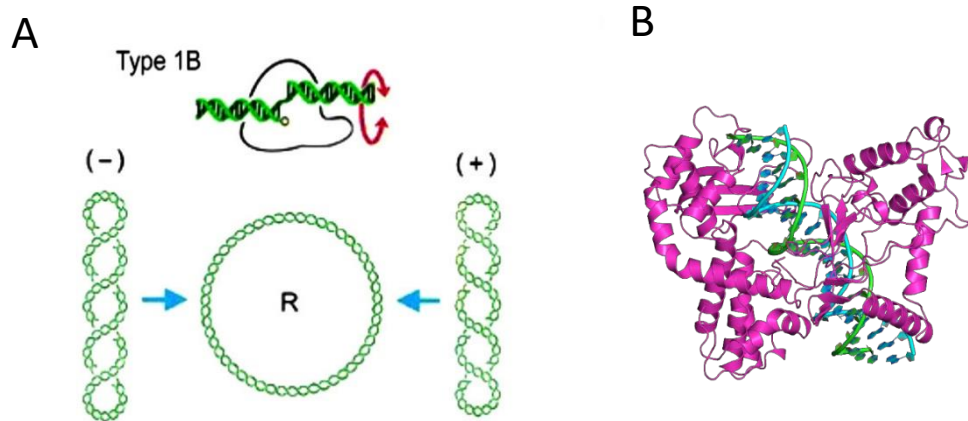


**Figure 12 – Type-1B topoisomerases** (A) Type-1B topoisomerases interact with duplex DNA and transiently nick one of the two strands. The 5' end of the cleaved strand then becomes free to swivel around the uncleaved strand. This rotation mechanism efficiently removes the DNA's (+) and (-) torsional stress. (B) Ribbon representation of the central core of human topoisomerase I bound to DNA (blue and green).

**Type-2A topoisomerases** are homodimeric enzymes that transiently cleave the two DNA strands, such that the two tyrosines of the active center of the enzyme are covalently linked to each of the 5'-phosphate ends of the DNA (G-segment). Then they pass another double-stranded DNA segment (T-segment) through the previously cleaved one in an ATP dependent manner (Figure 13A) (T.-S. Hsieh, 1990).

All type-2A topoisomerases present three highly evolutionary conserved domains that correspond to 3 gates: the ATPase or N-gate domain, the DNA binding or DNA-gate domain and the pivot or C-gate domain (Figure 13B). The first step in the transport cycle is the union of the G-segment to the DNA-gate domain. The second step is the binding of ATP to the ATPase domain which causes the N-gate to close (Roca & Wang, 1992). This closure allows the capture of the T-segment into the enzyme. Then, the T-segment is pushed through the transiently cleaved G-segment (Roca & Wang, 1992). Finally, the T-segment can exit through the C-gate. With this transport cycle the T-segment completely crosses the dimeric interface of the enzyme (Figure 13B) (Roca & Wang, 1994; Roca et al., 1996). However, after crossing the cleaved G-segment, the T-segment can sometimes go back and out again through the N-gate (backtracking). In this case, there is no topological change in the DNA (Figure 13B) (Martinez-Garcia et al., 2014).

## Introduction

When the G- and T-segments are in the same DNA molecule, the result of the transport cycle can either increase or reduce the number of DNA supercoils, or can produce or resolve DNA knots (Figure 13C). In either case, the type-2A topoisomerases change the value of  $Lk$  in +2 or -2 units, depending on whether a negative or positive supercoil is inverted, respectively. When the G- and T-segments are on different molecules, the result of the reaction cycle is the catenation or decatenation of the two DNA molecules (Figure 13C) (Roca, 2011).

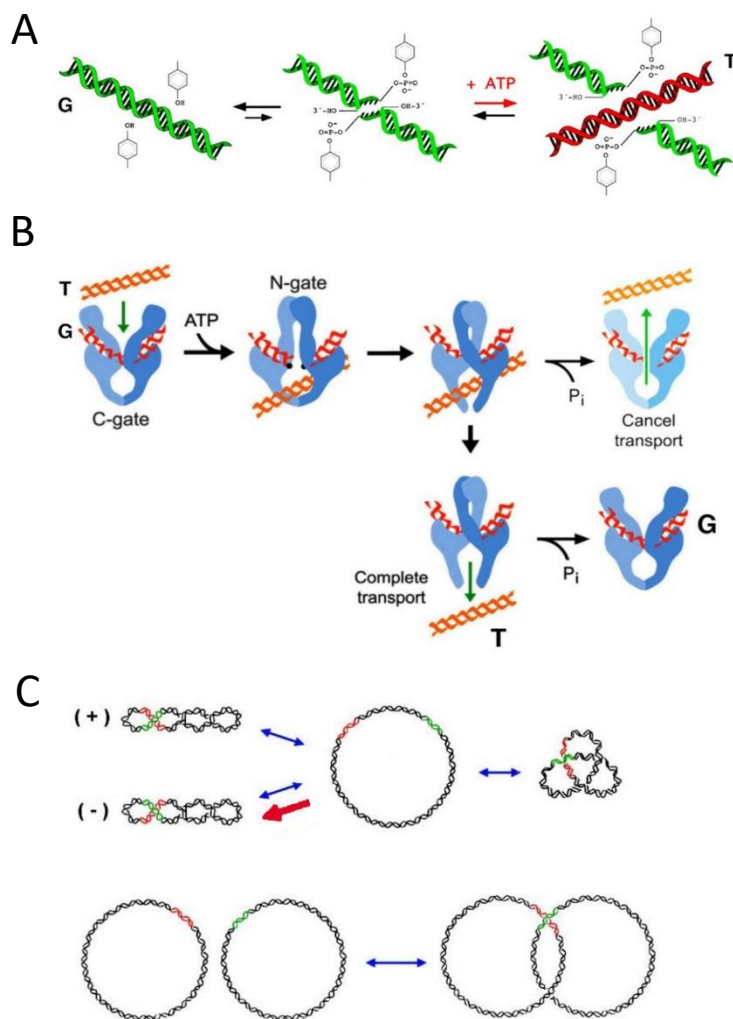


**Figure 13 – Type-2A topoisomerases.** (A) Mechanism. The DNA G-segment is transiently cleaved to allow the passage of the T-segment in an ATP dependent manner. (B) The three gates. Once the G-segment binds to the DNA-gate domain, a T-segment can be captured by the N-gate. The T-segment is then passed across the cleaved G-segment and exits the enzyme through the C-gate. Alternatively, the T-segment might backtrack and exit through the N-gate. (C) Intra-molecular DNA transport allows the removal of (+) and (-) supercoils, as well as formation or resolution of DNA knots. However, DNA gyrase only introduces (-) supercoils (red arrow). Inter-molecular DNA transport allows to catenate or decatenate DNA.

Within the type-2A enzyme subfamily, we can find topoisomerase II present in all eukaryotic cells and topoisomerase IV present in eubacteria (Kato et al., 1990). As mentioned before topoisomerases II and IV are proficient in simplifying the DNA's topology: they relax positive and negative supercoils, and remove knots and catenates. Moreover, *in vitro* experiments show that they are even able to simplify the DNA's topology below the thermodynamic equilibrium (Rybenkov et al., 1997). This means that they can reduce the variance of Lk thermal distributions, and also reduce the number of knots and catenates present in the DNA even when it is prone to be naturally entangled.

Lastly, a special type-2A enzyme of this subfamily is the DNA gyrase, which is present in eubacteria (Gellert et al., 1976). Unlike topoisomerases II and IV, DNA gyrase introduces negative supercoils into the DNA, a reaction that requires the enzyme to dictate the orientation of the T-segment with respect to the G-segment (Figure 13C). To do so, the gyrase wraps around 130 bp of DNA in a right-handed sense, to produce a positive supercoil between the G- and T-segments. Then, it inverts this crossing to produce a negative supercoil (Kampranis et al., 1999). The gyrase is therefore inefficient in relaxing negative supercoiling and/or altering the catenated or knotted state of the DNA.

**Type-2B topoisomerases** are homodimeric enzymes that have many structural and mechanistic similarities with the Type-2A family (Figure 14). They both form transient covalent bonds with the 5'-phosphate of both strands of the cleaved DNA duplex and function via a strand-passage mechanism. Furthermore, they both relax positive and negative supercoils, and can decatenate and unknot the DNA in an ATP dependent manner. However, Type-2B topoisomerases only have two protein gates or interfaces: the N-gate domain and the DNA-gate domain, lacking the C-gate domain (Figure 14). The enzyme that represents this group is topoisomerase VI. This enzyme is found throughout the archaea kingdom, in a few bacterial species, and in some plants and algae (Corbett & Berger, 2003; Wendorff & Berger, 2018). Their functional role is yet unclear. Remarkably, topoisomerase VI present analogies with the eukaryotic protein Spo11, which produces double-strand DNA breaks during meiotic recombination (Vrielynck et al., 2016).

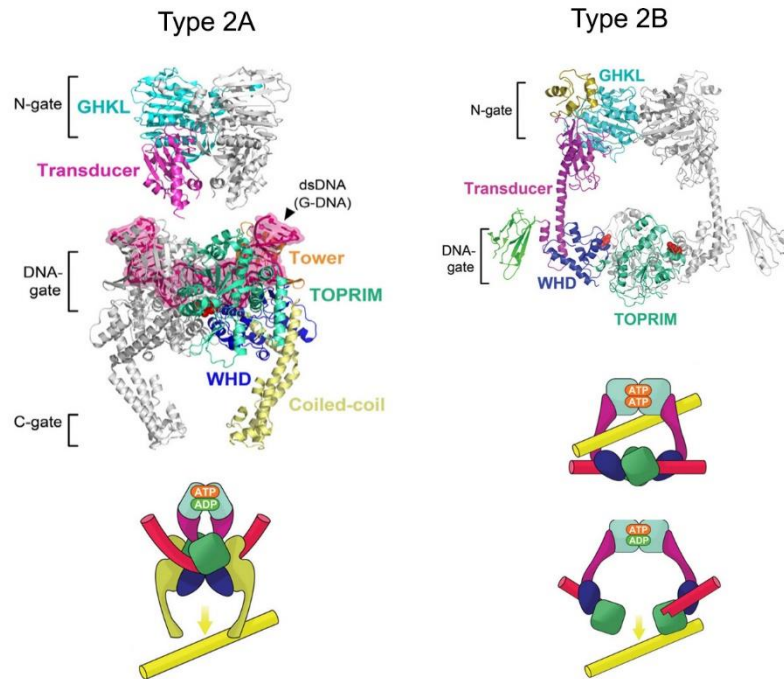


**Figure 14 – Structural and mechanistic similarities between type-2A and type-2B topoisomerases.** Both enzymes have an N-gate domain (that closes upon ATP binding) and a DNA-gate domain (that transiently cleaves the DNA). However, type-2B topoisomerases lack a C-gate domain (Adapted from Chen et al., 2013).

### 2.1.4 Main functions of DNA topoisomerases

DNA topological problems are widespread and affect both eukaryotes and prokaryotes in very similar ways. That is why, topoisomerases have high resemblances in both type of organisms (Champoux, 2001; Wang, 2002). In all cases DNA transcription generates (+) and (-) helical stress ahead of and behind the moving RNA polymerases, respectively (Figure 15A) (Roca, 2011). Similarly, the process of DNA replication generates (+) helical tension ahead of the replication forks (Figure 15B) (Roca, 2011). Relaxation of (+) helical tension is essential to allow the progression of transcription and replication. Relaxation of excessive (-) helical tension during transcription is also required to prevent the formation of R-loops and DNA damage (Wang, 2002). In eubacteria, type-1A topoisomerase I relaxes (-) helical tension, gyrase relaxes the (+) one while topoisomerase IV relaxes both. In eukaryotic cells, both type-1B topoisomerase I and

type-2A topoisomerase II participate in relaxing both (+) and (-) helical tension (Champoux, 2001).

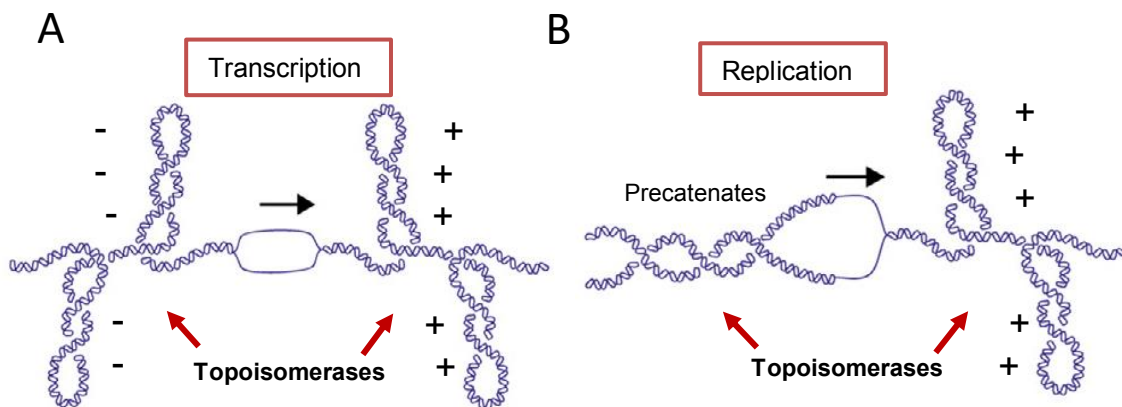


**Figure 15 – Common topological DNA problems in prokaryotes and eukaryotes.** (A) The progression of the transcription machinery generates (+) and (-) helical tension in front of and behind the RNA polymerase, respectively. (B) The advancement of the replication forks generates (+) helical tension in front and causes catenation between the newly replicated duplexes behind the replication fork (Adapted from McKie et al., 2021).

Another topological problem that arises during DNA replication is the catenation between the newly formed double helices which tend to be interweaved behind the replication fork (Figure 15B). Topoisomerase IV in eubacteria and topoisomerase II in eukaryotes are essential to eliminate these catenates in order to allow chromosome segregation during cell division (Cortés et al., 2003; Nitiss, 2009).

In addition to the general roles mentioned above, topoisomerases have been involved in other functions. In eukaryotes, topoisomerase II is often found located at promoter regions and at TAD boundaries (Uuskula-Reimand et al., 2016; Canela et al., 2017). It is unclear whether the enzyme's activity at these sites is to cleave the DNA, to alter its topology, or to perform some structural role. Likewise, experimental data shows that topoisomerase II is essential to perform mitotic chromosome condensation and decondensation (Antonin & Neumann, 2016; Nielsen et al., 2020). Yet again, the mechanism of topoisomerase II that activates these processes is poorly understood.

Regarding the functional roles of eukaryotic topoisomerases, our laboratory has pioneered in two lines of research: 1) The interplay of eukaryotic topoisomerases with

## Introduction

supercoiled nucleosomal fibers; 2) The DNA knotting-unknotting activity of topoisomerase II in vivo.

Specifically, experiments performed in our laboratory uncovered that, while type-1B topoisomerase I is more efficient at relaxing naked DNA, type-2A topoisomerase II is more efficient at relaxing nucleosome fibers (Salceda et al., 2006). These findings indicated that nucleosome fibers make DNA axial rotation difficult and consequently hard to relax via topoisomerase I (Figure 16). Instead, nucleosome fibers facilitate DNA segment juxtaposition and allow a very efficient topoisomerase II activity.

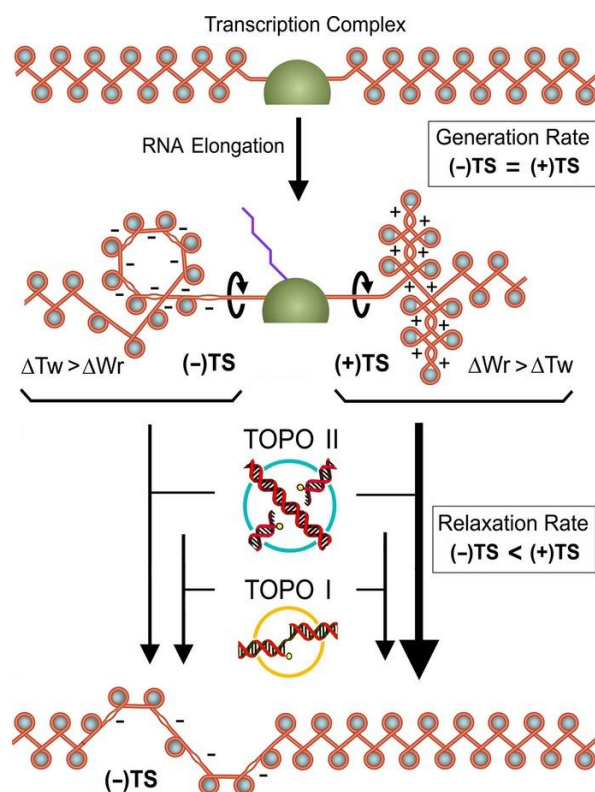


**Figure 16 – The conformational response of chromatin is distinct for (+) and (-) helical tension.** Chromatin under (+) helical tension alters mainly the writhe of the DNA ( $\Delta Wr > \Delta Tw$ ). These Wr deformations configure multiple DNA crossovers that are perfect substrates for the DNA cross-inversion mechanism of topoisomerase II. Conversely, chromatin under (-) helical tension alters mainly the DNA's twist ( $\Delta Tw > \Delta Wr$ ) which leads towards double-helical unwinding. Consequently, during DNA transcription, while the strand-rotation mechanism of topoisomerase I (yellow) relaxes (-) and (+) helical at similar rates, the DNA cross-inversion mechanism of topoisomerase II relaxes (+) helical tension quicker than the (-) one. As a result, (-) helical tension persists longer than the (+) one (Adapted from Fernández et al., 2014).

In the same line of research, our laboratory also found that in chromatin fibers, topoisomerase II is more proficient at relaxing (+) than (-) helical tension (Figure 16) (Salceda et al., 2006). This preference corroborated the knowledge that chromatin fibers deform differently as they accommodate (+) or (-) helical tension (Bancaud et al., 2006a).

The different ability of topoisomerases I and II to relax chromatin fibers, and their different efficiency to relax (+) vs (-) helical tension, has relevant implications. Whereas (+) and (-) helical tension are generated simultaneously and symmetrically during DNA transcription *in vivo*, (+) helical tension is relaxed faster than the (-) one (Figure 16) (Fernández et al., 2014). Such an asymmetry in the relaxation process allows maintenance of the (-) helical tension for a longer period of time and that could be relevant to regulate genomic activities (Fernández et al., 2014).

In contrast with the role of topoisomerases in the modulation of DNA supercoiling, and in the resolution of catenates between newly replicated DNA molecules, which have been widely studied in a great variety of biological systems, the knotting-unknotting activity of topoisomerases has been largely overlooked over the years (Bates & Maxwell, 2005). Therefore, in addition to the interplay of topoisomerases with supercoiled chromatin, in recent years our laboratory has initiated the study of the DNA knotting-unknotting activity of topoisomerase II *in vivo*. Before dealing with this new topic, I shall first introduce what a knot is, how the DNA becomes knotted, and how DNA knots are analyzed.

### **3. WHAT IS A KNOT?**

Mathematically, a knot is defined as a closed curve in space with irreducible intersections (crossovers). These intersections cannot be eliminated by deforming the curve in any way such as stretching, bending or twisting. The only possible way to reduce these crossovers is by cutting the closed curve and passing one segment through another and finally connecting the loose ends back together to close the curve (Chirikjian, 2013; Michieletto et al., 2017).

## Introduction

Knots are classified by their number of irreducible crossovers, each of which can be topologically (+) or (-) (Figure 17). The simplest knot of all is the unknotted circle (trivial knot), which corresponds to a closed curve that lacks irreducible intersections ( $0_1$ ). However, the first real knot has 3 irreducible intersections ( $3_1$ ) and it is called the trefoil knot (note that it is not possible to form a knot with less than 3 intersections). Following the trefoil knot, there are knots with 4 intersections ( $4_1$ ), two possible knot forms with 5 intersections ( $5_1$  and  $5_2$ ), three different possible knot forms with 6 intersections and so on (Figure 17A). As you add complexity to knots by adding more crossings the number of knots per group keeps increasing exponentially (Ernst & Sumners, 1987). All of these knots are known to be distinct. If we made one of them out of string, we would not be able to deform it to look like any of the others. We call these types of knots: prime knots. Knots that are expressed as the composition of two prime knots, neither of which being a trivial knot, are called composite knots (Figure 17B).

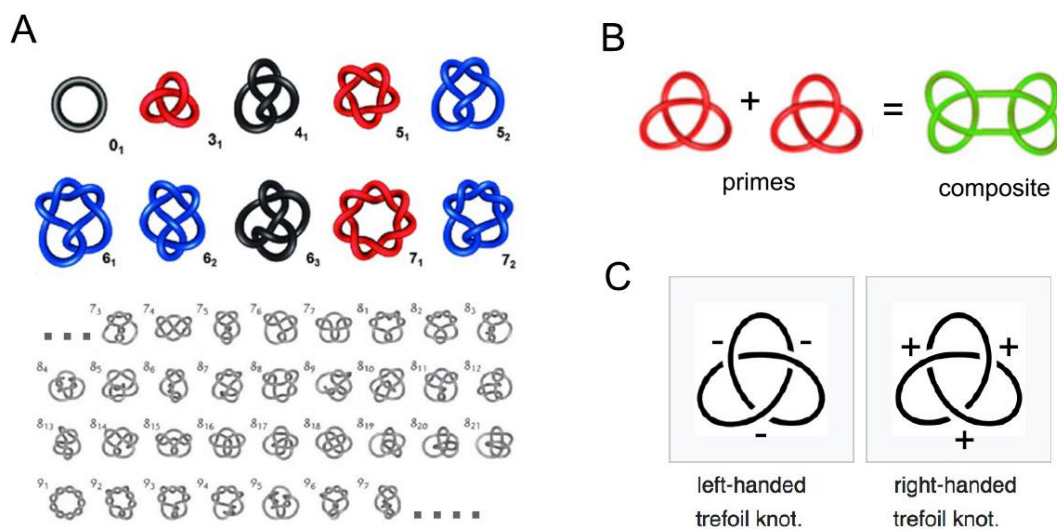


**Figure 17 – Types of knots.** (A) Classification of prime knots by their irreducible number of crossings. Knots of the toroidal family (red) and twist family (blue) are indicated. (B) Example of a composite knot formed by two primes (trefoils). (C) Example of the two chiral forms (mirror images) of the trefoil knot.

Another important fact is that most knots are chiral, which means that they cannot be deformed to their mirror image. As mentioned above, each knot crossover can be topologically (+) or (-). The trefoil knot, for instance, is a chiral knot and therefore it can



be found in two different chiral forms: with all three positive crossings  $3_1 (+)$  or its specular image  $3_1 (-)$ , with all three negative crossings (Figure 17C). However, the knot with four crossings  $4_1$  is achiral, always having two positive and two negative crossings, allowing the  $4_1$  knot to be deformed into its mirror image (Fielden et al., 2017).

### 3.1 How do DNA molecules become knotted?

DNA knots can be formed through three mechanisms: upon circularizing a linear DNA molecule, through the action of type-2 topoisomerases and through intramolecular recombination processes (Figure 18).

The circularization of linear DNA molecules *in vitro* can lead to the formation of DNA knots (Rybenkov et al., 1993; S. Shaw & Wang, 1993). The knotting probability when closing a DNA circle in free solution depends on its length and flexibility, which as previously mentioned, can vary with the ionic environment (Figure 18A).

The mechanism of type-2A topoisomerases (topoisomerases II and IV), allows the formation and resolution of DNA knots. More precisely, they allow the continuous passing of DNA segments through one another (Roca & Wang, 1992), which results in an equilibrium of knotting and unknotting events (Figure 18B). The equilibrium fractions of knotted and unknotted molecules will once again depend on DNA length and flexibility. However, other factors that promote the juxtaposition of intra-molecular DNA segments will also increase the fraction of knotted molecules by type-2A topoisomerases. These factors include supercoiling or the presence of proteins that condense the DNA (Hsieh, 1983; Wasserman & Cozzarelli, 1991).

Finally, DNA can become knotted as a result of intramolecular recombination processes (Figure 18C). These knots are specific depending on the recombinase and the orientation of the DNA segments at the time of recombination (Wasserman et al., 1985). DNA knots formed during recombination, are usually removed by type-2 topoisomerases without affecting the recombination product.

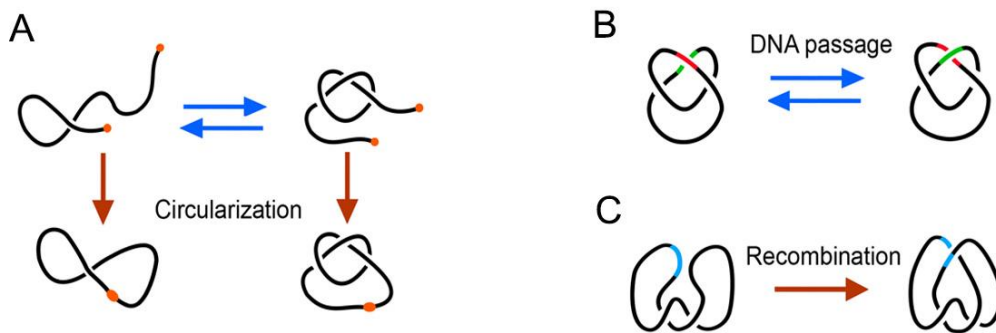


**Figure 18 – Mechanisms to form DNA knots.** (A) Circularization of a linear DNA molecules. (B) DNA strand passage activity of type-2A topoisomerases. (C) Recombination processes.

### 3.2 How are DNA knots analyzed?

There are two main approaches for DNA knot characterization: direct visualization of knotted DNA molecules via electron microscopy (EM); and DNA electrophoresis in one-dimensional (1D) or two-dimensional (2D) agarose gels.

In order to be able to visualize DNA knots it is necessary to eliminate all helical tension from the DNA molecule. To do this, one strand of the double DNA helix is nicked with an endonuclease. By producing this nick, the tension is eliminated but the knot crossovers are not altered, which allows knotted molecules to be differentiated from merely supercoiled ones (Figure 19) (Levene & Tsen, 1999).

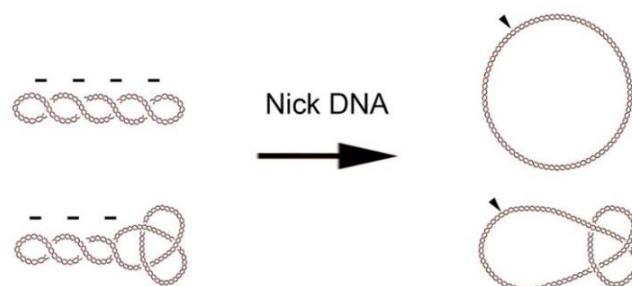


**Figure 19 – Effect of nicks on knotted DNA.** Nicking removes the DNA's helical tension. Consequently, the DNA crossovers that belonged to supercoiling disappear, but the irreducible crossovers of a knot remain.

Following the nicking step, to observe knots by means of EM the DNA sample has to be coated with Rec-A protein. This coating makes the DNA contour thicker to the EM machine, allowing it to differentiate the DNA segment on top and the one on the bottom for each DNA crossover (Figure 20). Through EM, it is thereby possible to draw the path of each knotted molecule, which allows the identification of the knot type and its chirality (Lynn & Crisona, 1999; Sogo et al., 1999). However, the main limitation of this technique is that knots have to be analyzed individually making it hard to get statistics. Moreover, this kind of analysis is unviable in biological samples that are extremely heterogenous and contain little amounts of knotted DNA forms.

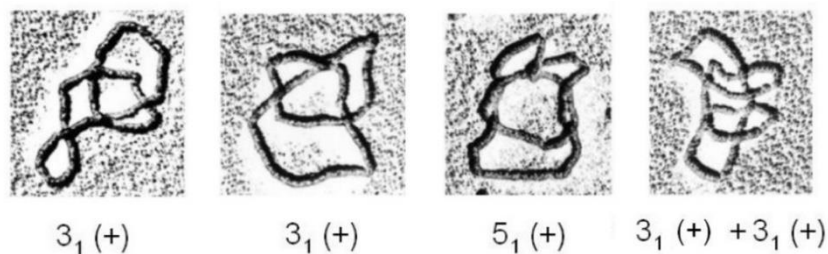


**Figure 20 – EM images of knotted DNA rings.** DNA is nicked and coated with RecA protein (Adapted from Kimura et al., 1999).

The most convenient way to characterize DNA knots is by agarose gel electrophoresis. Upon nicking the circular DNA to remove any supercoils (Figure 19), the knotted molecules will be more compact than the unknotted ones and consequently move faster in an agarose gel. Moreover, as the speed of DNA molecules correlates to their compaction, the more crossings one knot has, the greater its compaction and speed will be. Accordingly, each knot type will have a speed that is nearly proportional to its number of irreducible crossings (Figure 21) (G. Buck, 1998; Stasiak et al., 1996).

When knotted molecules are run in 1D gels, their positions can overlap with linear DNA fragments, which are especially present in *in vivo* samples. To solve this problem, our laboratory developed a high-resolution 2D electrophoresis method (Figure 21) (Trigueros et al., 2001). The first dimension of the electrophoresis allows the knots to be separated depending on their irreducible number of crossings. The added second

## Introduction

dimension allows knot populations to be separated from linear DNA fragments. Moreover, it can also allow knot populations to be separated between primes and compounds with the same number of crossings.

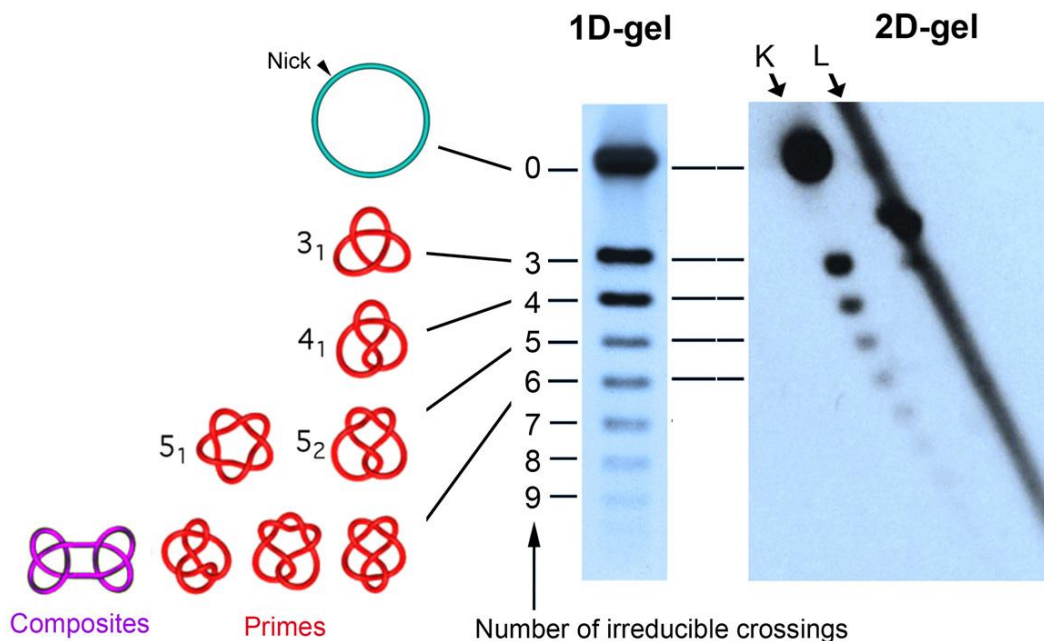


**Figure 21 – Mobility of DNA knots in 1D and 2D gel electrophoresis.** In 1D gels, the knot speed is proportional to its number of irreducible crossings. Adding a second dimension (2D) allows knot populations (K) to be separated from linear DNA fragments (L), which are abundant in cellular extractions.

Upon blotting and probing the DNA sequences in 1D or 2D agarose gel electrophoresis, DNA knots can be detected even in complex mixtures and in *in vivo* samples. From the intensity of each gel band, the relative abundance of each knot can be calculated. In addition, the total fraction of knotted molecules indicates the knotting probability of the DNA in a given experimental condition.

One limitation that the agarose gel electrophoresis presents is that it cannot separate the two chiral forms of a knot, given that they have identical compaction states. However, an earlier observation indicated that the two chiral forms of a purified trefoil knot (3<sub>1</sub>(+) and 3<sub>1</sub>(-)) acquire slightly different electrophoretic velocity when the DNA is supercoiled (i.e., not nicked) (Shaw & Wang, 1997). Using this knowledge, our laboratory has recently developed a 2D electrophoretic technique that can separate the chiral

forms of the trefoil knot in complex DNA samples that are largely unknotted (Figure 22) (Valdés et al., 2019).

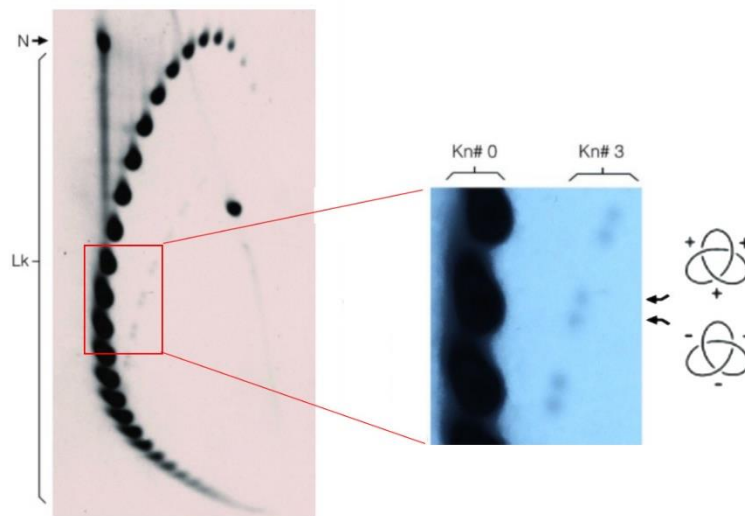


**Figure 22 - Separation of the two chiral forms of the trefoil knot.** In this 2D-gel technique, given that the DNA is not nicked, the Lk topoisomers are resolved as in Figure 7. However, the gel resolution is improved allowing to observe a secondary arch of supercoiled-knotted molecules.

### 3.3 Factors determining DNA knotting probability

DNA knotting probability ( $P^{kn}$ ) depends on several physical factors such as its: chain length, stiffness, thickness, and compaction (Figure 23). The effect of these parameters can be analyzed using computer simulations and contrasted with in vitro experiments.

It is quite intuitive to think that the longer a polymer, the higher its  $P^{kn}$ . Computer simulations performed with the random walk algorithm have demonstrated the correlation between these two parameters (Figure 23A). The random walk algorithm provides all possible random paths of a polymer in a 3D space, and then checks which paths lead to knot formation and which don't. These simulations showed an almost perfect linear correlation between polymer length and  $P^{kn}$  (Frank-Kamenetskii, 1997). Around the same time in vitro experiments were carried out using naked DNA molecules with different lengths. Linear DNA molecules were circularized with a ligase and then analyzed by agarose electrophoresis, which revealed how many of the formed DNA

## Introduction

circles had entrapped a knot. As expected, the higher the DNA length was, the higher the  $P^{kn}$  (Rybenkov et al., 1993; Shaw & Wang, 1993).

Similarly, it also follows that, irrespective of its length, a polymer's stiffness or flexibility must also largely affect its  $P^{kn}$ . Polymers with a large persistence length ( $P_L$ ) are more rigid and therefore will have lower  $P^{kn}$ . Conversely, very flexible polymers (with a small  $P_L$ ) will produce knots more easily and will have a large  $P^{kn}$ . This notion has been corroborated by computational simulations using the random walk algorithm, in which the  $P_L$  of the polymers is modeled by the size and orientation of the several steps (segments) used to perform the random walk (Figure 23A) (Frank-Kamenetskii, 1997). Thus, a very short but highly flexible polymer can have a larger  $P^{kn}$  than a much longer one that is more rigid.

Finally, in addition to the stiffness, the thickness or effective diameter of a polymer chain also affects its  $P^{kn}$ . Computer simulations demonstrated that, given two polymers of identical lengths and flexibility, a thinner one will have a larger  $P^{kn}$  than a much thicker one (Figure 23B) (Klenin et al., 1988).

The length, stiffness and thickness can determine the  $P^{kn}$  of any polymer chain in a free space. However, in most cases, a polymer chain such as DNA is not found in free solution; instead, it is condensed or restricted by biological ensembles. Computer analyses have demonstrated through polymer simulations that the  $P^{kn}$  exponentially increases with the effect of condensation and confinement (Figure 23C).

One way to conduct this simulation is by restricting the random paths of a polymer to a specific volume (Arsuaga et al., 2002). Another way to do it is by progressively deforming a circular chain until it can be fitted inside a desired volume. During this deformation process, the chain is allowed to behave as a "phantom chain" such that it can freely pass through itself (mimicking what a type-2 topoisomerase would do with the DNA) (Dorier & Stasiak, 2009). Thereby, the chain can topologically equilibrate by forming and dissolving its entanglements. In this regard, computer simulations have predicted that long DNA molecules confined in biological systems (for instance, the cell nucleus) would

be massively entangled if type-2A topoisomerases could freely equilibrate their global topology (Micheletti et al., 2008; Dorier & Stasiak, 2009).

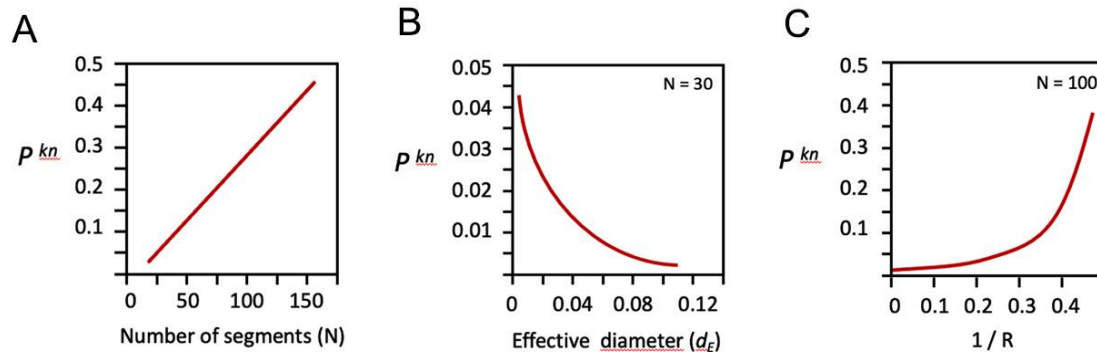


**Figure 23 – Factors determining DNA Knotting probability ( $P^{kn}$ ).** (A) Plotted results obtained by computer simulations of the  $P^{kn}$  of different polymer chains as a function of the chain's length and flexibility. The length and flexibility are modelled using a number of joined segments ( $N$ ), which length correlates to the  $P_L$ . (B) Plotted results obtained from computer simulations that analyzed the effect of the effective diameter on the  $P^{kn}$ . (C) Plotted results from computer simulations that studied the effect of confinement on the  $P^{kn}$ . The confinement is modelled by restricting the path of a chain within spheres of decreasing radius ( $R$ ).

Lastly, the DNA's condensation is usually a result of its interactions with proteins that bring DNA segments to close proximity or due to helical tension that supercoil the DNA or chromatin fibers by producing solenoids or plectonemes. In this regard, in vitro experiments have shown that, when DNA is condensed by proteins and/or supercoiling, knot formation by type-2 topoisomerase largely increases due to a higher juxtaposition of the DNA segments. (Hsieh, 1983; Wasserman & Cozzarelli, 1991; Roca et al., 1993).

### 3.4 Why are DNA knots informative?

The analysis of knots that are present in circular DNA molecules provides precious information regarding the DNA's biophysical properties, such as its  $P_L$  and its effective diameter ( $d_E$ ). For example, to obtain the DNA's  $P_L$ , the  $P^{kn}$  of DNA molecules that had been circularized in free solution were compared with the knotting probabilities

## Introduction

obtained by computer simulations using polymer chains with increasing flexibility. This analysis concluded that the  $P_L$  of double stranded DNA was 50nm (Klenin et al., 1988).

Similarly, to obtain the  $d_E$  of the DNA in a physiological environment, the  $P^{kn}$  obtained via computer simulations of polymers with increasing diameter were compared to the DNA's  $P^{kn}$  in physiological conditions. This allowed obtaining the  $d_E$  of the DNA in a physiological environment (5nm), which is larger than its geometric diameter (2nm) (Rybenkov et al., 1993; Shaw & Wang, 1993). The difference between the two values occurs because the  $d_E$  takes into account the repulsion and attraction of the negatively charged DNA segments. Consequently, when the ionic environment of DNA is altered, its  $d_E$  changes and so does its  $P^{kn}$  (Rybenkov et al., 1993; Shaw & Wang, 1993).

Seeing that the  $P^{kn}$  has allowed calculating the stiffness ( $P_L$ ) and diameter ( $d_E$ ) of naked DNA, we thought that it could be applied in the same way to DNA folded into nucleosomal fibers. As discussed later in this thesis, the  $P^{kn}$  obtained from nucleosomal fibers revealed that they are much more flexible than naked DNA (Valdes et al., 2018).

Finally, knots are very informative because they capture the DNA's spatial path. In other words, a knot is a topological invariant that preserves a 3D footprint of the DNA's trajectory. In this regard, computer simulations demonstrated that when DNA (or any polymer) follows a random path, the type of knots obtained will also be random. However, when a DNA follows a non-random path, it will result in specific types of knots. Moreover, when a DNA molecule follows a random path, it will produce knots of any chirality. However, if the followed path is chiral (i.e., more (+) crossing than (-), or vice-versa), then the resulting knots will also have a specific chirality.

These principles were used to work out several matters such as how different recombinases interact with DNA during homologous recombination (Wasserman et al., 1985). As explained below, in our laboratory, these principles were used to study the type of knots formed inside viruses, which allowed us to deduce how DNA is folded in viral capsids (Figure 24) (Arsuaga et al., 2005).



Lastly, it should be highlighted that the capture and subsequent analysis of DNA knots is virtually free of experimental artifacts and can provide reliable conformational information of the chromatin's dynamics and its spatial trajectory in short length scales (< 10Kb). These advantages contrast with other more invasive approaches that examine the path of intracellular chromatin at a resolution of tens to hundreds of DNA Kb.

### 3.5 Occurrence of DNA knots in biological systems

The first experimental observations of DNA knots in a biological system were made in bacteriophages at the beginning of the 1980s (Liu, Davis, et al., 1981; Liu, Perkocho, et al., 1981). Most bacteriophages contain linear DNA molecules with sticky ends. For example, the bacteriophage P4 genome consists of an 11 Kb linear DNA molecule, with 16 bp sticky ends. After extracting DNA from the capsid of these viruses, an extremely high amount of knotted DNA molecules was observed. Years later, our laboratory characterized these knots by means of 1D and 2D gel electrophoresis and compared the results with computer simulations that modeled the formation of knots in restricted volumes (Trigueros et al. 2001). The results indicated that these knots are formed during an accidental circularization of the DNA within the small volume of the phage capsids (Arsuaga et al., 2002). Moreover, analyses of the type of knots obtained from these analyses revealed an enrichment of chiral and toroidal knot forms. These observations demonstrated that the DNA is not randomly packaged inside viral capsids (Figure 24) (Arsuaga et al., 2005).

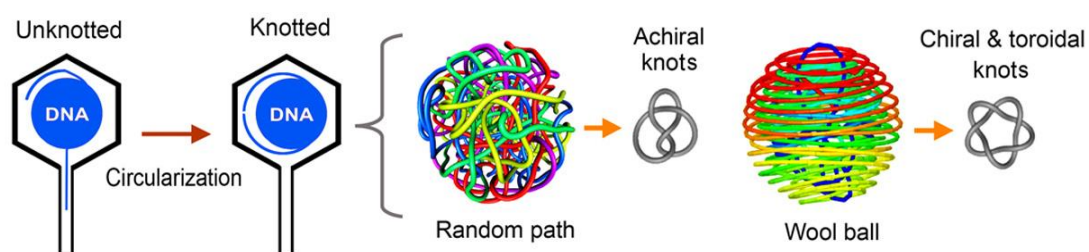


**Figure 24 – Knotted DNA in phages.** Given that the DNA is highly condensed (500 mg/mL) inside phage capsids; its circularization produced abundant and very complex knots. Most of these knots were chiral and toroidal, which led computer simulations to propose that the DNA in phages folded like a woolen ball.

## Introduction

A few years after the first observation of knots in bacteriophages, knotted DNA was found in bacteria (Shishido et al., 1987). These knots were mainly observed in plasmids extracted from *E. coli* strains, in which the activity of DNA topoisomerases, was altered (Shishido et al., 1987; Ishii et al., 1991). Remarkably, the spectrum of these knots was not random. Most of them presented an odd number of irreducible crossings (i.e., 3, 5, 7, 9, 11...). Three decades later, the mechanism that produces these knots remains unknown. DNA knot formation has also been observed in bacterial plasmids in which the replication forks have been hindered, leading to partially replicated molecules. These knots were mainly trefoils and were found in the replicated sections. The mechanism that drives their formation also remains poorly understood (Sogo et al., 1999; Olavarrieta et al., 2002).

In the case of eukaryotic cells, the existence of DNA knots had never been documented until recently in our laboratory (Valdes et al., 2018). Up until then, it was generally assumed that intracellular DNA was knot-free, since in vitro experiments had shown that DNA knots interfere with nucleosome assembly and DNA transcription (Portugal & Rodriguez-Campos, 1996; Rodriguez-Campos, 1996). However, given the high concentration of DNA in chromatin fibers and the abundance of soluble topoisomerase II inside the cell nucleus, it was likely that intracellular DNA could sometimes become knotted.

To test this possibility, our laboratory examined the topology of different circular minichromosomes in budding yeast (*Saccharomyces cerevisiae*). These minichromosomes varied in size (1.4 to 13 Kb) and contained different structural and functional elements. Upon growing the cells, they were fixed to conserve their DNA topology and then the total DNA was extracted. One half of each DNA sample was electrophoresed in 2D gels containing chloroquine, which allowed the distribution of Lk topoisomers to be displayed (Figure 25). As expected, since each nucleosome restrains about one negative supercoil, the minichromosomes presented negative  $\Delta Lk$  values that were proportional to their size (i.e., number of nucleosomes). The other half of each DNA sample was nicked with an endonuclease in order to remove the DNA supercoils.

The nicked DNA sample was electrophoresed in 2D gels to test the occurrence of DNA knots (Figure 25) (Valdes et al. 2018).

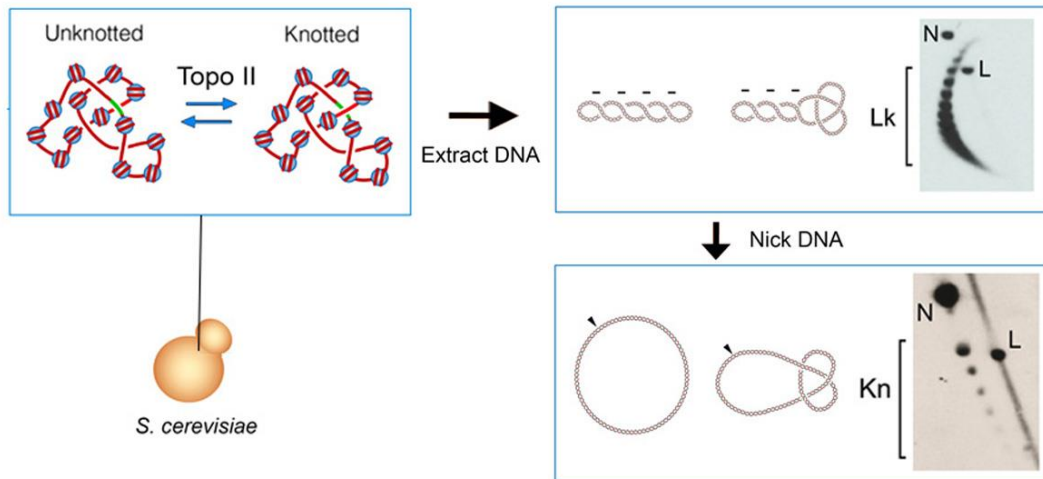


**Figure 25 – Experimental outline to study DNA knotting in eukaryotic chromatin.** The topology of yeast circular minichromosomes of different sizes and containing different elements was fixed *in vivo* and their DNA extracted. 2D gel electrophoresis of Lk topoisomers showed the negative supercoils (Lk) that were restrained by nucleosomes *in vivo*. Upon nicking the DNA, the 2D gels revealed the presence of knotted DNA molecules (Kn). N, nicked circles. L, linear DNA.

The analysis of the DNA knots found in yeast chromatin provided interesting and striking results, as explained below.

First, small amounts of DNA knots were present in most circular minichromosomes regardless of their structural and functional elements. Moreover, DNA knots happened irrespective of DNA replication and cell proliferation, although their abundance was slightly altered during DNA transcription. All these changes occurred in a topoisomerase II dependent manner. These observations strongly suggested that steady state fractions of DNA knots produced by topoisomerase II are common in eukaryotic chromatin (Figure 26).

Second, the  $P^{kn}$  of intracellular chromatin correlated linearly with DNA length until minichromosomes reached a size of around 5 Kb (i.e., about 25 nucleosomes). For this

## Introduction

size,  $P^{kn}$  was close to 0.025. The linear increase and type of knots observed were comparable to the knots produced via computer simulations that modeled knot formation in phantom chains (Frank-Kamenetskii et al., 1975; Hagerman, 1988; Rybenkov et al., 1993). Consequently, from the  $P^{kn}$  values obtained in these analyses the apparent  $P_L$  and  $d_E$  of nucleosomal fibers in vivo could be calculated. Surprisingly, the nucleosomal fibers presented  $P^{kn}$  values comparable to a polymer chain with a  $P_L$  of  $10 \pm 3$  nm and an  $d_E \approx 0$ . A larger  $P_L$  value would imply a negative  $d_E$  value, as if the nucleosomes present in the minichromosomes were strongly attracted to each other instead of repelled by electrostatic forces. Equally,  $d_E$  values approaching the geometrical diameter of the DNA (2nm) would imply extremely low  $P_L$  values ( $< 3$  nm). In any case, the in vivo DNA knotting data indicated that nucleosomal fibers ( $P_L$  of  $10 \pm 3$  nm) are much more flexible than naked DNA ( $P_L = 50$  nm) (Figure 26).

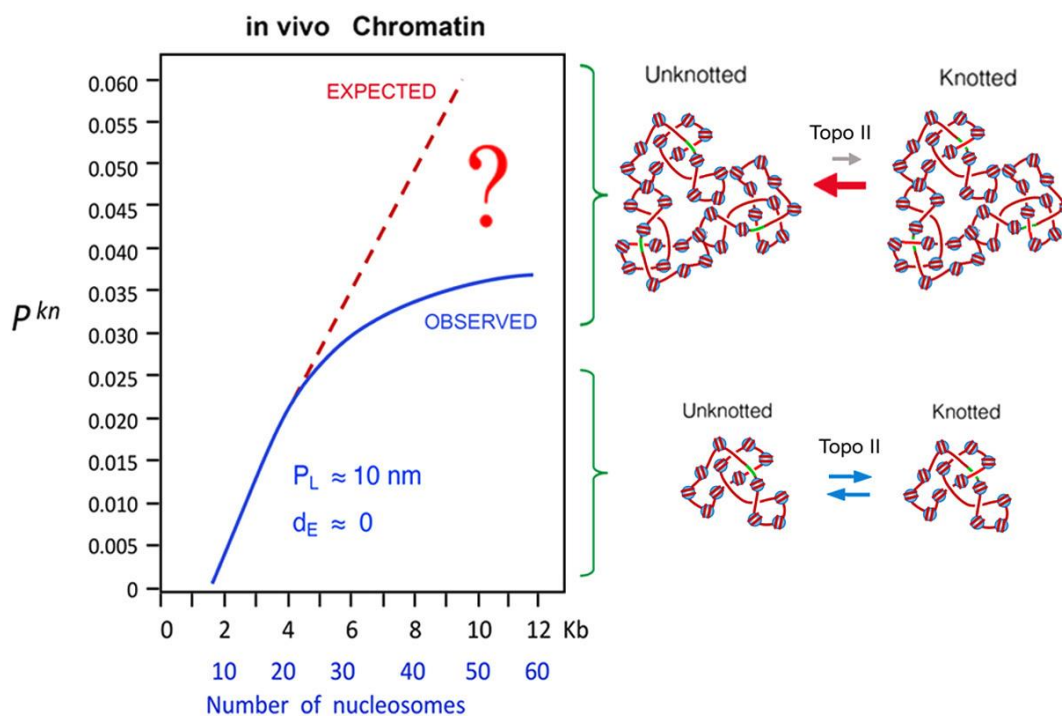


**Figure 26 – Chromatin  $P^{kn}$  as a function of its length.** The  $P^{kn}$  increases linearly up to a DNA length of about 25 nucleosomes, irrespective of chromatin elements or cell cycle stage. However, the  $P^{kn}$  of chromatin domains with >25 nucleosomes no longer follow the "expected" linear correlation with length. Therefore, the  $P^{kn}$  of in vivo chromatin is attenuated by some mechanism.

Third, the DNA  $P^{kn}$  was strongly attenuated when the size of the minichromosomes was larger than 5 Kb (i.e., more than 25 nucleosomes). The  $P^{kn}$  barely increased in nucleosomal fibers spanning from 6 to 13 Kb. This inflection was unexpected because all in silico analyses and in vitro studies with naked DNA demonstrated that the  $P^{kn}$  should increase proportionally to chain length. These findings indicated that, while high flexibility of nucleosomal fibers facilitate DNA knotting in short length scales (<5 Kb), some mechanism must minimize the scaling of DNA knot formation throughout intracellular chromatin (Figure 26).

One possibility to explain the inflection in the  $P^{kn}$  could be a length-dependent transition in the packaging mode of the nucleosomal fibres. For instance, minichromosomes (i.e., chromatin domains) containing up to 20-30 nucleosomes might fold into intricate disordered structures that can easily be entangled by topoisomerase II. However, larger chromatin domains might be able to adopt a more ordered or compacted configuration of their nucleosomes. This transition could then avoid random knotting by hindering the access of topoisomerase II to entangle the embedded DNA. However, no experimental evidence supports such abrupt length-dependent transition of nucleosome arrays (Bancaud et al., 2006a; Maeshima et al., 2016). Instead, rather than ordered and regular packing models (Dorigo et al., 2004; Song et al., 2014), numerous evidence indicates that native nucleosomal fibres present irregular folding in vitro and in vivo (Ricci et al., 2015; Grigoryev et al., 2016; Maeshima et al., 2016). Chromatin folding studies and super-resolution nanoscopy have indicated that chromatin folds into irregular clusters of 10–50 nucleosomes, termed “nucleosome clutches” (Hsieh et al., 2015; Ricci et al., 2015). Moreover, EM tomography has corroborated that intracellular chromatin is a disordered 5- to 24-nm diameter granular chain (Ou et al., 2017). Therefore, these irregular architectures could hardly explain why the  $P^{kn}$  of chromatin is minimized.

The purpose of the present thesis is to uncover the mechanism that is reducing the  $P^{kn}$  of chromatin. The existence of this mechanism is likely to be crucial to prevent the massive entanglement of intracellular DNA. To this end, we considered 3 hypotheses that could be experimentally tested in our laboratory (Figure 27).

## Introduction

The first hypothesis is based on the idea that DNA supercoiling drives topoisomerase II to unknot the DNA (Burnier et al., 2008; Witz et al., 2011).

The second hypothesis is based on the in vitro observation that topoisomerase II has an intrinsic capacity to reduce the equilibrium fractions of DNA knots (Rybenkov et al., 1997; Stuchinskaya et al., 2009).

The third hypothesis is based on computer simulations which suggest that extrusion of DNA loops via the activity of SMC complexes favors knot removal by topoisomerase II (Goloborodko, Marko, et al., 2016; Orlandini et al., 2019a). These three hypotheses are detailed below.

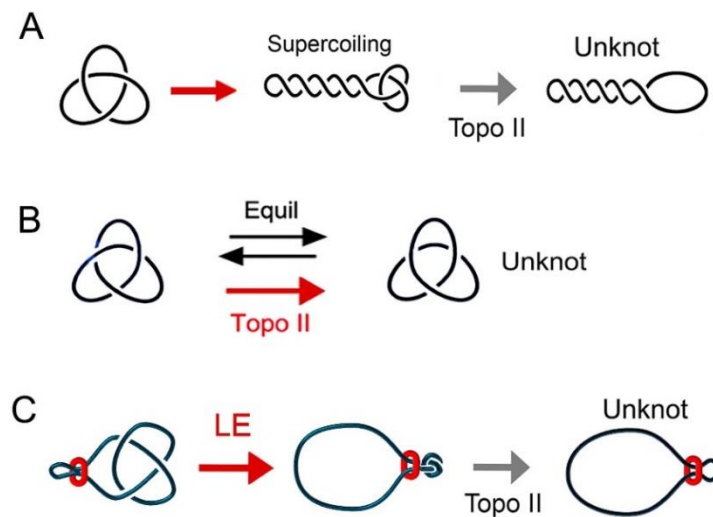


**Figure 27 – Three hypothetical mechanisms that could minimize the  $P^{kn}$  of intracellular DNA.** (A) Tightening of DNA knots by means of supercoiling. (B) Intrinsic capacity of topoisomerase II to reduce the equilibrium fraction of knotted DNA. (C) Tightening of DNA knots by means of loop extrusion.

### 3.5.1 Supercoiling as a way to reduce knotting

The idea that DNA supercoiling can alter DNA knotting has been tested by computer simulations (Podtelezhnikov et al., 1999; Burnier et al., 2008). These in silico studies showed that supercoiling could provoke the tightening of knotted regions (Buck & Lynn Zechiedrich, 2004; Witz et al., 2011) and confine them over biologically relevant timescales (Coronel et al., 2018). Such tightening would then facilitate the removal of knots by topoisomerase II (Figure 27A).

To test whether DNA supercoiling can promote the minimization of DNA knotting *in vivo*, we used yeast strains in which (+) or (-) supercoiling can be accumulated in circular minichromosomes. Using these strains, we could then check the  $P^{kn}$  of such minichromosomes by analyzing their DNA via high definition 2D electrophoresis gels. These experiments will constitute the 1<sup>st</sup> OBJECTIVE of the present thesis.

### 3.5.2 Intrinsic capacity of topoisomerase II to simplify DNA knots

In 1997, Rybenkov et al. discovered that, when DNA is naked in free solution, topoisomerases II and IV are able to produce steady-state fractions of DNA catenates, knots and supercoils that are lower than their corresponding equilibrium fractions (Figure 27B). Since then, several studies have addressed the question of how these topoisomerases could simplify the level of DNA entanglements (Stuchinskaya et al., 2009). Several models were proposed such as the sliding model (Rybenkov et al., 1997), the G-segment hairpin model (Vologodskii et al., 2001) or the three-segment interaction model (Trigueros et al., 2004). However, none of these models was satisfactory since they were experimentally disproven or did not fully explain the extent of DNA topology simplification experimentally observed.

Years later, *in vitro* studies carried out in our laboratory clarified the mechanism by which topoisomerase II simplifies the DNA equilibrium topology (Martinez-Garcia et al., 2014). These studies uncovered that topoisomerase II does not always release the T-segment through the exit gate (C-gate). Sometimes, after crossing the G-segment, the T-segment backtracks and exits through the entrance gate (N-gate).

Remarkably, when the backtracking of the T-segment is prevented by blocking the N-gate or by keeping the C-gate open, topoisomerase II loses its capacity to simplify the DNA's equilibrium topology (Martinez-Garcia et al., 2014). These observations opened the possibility to test whether topoisomerase II also simplifies the equilibrium topology

of nucleosomal fibers in vivo. These experiments will constitute the 2<sup>nd</sup> OBJECTIVE of the present thesis.

### **3.5.3 Removal of DNA entanglements via loop extrusion**

As mentioned before, SMC complexes (i.e., condensin and cohesin) dictate the long-range architecture of chromatin during interphase and mitosis through their capacity to form DNA loops (Zhang et al., 2019; Yatskevich et al., 2019; Davidson & Peters, 2021).

Although the loop extrusion process is thought to allow the ordered folding of intracellular DNA, another possible outcome of this process is that it could push any entanglement towards the outside of the growing loop. Therefore, if an entanglement becomes constricted in a small domain, it would easily be removed by topoisomerase II (Figure 27C). In this respect, computer simulations have demonstrated that the synergy of DNA loop extrusion activity with topoisomerase II could remove most of the interlinks and knots that are generated during the topological equilibration of intracellular DNA (Goloborodko, Marko, et al., 2016; Racko et al., 2018; Orlandini et al., 2019).

Since yeast cells carrying thermo-sensitive mutations to inactivate the SMC complexes are available, it was possible for our laboratory to test whether inactivation of condensin or cohesin would alter the  $P^{kn}$  of intracellular chromatin. These experiments will constitute the 3<sup>rd</sup> OBJECTIVE of the present thesis.



---

# Objectives

---



## **OBJECTIVES**

Find the mechanism that minimizes the entanglement of intracellular DNA.

1. Determine how intracellular DNA supercoiling correlates with DNA knotting probability.
2. Determine whether the intrinsic capacity of topoisomerase II to simplify the topology of DNA in vitro affects the knotting probability of chromatin in vivo.
3. Determine whether the activity of SMC complexes, such as condensin and cohesin, affects the knotting probability of chromatin in vivo.



---

# Publications

---



## PUBLICATIONS

### THESIS SUPERVISOR REPORT

#### ARTICLE #1

##### **DNA knots occur in intracellular chromatin**

Antonio Valdés, Joana Segura, Sílvia Dyson, Belén Martínez-García and Joaquim Roca\*

**Nucleic Acids Res.** Vol 48 n2, pages 650-660 (2018)

DOI: <https://doi.org/10.1093/nar/gkx1137>

Journal Impact IF 2018 : 11.2

This article is the first report of the existence of DNA knots in eukaryotic chromatin. Intriguingly, the results uncovered that some mechanism is minimizing the knotting probability of intracellular DNA. Therefore, this study establishes the starting point of the present thesis, which is to uncover such mechanism. Most results of this study were included in the doctoral thesis of Antonio Valdés, a former student in the laboratory and first author of the article. Sílvia Dyson contributed to this work by running samples of DNA knots in 2D gels and helping in the characterization of DNA knots during different stages of the cell cycle.

#### ARTICLE #2

##### **Transcriptional supercoiling boosts topoisomerase II-mediated knotting of intracellular DNA**

Antonio Valdés, Lucia Coronel, Belén Martínez-García, Joana Segura, Sílvia Dyson, Ofelia Díaz-Ingelmo, Cristian Micheletti, and Joaquim Roca\*

**Nucleic Acids Res.** Vol 47, n13, pages 6946–6955 (2019)

DOI: <https://doi.org/10.1093/nar/gkz491>

Journal Impact IF 2019: 11.5

This article demonstrates that positive supercoiling of intracellular DNA concurs with an increase of DNA knot formation. This finding was reported in the doctoral thesis of

## Publications

Antonio Valdés, a former student in the laboratory and first author of the article. Sílvia Dyson contributed to this work by helping in the characterization of DNA knots and by examining the effect of negative DNA supercoiling in DNA knot formation. She found that negative supercoiling does not have any significant effect. Therefore, this study discards DNA supercoiling as the mechanism that minimizes knot formation (objective 1 of the thesis).

### ARTICLE #3

#### **Condensin minimizes topoisomerase II-mediated entanglements of DNA *in vivo***

Sílvia Dyson, Joana Segura, Belén Martínez-García, Antonio Valdés, and Joaquim Roca\*

**The EMBO Journal** 40:e105393 (2021)

DOI: <http://dx.doi.org/10.15252/embj.2020105393>

Journal Impact IF 2019: 9.9

The experiments published in this article addressed the objectives 2 and 3 of this thesis. The results indicate that the intrinsic capacity of topoisomerase II to simplify the equilibrium topology of naked DNA *in vitro* does not affect the knotting probability of intracellular DNA (objective 2); and that, whereas inactivation of cohesin decreases knot formation, inactivation of condensin markedly increases it and restores the expected linear correlation between DNA knot formation and chromatin length (objective 3). These findings strongly suggest that loop extrusion activity of condensin is the main mechanism that minimizes the entanglement of intracellular DNA.

Sílvia Dyson is the first author of this article since she designed and conducted most of the reported experiments and analyzed the significance of the results. She also contributed to the writing of the manuscript.



Joaquim Roca Bosch

Thesis Supervisor



---

# Article #1

---



# DNA knots occur in intracellular chromatin

Antonio Valdés, Joana Segura, Sílvia Dyson, Belén Martínez-García and Joaquim Roca\*

Molecular Biology Institute of Barcelona (IBMB); Spanish National Research Council (CSIC); Barcelona 08028; Spain

Received August 25, 2017; Revised October 24, 2017; Editorial Decision October 26, 2017; Accepted October 28, 2017

## ABSTRACT

**In vivo DNA molecules are narrowly folded within chromatin fibers and self-interacting chromatin domains. Therefore, intra-molecular DNA entanglements (knots) might occur via DNA strand passage activity of topoisomerase II. Here, we assessed the presence of such DNA knots in a variety of yeast circular minichromosomes. We found that small steady state fractions of DNA knots are common in intracellular chromatin. These knots occur irrespective of DNA replication and cell proliferation, though their abundance is reduced during DNA transcription. We found also that *in vivo* DNA knotting probability does not scale proportionately with chromatin length: it reaches a value of  $\sim 0.025$  in domains of  $\sim 20$  nucleosomes but tends to level off in longer chromatin fibers. These figures suggest that, while high flexibility of nucleosomal fibers and clustering of nearby nucleosomes facilitate DNA knotting locally, some mechanism minimizes the scaling of DNA knot formation throughout intracellular chromatin. We postulate that regulation of topoisomerase II activity and the fractal architecture of chromatin might be crucial to prevent a potentially massive and harmful self-entanglement of DNA molecules *in vivo*.**

## INTRODUCTION

DNA topoisomerases are nature's solution for removing the DNA entanglements that occur during the genome transactions. In particular, the type-2A topoisomerases bacterial topo IV and eukaryotic topo II use ATP to catalyze the passage of one segment of duplex DNA through an enzyme-mediated transient double-strand break in another (1). By this mechanism, inter-molecular passage of DNA segments leads to the catenation or decatenation of different DNA molecules, whereas intra-molecular DNA passage leads to change the number of DNA supercoils within a topological domain (1). The activity of topo IV and topo II is essential for chromosome replication and segregation, during which they remove the intertwinings between the newly replicated DNA molecules (2,3). Type-2A enzymes are also necessary for the normal progression of DNA replication and tran-

scription, during which they relax the positive DNA supercoils generated ahead of the DNA and RNA polymerases (2,3).

Another possible outcome of the type-2A topoisomerase activity is that intra-molecular DNA passage can lead to the formation or removal of DNA knots (4). *In vitro* studies had shown that type-2A enzymes produce abundant and complex DNA knots when juxtaposition of intra-molecular DNA segments is enhanced by DNA supercoiling, protein–DNA interactions or other DNA condensing agents (5–7). In turn, when knotted DNA molecules are naked in free solution, topo IV and topo II unknot them efficiently and are able to reduce the fractions of knotted molecules to values below than those corresponding to the thermodynamic equilibrium (8).

Whereas the implication of type-2A topoisomerases in the modulation of DNA supercoiling and in the resolution of intertwinings between the newly replicated DNA molecules has been widely studied, little is known about their DNA knotting-unknotting activity *in vivo*. Indeed, the occurrence of DNA knots has been scarcely documented in living cells. In the context of bacteria, DNA knots have been found to accumulate in plasmids hosted in *Escherichia coli* strains that harbor mutations in topoisomerase genes (9,10). DNA knot formation has also been observed in replication bubbles of bacterial plasmids when replication forks are stalled (11,12). These knots are produced and eventually removed by the activity of topo IV (13,14). In the case of eukaryotes, to the best of our knowledge the occurrence of DNA knots has not been reported to date. In this regard, *in vitro* experiments had shown that DNA knots interfere with chromatin assembly and DNA transcription (15,16). Thus, a general assumption is that eukaryotic DNA is virtually knot-free. Consistent with this view, genome-wide analyses of chromosome architecture show little topological complexity (knotting or inter-linking) between the self-interacting domains (TADs) of eukaryotic chromatin (17,18). However, these experimental approaches have a resolution of tens to hundreds of DNA kilobases and are unable to discern whether intracellular DNA is entangled in shorter length scales. In that respect, computer simulations of polymer physics predict a high knotting probability when DNA molecules are condensed or confined in reduced volumes (19–21). Consequently, the occurrence of knots in chromatinized DNA could be significant within short length scales

\*To whom correspondence should be addressed. Tel: +34 934020117; Email: joaquim.roca@ibmb.csic.es

given the high concentration of DNA segments packaged within chromatin fibers and the abundant topo II activity that can pass such DNA segments through each other.

Here, we present the first evidence and analysis of the occurrence of DNA knots in eukaryotic chromatin. To this end, we used high resolution two-dimensional electrophoresis to assess the presence of DNA knots in yeast circular minichromosomes of distinct size and genetic configuration. We examined the relation of knot formation with DNA replication and transcription, and measured the dependence of DNA knotting probability on the size of the minichromosomes. We show that steady-state fractions of DNA knots are common in eukaryotic chromatin. This experimental finding sheds new light on the configuration and dynamics of nucleosomal fibers *in vivo*. We show also that the occurrence of DNA knots does not scale proportionally to the length of the nucleosomal fibers. This observation denotes the existence of a crucial mechanism that prevents the massive entanglement of intracellular DNA.

## MATERIALS AND METHODS

### Yeast strains, circular minichromosomes and knotted plasmids

Experiments were conducted with the *Saccharomyces cerevisiae* strain FY251 (S288C genetic background *MATa his3-D200 leu2-D1 trp1-D63 ura3-52*) and its derivatives. The  $\Delta top1$  deletion mutant and the thermo-sensitive *top2-4* mutant were obtained as described previously (22). Minichromosomes YRp3, YRp4, YRp401, YEp24, YCp50, YEp13 and YRp21 (Supplementary Figure S1) were amplified and purified as bacterial plasmids from *Escherichia coli*. Minichromosomes YRp1 and YRp2, which lack bacterial sequences, were constructed by circularization of linear DNA fragments. Monomeric forms of plasmids and DNA circles were gel-purified to transform yeast following standard procedures. Production of DNA knots *in vitro* was done by reacting purified bacterial plasmids with molar excess of topo II as described in Supplementary Figure S2.

### Yeast culture and DNA extraction

Yeast cells were grown at 26°C in yeast synthetic media containing adequate dropout supplements and 2% glucose. Liquid cultures were monitored by optical density and flow cytometry for DNA content. *pGALI* promoter was activated or repressed by transferring sedimented cells into YP Broth media containing 2% galactose or 2% glucose, respectively. Before harvesting yeast cells, the DNA topology of circular minichromosomes was fixed *in vivo* as described previously (23) by quickly mixing the liquid cultures with one cold volume (−20°C) of ETol solution (ethanol 95%, 28 mM Toluene, 20 mM Tris–HCl pH 8.8, 5 mM EDTA). Fixed cells from a 25 ml culture were sedimented, washed twice with water, resuspended in 400  $\mu$ l of TE (10 mM Tris HCl pH 8.8, 1 mM EDTA) and transferred to a 1.5-ml microfuge tube containing 400  $\mu$ l of phenol and 400  $\mu$ l of acid-washed glass beads (425–600  $\mu$ m, Sigma). Mechanic lysis of >80% cells was achieved by shaking the tubes in a FastPrep<sup>®</sup> apparatus for 10 s at power 5. The aqueous

phase of the cell lysates was collected, extracted with chloroform, precipitated with ethanol, and dissolved in 100  $\mu$ l of TE containing RNase-A. Following 10 min incubation at 37°C, ammonium acetate was added to 0.5 M and DNA was precipitated with ethanol. Each DNA sample was dissolved in 50  $\mu$ l of TE.

### DNA electrophoresis

To observe the *Lk* distribution of the minichromosomes, 10  $\mu$ l of each DNA sample was electrophoresed in a two-dimensional agarose gel in TBE buffer (89 mM Tris-borate, 2m M EDTA) containing 0.6  $\mu$ g/ml chloroquine in the first dimension and 3  $\mu$ g/ml chloroquine in the second dimension. To observe the knot species present in the minichromosomes, 40  $\mu$ l of each DNA sample was reacted with nicking endonuclease BstNB1 (NEB). Serial dilutions of the nicked DNA samples were electrophoresed in two-dimensional agarose gel in TBE buffer and run at low and high voltage as described previously (24). Electrophoresis settings (agarose concentration, voltage and running time) were adjusted to the size of each minichromosome and are specified in Supplementary Table S1. Gels were blot-transferred to a nylon membrane and probed with minichromosome-specific DNA sequences labeled with AlkPhos Direct (GE Healthcare<sup>®</sup>) or radio-labeled with <sup>32</sup>P. Probe signals of increasing exposure periods were recorded on X-ray films and by phosphorimaging.

### DNA topology and numerical analyses

*Lk* distributions were analyzed as described previously (23).  $\Delta Lk$  was calculated by counting the number of *Lk* topoisomers spanning from the center of the interrogated *Lk* distribution to the center of the *Lk* distribution of relaxed DNA. Individual knot populations were quantified by using the ImageJ software on non-saturated signals obtained with serial dilutions (1, 0.1, 0.01, 0.001) of DNA samples loaded in the 2D gels. The relative abundance of individual knot populations was calculated with respect to total amount of unknotted and knotted DNA circles. The graph that correlates knot complexity and the persistence length ( $P_L$ ) of a thin chain was generated with the data of Frank-Kamenetskii *et al.* (25). Using these data, the relative abundance of knots of more than three crossings ( $Kn > 3$ ) was plotted as a function of the  $P_L$  (nm) of a chain of contour length 380 nm. The graph that correlates knot probability with the  $P_L$  and effective diameter  $d_E$  of a simulated chain was generated with the data of Rybenkov *et al.* (26), which described that the probability  $K^P$  of a knot of  $n$  statistical Kuhn lengths (*Kuhn length* =  $2 \cdot P_L$ ) and diameter  $d$  is given by the empirical equation  $K^P(n, d) = K^P(n, d \text{ zero}) \exp(-r \cdot d/b)$ , where  $b$  is the Kuhn length and  $r$  depends on the knot type and equals 22 for knot  $3_1$ . Corresponding  $P_L$  and  $d_E$  values were determined for a chain of contour length 380 nm that produced the  $3_1$  knot with a probability of 0.017 (like minichromosome YRp4).

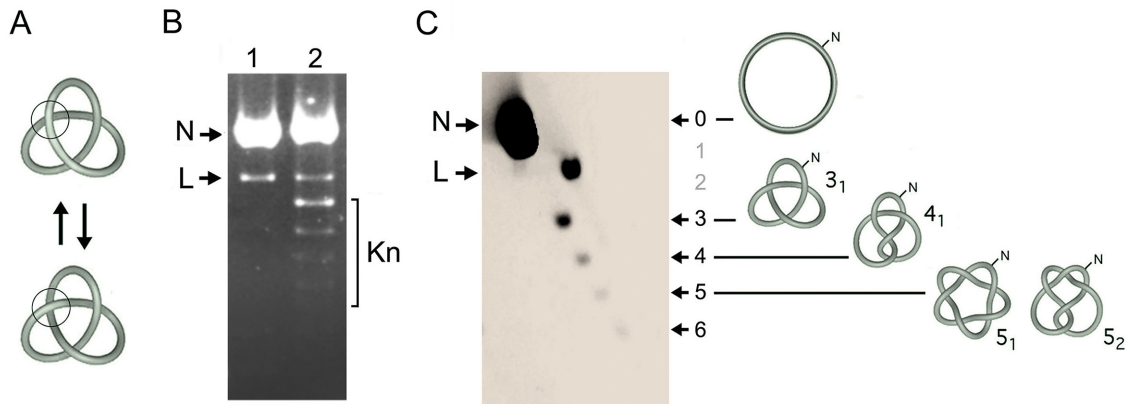


**Figure 1.** Identification of DNA knot species by 2D gel electrophoresis. (A) Interconversion of the unknotted (top) and knotted (bottom) forms of a double-stranded DNA circle by the DNA passage activity of topo II (ball). (B) The agarose gel shows a 4.4 kb DNA plasmid before (lane 1) and after incubation with an excess of topo II to favor knot formation (lane 2). Before loading the gel, plasmid samples were nicked with a site-specific endonuclease to eliminate DNA supercoils. N, unknotted nicked circles. L, linearized DNA. Kn, knotted nicked circles. (C) The previous sample of lane 2 was examined in a 2D agarose gel electrophoresis. The first gel dimension (top to bottom at low voltage) separated knot species by their irreducible number DNA crossings, Kn, indicated as 3, 4, 5, 6. The position corresponding to 0 crossings (un-knotted ring or trivial knot) and the two empty slots corresponding to 1 and 2 crossings are indicated. The second gel dimension (left to right at high voltage) segregated the ladder of knot forms from the linear DNA molecules (L), which acquired higher gel velocity. Illustrations depict ideal shapes of the un-knotted nicked ring, the knot of three crossings (trefoil knot or  $3_1$ ), four crossing ( $4_1$ ), and the two knots of five crossings ( $5_1$  and  $5_2$ ). The 2D-gel electrophoresis was conducted, blotted and probed as described in the methods and Supplementary Table S1.

## RESULTS

### Electrophoretic characterization of knotted DNA

The DNA passage activity of topo II in a circular molecule of double-stranded DNA can result in the inversion of supercoil crossings but also in the formation or removal of DNA knots (Figure 1A). When the resulting DNA molecules are nicked, their helical tension (supercoiling) dissipates because the duplex can swivel around the un-cleaved strand. However, the knots remain entrapped in the circular molecule. Since nicked DNA rings containing a knot are more compacted than the unknotted nicked circles, these forms have different velocities during agarose gel electrophoresis (Figure 1B). However, identification of knotted nicked DNA circles in one-dimensional gels can be ambiguous because they overlap with linear DNA fragments. This overlying can completely mask knotted molecules in DNA samples that contain abundant fragments of genomic DNA (i.e. whole cell extracts). This problem is solved by running a high resolution two-dimensional (2D) gel electrophoresis (Figure 1C). In the first gel-dimension, which is done at low voltage, knotted molecules have a gel velocity that correlates about linearly to knot complexity (i.e. the irreducible number of DNA crossings in a knot, Kn) (27). Accordingly, relative to the position of the unknotted circle that has zero crossings (trivial knot), positions corresponding to one and two crossings are empty because the simplest knot that has three crossings (trefoil knot or  $3_1$ ) (Figure 1C). Knot populations of increasing complexity form then a ladder that begins with  $3_1$  followed by the knot with four crossing ( $4_1$ ), two knots with five crossings ( $5_1$  and  $5_2$ ), and so on (Figure 1C). In the second gel-dimension, the gel is turned in orthogonal direction and electrophoresis is done at high voltage. In these conditions, the ladder of knotted molecules is retarded relative to the diagonal of linear DNA fragments

(L) (24), thereby allowing unambiguous identification and quantification of individual knot populations (Figure 1C).

### DNA knots occur in eukaryotic chromatin

In order to examine the occurrence of DNA knots *in vivo*, we used yeast cells that hosted a variety of circular minichromosomes (Supplementary Figure S1). We grew the cells to exponential phase and fixed them quickly with a cold ethanol-toluene solution. As described in previous studies (23), this fixation step inactivates the cellular topoisomerases and precludes plausible alterations of the DNA topology of the minichromosomes during DNA extraction and subsequent manipulations. We loaded one part of the DNA sample in a 2D gel containing chloroquine in order to examine the DNA linking number (Lk) of the minichromosomes. We enzymatically nicked the remaining DNA sample and loaded it in a 2D gel of low-high voltage to test the presence of DNA knots. Figure 2 shows the results obtained with cells containing the replicative minichromosome YRp4 (4.4 kb). This minichromosome presented a Gaussian distribution of Lk values *in vivo*, which denoted the absence of subpopulations with unconstrained positive or negative DNA supercoiling. Comparison of the Lk distribution of YRp4 *in vivo* with that of the relaxed DNA *in vitro* indicated that the minichromosome has a Lk difference ( $\Delta Lk$ ) of about  $-22$  (Figure 2A). As indicated in previous studies (28), this  $\Delta Lk$  value was consistent with the stabilization of about one negative supercoil ( $\Delta Lk \approx -1$ ) per nucleosome (29) and the presence of 22 nucleosomes since the nucleosomal density of yeast chromatin is about 1 nucleosome/200 base pairs (30). Upon nicking the YRp4 DNA, all the supercoils were eliminated and the presence of knots was revealed (Figure 2B). A prominent knot  $3_1$  was followed by a monotonic ladder of knot species of increasing complexity. Knots with more than eight DNA



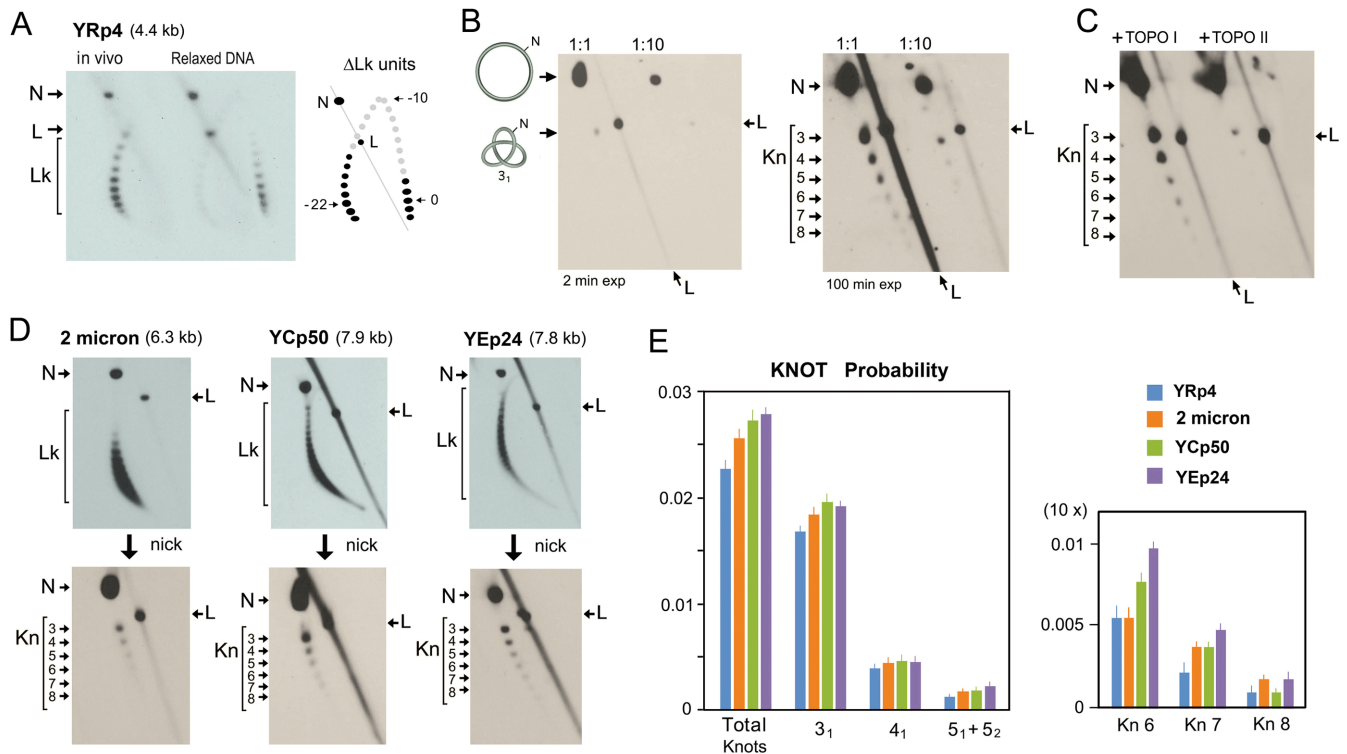


**Figure 2.** Yeast minichromosomes contain complex DNA knots. (A) Typical 2D gel electrophoresis of covalently closed DNA in presence of chloroquine, which displays the DNA linking number (Lk) distribution of the YRp4 minichromosome *in vivo* and of the YRp4 DNA relaxed *in vitro*. The Lk difference was calculated as the distance ( $\Delta$ Lk units) between the center of both Lk distributions across the arch of individual Lk topoisomers. (B) The *in vivo* DNA sample of YRp4 was enzymatically nicked and loaded in a 2D gel for analysis of DNA knotting. Gel lanes show 1:1 and 1:10 dilutions of the sample. Left and right panels show, respectively, short (2 min) and long exposures (100 min) of the gel-blot. (C) Result of the incubation of the nicked DNA sample of YRp4 with yeast topoisomerase I (TOPO I) and yeast topoisomerase II (TOPO II). (D) Lk distributions and knots species of the yeast 2-micron plasmid, YCp50 and Yep24 minichromosomes. The 2D gels in A-D were conducted, blotted and probed as described in the methods and Supplementary Table S1. The signals of nicked unknotted circles (N), linear DNA (L), Lk distributions (Lk) and knot populations with different irreducible number DNA crossings, Kn, (3–8) are indicated. (E) Total DNA knot probability and of knots  $3_1$ ,  $4_1$ ,  $5_1+5_2$ , and knot species of 6 to 8 crossings (Kn6, Kn7, Kn8) in the indicated yeast minichromosomes. The plots show the mean and  $\pm$ SD of three experiments.

crossings were discernible after long-exposure of the 2D gel-blot (Figure 2B). We corroborated that this ladder was formed by knotted double-stranded DNA circles because it was reduced when we reacted the DNA sample with topo II (Figure 2C). However, no change was produced when we treated the sample with topo I (Figure 2C). We conducted analogous experiments to that of YRp4 with other yeast minichromosomes (Supplementary Figure S1), such as the yeast endogenous 2-micron plasmid (6.3 kb), the episomal plasmid YEp24 (7.8 kb) and the centromeric plasmid YCp50 (7.9 kb) (Figure 2D). We found that all these minichromosomes had a DNA knotting probability ( $k^P_{CHR}$ ) comparable to that of YRp4 ( $k^P_{CHR}$  between 0.02 and 0.03) and presented similar patterns of knot complexity (Figure 2E).

### Chromatin knots are not a byproduct of DNA replication

Minichromosomes YRp4, YEp24, YCp50 and the endogenous 2-micron plasmid differ in copy number and have distinct DNA replication origins and DNA transcription units (Supplementary Figure S1). The observation that they all presented similar DNA knotting probability and complexity suggested that knot formation was not related to DNA

transactions (i.e. replication and transcription) or the presence of specific chromatin elements (i.e. centromeres). Consistent with this, we found that the  $k^P_{CHR}$  values were not meaningfully altered when yeast cultures passed from exponential growth to stationary phase and quiescence (Figure 3A). Accordingly,  $k^P_{CHR}$  values did not correlate with the relative abundance of DNA replicating cells (Figure 3B). We next examined knot formation in yeast topoisomerase mutants. Knotted fractions did not present significant changes in cells lacking topo I ( $\Delta top1$ ) or in cells with reduced topo II activity (*top2-ts*) (Figure 3C and D). Upon thermal inactivation of topo II, dimeric catenanes of newly replicated minichromosomes accumulated. These replication catenanes migrated as compacted structures in the 2D gels used for Lk analysis (Figure 3D). After nicking the DNA, these catenanes produced a ladder of species that differed in the number of catenation links (Figure 3D). Even in this condition, the fraction of knotted molecules was not significantly altered, thereby corroborating that the knots observed were not a byproduct of DNA replication (Figure 3E).

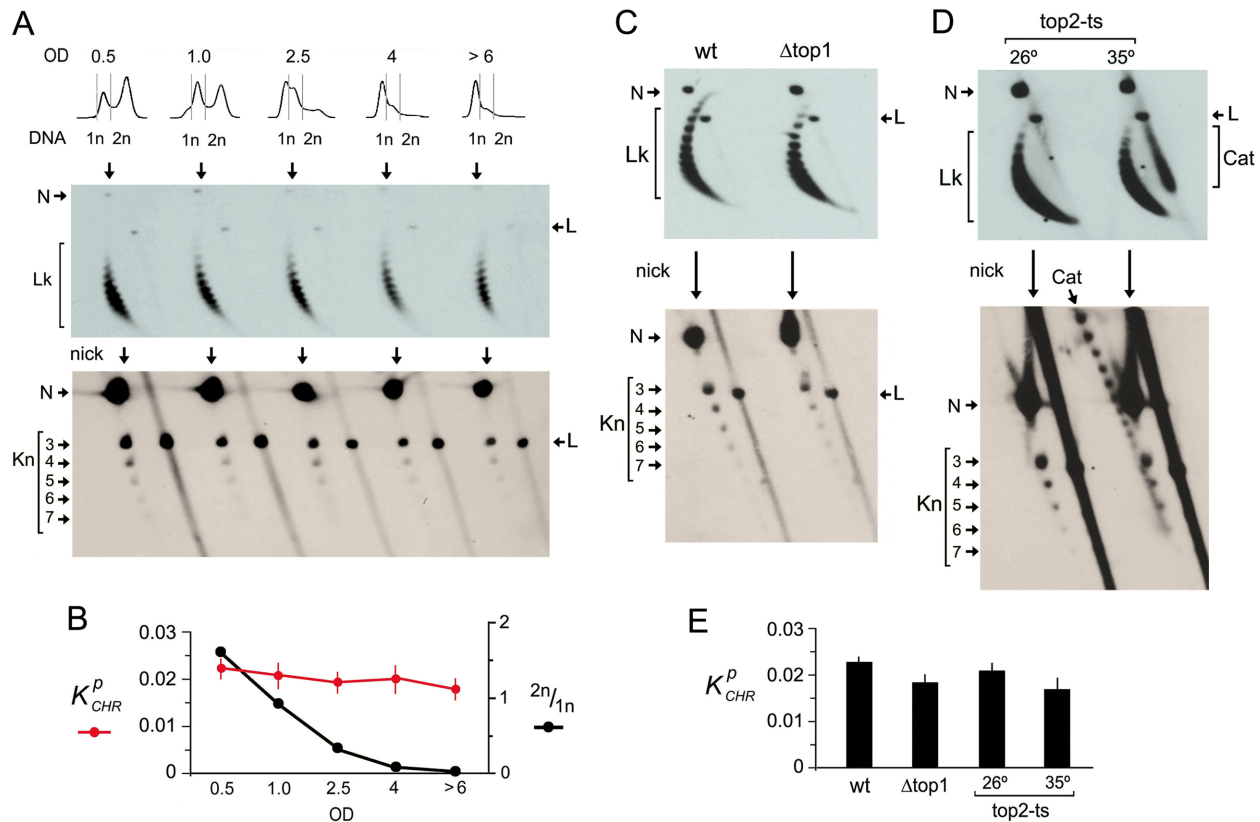


**Figure 3.** Chromatin knots occur irrespective of cell proliferation and DNA replication. (A) Cells containing the YRp4 minichromosome were sampled during exponential growth (OD 0.5 and 1.0), during the shift to stationary phase (OD 2.5 and 4) and during the quiescent stage (OD > 6). The cellular DNA content (1n, 2n), the *Lk* distribution and the knot species of YRp4 present in each sample are shown. (B) Comparison of  $k_{CHR}^P$  values and the abundance of replicating cells ( $2n/1n$ ) (mean and  $\pm$ SD of three experiments). (C and D) *Lk* distribution and knot species of YRp4 present in *wt* cells,  $\Delta top1$  mutants and *top2-ts* mutants before (26°C) and after thermal inactivation of topoisomerase II (35°C during 2 h). The 2D-gel electrophoreses in A, C and D were run, blotted and probed as described in the methods and Supplementary Table S1. Gel signals are annotated as described in Figure 2. Position of un-nicked and nicked replication catenanes (Cat) are indicated in the gels for *Lk* analysis and knot analysis, respectively. (E)  $k_{CHR}^P$  values (mean and  $\pm$ SD of three experiments) in *wt* cells,  $\Delta top1$  mutants and *top2-ts* mutants.

### Steady state fractions of knots are maintained by topoisomerase II

The above results suggested that the DNA knotting probability of yeast minichromosomes reflected a general property of the *in vivo* chromatin structure. We envisaged that the occurrence of knots could be then altered by enforcing a structural change in a whole population of minichromosomes. To test this notion, we used the minichromosome YRp401 (8.1 kb), which carries the sugar-regulatable *pGAL1* promoter on a reporter *LacZ* gene (Supplementary Figure S1). We examined knot formation in YRp401 before and after the induction of high rates of DNA transcription (Figure 4). When *pGAL1* was repressed in glucose-containing media, YRp401 had a  $k_{CHR}^P$  of 0.027, a knotting probability comparable to that of the endogenous 2-micron circle present in the same cells. However, when the *pGAL1* promoter was activated in galactose-containing media, the  $k_{CHR}^P$  of YRp401 was reduced about four-fold, and when transcription was repressed again in glucose-containing media, the initial  $k_{CHR}^P$  value of this minichromosome was recovered. We next questioned whether this unknotting and re-knotting process was mediated by topo II activity. We therefore repeated the same experiment in

the *top2-ts* mutant strain, in which we inhibited topo II before activating *pGAL1* (Figure 4). In this condition, transcription of the *LacZ* gene was similarly induced and repressed, as denoted by  $\beta$ -galactosidase activity. However, the unknotting and re-knotting process did not occur. These observations indicated that the formation and resolution of the DNA knots is a dynamic process that relies on the DNA-strand passage activity of topo II and that steady-state fractions of knots reflect a general trait of chromatin conformation *in vivo*.

### DNA knot formation does not increase proportionally to chromatin length

Computer simulations had predicted that the knotting probability of a random chain increases proportionally to the chain length (25). Subsequent *in vitro* experiments corroborated that the knotting probability of DNA during the circularization of linear DNA molecules in free solution increases proportionally to their length (26,31). We have observed that a similar length dependence appears also when DNA plasmids of different sizes are knotted by treating them with a molar excess of topo II *in vitro* (Supplementary Figure S2). In this regard, we noticed that such length

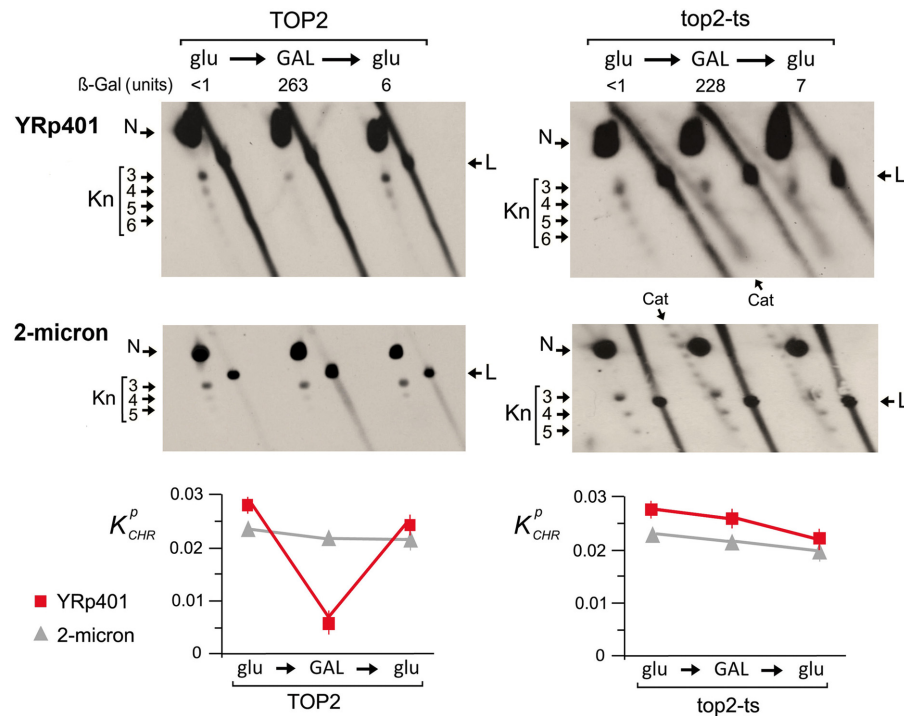


**Figure 4.** Chromatin knots are removed and reformed by topoisomerase II. The 2D gels compare knot formation in the YRp401 minichromosome, which carries pGAL1:LacZ. Experiments were conducted in *TOP2* and *top2-ts* yeast cells, and the knots produced in YRp401 were contrasted with the knots produced in the endogenous 2-micron plasmid. Yeast cultures were sampled during exponential growth at 26°C in glucose-containing media (glu), after shifting them 3 h at 35°C in galactose-containing media (GAL), and after 3 h back in glucose-containing media (glu). Lac Z transcription was monitored by the  $\beta$ -galactosidase activity of cell lysates. The 2D-gel electrophoreses were run, blotted and probed as described in the methods and Supplementary Table S1. Gel signals are annotated as described in Figures 2 and 3. The plots show mean mean and  $\pm$ SD of  $k_{CHR}^P$  of the YRp401 minichromosome and the 2-micron plasmid in two experiments.

dependence did not occur *in vivo* with the minichromosomes between 4.4 and 7.9 kb, since they all presented similar  $k_{CHR}^P$  values (Figure 2E). Thus, we measured  $k_{CHR}^P$  in a broader range of minichromosome sizes (Supplementary Figure S1). On the one hand, the episomal YEp13 (10.7 kb) and the replicative YRp21 (11.7 kb) presented a  $k_{CHR}^P$  of  $\sim 0.028$  (Figure 5A). This value was still comparable to that of minichromosomes of half their length. Regarding knot complexity, YEp13 and YRp21 showed a monotonic ladder of prime knots (i.e. indecomposable knots) alike the minichromosomes between 4.4 to 7.9 kb. However, YEp13 and YRp21 presented additional composite knots (i.e.  $3_1+3_1$  and  $3_1+4_1$ ), which we could not detect in shorter constructs. These composite knots migrated according to their minimal number of crossings in the first dimension, but moved faster than prime knots in the second dimension (Figure 5A). On the other hand, the  $k_{CHR}^P$  values dropped sharply in minichromosomes of size  $< 4$  kb (Figure 5B). Minichromosomes YRp3 (3.2 kb) and YRp2 (2 kb) had a  $k_{CHR}^P$  of 0.015 and 0.005, respectively. Their knot complexity was also reduced. We distinguished knot species of up to seven crossings in YRp3, but we detected just the knot  $3_1$  in YRp2. Finally, we did not find any trace of knot formation in YRp1 (1.4 kb), a well characterized minichromosome that results from the circularization of the genomic *TRPIARSI* segment of yeast and contains only seven nucleosomes (32). Therefore,  $k_{CHR}^P$  appeared to scale quickly in the minichromosomes of length up to about 4 kb. How-

ever, above this length, the slope of  $k_{CHR}^P$  was reduced  $\sim 5$ -fold such that knot formation barely increased from 4 to 12 kb (Figure 5C). The probability of individual knot species analyzed is specified in Supplementary Table S2.

## DISCUSSION

Our study provides the first evidence of the formation of DNA knots in eukaryotic cells. The results revealed that small amounts of DNA knots are present *in vivo* regardless of structural and functional elements of chromatin. These knots happen irrespective of DNA replication and cell proliferation, though their abundance is transiently reduced during DNA transcription in a topo II dependent manner. All together, these observations strongly suggest that steady state fractions of DNA knots produced by topo II are common in eukaryotic chromatin. This finding is not surprising when considering the high concentration of DNA segments within chromatin fibers and the abundant topo II activity that can potentially pass these segments through each other. Alternatively, DNA knots could be generated via intra-molecular DNA recombination. However, recombination events occur usually within specific DNA sequences, produce DNA insertions or deletions, and create distinctive populations of knot types (33–35). If the DNA knots uncovered here are consequent to random DNA passage activity of topo II, they should reflect biophysical and conformational properties of chromatin *in vivo*, as we discuss below.



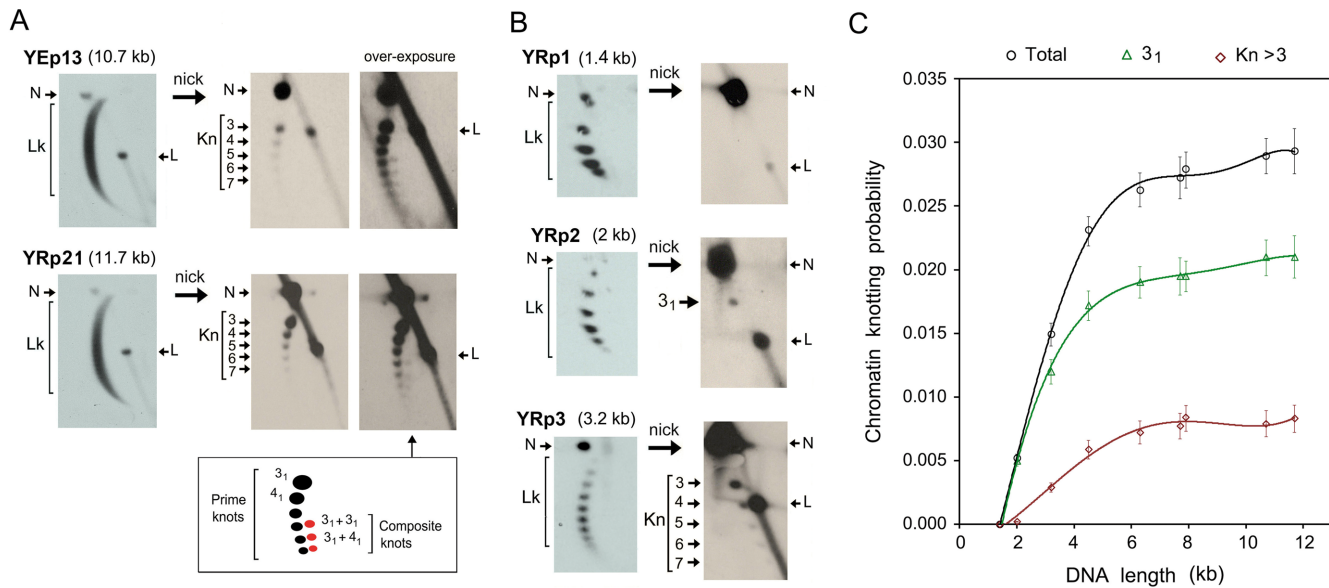


**Figure 5.** Dependence of DNA knotting probability on chromatin length. (A) Lk distributions and knotted forms of the minichromosomes YEpl3 (10.7 kb) and YRp21 (11.7 kb). Over-exposure of the gel-blots shows composite knots of six nodes ( $3_1 + 3_1$ ) and of seven nodes ( $3_1 + 4_1$ ). (B) Lk distributions and knotted forms of the minichromosomes YRp1 (1.4 kb), YRp2 (2 kb) and YRp3 (3.2 kb). The 2D-gel electrophoreses in A and B were run, blotted and probed as described in the methods and Supplementary Table S1. Gel signals are annotated as described in Figure 2. (C) DNA knotting probability of yeast minichromosomes in the size range 1.4–11.7 kb. The plot shows the probability (mean and  $\pm$ SD of three experiments) of all knot species (Total), the trefoil knot ( $3_1$ ) and knots with more than three irreducible nodes ( $\text{Kn} > 3$ ).

The probability of DNA knot formation in eukaryotic chromatin ( $k^P_{CHR}$ ) reported here contrasts markedly with the knotting probability of DNA during the circularization of linear DNA molecules in free solution ( $k^P_{DNA}$ ) (Figure 6A). The value of  $k^P_{DNA}$  increases proportionally to the DNA length and has a slope that depends on the duplex flexibility and its effective diameter (26,31). The DNA flexibility is denoted by its persistence length ( $P_L$ ), which is about 50 nm (36). The DNA effective diameter ( $d_E$ ) depends on the ionic environment and it was calculated to be about 5 nm in physiological salt concentrations (26,31). Our study shows that, up to a minichromosome size of about 4 kb,  $k^P_{CHR}$  increases with a slope higher than that of  $k^P_{DNA}$  and that, above this size, the slope of  $k^P_{CHR}$  is abruptly reduced. These differences were more noteworthy when we plotted  $k^P_{CHR}$  against the actual contour length of the minichromosomes, which equals to the sum of inter-nucleosomal DNA segments (Figure 6A).

The simplest interpretation of the sharp slope of  $k^P_{CHR}$  values is that juxtaposition of intramolecular DNA segments *in vivo* is much higher than in DNA in free solution and, consequently, the probability of knot formation upon topo II-mediated DNA passage. Since juxtaposition of intramolecular DNA segments can be promoted by DNA supercoiling, some studies have already tackled the effects of supercoiling on knot formation and resolution. On the one side, several *in vitro* experiments with bacterial plasmids had revealed that DNA supercoils enhance DNA knotting by type-2 topoisomerases (5–7). On the other side, computer simulations had led to the proposal that DNA supercoiling could tighten existing DNA knots and facilitate their removal (37). However, the Lk distributions of the minichromosomes analyzed in our study showed no evidence of un-

constrained supercoils that could promote DNA knot formation or resolution *in vivo*. Therefore, we excluded a significant role of DNA supercoiling to explain the observed  $k^P_{CHR}$  values. A more plausible explanation is that juxtaposition of DNA segments is due to the high flexibility of nucleosomal fibers in comparison to naked DNA. In this respect, *in vivo* analyses of DNA looping (38) and single particle tracking (39) evidenced the high flexibility of nucleosomal fibers, its  $P_L$  being qualitatively estimated to be shorter than the DNA linker length (10–20 nm). Here, we determined the apparent  $P_L$  and  $d_E$  values of the nucleosomal fibers *in vivo* by comparing our  $k^P_{CHR}$  data with previous simulations of knot formation in random polymer chains (25,26,40). To this end, we had to assume that the minichromosome knots were produced by topo II-mediated random passage of DNA segments. By considering the knot complexity (Figure 6B) and the probability of the  $3_1$  knot (Figure 6C), we calculated that nucleosomal fibers *in vivo* have knotting probability similar to that of a thin random polymer chain with a  $P_L$  of 8 and 14 nm, respectively. Larger  $P_L$  values would imply a negative  $d_E$  value, as if DNA linker segments were strongly attracted instead of repelled by electrostatic potential. Conversely,  $d_E$  values approaching the physical thickness of DNA (2 nm) would imply extremely low  $P_L$  values (<3 nm), less than one turn of the double helix.

The high flexibility of nucleosomal fibers is mainly due to the adaptable angle between the entry and exit segments of the nucleosomal DNA, (41). In this respect, if DNA linker segments were to behave as nearly rigid sticks, another way to qualitatively interpret our  $k^P_{CHR}$  data is based on the minimum stick number to form a knot (42). This theory stabilizes that at least six self-avoiding sticks are required to

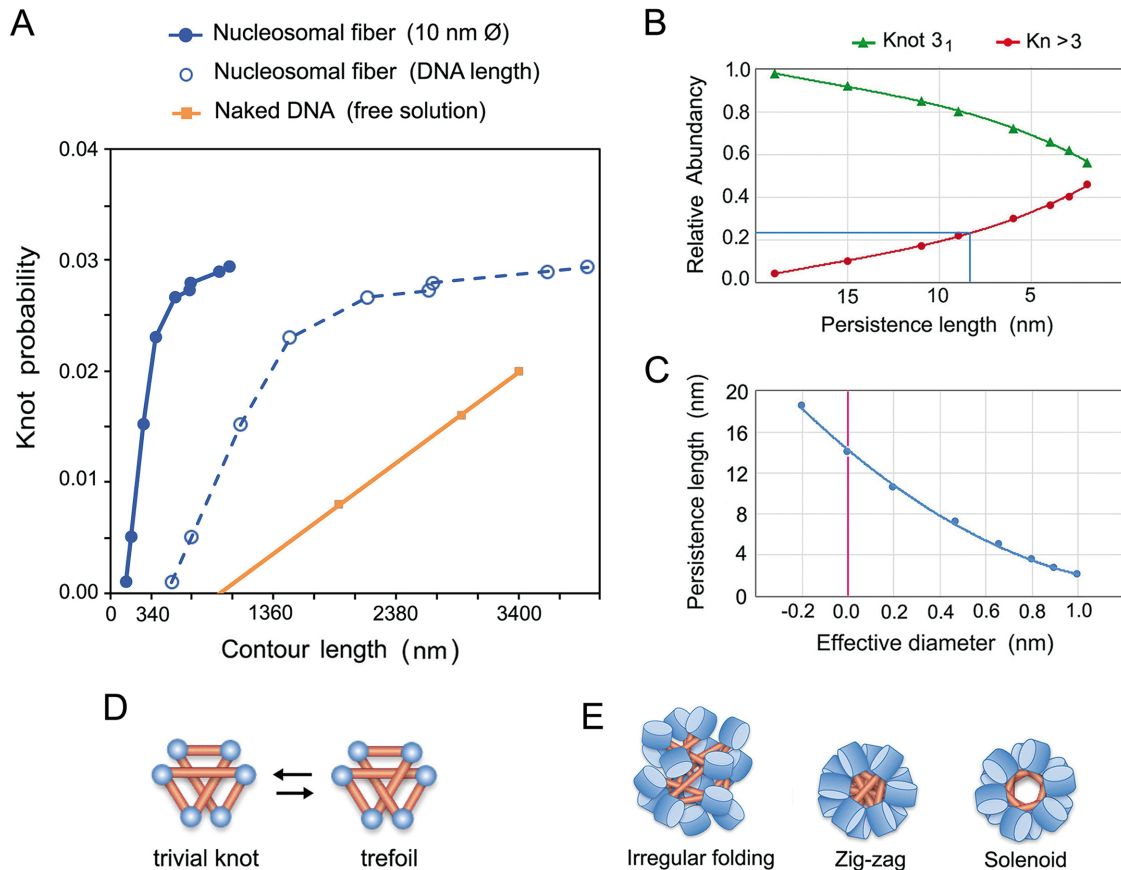


**Figure 6.** Properties of nucleosomal fibers deduced from DNA knot analysis. **(A)** Comparison of knotting probability of naked DNA in free solution (orange) with that of nucleosomal fibers (blue) as a function of their contour length (nm). Values of naked DNA are from previous studies (26,31). Values of chromatin are plotted against the total DNA length (dashed line) and against the length of a stretched 10 nm nucleosomal fiber (solid line). **(B)** Relative abundance of knot  $3_1$  and knots of more than three crossings ( $Kn > 3$ ) as a function of  $P_L$  of a thin chain that has contour length 380 nm (as minichromosome YRp4). **(C)**  $P_L$  and  $d_E$  values of a simulated chain with a contour length of 380 nm that would produce the knot  $3_1$  with a probability of 0.017 (as the minichromosome YRp4). **(D)** At least six self-avoiding sticks are required to conform the trefoil knot. **(E)** Juxtaposition of DNA linker segments in solenoid, zig-zag and irregular folding models of nucleosomal fibers.

conform the knot  $3_1$  (Figure 6D). This view could explain why we did not detect knots in the YRp1 minichromosome (1.4 kb), which has only seven nucleosomes, a stick number close to the theoretical minimum. However, the  $3_1$  knot was readily formed in the slightly larger YRp2 minichromosome (2 kb) and knots of up to seven crossings were produced in YRp3 (3.2 kb). Then, in terms of chromatin architecture, our  $k^P_{CHR}$  data support zig-zag or intricate folding models of the nucleosomal fiber (43,44), in which DNA linker segments cross each other with higher frequency than in solenoid packaging models (45) (Figure 6E). Finally, another indication that DNA knot formation might be facilitated by intricate clustering of nearby nucleosomes was the decrease of knot abundance induced by DNA transcription (Figure 4). During DNA transcription, chromatin locally unfolds and thereby the juxtaposition of intra-molecular DNA segments is reduced (46) (Figure 7 A). Other processes, such as DNA supercoiling waves and topoisomerase activities associated to DNA transcribing complexes, could also alter steady state fractions of DNA knots. Future research might determine in more detail the interplay between chromatin dynamics and DNA knot turnover.

The abrupt reduction of the  $k^P_{CHR}$  slope when the size of the minichromosomes surpassed 4 kb (about 20 nucleosomes) was striking but likely to have a strong biological relevance. Computer simulations (25), circularization of linear DNA molecules in free solution (26,31), and topo II-mediated knotting of DNA plasmids *in vitro* (Supplementary Figure S2) indicated that DNA knotting probability increases proportionally to the DNA length. Therefore, some mechanism prevents the high knotting probability of nucleosomal fibers to keep climbing as their length increases, which would produce a massive entanglement of intracellular DNA. One possibility is that this inflection is achieved via the topo II ability to simplify the equilibrium DNA topology (8). In this regard, previous *in vitro* studies indicated that topo II is less efficient in simplifying thermal supercoils when the contour length of DNA decreases (47). A similar length dependence could explain why intracellular topo II unknots more efficiently the large than the small minichromosomes. Other mechanisms might direct also the activity of topo II to prevent the scaling of DNA knot formation. In this respect, recent studies indicated that the torsional state of chromatinized DNA (48) and the activity of

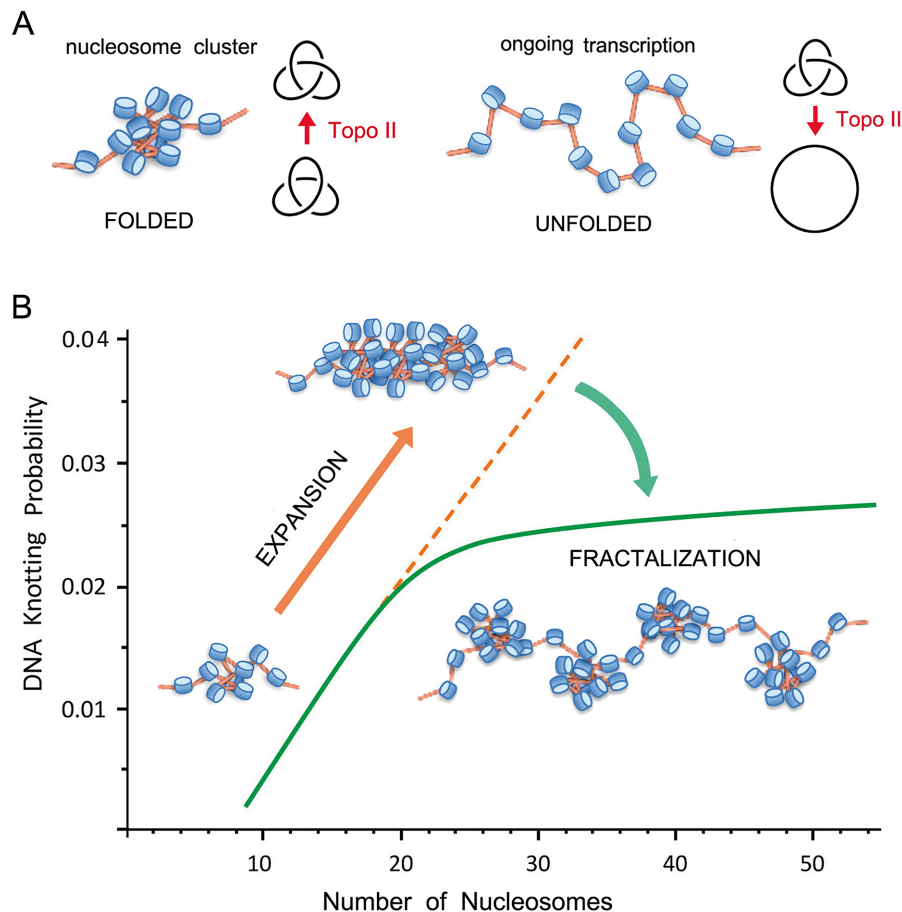


**Figure 7.** Model of chromatin architecture inferred from DNA knotting probability. (A) Intricate folding of nucleosome arrays favors topo II-mediated knotting of intracellular DNA. Knotted fractions are reduced when nucleosomal clusters unfold during DNA transcription. (B) Uninterrupted expansion of nucleosomal fibers would produce proportional scaling of DNA knot formation (orange dashed line). Fractalization of the chromatin architecture minimizes instead the potentially harmful scaling of DNA entanglements (green line). The  $k_{CHR}^P$  data supports a fractal model, in which the ‘beads on a string’ architecture of the 10 nm nucleosomal fiber reiterates in its next level of organization by forming clusters of about 20 nucleosomes.

condensins (49,50) can regulate DNA passage preferences of topo II *in vivo*.

A different feature that could explain the inflection of the  $k_{CHR}^P$  slope is a length-dependent transition in the packaging mode of the nucleosomal fiber. The folding architecture of chromatin fibers has been hotly debated (51–53). In addition to regular packing models (43–45), irregular folding models that incorporate variability in the nucleosome repeat length and other heteromorphic structures have been proposed in recent years (54–56). We envision two models that might explain the leveling of DNA knotting when a chromatin fiber reaches a length of about 20 nucleosomes. Both models invoke the transition from a globular to a fibrillary architecture. One possibility is that, below this length, strings of nucleosomes fold into intricate disordered structures that can be entangled by topo II. Above this length, nucleosomal fibers adopt a highly ordered or compacted configuration, which hampers the access of topo II to entangle the embedded DNA. However, no experimental evidence supports such abrupt length-dependent transition during the folding of nucleosome arrays (41,56). A more plausible mechanism through which the scaling of knot formation could be minimized is the fractalization of

chromatin architecture. In this regard, our results support a model in which ‘beads on a string’ organization of the 10-nm nucleosome fiber reiterates in the next level of organization, in which the ‘bead’ unit is a cluster of about 20 nucleosomes (Figure 7B). As a result, DNA knot abundance and complexity do not scale as would occur in an uninterrupted mesh of nucleosomes. According to this fractal organization, the small minichromosomes (<4 kb) examined in our study configured a single cluster of nucleosomes, whereas the larger ones configured two or more clusters. This architecture could explain the presence of composite knots in the larger minichromosomes, where prime knots might concur in separate nucleosome clusters. Remarkably, this fractal configuration is in line with most recent observations of intracellular chromatin. Mapping chromosome folding at nucleosome resolution indicated that yeast chromatin folds into clusters of 10–50 nucleosomes (57). Super-resolution nanoscopy showed that chromatin fibers are formed by heterogeneous clutches of nucleosomes (54). EM tomography revealed that intracellular chromatin is a disordered 5- to 24-nm-diameter granular chain (58). Minimization of DNA knot complexity might be therefore a fundamental outcome of the fractal architecture of intracellular chromatin.



In this discussion, we have assumed that the small fractions of DNA knots present in eukaryotic chromatin are merely a side effect of the ubiquitous DNA passage activity of topo II. However, it cannot be discarded that DNA knot formation *in vivo* might have regulatory and structural roles in other instances. Future research might clarify whether topo II activity and chromatin structure are modulated not only to lessen the potentially harmful entanglement of intracellular DNA but also to promote DNA knotting at specific sites. In this respect, earlier studies had been able to infer the spatial path of DNA in macromolecular ensembles from the characterization of DNA knots produced *in vitro* (59,60). Similar analyses with DNA knots formed *in vivo* might constitute a unique non-invasive approach to disclose the spatial trajectory of DNA during genome transactions.

## SUPPLEMENTARY DATA

Supplementary Data are available at NAR online.

## ACKNOWLEDGEMENTS

We thank R. Joshi for critical reading of the manuscript.

## FUNDING

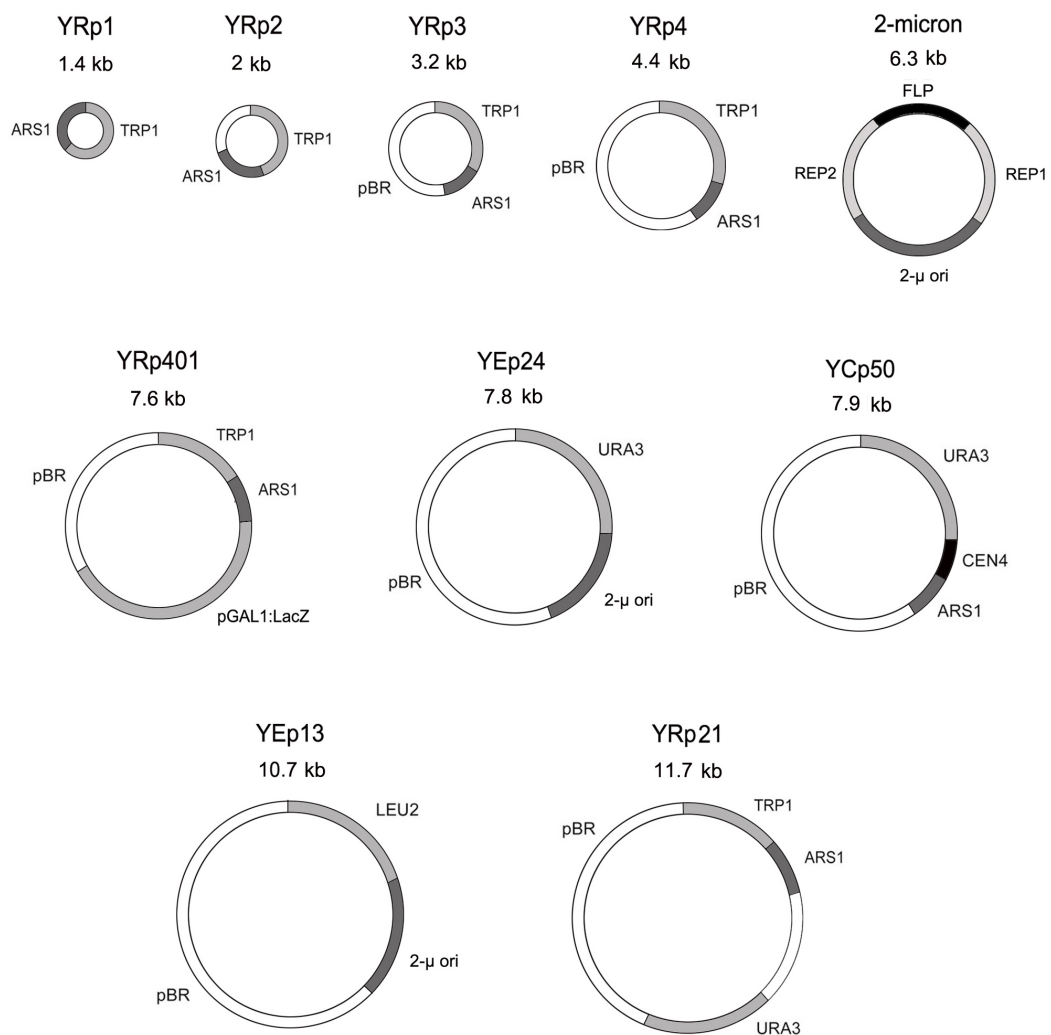
Plan Estatal de Investigación Científica y Técnica of Spain [BFU2015-67007-P and MDM-2014-0435-02 to J.R., BES-2015-071597 to A.V.]. Funding for open access charge: Plan Estatal de Investigación Científica y Técnica of Spain.  
*Conflict of interest statement.* None declared.

## REFERENCES

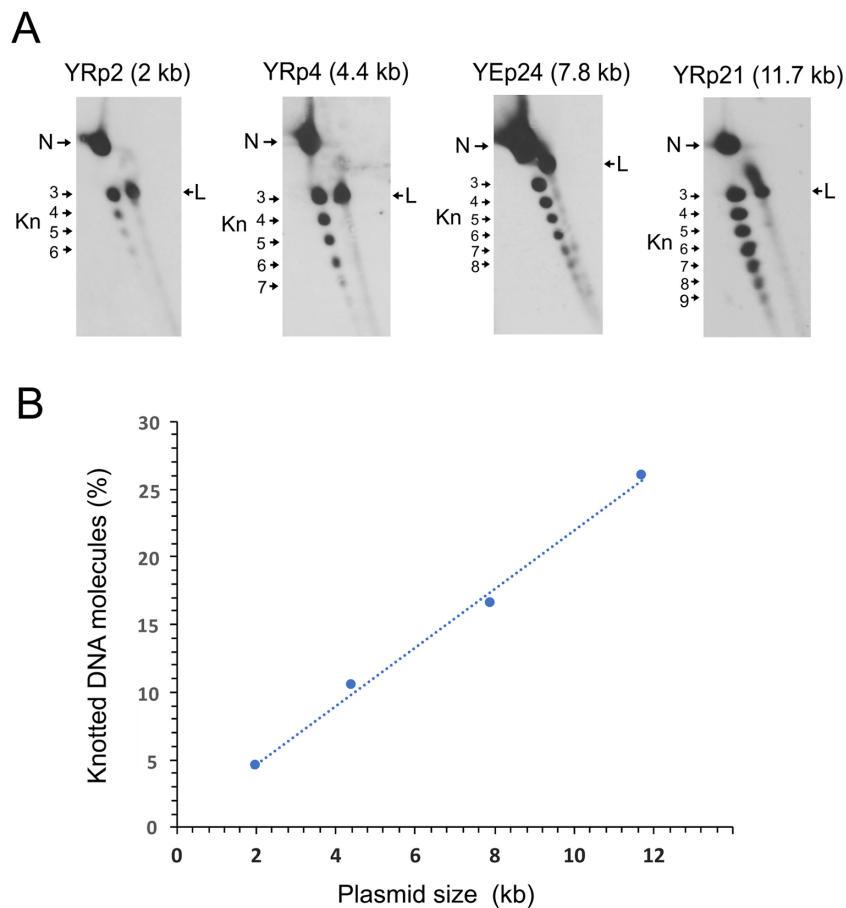
- Wang, J.C. (1998) Moving one DNA double helix through another by a type II DNA topoisomerase: the story of a simple molecular machine. *Q. Rev. Biophys.*, **31**, 107–144.
- Champoux, J.J. (2001) DNA topoisomerases: structure, function, and mechanism. *Annu. Rev. Biochem.*, **70**, 369–413.
- Wang, J.C. (2002) Cellular roles of DNA topoisomerases: a molecular perspective. *Nat. Rev. Mol. Cell Biol.*, **3**, 430–440.
- Liu, L.F., Liu, C.C. and Alberts, B.M. (1980) Type II DNA topoisomerases: enzymes that can unknot a topologically knotted DNA molecule via a reversible double-strand break. *Cell*, **19**, 697–707.
- Hsieh, T. (1983) Knotting of the circular duplex DNA by type II DNA topoisomerase from *Drosophila melanogaster*. *J. Biol. Chem.*, **258**, 8413–8420.
- Wasserman, S.A. and Cozzarelli, N.R. (1991) Supercoiled DNA-directed knotting by T4 topoisomerase. *J. Biol. Chem.*, **266**, 20567–20573.
- Roca, J., Berger, J.M. and Wang, J.C. (1993) On the simultaneous binding of eukaryotic DNA topoisomerase II to a pair of double-stranded DNA helices. *J. Biol. Chem.*, **268**, 14250–14255.
- Rybenkov, V.V., Ullsperger, C., Vologodskii, A.V. and Cozzarelli, N.R. (1997) Simplification of DNA topology below equilibrium values by type II topoisomerases. *Science*, **277**, 690–693.
- Shishido, K., Komiyama, N. and Ikawa, S. (1987) Increased production of a knotted form of plasmid pBR322 DNA in *Escherichia coli* DNA topoisomerase mutants. *J. Mol. Biol.*, **195**, 215–218.
- Ishii, S., Murakami, T. and Shishido, K. (1991) Gyrase inhibitors increase the content of knotted DNA species of plasmid pBR322 in *Escherichia coli*. *J. Bacteriol.*, **173**, 5551–5553.
- Sogo, J.M., Stasiak, A., Martinez-Robles, M.L., Krimer, D.B., Hernandez, P. and Schwartzman, J.B. (1999) Formation of knots in partially replicated DNA molecules. *J. Mol. Biol.*, **286**, 637–643.
- Olavarrieta, L., Martinez-Robles, M.L., Sogo, J.M., Stasiak, A., Hernandez, P., Krimer, D.B. and Schwartzman, J.B. (2002) Supercoiling, knotting and replication fork reversal in partially replicated plasmids. *Nucleic Acids Res.*, **30**, 656–666.
- Deibler, R.W., Rahmati, S. and Zechiedrich, E.L. (2001) Topoisomerase IV, alone, unknots DNA in *E. coli*. *Genes Dev.*, **15**, 748–761.
- Lopez, V., Martinez-Robles, M.L., Hernandez, P., Krimer, D.B. and Schwartzman, J.B. (2012) Topo IV is the topoisomerase that knots and unknots sister duplexes during DNA replication. *Nucleic Acids Res.*, **40**, 3563–3573.
- Rodriguez-Campos, A. (1996) DNA knotting abolishes *in vitro* chromatin assembly. *J. Biol. Chem.*, **271**, 14150–14155.
- Portugal, J. and Rodriguez-Campos, A. (1996) T7 RNA polymerase cannot transcribe through a highly knotted DNA template. *Nucleic Acids Res.*, **24**, 4890–4894.
- Schmitt, A.D., Hu, M. and Ren, B. (2016) Genome-wide mapping and analysis of chromosome architecture. *Nat. Rev. Mol. Cell Biol.*, **17**, 743–755.
- Denker, A. and de Laat, W. (2016) The second decade of 3C technologies: detailed insights into nuclear organization. *Genes Dev.*, **30**, 1357–1382.
- Arsuaga, J., Vazquez, M., Trigueros, S., Summers, D. and Roca, J. (2002) Knotting probability of DNA molecules confined in restricted volumes: DNA knotting in phage capsids. *Proc. Natl. Acad. Sci. U.S.A.*, **99**, 5373–5377.
- Micheletti, C., Marenduzzo, D., Orlandini, E. and Summers, D.W. (2008) Simulations of knotting in confined circular DNA. *Biophys. J.*, **95**, 3591–3599.
- Arsuaga, J., Jayasinghe, R.G., Scharein, R.G., Segal, M.R., Stolz, R.H. and Vazquez, M. (2015) Current theoretical models fail to predict the topological complexity of the human genome. *Front. Mol. Biosci.*, **2**, 48.
- Trigueros, S. and Roca, J. (2002) Failure to relax negative supercoiling of DNA is a primary cause of mitotic hyper-recombination in topoisomerase-deficient yeast cells. *J. Biol. Chem.*, **277**, 37207–37211.
- Diaz-Ingelmo, O., Martinez-Garcia, B., Segura, J., Valdes, A. and Roca, J. (2015) DNA topology and global architecture of point centromeres. *Cell Rep.*, **13**, 667–677.
- Trigueros, S., Arsuaga, J., Vazquez, M.E., Summers, D.W. and Roca, J. (2001) Novel display of knotted DNA molecules by two-dimensional gel electrophoresis. *Nucleic Acids Res.*, **29**, E67.
- Frank-Kamenetskii, M.D., Lukashin, A.V. and Vologodskii, A.V. (1975) Statistical mechanics and topology of polymer chains. *Nature*, **258**, 398–402.
- Rybenkov, V.V., Cozzarelli, N.R. and Vologodskii, A.V. (1993) Probability of DNA knotting and the effective diameter of the DNA double helix. *Proc. Natl. Acad. Sci. U.S.A.*, **90**, 5307–5311.
- Stasiak, A., Katritch, V., Bednar, J., Michoud, D. and Dubochet, J. (1996) Electrophoretic mobility of DNA knots [letter]. *Nature*, **384**, 122.
- Salceda, J., Fernandez, X. and Roca, J. (2006) Topoisomerase II, not topoisomerase I, is the proficient relaxase of nucleosomal DNA. *EMBO J.*, **25**, 2575–2583.
- Simpson, R.T., Thoma, F. and Brubaker, J.M. (1985) Chromatin reconstituted from tandemly repeated cloned DNA fragments and core histones: a model system for study of higher order structure. *Cell*, **42**, 799–808.
- Yuan, G.C., Liu, Y.J., Dion, M.F., Slack, M.D., Wu, L.F., Altschuler, S.J. and Rando, O.J. (2005) Genome-scale identification of nucleosome positions in *S. cerevisiae*. *Science*, **309**, 626–630.
- Shaw, S.Y. and Wang, J.C. (1993) Knotting of a DNA chain during ring closure. *Science*, **260**, 533–536.
- Thoma, F., Bergman, L.W. and Simpson, R.T. (1984) Nuclease digestion of circular TRP1ARS1 chromatin reveals positioned nucleosomes separated by nuclease-sensitive regions. *J. Mol. Biol.*, **177**, 715–733.
- Wasserman, S.A., Dungan, J.M. and Cozzarelli, N.R. (1985) Discovery of a predicted DNA knot substantiates a model for site-specific recombination. *Science*, **229**, 171–174.
- Buck, D. and Flapan, E. (2007) Predicting knot or catenane type of site-specific recombination products. *J. Mol. Biol.*, **374**, 1186–1199.

35. Deibler, R.W., Mann, J.K., Summers, W.L. and Zechiedrich, L. (2007) Hin-mediated DNA knotting and recombining promote replicon dysfunction and mutation. *BMC Mol. Biol.*, **8**, 44
36. Hagerman, P.J. (1988) Flexibility of DNA. *Annu. Rev. Biophys. Biophys. Chem.*, **17**, 265–286.
37. Witz, G., Dietler, G. and Stasiak, A. (2011) Tightening of DNA knots by supercoiling facilitates their unknotting by type II DNA topoisomerases. *Proc. Natl. Acad. Sci. U.S.A.*, **108**, 3608–3611.
38. Ringrose, L., Chabanis, S., Angrand, P.O., Woodroffe, C. and Stewart, A.F. (1999) Quantitative comparison of DNA looping in vitro and in vivo: chromatin increases effective DNA flexibility at short distances. *EMBO J.*, **18**, 6630–6641.
39. Hajjoul, H., Mathon, J., Ranchon, H., Goiffon, I., Mozziconacci, J., Albert, B., Carrivain, P., Victor, J.M., Gadal, O., Bystricky, K. *et al.* (2013) High-throughput chromatin motion tracking in living yeast reveals the flexibility of the fiber throughout the genome. *Genome Res.*, **23**, 1829–1838.
40. Klenin, K.V., Vologodskii, A.V., Anshelevich, V.V., Dykhne, A.M. and Frank-Kamenetskii, M.D. (1988) Effect of excluded volume on topological properties of circular DNA. *J. Biomol. Struct. Dyn.*, **5**, 1173–1185.
41. Bancaud, A., Conde e Silva, N., Barbi, M., Wagner, G., Allemand, J.F., Mozziconacci, J., Lavelle, C., Croquette, V., Victor, J.M., Prunell, A. *et al.* (2006) Structural plasticity of single chromatin fibers revealed by torsional manipulation. *Nat. Struct. Mol. Biol.*, **13**, 444–450.
42. Huh, Y. and Oh, S. (2011). An upper bound on stick number of knots. *J. Knot Theory Ram.* **5**, 741–747.
43. Dorigo, B., Schalch, T., Kulangara, A., Duda, S., Schroeder, R.R. and Richmond, T.J. (2004) Nucleosome arrays reveal the two-start organization of the chromatin fiber. *Science*, **306**, 1571–1573.
44. Song, F., Chen, P., Sun, D., Wang, M., Dong, L., Liang, D., Xu, R.M., Zhu, P. and Li, G. (2014) Cryo-EM study of the chromatin fiber reveals a double helix twisted by tetranucleosomal units. *Science*, **344**, 376–380.
45. Ghirlando, R. and Felsenfeld, G. (2008) Hydrodynamic studies on defined heterochromatin fragments support a 30-nm fiber having six nucleosomes per turn. *J. Mol. Biol.*, **376**, 1417–1425.
46. Kornberg, R.D. and Lorch, Y. (1995) Interplay between chromatin structure and transcription. *Curr. Opin. Cell Biol.*, **7**, 371–375.
47. Trigueros, S., Salceda, J., Bermudez, I., Fernandez, X. and Roca, J. (2004) Asymmetric removal of supercoils suggests how topoisomerase II simplifies DNA topology. *J. Mol. Biol.*, **335**, 723–731.
48. Fernandez, X., Diaz-Ingelmo, O., Martinez-Garcia, B. and Roca, J. (2014) Chromatin regulates DNA torsional energy via topoisomerase II-mediated relaxation of positive supercoils. *EMBO J.*, **33**, 1492–1501.
49. Sen, N., Leonard, J., Torres, R., Garcia-Luis, J., Palou-Marin, G. and Aragon, L. (2016) Physical proximity of sister chromatids promotes Top2-dependent intertwining. *Mol. Cell*, **64**, 134–147.
50. Piskadlo, E., Tavares, A. and Oliveira, R.A. (2017) Metaphase chromosome structure is dynamically maintained by condensin I-directed DNA (de)catenation. *Elife*, **6**, e26120.
51. Fussner, E., Ching, R.W. and Bazett-Jones, D.P. (2011) Living without 30nm chromatin fibers. *Trends Biochem. Sci.*, **36**, 1–6.
52. Luger, K., Dechassa, M.L. and Tremethick, D.J. (2012) New insights into nucleosome and chromatin structure: an ordered state or a disordered affair? *Nat Rev Mol Cell Biol*, **13**, 436–447.
53. Maeshima, K., Imai, R., Tamura, S. and Nozaki, T. (2014) Chromatin as dynamic 10-nm fibers. *Chromosoma*, **123**, 225–237.
54. Ricci, M.A., Manzo, C., Garcia-Parajo, M.F., Lakadamyali, M. and Cosma, M.P. (2015) Chromatin fibers are formed by heterogeneous groups of nucleosomes in vivo. *Cell*, **160**, 1145–1158.
55. Grigoryev, S.A., Bascom, G., Buckwalter, J.M., Schubert, M.B., Woodcock, C.L. and Schlick, T. (2016) Hierarchical looping of zigzag nucleosome chains in metaphase chromosomes. *Proc. Natl. Acad. Sci. U.S.A.*, **113**, 1238–1243.
56. Maeshima, K., Rogge, R., Tamura, S., Joti, Y., Hikima, T., Szerlong, H., Krause, C., Herman, J., Seidel, E., DeLuca, J. *et al.* (2016) Nucleosomal arrays self-assemble into supramolecular globular structures lacking 30-nm fibers. *EMBO J.*, **35**, 1115–1132.
57. Hsieh, T.H., Weiner, A., Lajoie, B., Dekker, J., Friedman, N. and Rando, O.J. (2015) Mapping nucleosome resolution chromosome folding in yeast by micro-C. *Cell*, **162**, 108–119.
58. Ou, H.D., Phan, S., Deerinck, T.J., Thor, A., Ellisman, M.H. and O’Shea, C.C. (2017) ChromEMT: Visualizing 3D chromatin structure and compaction in interphase and mitotic cells. *Science*, **357**, eaag0025.
59. Kimura, K., Rybenkov, V.V., Crisona, N.J., Hirano, T. and Cozzarelli, N.R. (1999) 13S condensin actively reconfigures DNA by introducing global positive writhe: implications for chromosome condensation. *Cell*, **98**, 239–248.
60. Arsuaga, J., Vazquez, M., McGuirk, P., Trigueros, S., Summers, D. and Roca, J. (2005) DNA knots reveal a chiral organization of DNA in phage capsids. *Proc. Natl. Acad. Sci. U.S.A.*, **102**, 9165–9169.

## **Supplementary Information**



**Supplementary Figure 1. Size and genetic configuration of yeast minichromosomes analyzed in the study.** YRp3, YRp4, YRp401, YEp24, YCp50, YEp13 and YRp21 were amplified as bacterial plasmids in *Escherichia coli*. YRp1 and YRp2, which lack bacterial sequences, were constructed by circularization of linear DNA fragments generated via PCR amplification. Minichromosomes were transfected into *Saccharomyces cerevisiae* cells by electroporation. The 2-micron plasmid was endogenous in the yeast strains used.



**Supplementary Figure 2. Dependence of topo II-mediated knotting of DNA on plasmid size.** (A) DNA knots produced by topo II in bacterial plasmids YRp2 (2 kb), YRp4 (4.4 kb), YEp24 (7.8 kb), and YRp21 (11.7 kb). Reactions were done in 20  $\mu$ l of 50 mM Tris-HCl pH 8, 1 mM EDTA, 50 mM NaCl, 10 mM  $MgCl_2$ , 7 mM 2-mercaptoethanol, 100 mg/ml of bovine serum albumin, and contained 10 ng of plasmid DNA and 10 ng of yeast topo II. Following incubation at 30°C for 5 min, AMPPNP was added to 1 mM final concentration to effect DNA transport. Reactions were terminated after 10 min and each sample was phenol-extracted and ethanol precipitated. Recovered DNA samples were nicked with endonuclease BstNB1 (NEB) and examined in a two-dimensional agarose gel electrophoresis as described in Supplementary Table I. Gels were blotted and probed as described in the methods. Signals of nicked unknotted circles (N), linear DNA (L), and knots (Kn) with increasing number of crossings (3 to 9) are indicated. (B) The graph plots the fraction of knotted molecules (%) produced by plasmid size (kb).



DNA (Kb)	Electrophoresis of Lk distributions Agarose gel of 20 x 20 cm			Electrophoresis of DNA knots Agarose gel of 20 x 20 cm		
		Dimension I Chloroquine 0.6 µg/mL	Dimension II Chloroquine 3.0 µg/mL		Dimension I	Dimension II
	Agarose (w/v)	volts x time	volts x time	Agarose (w/v)	volts x time	volts x time
YRp1 (1.5 kb)	2 %	40V x 24h	100V x 4h	2 %	40V x 24h	200V x 3h
YRp2 (2 kb)	1.8 %	65V x 15h	100V x 4h	1.8 %	65V x 15h	165V x 3h
YRp3 (3.2kb)	1.2 %	65V x 15h	100V x 4h	1.2 %	65V x 15h	150V x 3h
YRp4 (4.4kb)	0.7 %	50V x 16h	70V x 4h	0.9 %	33V x 42h	150V x 3h
2-micron (6.3kb)	0.6 %	22V x 42h	90V x 4h	0.6 %	22V x 42h	125V x 3h
YEp24 (7.8 kb) YCp50 (7.9 kb)	0.6 %	22V x 42h	90V x 4h	0.45 %	22V x 42h	125V x 4h
YEp13 (10.7 kb) YRp21 (11.7kb)	0.4 %	20V x 42h	90V x 4h	0.4 %	33V x 42h	125V x 4h

**Supplementary Table 1**  
Settings for 2D-gel electrophoresis

Chromosome	Length (Kb)	$K_{CHR}^P$	Kn 3	Kn 4	Kn 5	Kn 6	Kn 7	Kn 8
YRp1	1,4	0,00						
YRp2	2,0	0,52	0,52					
YRp3	3,2	1,49	1,20	0,21	0,06	0,02		
YRp4	4,4	2,31	1,72	0,39	0,12	0,05	0,02	0,01
2-micron	6,3	2,62	1,90	0,44	0,17	0,05	0,04	0,02
YEp24	7,8	2,72	1,95	0,46	0,18	0,08	0,04	0,01
YCp50	7,9	2,79	1,95	0,45	0,22	0,10	0,05	0,02
YEp13	10,7	2,89	2,10	0,40	0,23	0,09	0,05	0,02
YRp21	11,7	2,93	2,10	0,40	0,25	0,11	0,05	0,02

$K_{CHR}^P$ : Total DNA knotting probability

Kn3 to Kn8: Probability (100 x) of DNA knot species of different number of crossings (3 to 8)

### Supplementary Table 2

DNA knotting probability of yeast minichromosomes

---

# Article #2

---



# Transcriptional supercoiling boosts topoisomerase II-mediated knotting of intracellular DNA

Antonio Valdés<sup>1</sup>, Lucia Coronel<sup>2</sup>, Belén Martínez-García<sup>1</sup>, Joana Segura<sup>1</sup>, Sílvia Dyson<sup>1</sup>, Ofelia Díaz-Ingelmo<sup>1</sup>, Cristian Micheletti<sup>2</sup> and Joaquim Roca<sup>1,\*</sup>

<sup>1</sup>Molecular Biology Institute of Barcelona (IBMB), Spanish National Research Council (CSIC), Barcelona 08028, Spain and <sup>2</sup>Scuola Internazionale Superiore di Studi Avanzati (SISSA), 34136 Trieste, Italy

Received March 19, 2019; Revised May 9, 2019; Editorial Decision May 22, 2019; Accepted May 22, 2019

## ABSTRACT

Recent studies have revealed that the DNA cross-inversion mechanism of topoisomerase II (topo II) not only removes DNA supercoils and DNA replication intertwinings, but also produces small amounts of DNA knots within the clusters of nucleosomes that conform to eukaryotic chromatin. Here, we examine how transcriptional supercoiling of intracellular DNA affects the occurrence of these knots. We show that although (–) supercoiling does not change the basal DNA knotting probability, (+) supercoiling of DNA generated in front of the transcribing complexes increases DNA knot formation over 25-fold. The increase of topo II-mediated DNA knotting occurs both upon accumulation of (+) supercoiling in topoisomerase-deficient cells and during normal transcriptional supercoiling of DNA in *TOP1 TOP2* cells. We also show that the high knotting probability ( $P^{kn} \geq 0.5$ ) of (+) supercoiled DNA reflects a 5-fold volume compaction of the nucleosomal fibers *in vivo*. Our findings indicate that topo II-mediated DNA knotting could be inherent to transcriptional supercoiling of DNA and other chromatin condensation processes and establish, therefore, a new crucial role of topoisomerase II in resetting the knotting–unknotting homeostasis of DNA during chromatin dynamics.

## INTRODUCTION

During DNA transcription, rotation of the duplex relative to the RNA polymerase produces positive supercoiling of DNA ((+)S) in front of the transcribing complex and negative supercoiling ((–)S) behind it (1,2). In eukaryotic cells, topoisomerases I and II (topo I and topo II) facilitate RNA synthesis by relaxing the transcriptional supercoiling of DNA (3,4). Topo I produces transient DNA nicks to allow swiveling of the duplex and thus relaxation of (+)S and

(–)S (5). Topo II produces transient DNA double-strand breaks and passes across them another segment of DNA (6). This DNA cross-inversion mechanism allows the relaxation of (+)S and (–)S, as well as the elimination of the DNA intertwinings that arise during chromosome replication (3,4) (Figure 1A).

Although either topo I or topo II suffices to relax (+)S and (–)S *in vivo*, fine-tuning of chromosomal DNA topology requires the interplay of both topoisomerases with chromatin architecture (7,8). Whereas topo I relaxes efficiently naked DNA regions, topo II is more proficient in chromatinized DNA (9). Accordingly, topo I is recruited in adjoining DNA-transcribing complexes, where nucleosomes are transiently disrupted and spinning of the duplex is fast (10), whereas topo II is recruited mainly in intergenic regions, away from open reading frames (11,12) (Figure 1A).

The chromatin architecture also determines the dissipation and relaxation rates of (+)S and (–)S. The organization of cellular chromosomes into topological domains and the rotational drag of chromatin fibers delay the diffusion and cancellation of DNA supercoiling waves (13,14). Accordingly, domains with different levels of (+)S and (–)S have been mapped within transcriptionally active regions throughout chromosomes of yeast (15), *Drosophila* (16) and human cells (17,18). Detection of these (+)S and (–)S domains also indicates that transcriptional supercoiling of DNA is not instantaneously relaxed or dissipated. In this respect, the activity of intracellular topoisomerases has been found to relax (+)S domains faster than (–)S domains (19). Since (+)S and (–)S are generated at similar rates during DNA transcription, their asymmetric rate of relaxation produces a homeostatic excess of (–)S, thereby overcoming the necessity of a DNA-unwinding topoisomerase (i.e. bacterial DNA gyrase) in eukaryotic cells (19).

Efficient relaxation of (+)S facilitates transcriptional elongation, and the activity of either topo I or topo II can fulfil this task. However, studies in mouse and human cells demonstrate that a combined function of topo I and topo II is required for proper transcription elongation, particularly

\*To whom correspondence should be addressed. Tel: +34 9340 20117; Email: jrbbmc@ibmb.csic.es

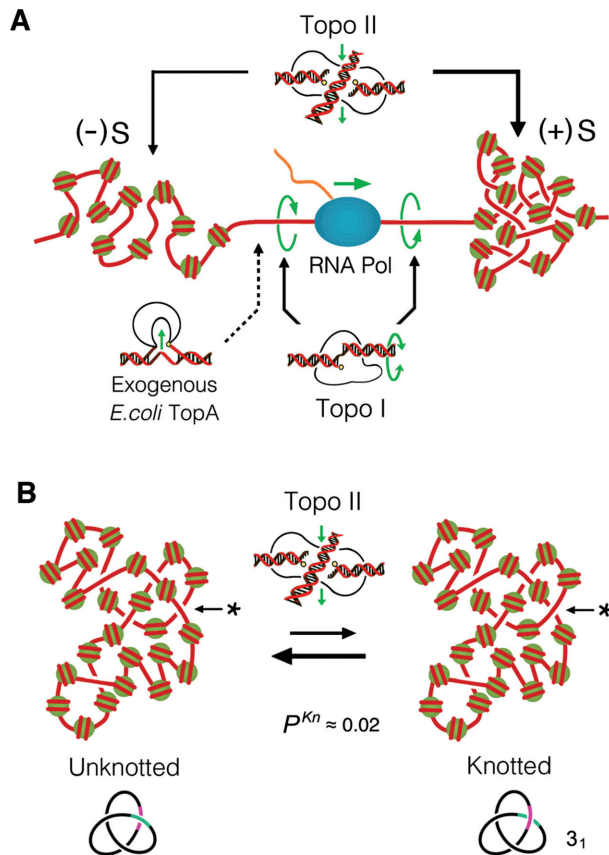


**Figure 1.** Topoisomerase activities that modulate supercoiling and knotting of intracellular DNA. (A) Both topo I and topo II can relax the (+)S and (-)S of DNA generated, respectively, in front of and behind the transcribing complex. The DNA-swiveling mechanism of topo I performs nearby the RNA polymerase, whereas the DNA cross-inversion mechanism of topo II performs at DNA crossings formed within nucleosomal fibers. Exogenous expression of *Escherichia coli TopA* relaxes (-)S only and thereby leads to the accumulation of (+)S, when topo I and topo II are inactivated. (B) The mechanism of topo II can produce and remove DNA knots by inverting juxtapositions of DNA linker segments (\*) within nucleosomal fibers. The scheme illustrates the formation and resolution of a trefoil knot (31) in a circular minichromosome of ~25 nucleosomes, whose DNA knotting probability ( $P^{Kn}$ ) *in vivo* is  $\approx 0.02$ .

during the synthesis of long RNA transcripts (20–22). This requirement affects long genes involved in neural development (20) and synaptic function (23) and linked to autism (24). Likewise, in yeast cells, proper transcription of long genes requires both topoisomerases and becomes blocked when topo II is inactivated (25). Strikingly, this stalling of RNA polymerases can be rescued by exogenous expression of type-2 (topo II), but not type-1 (topo I) topoisomerases (25). These observations led us to hypothesize that the constraints impairing transcription elongation could be DNA knots (i.e. intramolecular entanglements of DNA), since only type-2 topoisomerases can knot–unknot duplex DNA (3,6). Supporting this hypothesis, *in vitro* studies have shown that DNA knots are able to impair DNA transcription (26). In this respect, we recently uncovered that DNA knots are present in intracellular chromatin (27). Topo II-mediated knotting of DNA occurs within stretches of ~25 nucleosomes with a probability of ~0.02 (Figure 1B). These find-

ings opened up the question of how the knotting probability of intracellular DNA affects or is affected by genome activities and chromatin architecture.

Here, we examine how the occurrence of intracellular DNA knots is affected by transcriptional supercoiling of DNA. We show that (+)S increases topo II-mediated knotting of DNA over 25-fold and that this increase is consequent to chromatin compaction. Our findings show that DNA knotting concurs normally with transcriptional supercoiling and other chromatin condensation processes, and establish therefore a new crucial role of topo II in resetting the DNA knotting–unknotting balance during the conformational transitions of intracellular chromatin.

## MATERIALS AND METHODS

### Yeast strains, plasmids and enzymes

All experiments were conducted in *Saccharomyces cerevisiae* strains JCW25 (*TOP1 TOP2*) and JCW28 ( $\Delta top1 top2-4$ ), which are derivatives of FY251 (*MATa his3- $\Delta$ 200 leu2- $\Delta$ 1 trp1- $\Delta$ 63 ura3-52*). JCW28 carries the null mutation  $\Delta top1$  and the thermosensitive mutation *top2-4* (28). When indicated, JCW25 and JCW28 were transformed with pJRW13, a plasmid that carries the *Escherichia coli TopA* gene under the constitutive pGPD yeast promoter (9). Circular minichromosomes YRp4 (27), YEp24 (27) and pYR121 (29) were amplified as bacterial plasmids in *E. coli* and used to transform *S. cerevisiae* following standard procedures. Topo I of vaccinia virus was purified from *E. coli* cells harboring the expression clone pET11vtop1 as described previously (30). Topo II of *S. cerevisiae* was purified from yeast cells harboring the expression clone YEpTOP2GAL1 as described previously (31). The DNA-nicking endonuclease BstNB1 was purchased from NEB.

### Yeast culture and DNA extraction

Yeast cells were grown at 26°C in yeast synthetic media containing adequate dropout supplements and 2% glucose. Thermal inactivation of topo II was carried out during exponential growth (OD  $\approx 0.8$ ) by shifting cell cultures to 37°C for the indicated time periods. Activation of the *GAL1 GAL10* promoter of pRY121 was performed by transferring the cells that grew in media containing 2% glucose into YP Broth media containing 2% galactose for 3 h. Before harvesting yeast cells, intracellular DNA topology was fixed as described previously (32) by quickly mixing the liquid cultures with one cold volume (-20°C) of ETol solution (ethanol 95%, 28 mM toluene, 20 mM Tris-HCl, pH 8.8, 5 mM EDTA). Fixed cells from a 25 ml culture were sedimented, washed twice with water, resuspended in 400  $\mu$ l of TE (10 mM Tris-HCl, pH 8.8, 1 mM EDTA) and transferred to a 1.5-ml microfuge tube containing 400  $\mu$ l of phenol and 400  $\mu$ l of acid-washed glass beads (425–600  $\mu$ m, Sigma). Mechanic lysis of >80% cells was achieved by shaking the tubes in a FastPrep® apparatus for 10 s at power 5. The aqueous phase of the cell lysates was collected, extracted with chloroform, precipitated with ethanol and dissolved in 100  $\mu$ l of TE containing RNase-A. Following 10 min of incubation at 37°C, DNA was precipitated with am-

monium acetate and ethanol, and then dissolved in 40  $\mu$ l of TE.

### DNA topology analysis by 2D-gel electrophoresis

To examine the Lk distribution of minichromosomes, 2D-electrophoreses of YRp4 and 2-micron circles were carried out in 0.8% agarose gels (20 cm  $\times$  20 cm) in TBE buffer (89 mM Tris-borate, 2 mM EDTA) plus 0.6  $\mu$ g/ml of chloroquine at 50 V for 14 h in the first dimension, and TBE buffer plus 3  $\mu$ g/ml of chloroquine, at 60 V for 8 h in the second dimension. 2D-electrophoreses of YEp24 and pRY121 were carried out in 0.6% agarose in TBE buffer plus 0.6  $\mu$ g/ml of chloroquine at 30 V for 36 h in the first dimension, and TBE buffer plus 3  $\mu$ g/ml of chloroquine, at 80 V for 4 h in the second dimension. To examine the DNA knots formed in the minichromosomes, their DNA were nicked with endonuclease BstNBI and loaded in a 20 cm  $\times$  20 cm agarose gel. 2D-electrophoreses of YRp4 were carried out in a 0.9% agarose gel in TBE buffer at 33 V for 40 h in the first dimension, and at 150 V for 3 h in the second dimension. 2D-electrophoreses of 2-micron circles, YEp24 and pYR121 were carried out in 0.6% agarose (2-micron) or 0.45% agarose (YEp24 and pYR121) in TBE buffer at 25 V for 40 h in the first dimension, and at 125 V for 4 h in the second dimension. 2D-gels were blot-transferred to a nylon membrane and probed with minichromosome-specific DNA sequences labeled with AlkPhos Direct (GE Healthcare®). Probe signals of increasing exposure periods were recorded on X-ray films. DNA knot probability ( $P^{Kn}$ ) was calculated as described previously (27), as the total fraction of nicked knotted DNA circles (irrespective of the knot complexity) relative to the total amount of nicked DNA circles (knotted and unknotted).

### Numerical simulation of DNA knotting in modeled nucleosomal fibers

The YRp4 minichromosome was modeled as a ring made of 25 spherical beads of diameter  $D$ , each representing a nucleosome, and infinitely thin straight segments connecting the centers of neighboring beads, such that the free portion of a segment, of length  $L$ , represented a DNA linker. A Metropolis Monte Carlo scheme based on crankshaft moves was used to evolve the system, which was initially prepared in a circular arrangement. Excluded volume effects were introduced by assigning infinite energy to configurations with overlapping beads, and zero energy otherwise. The Monte Carlo moves allowed the linkers to cross so that the sampled space corresponded to torsionally relaxed and topology unrestricted minichromosomes. For different combinations of the  $D/L$  ratio in the [0:1] range, we collected  $10^5$  uncorrelated conformations (i.e. picked at time intervals larger than the autocorrelation time of the radius of gyration radius,  $R_g$ ) that were topologically profiled by comparing the Dowker code of their 2D projections against tabulated values. The Knotscape software (<http://pzacad.pitzer.edu/~jhoste/hostewebpages/kntscp.html>) was used for this purpose. As the basal  $P^{Kn} \sim 0.02$  of YRp4 *in vivo* was recovered for  $D/L \sim 0.47$ , the effect of compaction at this value of  $D/L$  was accounted for by keeping only configurations with relative gyration radius smaller

than a threshold value,  $\max R_g$ , out of a more extensive set of  $\sim 4 \times 10^6$  uncorrelated conformers, which yielded an average (root mean square) gyration radius  $R_g^0/(D + L)$  of 1.63. Absolute writhe ( $|Wr|$ ) was computed by averaging the sum of the signed crossings (defined according to the right-hand rule after orienting the curve) over hundreds of projections. For each sampled conformation,  $R_g/R_g^0$  was averaged for different (binned) ranges of  $|Wr|$ .

## RESULTS

### DNA knotting probability changes differently during (+) and (–) supercoiling of intracellular chromatin

As in previous studies, we used yeast circular minichromosomes to analyze DNA knot formation in intracellular chromatin (27). Since (+)S and (–)S cancel each other in circular DNA domains, we accumulated (+)S and (–)S separately to reproduce the conformations generated during transcriptional supercoiling of chromosomal DNA. We generated (+)S upon topo II inactivation in  $\Delta top1 top2-4$  cells that constitutively expressed *E. coli TopA* (2). In these conditions, *TopA* relaxes the (–)S but not the (+)S generated during DNA transcription. Likewise, we generated (–)S upon thermal inactivation of topo II in  $\Delta top1 top2-4$  cells. In these conditions, preferential relaxation of (+)S by residual topo II leads to the accumulation of (–)S (19) (Figure 1A).

Upon fixing the DNA topology of the minichromosomes *in vivo* (32), we examined the superhelicity of their DNA by means of 2D-gel electrophoresis (33). In these gels (Figure 2A), linking number topoisomers (Lk) of circular DNA distribute along an arch, in which Lk values increase in the clockwise direction. Accumulation of (+)S is thus denoted by a clockwise displacement of the Lk distribution, whereas increase of (–)S is denoted by a counterclockwise shift. To examine the presence of DNA knots in the supercoiled minichromosomes, we nicked their DNA to eliminate any supercoiling and conducted a different kind of 2D-gel electrophoresis (34). In these gels (Figure 2B), nicked DNA circles that contain knots move faster than the unknotted nicked circle, and their velocity correlates to the knot complexity (the number of irreducible DNA crossings of a knot,  $Kn\#$ ).

Figure 2C shows the DNA supercoiling (top gel) and DNA knotting (bottom gel) states of YRp4, a 4.5-kb minichromosome, in  $\Delta top1 top2-4$  cells. Before topo II inactivation (lane 1), the Lk distribution reflected the negative supercoils that are normally constrained by native nucleosomes. Upon thermal inactivation of topo II (lane 2), accumulation of (–)S was evidenced by a counterclockwise shift of the Lk distribution. However, the signals of DNA knots did not significantly change with the generation of (–)S (bottom gel, compare lanes 1 and 2). Figure 2D shows the analogous experiment conducted in  $\Delta top1 top2-4 TopA+$  cells. In this case, the typical Lk distribution constrained by native nucleosomes (top gel, lane 1) was shifted entirely clockwise after the thermal inactivation of topo II (lane 2), denoting the accumulation of (+)S in all the minichromosomes. Strikingly, in this condition, the signals of DNA knots increased markedly with the accumulation of (+)S



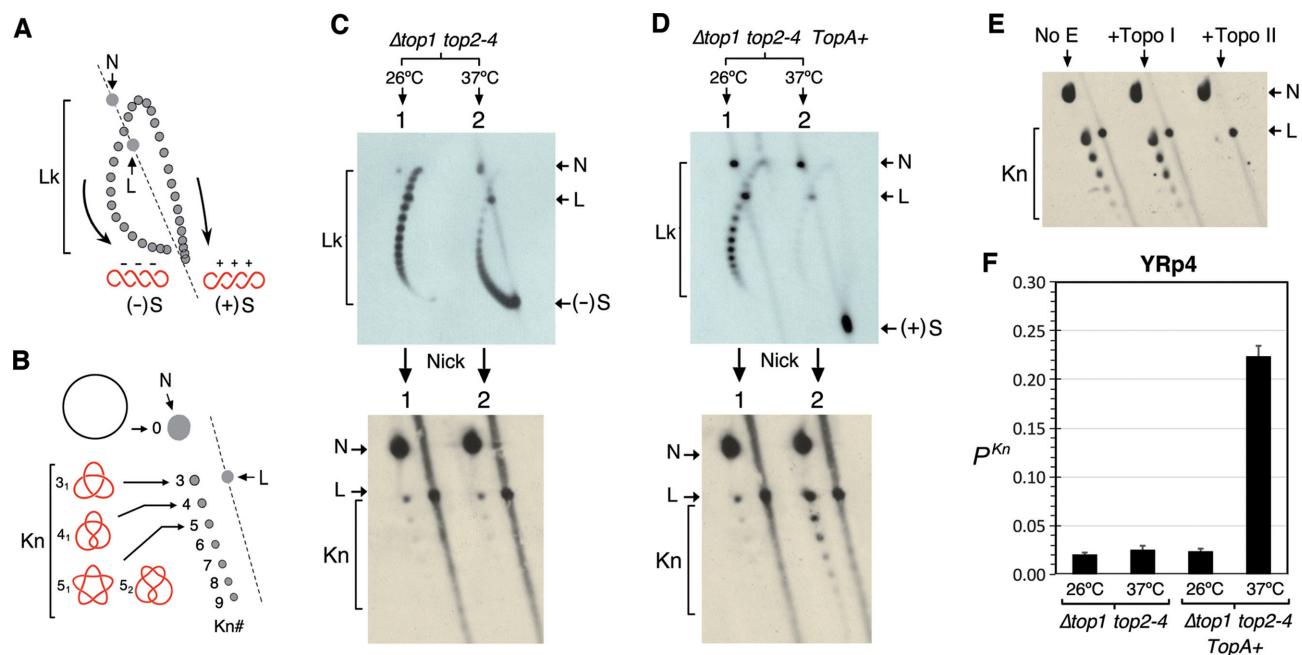


**Figure 2.** DNA knotting probability during (+) and (-) supercoiling of chromatin. (A) Lk distribution of DNA topoisomers (Lk) in a 2D-gel electrophoresis (first dimension, top to bottom; second dimension, left to right). Arrows denote Lk displacement upon increasing (+)S and (-)S of DNA; N, nicked DNA circles; L, linear DNA. (B) Relative position of unknotted (N) and knotted nicked DNA circles ( $Kn$ ) in a 2D-gel electrophoresis. The velocity of knotted molecules in the first gel dimension (top to bottom) correlates with their number of irreducible of DNA crossings ( $Kn\#$ ). Knots 3<sub>1</sub>, 4<sub>1</sub>, 5<sub>1</sub> and 5<sub>2</sub> are depicted. (C and D) DNA topology of YRp4 in  $\Delta top1 top2-4$  (C) and in  $\Delta top1 top2-4 TopA+$  (D) cells. Cells were sampled at 26°C (lane 1) and following 120 min at 37°C (lane 2). (E) Incubation of the nicked DNA sample of (+)S YRp4 (no E) with topo I and topo II activities *in vitro*. (F) DNA knotting probability ( $P^{Kn}$ ) of YRp4 in the four conditions analyzed in panels (C) and (D). Data in panel (F) are presented as mean  $\pm$  SD of three experiments.

(bottom gel, compare lanes 1 and 2). We corroborated that the increased signals were knots of double-stranded DNA by incubating the sample with topo I and topo II *in vitro*. As expected, only topo II was able to unknot the DNA and so reduce the increased signals (Figure 2E). Quantification of the DNA knot probability ( $P^{Kn}$ ) of YRp4 indicated that, prior to accumulation of (-)S or (+)S,  $P^{Kn}$  was  $\sim 0.02$ , similar to that previously observed in *TOP1 TOP2* cells (27).  $P^{Kn}$  did not change significantly with (-)S, but increased  $\sim 10$ -fold with (+)S (Figure 2F).

### (+) Supercoiling boosts DNA knotting probability and knot complexity

In previous studies, we showed that no significant changes of  $P^{Kn}$  occur in  $\Delta top1$  or  $top2-4$  cells, at either 26 or 37°C (27). For both these single mutants, since the action of topo II or topo I alone suffices to relax both (+)S and (-)S, the amount of transcriptional supercoiling is the same as *TOP1 TOP2* cells and so is the DNA knotting probability. Therefore, it is not likely that the boost of DNA knot formation observed in  $\Delta top1 top2-4 TopA+$  cells is an artifact due to manipulation of cellular topoisomerases. To discard the possibility that the increase of DNA knotting could be a product of the exogenous *TopA* activity, we examined knot formation in *TOP1 TOP2 TopA+* cells sampled at 26°C and following 120 min at 37°C (Figure 3A). In either condition, (+)S did not occur and  $P^{Kn}$  was about 0.02, similar to that observed in *TOP1 TOP2* cells (27) (Figure 3B). Likewise, to exclude the possibility that the increase of knot formation could be a singularity of YRp4, we examined the effect of

(-)S and (+)S on DNA knot formation in other chromatin constructs, such as the 2-micron circle, an endogenous 6.3-kb plasmid of *S. cerevisiae* (Figure 3C and D), and YEp24, a 7.6-kb circular minichromosome (Figure 3E and F). In all cases,  $P^{Kn}$  did not change significantly with (-)S, but increased about 10-fold with (+)S (Figure 3G and H).

To substantiate further the correlation of (+)S and knot formation, we compared the accumulation rate of (+)S molecules with that of knotted molecules by sampling the cells at different time points after inducing topo II inactivation (Figure 4A). DNA knot formation increased rapidly as soon as (+)S molecules started to appear, not before. However, whereas the accumulation of (+)S molecules continued until it became nearly complete after 100 min, the accumulation of DNA knots reached a plateau ( $P^{Kn}$  of  $\sim 0.2$ ) after 40–60 min of inducing topo II inactivation (Figure 4B, yellow bars). These distinct accumulation rates reflect the different mechanisms involved in DNA supercoiling and DNA knotting in the minichromosomes. Namely, upon inducing topo II inactivation, DNA transcription and relaxation of (-)S by *TopA* continue until virtually all minichromosomes are (+)S. Conversely, since  $P^{Kn}$  values result from the DNA knotting/unknotting balance produced by topo II, they change only as long as there is residual topo II activity. Consequently,  $P^{Kn}$  values stop increasing once topo II inactivation is complete. Since after 20–40 min of inducing topo II inactivation, the increased amount of knotted DNA molecules was nearly half the amount of (+)S molecules, the actual  $P^{Kn}$  in (+)S chromatin was  $\sim 0.5$  (Figure 4B, green bars). Therefore, the residual activity of topo II, assuming it



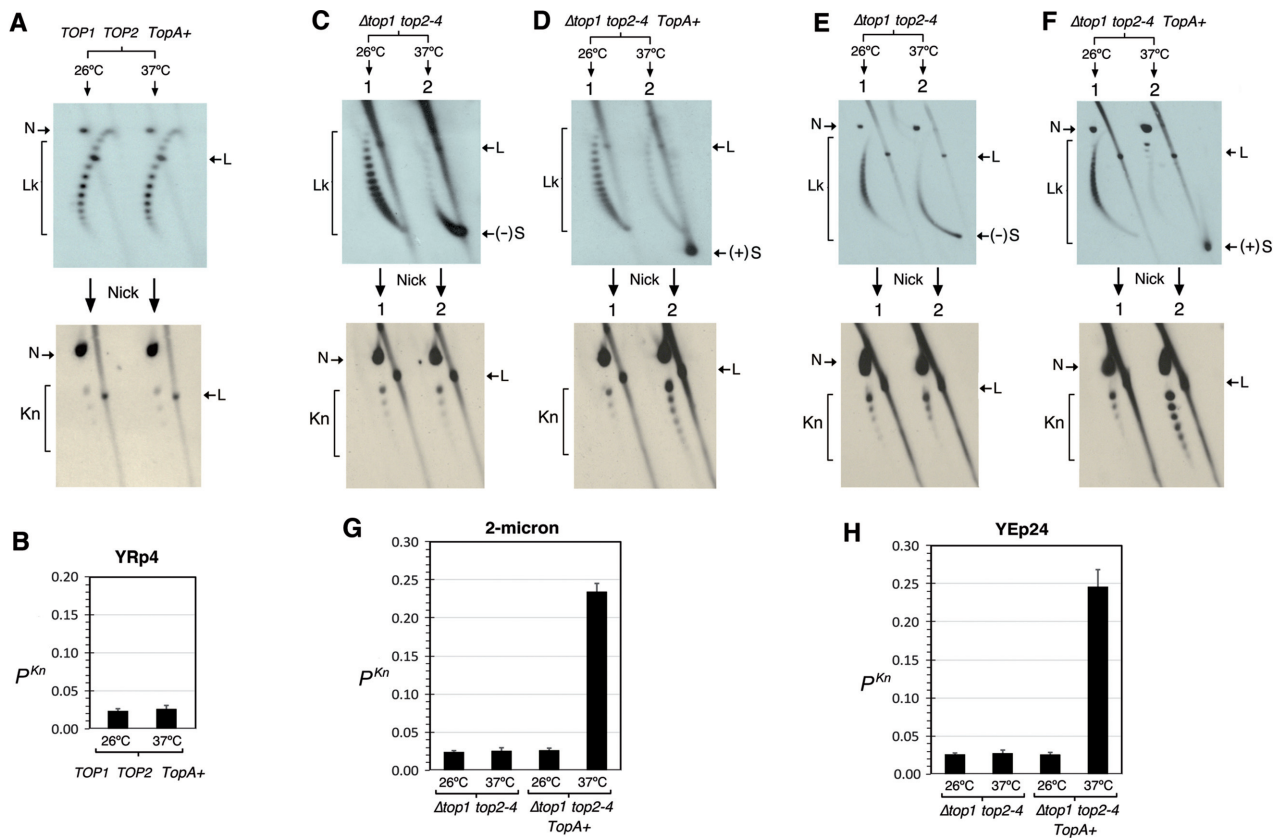


**Figure 3.** Increased knot formation is caused by (+) supercoiling of DNA. (A) DNA supercoiling and knotting of YRp4 in *TOP1 TOP2 TopA+* cells sampled at 26°C and following 120 min at 37°C. (B)  $P^{Kn}$  of YRp4 in *TOP1 TOP2 TopA+* cells. (C–F) DNA supercoiling and knotting of the 2-micron plasmid (C and D) and the YEp24 minichromosome (E and F) in  $\Delta top1 top2-4$  and in  $\Delta top1 top2-4 TopA+$  cells. Cells were sampled at 26°C (lane 1) and following 120 min at 37°C (lane 2). (–)S and (+)S, negatively and positively supercoiled DNA; Lk, linking number topoisomers; Kn, knotted DNA forms; N, nicked DNA circles; L, linear DNA molecules. (G and H)  $P^{Kn}$  of 2-micron and YEp24 in the conditions analyzed in panels (C) to (F). Data in panels (B), (G) and (H) are presented as mean  $\pm$  SD of three experiments.

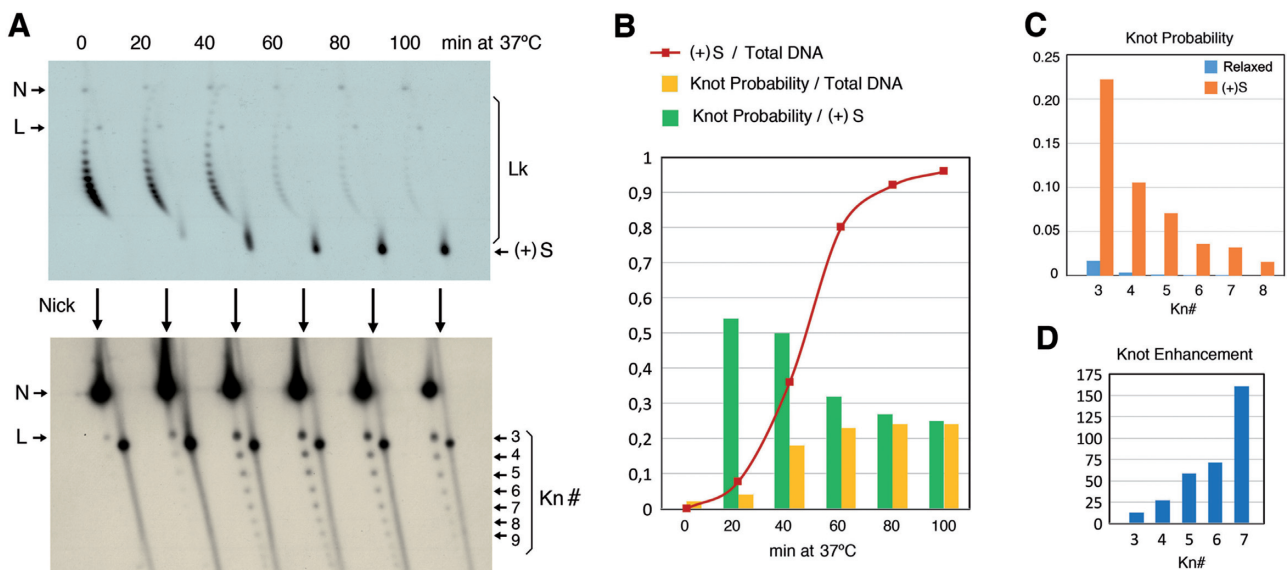


**Figure 4.** Correlation of (+)S with knot probability and complexity. (A) DNA supercoiling and knotting of YRp4 in  $\Delta top1 top2-4 TopA+$  cells sampled at different time points (min) after shifting the cultures to 37°C. (B) Comparison of the accumulation rate of (+)S (red),  $P^{Kn}$  values relative to total DNA (yellow) and  $P^{Kn}$  values relative to the fraction of (+)S DNA (green). (C) Probability of individual knot populations (Kn# 3–8) in cells sampled at 0 min (relaxed chromatin, blue) and after shifting them to 37°C for 100 min ((+)S chromatin, orange). (D) Enhancement of individual knot populations shown in panel (C) (Kn# 3–7) upon accumulation of (+)S.

to be the same for the wild-type and the thermosensitive mutant, increased 25-fold the basal  $P^{Kn}$  of intracellular DNA with accumulated (+)S.

We examined next whether the burst of DNA knot formation during (+)S of chromatin also changed the complexity of the knots. Both in relaxed and in (+)S chromatin, the knot  $3_1$  was the most abundant form followed by knot populations that gradually diminished as their  $Kn\#$  increased (Figure 4C). However, the enhancement of individual knot populations in (+)S markedly increased with knot complexity. The probability of knot  $3_1$  increased  $\sim 12$  times, that of knot  $4_1$   $\sim 25$  times and that of knots  $5_1 + 5_2$  over 60 times (Figure 4D). Therefore, (+)S increased both knot formation and knot complexity.

### Transcriptional supercoiling of DNA in *TOP1 TOP2* cells also increases DNA knot formation

Since (+)S is normally generated in front of the transcribing complexes, our results suggested that topo II-dependent DNA knotting should also increase during normal transcription in *TOP1 TOP2* cells. However, in our previous studies, we observed not only that transcription did not increase DNA knot formation, but also that it actually reduced the  $P^{Kn}$  values of the minichromosomes (27). These observations can be reasoned by considering that the lifetime of the transcriptional supercoils produced in the circular minichromosomes is probably extremely short. Not only are the transcriptional supercoils rapidly relaxed by cellular topoisomerases in *TOP1 TOP2* cells, but also the (+)S and (-)S waves quickly cancel each other at the opposite side of the transcribing complex in these circular constructs (Figure 5A). The transient wave of (+)S may thereby be too brief to establish a significant boost of topo II-mediated DNA knotting and alter the  $P^{Kn}$  values of the total population of minichromosomes. Basal  $P^{Kn}$  values could instead diminish due to the unfolded state of transcriptionally active chromatin (27).

The above premises led us to hypothesize that the transient increase of DNA knotting during DNA transcription in *TOP1 TOP2* cells could be perhaps detected in circular minichromosomes by preventing the cancellation of transcriptional supercoiling waves. To this end, we analyzed DNA knotting in a minichromosome (pRY121), in which high rates of bidirectional transcription are induced from the galactose-inducible *GAL1-GAL10* divergent promoter (29). In this minichromosome, high transcription rates preclude quick relaxation of DNA by cellular topoisomerases, whereas bidirectional transcription prevents the cancellation of (+) and (-) supercoiled domains (Figure 5A). We found that shifting *TOP1 TOP2* cells containing pRY121 from glucose- to galactose-containing media did not alter the basal DNA knot probability of the endogenous 2-micron plasmid (Figure 5B). However, the DNA knot probability of pRY121 increased  $\sim 3$ -fold following the galactose induction (Figure 5C and D). Remarkably, this increase of knot formation occurred with no net accumulation of (+)S or (-)S (Figure 5C), in agreement thus with the coexistence of twin supercoiled domains (Figure 5A). These results indicated that the boost of DNA knotting observed upon accumulation of (+)S in  $\Delta top1 top2-4 TopA+$  can also occur

during normal transcriptional supercoiling of DNA in *TOP1 TOP2* cells.

### DNA knots increase due to chromatin compaction driven by (+)S

*In vitro* studies have shown that topo II produces abundant and complex knots when DNA molecules are compacted (35–37). *In vitro* and *in vivo* studies have also indicated that (+)S rapidly compacts nucleosomal fibers (18,38,39). Therefore, we hypothesized that the burst of DNA knots observed *in vivo* was consequent to chromatin compaction driven by (+)S. In this respect, computer simulations of polymer chains have been useful to study the effect of compaction on knot probability and complexity (40–42). To test our notion, we then conducted numerical simulations of knot formation in nucleosomal fibers and examined the effect of compaction.

To obtain a representative beads-on-a-string model of the nucleosomal fiber, we generated random conformations of rings of  $N$  beads (nucleosomes) of diameter  $D$  connected by straight infinitely thin segments of length  $L$  (DNA linker) (Figure 6A). We then computed the knot probability of rings of 25 beads as a function of  $D/L$ . We found that the basal  $P^{Kn}$  of  $\sim 0.02$  observed *in vivo* in unconstrained minichromosomes containing  $\sim 25$  nucleosomes (e.g. YRp4) was matched by a  $D/L$  ratio of 0.47 (Figure 6B). We next used this reference model of the nucleosomal fiber to generate millions of random conformers and profiled this unbiased sample in terms of the impact of compaction on knot probability. To this end, we set various cutoff values for the gyration radius ( $R_g$ ) of the configurations and computed knot probabilities considering only those with a lower  $R_g$  (max  $R_g$ ). We then plotted the knot probability obtained for max  $R_g$  values relative to  $R_g^0$ , the gyration radius of the unconstrained distribution of conformers (Figure 6C). As expected,  $P^{Kn}$  values increased dramatically with increasing compaction. To reach the  $P^{Kn}$  of  $\sim 0.5$  produced by (+)S *in vivo*,  $R_g$  had to be reduced more than 60% relative to  $R_g^0$ , corresponding thus to a 5-fold volume compaction. We calculated next the enhancement of individual knot populations ( $3_1$ ,  $4_1$  and  $5_1 + 5_2$ ) produced by increasing compaction (Figure 6D). Akin to what was observed *in vivo*, the more complex a knot population the higher was its enhancement. Moreover, the enhancements of knots  $3_1$ ,  $4_1$  and  $5_1 + 5_2$  produced by (+)S *in vivo* (12, 25 and 60 times, respectively) all matched compression levels similar to those needed to increase  $P^{Kn}$  to 0.5 (i.e. a max  $R_g$  of  $\sim 60\%$  of  $R_g^0$ ). The simulation thus reproduced fairly well the spectrum of experimentally observed knots.

Finally, we asked how the compaction levels inferred from the simulation would correlate to DNA supercoiling. As an approximation to this problem, we computed the reduction of the radius of gyration of the conformers containing 25 beads ( $\langle R_g \rangle / R_g^0$ ) as a function of their absolute writhe ( $|Wr|$ ) (Figure 6E).  $R_g$  reduction correlated to increasing values of  $|Wr|$ , and the compaction levels needed to obtain the knot spectrum induced by (+)S *in vivo* involved  $|Wr|$  values  $\geq 9$ . These high  $Wr$  values are reachable *in vivo*, considering that the Lk of YRp4 increases more than 40 units when the minichromosome accumulates (+)S, and that

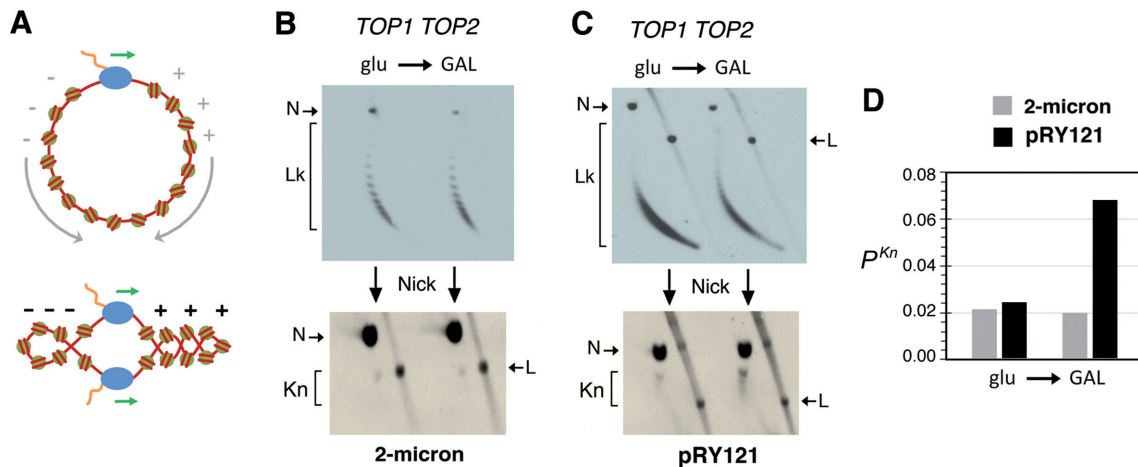


**Figure 5.** Transcriptional supercoiling increases knot formation in *TOP1 TOP2* cells. (A) Cancellation of the (+)S and (-)S waves generated by DNA transcription in circular minichromosomes (top) is precluded during bidirectional transcription, which produces separated (+)S and (-)S domains (bottom). (B and C) DNA supercoiling and knotting of the 2-micron plasmid (B) and the pRY121 minichromosome (C), which carries the *GAL1-GAL10* divergent promoter. *TOP1 TOP2* cells containing 2-micron and pRY121 were sampled during exponential growth at 26°C in glucose-containing media (glu) and after shifting them for 3 h in galactose-containing media (GAL); Lk, linking number topoisomers; Kn, knotted DNA forms; N, nicked DNA circles; L, linear DNA molecules. (D)  $P^{Kn}$  of 2-micron and pRY121 in the conditions analyzed in panels (B) and (C).

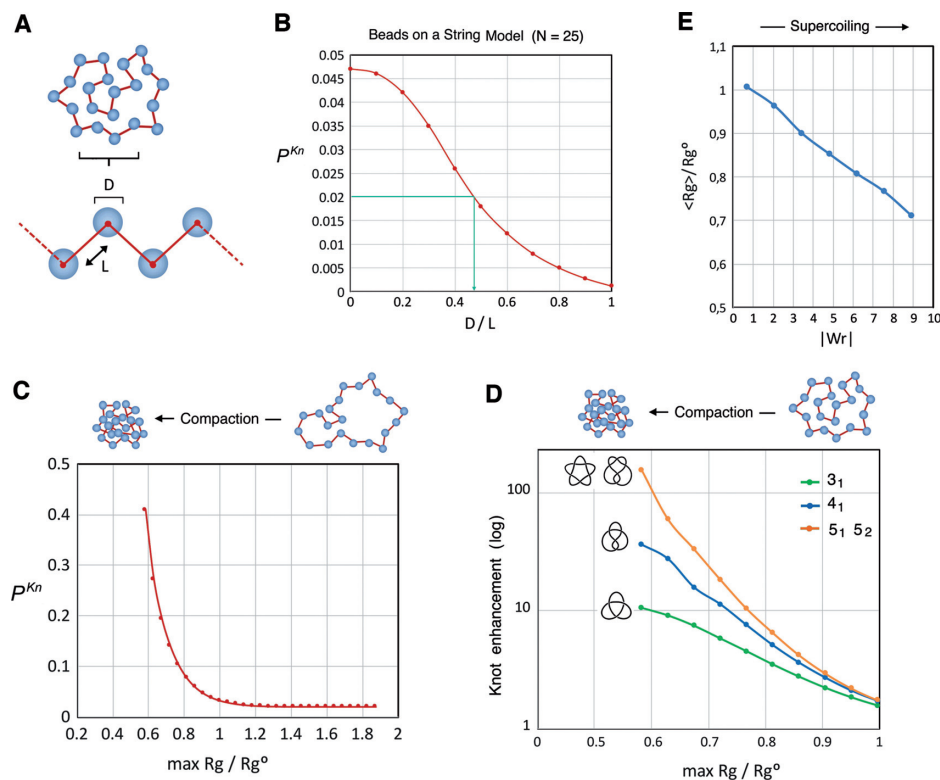


**Figure 6.** Computer simulations of the effect of chromatin compaction on DNA knot probability. (A) Beads-on-a-string model that simulates nucleosomal fibers. Beads of diameter  $D$  are connected by straight infinitely thin linkers of length  $L$ , such that the centers of two consecutive beads have a distance  $D + L$ . (B) Knot probability ( $P^{Kn}$ ) of random configurations of rings of 25 beads as a function of  $D/L$ . The  $P^{Kn}$  of 0.02 experimentally observed in unconstrained minichromosomes containing  $\sim 25$  nucleosomes is interpolated and matches  $D/L = 0.47$ . (C) Effect of compaction of knot probability.  $P^{Kn}$  values of the reference model of the nucleosomal fiber ( $N = 25$ ,  $D/L = 0.47$ ) are plotted as a function of the gyration radius ( $R_g$ ) of the random configurations. Each point computes the  $P^{Kn}$  of those configurations of  $R_g$  below a cutoff value ( $\max R_g$ ) relative to the average gyration radius of the entire distribution of conformers ( $R_g^0$ ). (D) Enhancement of individual knot populations by the effect of compaction. The enhancement of knots  $3_1$ ,  $4_1$  and  $5_1 + 5_2$  is computed for configurations of  $R_g$  below a cutoff value ( $\max R_g / R_g^0$ ). (E) Reduction of  $R_g / R_g^0$  as a function of the absolute writhe ( $|Wr|$ ). For each sampled conformation,  $R_g / R_g^0$  was computed and averaged for different (binned) ranges of  $|Wr|$ .



this Lk difference translates mostly into changes of Wr (9). The overall simulation data thus supported that the basal DNA knotting probability of minichromosomes ( $P^{Kn}$  0.02) increases ~25-fold ( $P^{Kn}$  0.5) as their nucleosomal fibers become compacted (a 5-fold volume reduction) during (+)S of DNA.

## DISCUSSION

The burst of DNA knots induced by (+)S in intracellular chromatin was not anticipated by previous theoretical models of the effect of supercoiling on knot formation and resolution. Computer simulations of polymer chains predicted that DNA supercoiling would inhibit DNA knotting (43). Supercoiling was also expected to facilitate DNA unknotting by topoisomerases by tightening the tangled regions (44–46) or confining them over biologically relevant timescales (44,47). Other mechanisms irrespective of DNA supercoiling were also expected to minimize knot formation in intracellular DNA. Topo II could use its *in vitro* capacity to reduce DNA knotting probability to levels below that of equilibrium conformations (48). DNA tracking motors, such as polymerases and condensins, could push and tighten DNA knots to facilitate their removal by topoisomerases (49). Clearly, none of these mechanisms appear to be effective to prevent the observed burst of DNA knots.

The alternative and simplest explanation for the increase of DNA knot formation is that (+)S compacts the nucleosomal fiber. In this respect, since interphase chromatin has a scaling behavior not dissimilar to that of a fractal globule (50,51), there is very little intermingling and so possible entanglements of DNA across topologically associating domains (TADs) and other high-order folds of chromatin (52,53). However, this is not the case within the length scales of nucleosomal fibers. Intramolecular DNA segments come in close proximity when nucleosome arrays are compacted by supercoiling or other mechanisms, thus increasing the incidence of DNA juxtapositions and thereby the chance that the DNA cross-inversion activity of topo II leads to DNA knots. Supporting this notion, topo II produces *in vitro* abundant and complex knots when DNA is compacted by supercoiling or other condensing agents (35–37). Likewise, numerical simulations demonstrated that the knotting probability and complexity of polymer chains largely increase by the effect of compaction (40–42). Our study extended these simulations of knot formation into a simplified model of the nucleosomal fiber. The results support that intracellular DNA knots are the statistically inevitable outcome of topo II activity, and show that the 25-fold increase of  $P^{Kn}$  and the knot spectrum induced by (+)S can be reproduced by reducing to 60% the radius of gyration of the nucleosomal fibers, which corresponds to a 5-fold volume compaction.

The burst of DNA knot formation as a consequence of chromatin compaction also accounts for the differential effects of (+)S and (–)S of DNA. *In vitro* studies have shown that DNA over-twisting compacts nucleosomal fibers quicker and further than DNA untwisting (38,39). *In vivo* studies have also indicated that chromosomal domains under (+)S are more compacted than those under (–)S (18). This asymmetry in the conformational response of chro-

matin to helical tension of DNA has already explained why topo II is more proficient in relaxing (+)S than (–)S *in vivo* (9,19). The possibility that (–)S was inhibiting DNA knotting by means of other mechanisms then seems unlikely. For instance, (–)S could promote the formation of extended RNA/DNA hybrids (54), which could preclude the activity of topo II (55). In this respect, our previous studies indicated that there are no R-loops or other molecular interactions stabilizing the (–)S accumulated in the minichromosomes (19). The different effects of (+)S and (–)S on DNA knot formation thus corroborate that (+)S compacts intracellular chromatin to a much larger extent than (–)S. DNA knot analysis thereby proved to be very revealing about the elusive architecture of chromatin *in vivo*.

The (+)S in the circular minichromosomes examined in our study is driven by DNA transcription (1,2). Eukaryotic RNA polymerases transcribe DNA at rates of ~100 bp/s, which means that DNA becomes over-twisted ~10 turns/s (56). The degree of (+)S attained in circular minichromosomes (supercoiling density > +0.04) thus denotes the lower limit against which the transcription machinery is able to elongate *in vivo* (9). This capacity of RNA polymerases to confront (+)S may be crucial to transcribe DNA along native chromosomes, in which twin supercoiling domains cannot be cancelled as in the case of circular minichromosomes. Moreover, high levels of (+)S may occur when transcribing complexes encounter twist diffusion barriers or converge with other transcribing units or replication forks. Topo II-mediated knotting of DNA in native chromosomes might then reach levels comparable to those observed in the circular minichromosomes. In normal conditions, though, the occurrence of these knots is likely to be short-lived because, as soon as (+)S is relaxed or dissipated, topo II activity must restore the basal knotting probability of intracellular chromatin. However, if (+)S levels remain elevated or topoisomerase activity is altered, DNA knots could then persist and obstruct DNA transcription and chromatin assembly, as it has been demonstrated *in vitro* with knotted DNA templates (26,57). Remarkably, this scenario could explain why inactivation of topo II in *TOP1 top2-ts* yeast cells produces the stalling of RNA polymerases during the transcription of long genes (25), and why this stalling is rescued by exogenous expression of type-2, but not type-1 topoisomerases that relax supercoils but cannot remove DNA knots (Figure 7A). The concurrence of DNA supercoiling and knotting might also account for the effects of topoisomerase dysfunction during the transcription of long genes in mammal cells (20–24). This dark side of the topo II activity should therefore be taken into account when interpreting structural and functional alterations of intracellular chromatin.

As in the case of transcriptional supercoiling, our results highlight that other processes that compact chromatin might concur with topo II-mediated knotting of the embedded DNA. In this respect, an interesting possibility is that DNA knotting might be exploited to stabilize specific chromatin conformations. Previous studies indicate that mitotic chromosomes are shaped by topo II-sensitive DNA entanglements (58), and that topo II activity is required for both resolution and formation of facultative heterochromatin (59). DNA knot formation and removal could operate, for instance, to lock and unlock conformational states of chro-

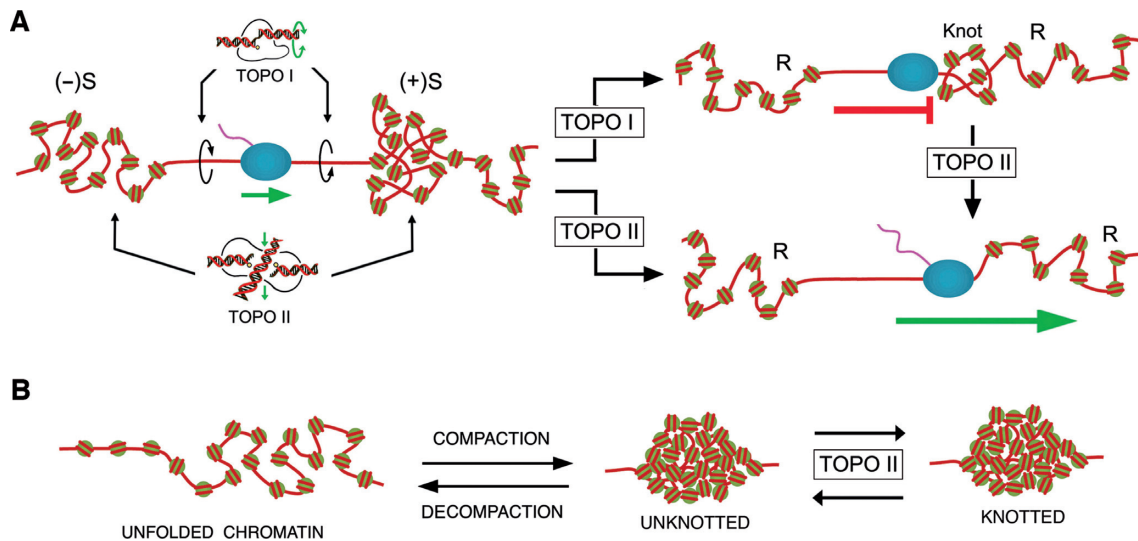


**Figure 7.** Implications of DNA knotting during gene transcription and chromatin compaction. (A) During normal DNA transcription, (+)S compacts chromatin and increases topo II-mediated knotting of DNA. Upon relaxation of (+)S, topo II dissolves DNA knots and transcription can continue. However, since topo I is not able to unknot DNA, the RNA polymerase is stalled by DNA knots when topo II fails to remove them. (B) Topo II-mediated knotting of DNA could be regulated to stabilize different conformational or compaction states of chromatin.

matin (Figure 7B). Future research will uncover whether intracellular DNA knots are the only statistically inevitable outcome of topo II activity or whether DNA knot formation is also actively regulated. So far, we have uncovered that the DNA knotting probability changes dramatically with chromatin dynamics. Therefore, in addition to removing DNA supercoils and replication intertwinings, topo II plays a crucial role in setting the DNA knotting–unknotting homeostasis of eukaryotic chromatin.

## ACKNOWLEDGEMENTS

*Author Contributions:* J.R. conceived the project. J.R. and A.V. designed experiments. A.V., J.S., O.D.-I., S.D and B.M.-G. performed experiments. L.C and C.M. conducted computer simulations. J.R. wrote the manuscript with inputs of C.M.

## FUNDING

Plan Estatal de Investigación Científica y Técnica of Spain [BFU2015-67007-P, MDM-2014-0435-02 to J.R., BES-2015-071597 to A.V.]; Italian Ministry of Education to C.M. Funding for open access charge: Plan Estatal de Investigación Científica y Técnica of Spain [BFU2015-67007-P].

*Conflict of interest statement.* None declared.

## REFERENCES

- Liu, L.F. and Wang, J.C. (1987) Supercoiling of the DNA template during transcription. *Proc. Natl. Acad. Sci. U.S.A.*, **84**, 7024–7027.
- Giaever, G.N. and Wang, J.C. (1988) Supercoiling of intracellular DNA can occur in eukaryotic cells. *Cell*, **55**, 849–856.
- Chen, S.H., Chan, N.L. and Hsieh, T.S. (2013) New mechanistic and functional insights into DNA topoisomerases. *Annu. Rev. Biochem.*, **82**, 139–170.
- Pommier, Y., Sun, Y., Huang, S.N. and Nitiss, J.L. (2016) Roles of eukaryotic topoisomerases in transcription, replication and genomic stability. *Nat. Rev. Mol. Cell Biol.*, **17**, 703–721.
- Stewart, L., Redinbo, M.R., Qiu, X., Hol, W.G. and Champoux, J.J. (1998) A model for the mechanism of human topoisomerase I. [see comments]. *Science*, **279**, 1534–1541.
- Wang, J.C. (1998) Moving one DNA double helix through another by a type II DNA topoisomerase: the story of a simple molecular machine. *Q. Rev. Biophys.*, **31**, 107–144.
- Roca, J. (2011) The torsional state of DNA within the chromosome. *Chromosoma*, **120**, 323–334.
- Vos, S.M., Tretter, E.M., Schmidt, B.H. and Berger, J.M. (2011) All tangled up: how cells direct, manage and exploit topoisomerase function. *Nat. Rev. Mol. Cell Biol.*, **12**, 827–841.
- Salceda, J., Fernandez, X. and Roca, J. (2006) Topoisomerase II, not topoisomerase I, is the proficient relaxase of nucleosomal DNA. *EMBO J.*, **25**, 2575–2583.
- Baranello, L., Wojtowicz, D., Cui, K., Devaiah, B.N., Chung, H.J., Chan-Salis, K.Y., Guha, R., Wilson, K., Zhang, X., Zhang, H. *et al.* (2016) RNA polymerase II regulates Topoisomerase I activity to favor efficient transcription. *Cell*, **165**, 357–371.
- Bermejo, R., Capra, T., Gonzalez-Huici, V., Fachinetti, D., Cocito, A., Natoli, G., Katou, Y., Mori, H., Kurokawa, K., Shirahige, K. *et al.* (2009) Genome-organizing factors Top2 and Hmo1 prevent chromosome fragility at sites of S phase transcription. *Cell*, **138**, 870–884.
- Sperling, A.S., Jeong, K.S., Kitada, T. and Grunstein, M. (2011) Topoisomerase II binds nucleosome-free DNA and acts redundantly with topoisomerase I to enhance recruitment of RNA Pol II in budding yeast. *Proc. Natl. Acad. Sci. U.S.A.*, **108**, 12693–12698.
- Nelson, P. (1999) Transport of torsional stress in DNA. *Proc. Natl. Acad. Sci. U.S.A.*, **96**, 14342–14347.
- Joshi, R.S., Pina, B. and Roca, J. (2010) Positional dependence of transcriptional inhibition by DNA torsional stress in yeast chromosomes. *EMBO J.*, **29**, 740–748.
- Bermudez, I., Garcia-Martinez, J., Perez-Ortin, J.E. and Roca, J. (2010) A method for genome-wide analysis of DNA helical tension by means of psoralen-DNA photobinding. *Nucleic Acids Res.*, **38**, e182.
- Teves, S.S. and Henikoff, S. (2014) Transcription-generated torsional stress destabilizes nucleosomes. *Nat. Struct. Mol. Biol.*, **21**, 88–94.
- Kouzine, F., Gupta, A., Baranello, L., Wojtowicz, D., Ben-Aissa, K., Liu, J., Przytycka, T.M. and Levens, D. (2013) Transcription-dependent dynamic supercoiling is a short-range genomic force. *Nat. Struct. Mol. Biol.*, **20**, 396–403.

18. Naughton, C., Avlonitis, N., Corless, S., Prendergast, J.G., Mati, I.K., Eijk, P.P., Cockroft, S.L., Bradley, M., Ylstra, B. and Gilbert, N. (2013) Transcription forms and remodels supercoiling domains unfolding large-scale chromatin structures. *Nat. Struct. Mol. Biol.*, **20**, 387–395.
19. Fernandez, X., Diaz-Ingelmo, O., Martinez-Garcia, B. and Roca, J. (2014) Chromatin regulates DNA torsional energy via topoisomerase II-mediated relaxation of positive supercoils. *EMBO J.*, **33**, 1492–1501.
20. Lyu, Y.L., Lin, C.P., Azarova, A.M., Cai, L., Wang, J.C. and Liu, L.F. (2006) Role of topoisomerase IIbeta in the expression of developmentally regulated genes. *Mol. Cell Biol.*, **26**, 7929–7941.
21. Ljungman, M. and Hanawalt, P.C. (1996) The anti-cancer drug camptothecin inhibits elongation but stimulates initiation of RNA polymerase II transcription. *Carcinogenesis*, **17**, 31–35.
22. Solier, S., Ryan, M.C., Martin, S.E., Varma, S., Kohn, K.W., Liu, H., Zeeberg, B.R. and Pommier, Y. (2013) Transcription poisoning by Topoisomerase I is controlled by gene length, splice sites, and miR-142-3p. *Cancer Res.*, **73**, 4830–4839.
23. Mabb, A.M., Kullmann, P.H., Twomey, M.A., Miriyala, J., Philpot, B.D. and Zylka, M.J. (2014) Topoisomerase I inhibition reversibly impairs synaptic function. *Proc. Natl. Acad. Sci. U.S.A.*, **111**, 17290–17295.
24. King, I.F., Yandava, C.N., Mabb, A.M., Hsiao, J.S., Huang, H.S., Pearson, B.L., Calabrese, J.M., Starmer, J., Parker, J.S., Magnuson, T. *et al.* (2013) Topoisomerases facilitate transcription of long genes linked to autism. *Nature*, **501**, 58–62.
25. Joshi, R.S., Pina, B. and Roca, J. (2012) Topoisomerase II is required for the production of long Pol II gene transcripts in yeast. *Nucleic Acids Res.*, **40**, 7907–7915.
26. Portugal, J. and Rodriguez-Campos, A. (1996) T7 RNA polymerase cannot transcribe through a highly knotted DNA template. *Nucleic Acids Res.*, **24**, 4890–4894.
27. Valdes, A., Segura, J., Dyson, S., Martinez-Garcia, B. and Roca, J. (2018) DNA knots occur in intracellular chromatin. *Nucleic Acids Res.*, **46**, 650–660.
28. Roca, J., Gartenberg, M.R., Oshima, Y. and Wang, J.C. (1992) A hit-and-run system for targeted genetic manipulations in yeast. *Nucleic Acids Res.*, **20**, 4671–4672.
29. West, R.W. Jr, Yocum, R.R. and Ptashne, M. (1984) *Saccharomyces cerevisiae* GAL1-GAL10 divergent promoter region: location and function of the upstream activating sequence UASG. *Mol. Cell Biol.*, **4**, 2467–2478.
30. Shuman, S., Golder, M. and Moss, B. (1988) Characterization of vaccinia virus DNA topoisomerase I expressed in *Escherichia coli*. *J. Biol. Chem.*, **263**, 16401–16407.
31. Worland, S.T. and Wang, J.C. (1989) Inducible overexpression, purification, and active site mapping of DNA topoisomerase II from the yeast *Saccharomyces cerevisiae*. *J. Biol. Chem.*, **264**, 4412–4416.
32. Diaz-Ingelmo, O., Martinez-Garcia, B., Segura, J., Valdes, A. and Roca, J. (2015) DNA topology and global architecture of point centromeres. *Cell Rep.*, **13**, 667–677.
33. Hanai, R. and Roca, J. (1999) Two-dimensional agarose-gel electrophoresis of DNA topoisomers. *Methods Mol. Biol.*, **94**, 19–27.
34. Trigueros, S., Arsuaga, J., Vazquez, M.E., Summers, D.W. and Roca, J. (2001) Novel display of knotted DNA molecules by two-dimensional gel electrophoresis. *Nucleic Acids Res.*, **29**, E67–67.
35. Hsieh, T. (1983) Knotting of the circular duplex DNA by type II DNA topoisomerase from *Drosophila melanogaster*. *J. Biol. Chem.*, **258**, 8413–8420.
36. Wasserman, S.A. and Cozzarelli, N.R. (1991) Supercoiled DNA-directed knotting by T4 topoisomerase. *J. Biol. Chem.*, **266**, 20567–20573.
37. Roca, J., Berger, J.M. and Wang, J.C. (1993) On the simultaneous binding of eukaryotic DNA topoisomerase II to a pair of double-stranded DNA helices. *J. Biol. Chem.*, **268**, 14250–14255.
38. Bancaud, A., Conde e Silva, N., Barbi, M., Wagner, G., Allemand, J.F., Mozziconacci, J., Lavelle, C., Croquette, V., Victor, J.M., Prunell, A. *et al.* (2006) Structural plasticity of single chromatin fibers revealed by torsional manipulation. *Nat. Struct. Mol. Biol.*, **13**, 444–450.
39. Lavelle, C., Victor, J.M. and Zlatanova, J. (2010) Chromatin fiber dynamics under tension and torsion. *Int. J. Mol. Sci.*, **11**, 1557–1579.
40. Arsuaga, J., Vazquez, M., Trigueros, S., Summers, D. and Roca, J. (2002) Knotting probability of DNA molecules confined in restricted volumes: DNA knotting in phage capsids. *Proc. Natl. Acad. Sci. U.S.A.*, **99**, 5373–5377.
41. Micheletti, C., Marenduzzo, D., Orlandini, E. and Summers, D.W. (2008) Simulations of knotting in confined circular DNA. *Biophys. J.*, **95**, 3591–3599.
42. Marenduzzo, D., Micheletti, C. and Orlandini, E. (2010) Biopolymer organization upon confinement. *J. Phys. Condens. Matter*, **22**, 283102.
43. Burnier, Y., Dorier, J. and Stasiak, A. (2008) DNA supercoiling inhibits DNA knotting. *Nucleic Acids Res.*, **36**, 4956–4963.
44. Buck, G.R. and Zechiedrich, E.L. (2004) DNA disentangling by type-2 topoisomerases. *J. Mol. Biol.*, **340**, 933–939.
45. Witz, G. and Stasiak, A. (2010) DNA supercoiling and its role in DNA decatenation and unknotting. *Nucleic Acids Res.*, **38**, 2119–2133.
46. Witz, G., Dietler, G. and Stasiak, A. (2011) Tightening of DNA knots by supercoiling facilitates their unknotting by type II DNA topoisomerases. *Proc. Natl. Acad. Sci. U.S.A.*, **108**, 3608–3611.
47. Coronel, L., Suma, A. and Micheletti, C. (2018) Dynamics of supercoiled DNA with complex knots: large-scale rearrangements and persistent multi-strand interlocking. *Nucleic Acids Res.*, **46**, 7533–7541.
48. Rybenkov, V.V., Ullsperger, C., Vologodskii, A.V. and Cozzarelli, N.R. (1997) Simplification of DNA topology below equilibrium values by type II topoisomerases. *Science*, **277**, 690–693.
49. Racko, D., Benedetti, F., Dorier, J. and Stasiak, A. (2018) Transcription-induced supercoiling as the driving force of chromatin loop extrusion during formation of TADs in interphase chromosomes. *Nucleic Acids Res.*, **46**, 1648–1660.
50. Grosberg, A., Rabin, Y., Havlin, S. and Neer, A. (1993) Crumpled globule model of the three-dimensional structure of DNA. *Europhys. Lett.*, **23**, 373–378.
51. Mirny, L.A. (2011) The fractal globule as a model of chromatin architecture in the cell. *Chromosome Res.*, **19**, 37–51.
52. Lieberman-Aiden, E., van Berkum, N.L., Williams, L., Imakaev, M., Ragozy, T., Telling, A., Amit, I., Lajoie, B.R., Sabo, P.J., Dorschner, M.O. *et al.* (2009) Comprehensive mapping of long-range interactions reveals folding principles of the human genome. *Science*, **326**, 289–293.
53. Stevens, T.J., Lando, D., Basu, S., Atkinson, L.P., Cao, Y., Lee, S.F., Leeb, M., Wohlfahrt, K.J., Boucher, W., O’Shaughnessy-Kirwan, A. *et al.* (2017) 3D structures of individual mammalian genomes studied by single-cell Hi-C. *Nature*, **544**, 59–64.
54. El Hage, A., French, S.L., Beyer, A.L. and Tollervy, D. (2010) Loss of Topoisomerase I leads to R-loop-mediated transcriptional blocks during ribosomal RNA synthesis. *Genes Dev.*, **24**, 1546–1558.
55. Wang, Y., Thyssen, A., Westergaard, O. and Andersen, A.H. (2000) Position-specific effect of ribonucleotides on the cleavage activity of human topoisomerase II. *Nucleic Acids Res.*, **28**, 4815–4821.
56. Dunder, M., Hoffmann-Rohrer, U., Hu, Q., Grummt, I., Rothblum, L.I., Phair, R.D. and Misteli, T. (2002) A kinetic framework for a mammalian RNA polymerase in vivo. *Science*, **298**, 1623–1626.
57. Rodriguez-Campos, A. (1996) DNA knotting abolishes in vitro chromatin assembly. *J. Biol. Chem.*, **271**, 14150–14155.
58. Kawamura, R., Pope, L., MO, C., Sun, M., Terekova, K., Boege, F., M’ielke, C., Andersen, A. and Marko, J. (2010) Mitotic chromosomes are constrained by topoisomerase II-sensitive DNA entanglements. *J. Cell Biol.*, **188**, 653–663.
59. Miller, E.L., Hargreaves, D.C., Kadoch, C., Chang, C.Y., Calarco, J.P., Hodges, C., Buenrostro, J.D., Cui, K., Greenleaf, W.J., Zhao, K. *et al.* (2017) TOP2 synergizes with BAF chromatin remodeling for both resolution and formation of facultative heterochromatin. *Nat. Struct. Mol. Biol.*, **24**, 344–352.

---


# Article #3

---





# Condensin minimizes topoisomerase II-mediated entanglements of DNA *in vivo*

Sílvia Dyson, Joana Segura, Belén Martínez-García, Antonio Valdés & Joaquim Roca\* 

## Abstract

The juxtaposition of intracellular DNA segments, together with the DNA-passage activity of topoisomerase II, leads to the formation of DNA knots and interlinks, which jeopardize chromatin structure and gene expression. Recent studies in budding yeast have shown that some mechanism minimizes the knotting probability of intracellular DNA. Here, we tested whether this is achieved via the intrinsic capacity of topoisomerase II for simplifying the equilibrium topology of DNA; or whether it is mediated by SMC (structural maintenance of chromosomes) protein complexes like condensin or cohesin, whose capacity to extrude DNA loops could enforce dissolution of DNA knots by topoisomerase II. We show that the low knotting probability of DNA does not depend on the simplification capacity of topoisomerase II nor on the activities of cohesin or Smc5/6 complexes. However, inactivation of condensin increases the occurrence of DNA knots throughout the cell cycle. These results suggest an *in vivo* role for the DNA loop extrusion activity of condensin and may explain why condensin disruption produces a variety of alterations in interphase chromatin, in addition to persistent sister chromatid interlinks in mitotic chromatin.

**Keywords** chromatin; DNA knot; DNA loop extrusion; DNA topology; SMC complex

**Subject Categories** Chromatin, Transcription & Genomics; DNA Replication, Recombination & Repair

**DOI** 10.15252/emboj.2020105393 | Received 23 April 2020 | Revised 10

September 2020 | Accepted 7 October 2020 | Published online 6 November 2020

**The EMBO Journal (2021) 40: e105393**

## Introduction

Type-2A topoisomerases, such as bacterial topo IV and eukaryotic topo II, pass one segment of duplex DNA through the transient double-stranded DNA break that they produce in another segment (Wang, 1998). This DNA-passage activity is essential to remove the intertwinings generated between newly replicated DNA molecules and to modulate DNA supercoiling during genome transactions (Corbett & Berger, 2004; Nitiss, 2009). However, the activity of type-2A topoisomerases also entails important threats. Firstly, the DNA cleaving step can be a source of chromosomal damage (Nitiss &

Wang, 1996). Secondly, the DNA-passage activity can entangle DNA molecules that are closely packed or folded via protein-DNA interactions (Hsieh, 1983; Wasserman & Cozzarelli, 1991; Roca *et al.*, 1993). Indeed, computer simulations have predicted that DNA molecules confined in biological systems would be massively entangled if type-2A topoisomerases could freely equilibrate their global topology (Arsuaga *et al.*, 2002; Micheletti *et al.*, 2008; Dorier & Stasiak, 2009). Fortunately, this prospect does not occur because the hierarchical folding of chromatin, which has a scaling behavior similar to that of a fractal globule, drastically reduces the topological complexity of chromosomes (Lieberman-Aiden *et al.*, 2009; Mirny, 2011). Accordingly, 3D analyses of the eukaryotic nuclear architecture revealed little intermingling of chromosomal territories and large chromatin domains (Denker & de Laat, 2016; Schmitt *et al.*, 2016). Reconstruction of 3D paths of high-order chromatin fibers in individual cells also evidenced the scarcity of long-range entanglements (Siebert *et al.*, 2017; Stevens *et al.*, 2017; Sulkowska *et al.*, 2018).

The hierarchical architecture of chromatin, however, cannot prevent the formation of DNA interlinks between chromatin fibers that come in close proximity or the formation of DNA knots within clusters of nucleosomes. Another mechanism must thereby operate to avoid these local DNA entanglements. This is exemplified by the sister chromatid interlinks (SCI), which are eliminated during prophase, even though sister chromatids remain cohesed until metaphase (Nagasaka *et al.*, 2016). Further evidence of such mechanism also emerged from the analysis of the knotting probability ( $P^{kn}$ ) of intracellular chromatin (Valdes *et al.*, 2018). These studies revealed that topo II-mediated knotting and unknotting of DNA normally occur within stretches of 10 to 60 nucleosomes (Fig 1A). However, the  $P^{kn}$  of chromatin does not scale proportionately to DNA length, as would be expected for any polymer chain. The slope of  $P^{kn}$  is progressively reduced in domains larger than 20 nucleosomes (Valdes *et al.*, 2018), as if some mechanism were counteracting the potential entanglement of intracellular DNA (Fig 1B).

Two mechanisms have been hypothesized that could minimize the entanglement of DNA *in vivo*. The first one relies on the intrinsic capacity of type-2A topoisomerases to simplify the equilibrium topology of DNA molecules in free solution (Rybenkov *et al.*, 1997). Namely, topo II uses a three-gate mechanism to pass one segment of DNA (T-segment) through another (G-segment) in an ATP-dependent manner (Wang, 1998). Upon topo II binding to the G-segment,

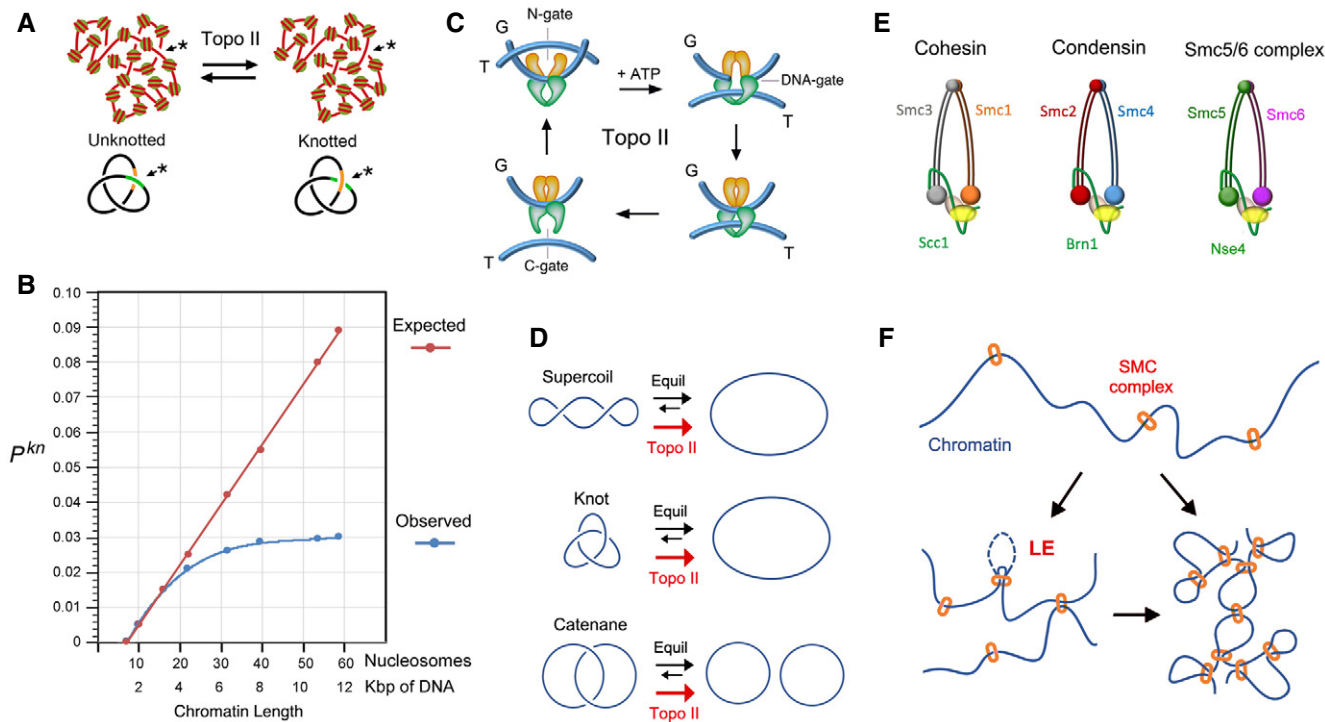


**Figure 1. Knotting probability of intracellular DNA and plausible regulatory mechanisms.**

A Topo II activity on random juxtapositions of DNA segments (\*) produces steady-state fractions of DNA knots in intracellular chromatin.  
 B DNA knotting probability ( $P^{kn}$ ) of intracellular chromatin (observed) does not scale proportionally to the length of DNA (expected). The slope of  $P^{kn}$  is reduced in chromatin stretches larger than 20 nucleosomes. Data from (Valdes *et al.*, 2018).  
 C Three-gate mechanism of topo II to pass one segment of DNA (T-segment) through another (G-segment). Upon ATP binding, the T-segment is captured by the entrance gate (N-gate) and passed through the transiently cleaved G-segment (DNA-gate). Upon re-ligation of the G-segment, the T-segment is released through the exit gate (C-gate).  
 D Topo II activity reduces the fractions of DNA supercoils, knots and catenates to below the topological equilibrium values (see details in Fig EV1).  
 E Architecture of the SMC complexes of *S. cerevisiae*. The Smc heterodimers (Smc1-Smc3, Smc2-Smc4, Smc5-Smc6) and kleisin (Scc1, Brn1, Nse4) subunits of cohesin, condensin, and the Smc5/6 complex are indicated.  
 F SMC complexes entrap segments of DNA to form chromatin loops and/or bridge nearby chromatin domains. Their loop extrusion activity (LE) ensures the co-entrapment of contiguously oriented intramolecular DNA segments.

the T-segment is captured by closing the entrance gate (N-gate) of the enzyme. The T-segment is then passed through the transiently cleaved G-segment (DNA-gate), and it is released outside the enzyme through the exit gate (C-gate) (Fig 1C). This mechanism allows DNA supercoils, knots, and catenates to be reduced. However, when topo II relaxes supercoiled DNA, it produces a linking number (Lk) distribution of DNA topoisomers that is narrower than the equilibrium Lk distribution (Figs 1D and EV1A). Likewise, when topo II unknots or decatenates DNA molecules, it reduces the fraction of knotted and catenated molecules to values below the topological equilibrium (Figs 1D and EV1B). The mechanism by which topo II is able to assess and locally reduce the equilibrium topology of large DNA molecules remains mysterious (Vologodskii, 2016). Moreover, the physiological relevance of this simplification activity is unknown since it has never been assessed *in vivo*. Yet, *in vitro* studies have shown that topo II does not simplify the equilibrium topology of DNA when the enzyme activity is quenched with the inhibitor ICRF-193 (Fig EV2A) or when the C-gate of the enzyme is deleted (Fig EV2B) (Martinez-Garcia *et al.*, 2014; Thomson *et al.*, 2014). These two observations opened up the

possibility to target the simplification activity of intracellular topo II and test whether that affects the  $P^{kn}$  of chromatin.

The second mechanism that could reduce intracellular DNA entanglements relies on the activity of structural maintenance of chromosomes (SMC) complexes, which are mainly identified as cohesin, condensin, and the Smc5/6 complex in eukaryotic cells (Uhlmann, 2016; Yatskevich *et al.*, 2019). Cohesin generates the DNA loops that organize chromatin during interphase and holds sister chromatids together from S-phase until metaphase (Onn *et al.*, 2008; Nasmyth & Haering, 2009). Condensin plays a key role in the compaction and individualization of chromatids during cell divisions (Hirano, 2012). The Smc5/6 complex has been mainly implicated in DNA repair via homologous recombination (Aragon, 2018). Despite their distinct roles, SMCs have similar architecture. They are large rod-shaped proteinic ensembles composed of a trimeric core formed by a heterodimer of Smc ATPases and a conserved kleisin, in addition to several additional regulatory subunits (Fig 1E). ATP binding and hydrolysis produce the opening and closure of distinct SMC compartments, which can embrace one or more segments of DNA (Hassler *et al.*, 2018; Yatskevich *et al.*, 2019).

Moreover, ATP usage can produce the translocation of the SMC complex along DNA (Terakawa *et al*, 2017) and the extrusion of DNA loops (Ganji *et al*, 2018; Davidson *et al*, 2019; Kim *et al*, 2019) (Fig 1F). The notion that SMCs can promote the removal of DNA entanglements was proposed in the context of sister chromatid resolution (Sen *et al*, 2016; Piskadlo *et al*, 2017). Former studies suggested that positive supercoils generated by condensin in mitotic chromosomes could produce a bias in topo II activity to eliminate the SCIs (Baxter *et al*, 2011; Sen *et al*, 2016). Subsequent computational simulations showed that DNA loop extrusion activity of SMCs would constrict DNA entanglements and so bias topo II to disentangle intermixed chromosomes (Goloborodko *et al*, 2016a) and minimize the occurrence of DNA knots (Racko *et al*, 2018; Orlandini *et al*, 2019).

Here, we show that precluding the capacity of topo II to simplify equilibrium topology of DNA does not alter the low knotting probability of intracellular chromatin. Inactivation of cohesin or the *smc5/6* complex also does not increase knot formation. However, inactivation of condensin markedly increases the occurrence of chromatin knots throughout the cell cycle. We propose that the requirement of condensin to minimize DNA entanglements might rely on its DNA loop extrusion activity. This function could explain the wide range of alterations that condensin inactivation produces both in interphase and mitotic chromatin.

## Results

### Topoisomerase II does not minimize the knotting probability of chromatin

We used two experimental approaches to assess whether the capacity of topo II to simplify the equilibrium topology of DNA was sustaining the low knotting probability ( $P^{kn}$ ) of intracellular chromatin. First, we used the topo II inhibitor ICRF-193 to impair the simplification activity of cellular topo II (Fig EV2A) (Martinez-Garcia *et al*, 2014). We carried out this experiment in a  $\Delta top1 TOP2$  yeast strain that hosted the circular minichromosome YEp13 (10.7 Kb) as the reporter of  $P^{kn}$  (Fig 2A). To verify that the simplification capacity of yeast topo II was targeted by ICRF-193, we added to crude lysates of the cells a negatively supercoiled DNA plasmid (YEp24, 7.8 Kb), which served as internal control of topo II activity (Fig 2A). When YEp24 was relaxed by a purified type-1B topoisomerase (topo I) (Fig 2B, lanes 1 and 2), it produced an equilibrium distribution of Lk topoisomers (Fig EV1A). However, when YEp24 was relaxed by the topo II activity present in the cell lysates, it produced a distribution of Lk topoisomers that was narrower than the equilibrium Lk distribution generated by topo I (Fig 2B, compare Lk plots of lanes 2 and 3). When we quenched the topo II activity by adding ICRF-193 to the mixture, the Lk distribution of YEp24 became broadened to an extent similar to that of the equilibrium Lk distribution (Fig 2B, compare Lk plots of lanes 2 and 4). Therefore, cellular topo II was able to simplify the equilibrium topology of naked DNA and this capacity was canceled by ICRF-193. We then examined what happened to the topology of the YEp13 minichromosome present in the above mixtures before and after the addition of ICRF-193 (Fig 2C). To this end, we first ran a 2D-gel electrophoresis containing chloroquine (Hanai & Roca, 1999) to resolve the Lk

distribution of the YEp13 DNA (Fig EV3). Before adding ICRF-193, YEp13 presented a distribution of topoisomers of negative  $\Delta Lk$  values (Fig 2C, Lk) consistent with the negative supercoils constrained by nucleosomes (Segura *et al*, 2018) (Fig EV3). Following the addition of ICRF-193, the Lk distribution of YEp13 was not significantly altered, which contrasted to what was observed in the control plasmid YEp24 (compare Lk plots in Fig 2C and 2B). Next, we nicked the DNA samples and ran a different 2D gel electrophoresis to reveal DNA knots (Trigueros *et al*, 2001) (Fig EV4). Both before and after adding ICRF-193, YEp13 presented a similar ladder of knotted molecules (Fig 2C, Kn), which started with the knot of three irreducible crossings (trefoil knot or  $3_1$ ) as the most abundant form (Fig EV4). We calculated  $P^{kn}$  as the relative abundance of total knotted molecules with respect to the total amount of unknotted and knotted DNA circles. In agreement with previous studies, the  $P^{kn}$  of YEp13 was about 0.03 (Valdes *et al*, 2018), three times lower than the value expected if  $P^{kn}$  scaled proportionally to DNA length (Fig 1B). Following the addition of ICRF-193, the  $P^{kn}$  of YEp13 was not significantly altered (Fig 2C).

Our second approach to test the simplification activity of topo II on chromatin was via the expression of a truncated topo II (*Top2- $\Delta 83$* ), in which the C-gate was removed (Martinez-Garcia *et al*, 2014) (Fig 2D, Fig EV2B). Similar to the type-2B class of topoisomerases that innately lack a C-gate (Fig EV2C), *Top2- $\Delta 83$*  is able to reduce DNA topology constraints but cannot simplify the equilibrium topology of free DNA (Martinez-Garcia *et al*, 2014; Thomson *et al*, 2014). We used the galactose-inducible *pGal1* promoter to express in  $\Delta top1 top2-4$  yeast cells either *Top2- $\Delta 83$*  or *TOP2* (full-length topo II) enzymes (Fig 2D). Upon inactivation of the *top2-4* thermo-sensitive allele, we examined the effects of the expressed enzymes on the topology of the control plasmid YEp24 and the minichromosome Yep13 present in these cells. As expected, in cells expressing *TOP2*, YEp24 was relaxed and presented a narrow (i.e., simplified) distribution of Lk topoisomers, whereas in cells expressing *Top2- $\Delta 83$* , the resulting Lk distribution was wider (Fig 2E). However, neither the Lk distribution nor the knotting probability of the Yep13 minichromosome was altered in the presence of the *TOP2* and *Top2- $\Delta 83$*  activities (Fig 2F). Therefore, in concordance with the ICRF-193 results, precluding the simplification capacity of topo II did not produce any significant effect on the topology of chromatinized DNA.

### Condensin inactivation boosts the occurrence of chromatin knots

To test whether the low knotting probability of intracellular DNA was achieved via the activity of SMC complexes, we examined the DNA topology of the Yep13 minichromosome in yeast strains previously characterized for carrying thermo-sensitive mutations that inactivate either condensin (*smc2-8*) (Freeman *et al*, 2000), cohesin (*scc1-73*) (Michaelis *et al*, 1997), or the Smc5/6 complex (*smc6-9*) (Torres-Rosell *et al*, 2005) (Appendix Fig S2). In each case, we grew the cells at a permissive temperature (26°C) and, upon reaching the exponential phase (OD 0.6-0.8), we shifted one half of the cultures to 35°C for 60 min. We then fixed the topology of intracellular DNA by quenching the cells with a cold ethanol-toluene solution and extracted their total DNA (Diaz-Ingelmo *et al*, 2015). As in the foregoing experiments, we ran a 2D-gel electrophoresis to examine the distribution of Lk topoisomers of YEp13; and we nicked the DNA to

examine the occurrence of DNA knots in a different 2D gel electrophoresis.

The Lk distribution of YEp13 in the three strains presented negative  $\Delta Lk$  values, which were not significantly altered upon inactivation of condensin, cohesin, or the Smc5/6 complex (Fig 3A-C).

Likewise, before inactivation of the SMCs, the knotting probability of YEp13 was low and similar in the three strains ( $p^{kn} \approx 0.03$ ) (Fig 3A-C). This concordance indicated that the knot minimization mechanism is robust and performs equally in most cells. However, upon inactivation of condensin,  $p^{kn}$  of YEp13 increased about

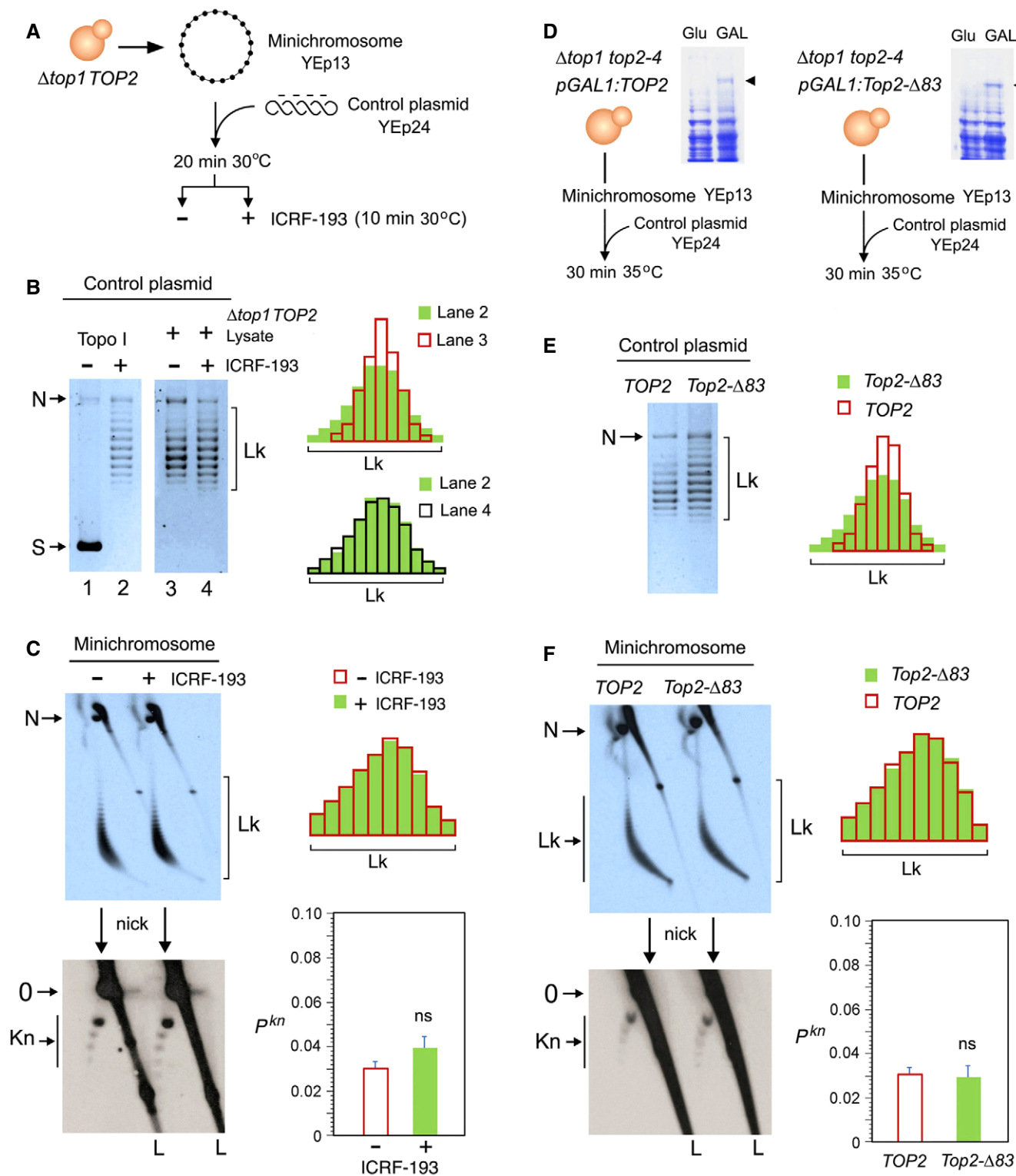


Figure 2.

**Figure 2. Topoisomerase II does not minimize the knotting probability of chromatin.**

- A Experimental layout to test the DNA topology simplification activity of cellular topo II upon the addition of ICRF-193.
- B Lanes 1 and 2: negatively supercoiled plasmid (YE<sub>p</sub>24) and its equilibrium distribution of Lk topoisomers upon its relaxation with Topo I. Lanes 3 and 4: distribution of Lk topoisomers of YE<sub>p</sub>24 upon its relaxation in lysates of  $\Delta top1 TOP2$  yeast cells in absence and after the addition of ICRF-193. Plots compare the relative intensity of individual topoisomers of the Lk distributions in lanes 2, 3, and 4.
- C Top: 2D gel electrophoresis of the Lk distributions of the YE<sub>p</sub>13 minichromosome present in the lysates of  $\Delta top1 TOP2$  yeast cells before and after the addition of ICRF-193 (see details in Fig EV3). Plots compare the relative intensity of the Lk distributions (divided into ten sections). Bottom: 2D gel electrophoresis of the same samples upon nicking the DNA in order to reveal the occurrence of knots (see details in Fig EV4). The graph shows  $P^{kn}$  of YE<sub>p</sub>13 (mean  $\pm$  SD from three independent experiments). P-values (Student's t test): ns,  $P > 0.05$ .
- D Experimental layout to compare the activities of *TOP2* and *Top2- $\Delta 83$*  on DNA and chromatin. Arrowheads indicate the extrachromosomal expression of *TOP2* and *Top2- $\Delta 83$*  under the inducible *pGAL1* promoter.
- E Lk distributions of the control plasmid (YE<sub>p</sub>24) relaxed by lysates of  $\Delta top1 top2-4$  yeast cells that expressed *TOP2* or *Top2- $\Delta 83$* . Plots compare the relative intensity of individual Lk topoisomers.
- F Top: 2D gel electrophoresis of the Lk distributions of the YE<sub>p</sub>13 minichromosome produced in the presence of *TOP2* or *Top2- $\Delta 83$* . Plots compare the relative intensity of the Lk distributions (divided into ten sections). Bottom: 2D gel electrophoresis of the same samples upon nicking the DNA in order to reveal the occurrence of knots. Graph:  $P^{kn}$  of YE<sub>p</sub>13 (mean  $\pm$  SD from three independent experiments).
- Gel signals are: N, nicked DNA circles; S, supercoiled DNA; L, diagonal of linear DNA fragments; Lk, distribution of Lk topoisomers; 0, unknotted DNA (nicked); Kn, ladder of knotted forms (nicked). P-values (Student's t test): ns,  $P > 0.05$ .

threefold ( $P^{kn} \approx 0.09$ ) (Fig 3A). Inactivation of cohesin produced a slight yet not significant reduction ( $P^{kn} \approx 0.02$ ) (Fig 3B). Inactivation of the Smc5/6 complex did not change the knot abundance (Fig 3C). To verify that the *smc2-8* allele was causing the threefold increase of  $P^{kn}$ , we introduced this mutation in strains JCW25 (*TOP2*) and JCW26 (*top2-4*) (Trigueros & Roca, 2001). Upon shifting these cells to 35°C, the  $P^{kn}$  of YE<sub>p</sub>13 increased again about threefold in the *smc2-8 TOP2* cells (Fig EV5). However, DNA knot formation did not change in the *smc2-8 top2-4* double mutant, which corroborated that topo II activity is required to produce the  $P^{kn}$  changes induced by condensin (Fig EV5).

Since the above experiments were done in asynchronous cell cultures, we considered whether the effects of SMC inactivation on  $P^{kn}$  would occur at different stages of the cell cycle. We conducted analogous experiments in cells arrested in G<sub>1</sub> and in metaphase (Fig 3D–3I). Arrested cells were sampled at 26°C and after shifting them to 35°C for 60 min during the arrest. Prior inactivation of the SMCs,  $P^{kn}$  of YE<sub>p</sub>13 in the G<sub>1</sub> and the metaphase-arrested cells were similar to that observed in the asynchronous cell cultures ( $P^{kn} \approx 0.03$ ) (Fig 3D–3I). This observation corroborated previous indications that the knotting probability of intracellular chromatin is not cell cycle-dependent (Valdes et al, 2018). Upon inactivation of condensin, the occurrence of knots in YE<sub>p</sub>13 increased about threefold both in G<sub>1</sub> ( $P^{kn} \approx 0.10$ ) and in metaphase-arrested cells ( $P^{kn} \approx 0.09$ ) (Fig 3D and 3E). Inactivation of cohesin produced a slight reduction of  $P^{kn}$  in G<sub>1</sub> ( $P^{kn} \approx 0.017$ ) and metaphase cells ( $P^{kn} \approx 0.022$ ) (Fig 3F and 3G). Inactivation of the Smc5/6 complex did not alter the knot abundance at any stage (Fig 3H and 3I). Thus, we concluded that inactivation of condensin markedly increases the occurrence of DNA knots throughout the cell cycle. Remarkably, this change of  $P^{kn}$  occurred without any notable alteration of the Lk distribution of the minichromosome. Therefore, the regulation of  $P^{kn}$  by condensin did not involve changes of DNA supercoiling or a major disruption of chromatin structure.

### Condensin inactivation restores the DNA length-dependent entanglement of chromatin

Next, we asked whether the effects of condensin, cohesin, and Smc5/6 activity on the knotting probability of YE<sub>p</sub>13 were reproduced in

other chromatin constructs. To this end, we transformed the SMCs mutant strains with circular minichromosomes that contained distinct functional elements (replication origins, transcription units, centromeres) and differed in DNA length. We inspected the topology of minichromosomes YRp3 (3.2 kb), YRp4 (4.4 kb), YRp5 (5.0 kb), YCp50 (7.9 kb), YRp21 (11.7 Kb), and of the endogenous 2-micron plasmid (6.3 kb) present in yeast cells (Appendix Fig S1). As in the foregoing experiments, we sampled exponentially growing cultures before and after inactivation of the SMCs.

In the *smc2-8* mutant (Fig 4), condensin inactivation did not significantly change the knot probability of YRp3, YRp4, and the 2-micron plasmid (Fig 4A–C). However, it augmented the occurrence of knots about twofold in YCp50 (Fig 4D), and over threefold in YRp21 (Fig 4E). Therefore, the effect of condensin inactivation on  $P^{kn}$  values appeared to vary with DNA length rather than with the presence of specific functional elements. Furthermore, plotting the  $P^{kn}$  changes of the distinct minichromosomes revealed that the inactivation of condensin increased  $P^{kn}$  to the levels expected if knot formation was to escalate proportionally to DNA length (Fig 4F).

In the *scc1-73* mutant (Fig 5), YRp3 and YRp4 could not be analyzed since the strain was *TRP+*. Cohesin inactivation did not change the knot probability of YRp5 and the 2-micron plasmid (Fig 5A and B). However, similar to that observed in YE<sub>p</sub>13 (Fig 3B), cohesin inactivation produced a slight reduction of  $P^{kn}$  in YCp50 and YRp21 (Fig 5C and D). Plotting these  $P^{kn}$  values versus the size of the minichromosomes revealed that the reduction of knot formation observed in the large minichromosomes (YCp50, YE<sub>p</sub>13, and YRp21) was overall significant (Fig 5E). Finally, as in the case of YE<sub>p</sub>13, inactivation of the Smc6/5 complex did not change DNA knotting probability in any of the constructs inspected (YRp4, 2-micron plasmid, YCp50 and YRp21) (Fig 6A–E).

The above experiments corroborated that the Lk distribution of the different minichromosomes did not change upon inactivation of the SMCs, thereby excluding that  $P^{kn}$  changes were consequent to alterations of DNA supercoiling or chromatin structure. The above results also evidenced that, before inactivation of the SMCs, the slope of  $P^{kn}$  as minichromosomes increased in size (Figs 4F, 5E, 6E) was alike in all the strains. This similarity corroborated that the knot minimization mechanism is constitutive and robust. This mechanism is apparently sustained by the activity of condensin, since its



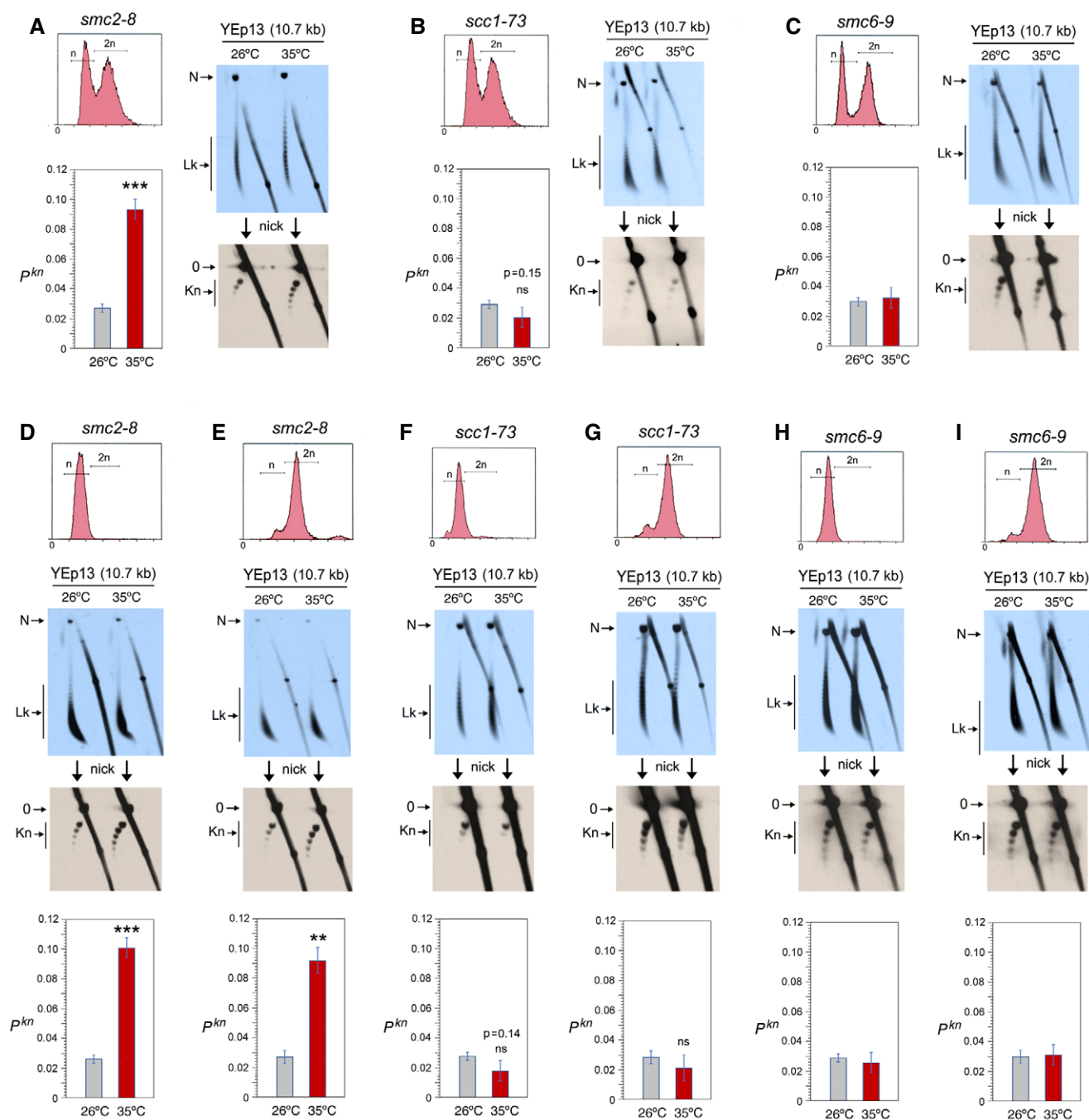


**Figure 3. Condensin inactivation boosts the occurrence of chromatin knots.**

- A** Top, DNA content ( $n/2n$ ) of exponentially growing ( $OD_{600} = 0.6-0.8$ ) *smc2-8* yeast cells. First blot: 2D gel electrophoresis of the distribution of Lk topoisomers (Lk) of the YEp13 DNA in cells quenched at 26°C and after shifting the culture to 35°C for 60 min. Second blot: 2D gel electrophoresis of the same samples upon nicking the YEp13 DNA in order to reveal the occurrence of knots (kn). Graph:  $P^{kn}$  of YEp13 before and after the inactivation of condensin.
- B** Experiments conducted as in (A) but in *scc1-73* yeast cells. Graph:  $P^{kn}$  of YEp13 before and after the inactivation of cohesin.
- C** Experiments conducted as in (A) but in *smc6-9* yeast cells. Graph:  $P^{kn}$  of YEp13 before and after the inactivation of the Smc5/6 complex.
- D, E** Experiments conducted as in (A), but in cells arrested in G<sub>1</sub> with alpha-factor (D) or in metaphase with nocodazole (E) for 2 h at 26°C and for one additional hour at 26°C or 35°C.
- F, G** Experiments conducted as in (B), but in cells arrested in G<sub>1</sub> with alpha-factor for 2 h at 26°C (F) or in metaphase with nocodazole (G) and for one additional hour at 26°C or 35°C.
- H, I** Experiments conducted as in (C), but in cells arrested in G<sub>1</sub> with alpha-factor (H) or in metaphase with nocodazole (I) for 2 h at 26°C and for one additional hour at 26°C or 35°C.

Data information: Gel signals (N, Lk, O, Kn) are as described in Fig 2. Graphs show mean  $\pm$  SD from three independent experiments in (A, B, D, E, F, G); and from two independent experiments in (C, H, I).  $P$ -values (Student's  $t$  test): ns,  $P > 0.05$ ; \*\* $P < 0.01$ ; \*\*\* $P < 0.001$ .

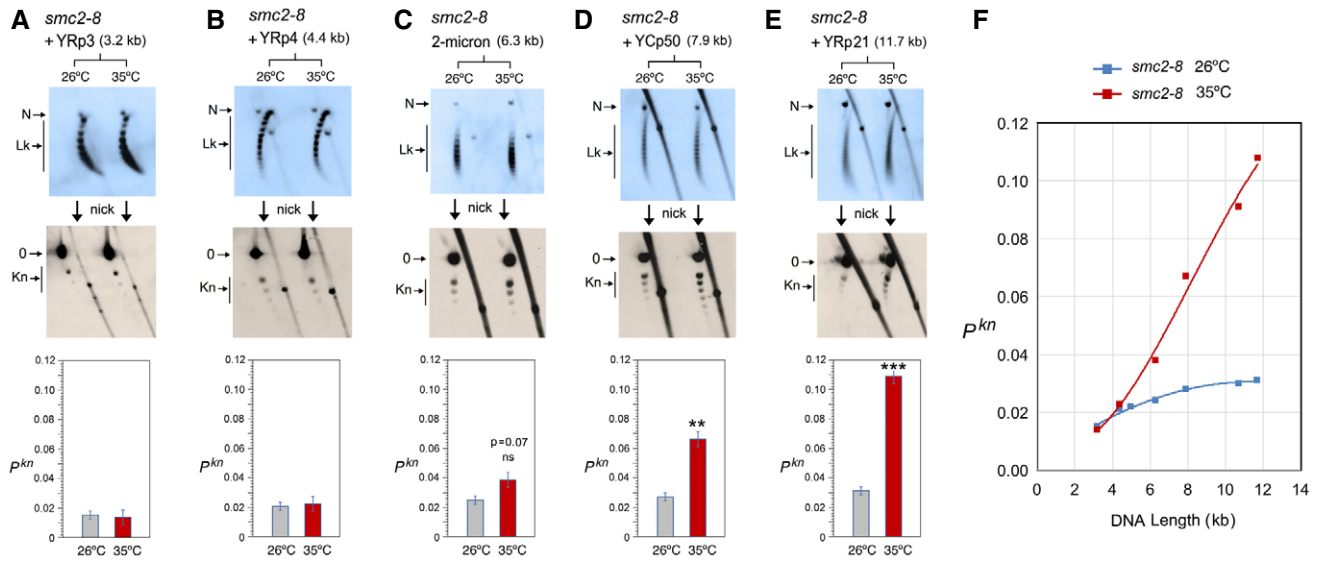


**Figure 4. DNA length dependence of the topological effects of condensin inactivation.**

A–E DNA topology of the indicated minichromosomes of increasing DNA length (kb) before (26°C) and after inactivation of condensin (35°C) in *smc2-8* cells. In each case, the first 2D gel resolves the Lk topoisomers (Lk), the second 2D gel uncovers the knotted forms (Kn). Gel signals are denoted as in Fig 2. Bottom graphs compare the  $P^{kn}$  before and after the inactivation of condensin (mean  $\pm$  SD from three independent experiments). P-values (Student's t test): ns,  $p > 0.05$ ; \*\* $p < 0.01$ ; \*\*\* $p < 0.001$ .

F Plot of  $P^{kn}$  values of minichromosomes of increasing DNA length (including YEp13) before and after inactivation of condensin.

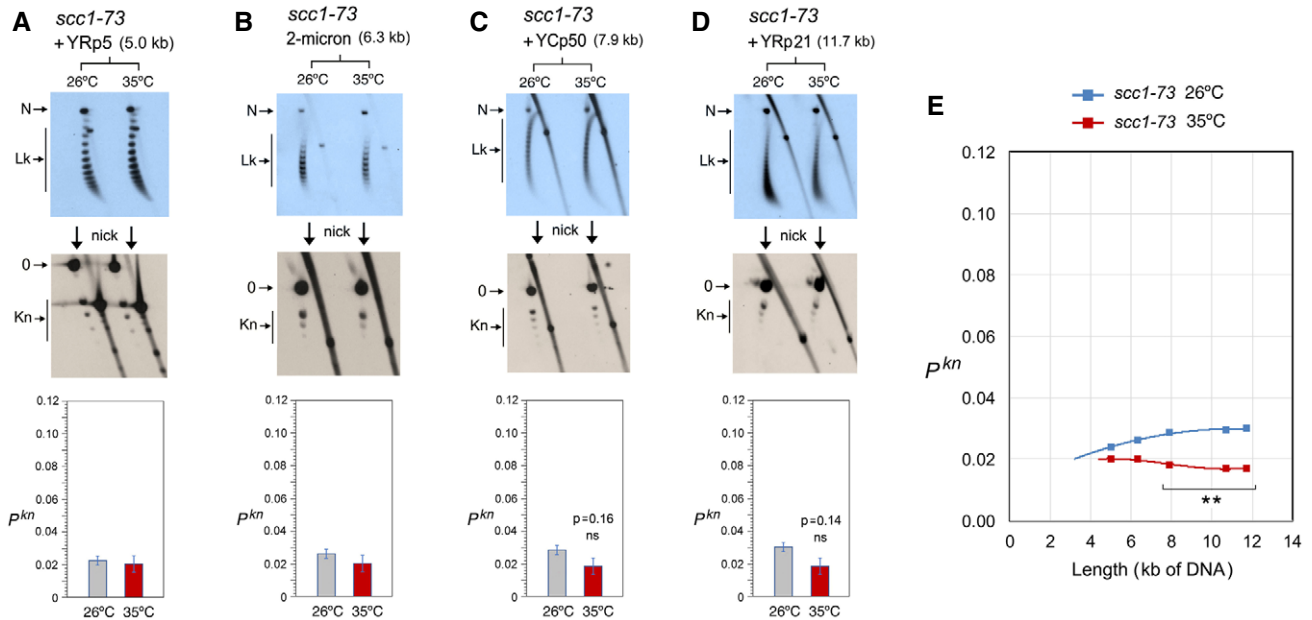


**Figure 5. DNA length dependence of the topological effects of cohesin inactivation.**

A–D DNA topology of the indicated minichromosomes of increasing DNA length (kb) before (26°C) and after inactivation of cohesin (35°C) in *scc1-73* cells. In each case, the first 2D gel resolves the Lk topoisomers (Lk), the second 2D gel uncovers the knotted forms (Kn). Gel signals are denoted as in Fig 2. Bottom graphs compare the  $P^{kn}$  before and after the inactivation of cohesin (mean  $\pm$  SD from three independent experiments). P-values (Student's t test): ns,  $P > 0.05$ .

E Plot of  $P^{kn}$  values of minichromosomes of increasing DNA length (including YEp13) before and after inactivation of cohesin. P-values (Student's t test): \*\* $P < 0.01$ .

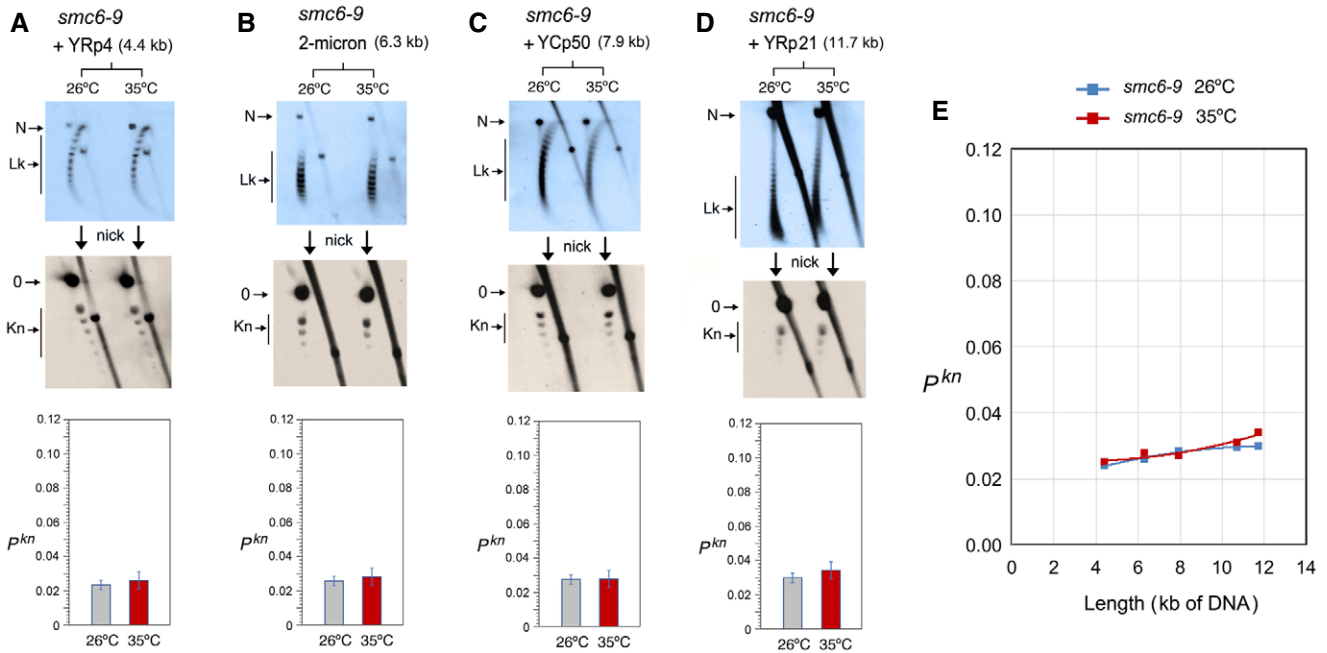


**Figure 6. DNA length dependence of the topological effects of Smc5/6 complex inactivation.**

A–D DNA topology of the indicated minichromosomes of increasing DNA length (kb) before (26°C) and after inactivation of Smc5/6 complex (35°C) in *smc6-9* cells. In each case, the first 2D gel resolves the Lk topoisomers (Lk), and the second 2D gel uncovers the knotted forms (Kn). Gel signals are denoted as in Fig 2. Bottom graphs compare the  $P^{kn}$  before and after the inactivation of Smc5/6 complex (mean  $\pm$  SD from two independent experiments).

E Plot of  $P^{kn}$  values of minichromosomes of increasing DNA length (including YE13) before and after inactivation of Smc5/6 complex.

inactivation restored the DNA length-dependent entanglement of chromatin (Fig 4F).

## Discussion

The intrinsic capacity of topoisomerase II to simplify the equilibrium topology of DNA in free solution is commonly stated as the mechanism that prevents indiscriminate entanglement of intracellular DNA. This assumption, however, had never been experimentally tested until the present study. Our results show that disrupting the simplification activity of cellular topo II does not increase DNA knotting in chromatin. Apparently, the equilibrium topology of chromatinized DNA is not recognized by topo II in the same way as in free DNA. While these negative results cannot formally discard some role of the simplification capacity of topo II *in vivo*, the marked effects produced by condensin indicate that minimizing the entanglement of intracellular DNA mainly depends on this SMC complex.

### Mechanism of condensin to minimize DNA entanglements

Our finding that condensin minimizes the knotting probability of intracellular DNA seems a priori counterintuitive. Normally, any condition that folds or compacts DNA should promote its topological entanglement, not the opposite. Consistent with this notion, early *in vitro* studies found that condensin markedly increases topo

II-mediated knotting of DNA (Kimura *et al*, 1999; Losada & Hirano, 2001). DNA knotting and catenation were also found stimulated by cohesin (Losada & Hirano, 2001), the Smc5/6 complex (Kanno *et al*, 2015), and bacterial SMCs (Petrushenko *et al*, 2006; Bahng *et al*, 2016). These observations supported the notion that SMCs can embrace or bring in close proximity two or more segments of DNA. However, since SMCs had to be added in large molar excess (> 30:1) over circular DNA molecules to stimulate knotting or catenation, these experiments did not reflect a physiological context. Conversely, current evidence that individual condensin complexes can translocate along DNA (Terakawa *et al*, 2017) and produce the extrusion of DNA loops (Ganji *et al*, 2018) explain how condensin might promote the removal of DNA knots. Computational simulations of LE activity indicated that the extrusion process would tighten any intra- or inter-molecular entanglement of DNA and enforce its removal by topo II (Goloborodko *et al*, 2016a; Racko *et al*, 2018; Orlandini *et al*, 2019). As a result, LE activity would reduce the equilibrium fractions of DNA links and knots, whereas LE inactivation would reestablish the equilibrium fractions (i.e., random entanglements of the DNA), which escalate proportionally to DNA length (Frank-Kamenetskii *et al*, 1975; Rybenkov *et al*, 1993; Shaw & Wang, 1993). Remarkably, this prospect matches with the effects of condensin inactivation on minichromosomes of increasing size (Fig 4F).

Since condensin minimizes intramolecular entanglements of DNA (knots), it might operate similarly to remove inter-molecular DNA tangles such as the sister chromatid interlinks (SCI) that arise



during DNA replication. A compaction-independent role of condensin has been involved in the removal of these linkages (D'Amours *et al*, 2004; Renshaw *et al*, 2010). Moreover, although sister chromatids remain in very close proximity by the effect of cohesin until anaphase, the removal of SCI is nearly completed at the end of prophase (Nagasaka *et al*, 2016). However, inactivation of condensin during metaphase results in de novo formation of SCI (Sen *et al*, 2016; Piskadlo *et al*, 2017), which implies that condensin promotes the unlinking of sister chromatids while their close proximity still favors interlinking. In this respect, it was proposed that positive DNA supercoils generated by condensin in mitotic chromatin produce a bias in topo II function to remove the SCIs (Baxter *et al*, 2011; Sen *et al*, 2016). However, *in vitro* studies indicated that condensin does not compact DNA by inducing DNA supercoiling (Eeftens *et al*, 2017). Moreover, recent *in vivo* studies have shown that positive supercoiling of DNA markedly increases the formation of DNA knots (Valdes *et al*, 2019). Accordingly, if condensin were generating supercoils to promote the removal of SCI, that would in turn increase knot formation in mitotic chromatin. This prospect is inconsistent with our results, which show that condensin minimizes the occurrence of knots without altering DNA supercoiling both in interphase and mitotic chromatin. Therefore, our findings support the notion that the removal of intra- and inter-molecular DNA entanglements could be promoted via the LE activity of condensin (Fig 7).

### Distinct effects of condensin and cohesin

In contrast to condensin, inactivation of cohesin and the smc5/6 complex did not increase knot formation. Moreover, cohesin inactivation slightly reduced  $P^{kn}$  both in G1 and mitotic cells. This observation indicates that the plausible implication of cohesin on knot formation must be independent of its role in sister chromatid cohesion. In that case, the distinct effects of condensin and cohesin on  $P^{kn}$  are striking since both complexes have LE activity (Davidson *et al*, 2019; Kim *et al*, 2019). Indeed, LE activity of cohesin *in vivo* accounts for the peaks and strikes observed in Hi-C matrices, which are commonly translated as topological associated regions (TADs) in G1 cells (Fudenberg *et al*, 2016; Sanborn *et al*, 2015). Recent studies confirmed that cohesin-mediated loops and the positions of TADs emerge quickly after telophase by producing contact patterns consistent with a LE process (Abramo *et al*, 2019; Zhang *et al*, 2019).

We can postulate several non-excluding hypotheses to explain the different effects of condensin and cohesin on DNA knotting. One possibility could rely on the dynamics of their LE activity (Fig 7). Cohesin is likely to conduct discrete LE events to generate structural loops within specific boundaries. Subsequent stabilization of such loops would then favor intramolecular entanglement of DNA, as has been demonstrated with polymer simulations (Najafi & Potestio, 2015). Conversely, condensin may perform more dynamic rounds of LE without specific boundaries to scan the presence of DNA entanglements and promote their removal genome-wide. This scenario might be analogous to that occurs in mitotic chromatin, where cohesin may favor SCI formation by maintaining sister chromatids in close proximity (Sen *et al*, 2016; Goloborodko *et al*, 2016b; Piskadlo *et al*, 2017), whereas condensin might be performing continuous rounds of LE to enforce

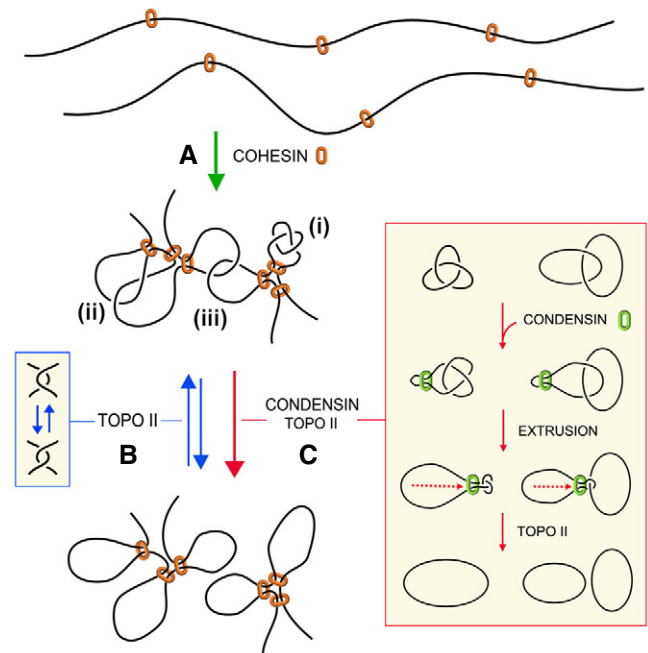


**Figure 7. Model of condensin role in the minimization of DNA entanglements.**

- A Cohesin generates and stabilizes DNA loops to organize interphase chromatin into topological domains.
- B Random DNA strand passage activity of topo II can either remove or produce DNA entanglements within and across such topological domains. Juxtapositions of DNA segments within a loop can lead to the formation of knots (i), whereas juxtapositions of DNA segments belonging to nearby loops or adjacent domains can lead to the formation of intra- (ii) or inter-molecular (iii) DNA interlinks.
- C To minimize the occurrence of these entanglements, condensin might use its DNA loop extrusion activity to constrict intra- and inter-molecular interlinks and so bias the DNA strand passage activity of topo II to remove them. This condensin function may operate during interphase to facilitate chromatin transactions and during cell division to enforce the removal of sister chromatid interlinks.

the removal of SCI. A second possibility could rely on distinct coordination of condensin and cohesin with topo II activity. Based on immunofluorescence and ChIP data, topo II occupies similar genomic loci to condensin and cohesin, but their functional interplay remains unknown. Some studies suggested that condensin can physically interact with topo II and stimulate its activity (Bhat *et al*, 1996; D'Ambrosio *et al*, 2008a). Yet, other studies have failed to confirm a physical interaction (Bhalla *et al*, 2002; Lavoie *et al*, 2002; Cuvier & Hirano, 2003) or a stimulatory effect (Charbin *et al*, 2014). Likewise, a physical or functional interaction of cohesin and topo II has been proposed, as both complexes colocalize at DNA loop boundaries (Uuskula-Reimand *et al*, 2016; Canela *et al*, 2017). Lastly, the distinct effects of condensin and cohesin could result from unequal binding to minichromosomes. This possibility, however, seems less likely considering the comparable abundance and broad chromosomal distribution of both complexes in budding yeast (Glynn *et al*, 2004; Wang *et al*, 2005). Accordingly, the effects of condensin and cohesin on  $P^{kn}$  are accentuated with DNA length independently of the functional elements present

in the minichromosomes. Only the lack of effects observed upon the inactivation of the Smc5/6 complex could be attributed to the lower abundance of this complex in comparison with cohesin and condensin (Aragon, 2018).

### Role of condensin during interphase

The generally established essential function of condensin is the compaction and individualization of sister chromatids to facilitate their segregation during cell divisions (Strunnikov *et al*, 1995; Hirano *et al*, 1997). To this end, condensin might play both an active role in promoting the removal of SCI (Sen *et al*, 2016; Piskadlo *et al*, 2017) and a structural role in organizing the axial architecture of mitotic chromosomes (Maeshima & Laemmli, 2003; Ono *et al*, 2003; Walther *et al*, 2018). These mitotic roles are achieved by the single condensin complex found in yeast cells and by the two condensin complexes (condensin I and II) found in metazoans (Hirota *et al*, 2004; Hirano, 2012). However, former studies in budding yeast revealed that condensin is also present in interphase chromatin (Freeman *et al*, 2000; Lavoie *et al*, 2002), where it is distributed over the length of every chromosome throughout the cell cycle (Wang *et al*, 2005; D'Ambrosio *et al*, 2008b). Likewise, condensin II is also present in interphase chromatin in metazoans (Hirano, 2012; Frosi & Haering, 2015). The role of condensin during interphase is unknown, but its inactivation causes large-scale changes in the chromatin structure of budding yeast (Bhalla *et al*, 2002; Lazar-Stefanita *et al*, 2017; Paul *et al*, 2018). Inactivation of condensin II produces intermixing of chromosomal territories in *Drosophila* (Rosin *et al*, 2018; Rowley *et al*, 2019) and an increase of inter-chromosome associations in mammals (Nishide & Hirano, 2014). Other studies concur that condensin disruption alters a wide range of processes including gene regulation, DNA repair and recombination (Frosi & Haering, 2015; Paul *et al*, 2019). It is intriguing how so many functions and phenotypes are connected to condensin activity. According to our findings, the answer could be that condensin is promoting the removal of harmful DNA knots and interlinks that topo II activity might produce during topological equilibration of chromatin fibers and domains (Fig 7). Such DNA entanglements can alter, for instance, the progression of RNA polymerases and the assembly of nucleosomes, as demonstrated by *in vitro* studies (Portugal & Rodriguez-Campos, 1996; Rodriguez-Campos, 1996). Therefore, the failure of condensin to promote DNA untangling is expected to interfere with multiple genome transactions during interphase, in addition to the individualization of chromosomes during cell division.

The unanticipated role of condensin in minimizing DNA entanglements raises new questions, such as how the LE activities of condensin and cohesin may interplay with each other throughout the cell cycle. A similar issue arises in mitotic chromatin, in which the cohesion of sister chromatids, the removal of SCI, and DNA looping along the axial architecture of chromosomes involve the coordination of distinct SMC activities. Another relevant matter is the interplay of SMCs and type-2 topoisomerases, which are highly conserved from bacteria to eukaryotes. The coordination of these two essential machineries might have been primordial throughout evolution to minimize DNA entanglements as genomes increased in size and complexity.

## Materials and Methods

### DNA constructs and yeast strains

Plasmids YEp13, YEp24, YRp21, YCp50, YRp5, YRp4, and YRp3 (Appendix Fig S1) were amplified in *Escherichia coli* and, when indicated, converted into circular minichromosomes by transforming *Saccharomyces cerevisiae* using standard procedures (Valdes *et al*, 2018). Cellular topo II assays were done in the topo I-deficient strains JCW27 (*MATa*,  $\Delta$ *top1*, *his3-D200*, *leu2-D1*, *trp1-D63*, *ura3-52*) and JCW28 (*MATa*,  $\Delta$ *top1*, *top2-4*, *his3-D200*, *leu2-D1*, *trp1-D63*, *ura3-52*) (Trigueros & Roca, 2001). Condensin function was tested in AS330 (*MATa*, *smc2-8*, *ura3*, *leu2*, *lys2*, *his3*, *ade2*) (Freeman *et al*, 2000). The *smc2-8* mutation was introduced in yeast strains JCW25 (*MATa*, *his3-D200*, *leu2-D1*, *trp1-D63*, *ura3-52*) and its derivative JCW26 (*top2-4*) by two-step gene replacement involving the counter selectable marker *URA3* (Rothstein, 1991). Cohesin function was tested in the strain K5832 (*MATa*, *scc1-73*, *ade2-1*, *ura3-52*, *TRP+*, *can1-100*, *leu2-3*, *112*, *his3-11*) (Michaelis *et al*, 1997). Smc5/6 function was tested in CCG1428 (*MATa*, *smc6-9*, *bar1 $\Delta$* , *leu2-3* *112*, *ura3-52*, *his3-D200*, *trp1-D63*, *ade2-1*, *lys2-801*, *pep4*) (Torres-Rosell *et al*, 2005). Thermo-sensitivity of SMC complexes and topoisomerase mutants was corroborated by drop growth assays (Appendix Fig S2).

### Topo II activity in crude yeast lysates

To target cellular topo II activity with ICRF-193 (Sigma-Aldrich), JCW27 ( $\Delta$ *top1*) cells bearing YEp13 were grown at 30°C in synthetic dropout -LEU media containing 2% glucose. Exponential 50 ml cultures ( $OD_{600} = 0.6-0.8$ ) were harvested and washed twice in TE (Tris-HCl 10 mM (pH 8) EDTA 1 mM) and resuspended at 4°C in 1 ml of lysis buffer (Tris-HCl 10 mM pH 8.0, EDTA 1 mM, EGTA 1 mM, NaCl 150 mM, DTT 1mM, Triton X-100 0.1%, pepstatin 1 $\mu$ g/ml, leupeptin 1 $\mu$ g/ml, PMSF 1 mM). Resuspended cells were transferred to 15-ml conic tubes and mixed with 1 ml of acid-washed glass beads (425–600  $\mu$ m, Sigma). Mechanic lysis of > 80% cells was achieved by stirring six times with a vortex apparatus for 30 sec at 4°C. Glass beads and large cell debris were removed by centrifugation (2000 g x 2 min at 4°C). Cell lysates (0.5 ml) were supplemented with 5 mM MgCl<sub>2</sub> and 2 mM ATP and with 100 ng of a negatively supercoiled control plasmid (YEp24). Following incubation at 30°C for 20 min, ICRF-193 was added (100  $\mu$ M) and incubation continued at 30°C for 10 min. Reactions were quenched by adding EDTA (20 mM) and SDS (0.2%) and extracted twice with phenol and once with chloroform. Nucleic acids were precipitated with ethanol and dissolved in 100  $\mu$ l of TE containing RNase-A. Following 10-min incubation at 37°C, ammonium acetate was added to 0.5 M and DNA was precipitated with ethanol. Each DNA sample was dissolved in 40  $\mu$ l of TE prior gel electrophoresis. To test *Top2- $\Delta$ 83* activity in yeast, JCW28 ( $\Delta$ *top1 top2-4*) cells bearing YEp13 and the expression plasmids *pGAL1T2* or *pGAL1T2 $\Delta$ 83* (Martinez-Garcia *et al*, 2014) were grown at 26°C in synthetic dropout -URA -LEU media containing 2% glucose. Exponentially growing cultures were diluted to  $OD_{600} = 0.1$  in YEP containing 2% raffinose. When  $OD_{600} = 0.6-0.8$  was reached at 26°C, galactose was added to a 2% final concentration and the cell cultures were shifted to 35°C for 2 h. Cells were harvested and crude lysates were prepared by

stirring with glass beads as described above. A sample of the lysates was loaded in SDS-PAGE gels to confirm the extrachromosomal expression of TOP2 and Top2-Δ83 proteins. Upon addition of 5 mM MgCl<sub>2</sub>, 2 mM ATP and 100 ng of negatively supercoiled plasmid YEp24, the lysates were incubated for 30 min at 35°C. Reactions were quenched and nucleic acids isolated for gel electrophoresis analyses as described above.

### SMC mutants culture and DNA extraction

Yeast strains bearing distinct circular minichromosomes were grown at 26°C in the adequate synthetic dropout media supplemented with 2% glucose. Exponentially growing cultures OD<sub>600</sub> = 0.6–0.8 were maintained at 26°C or shifted to 35°C for 60 min to inactivate the temperature-sensitive alleles. To arrest the cells in G1, alpha-factor to a final concentration of 2 mg/L was added to exponentially growing cultures every 30 min for 2 h at 26°C and then for one additional hour upon shifting one half of the cultures to 35°C. To arrest the cells in metaphase, nocodazole was added to exponentially growing cultures to a final concentration of 15 mg/mL for 2 h at 26°C and then for one additional hour upon shifting one half of the cultures to 35°C. Following the inactivation of the temperature-sensitive alleles, the DNA topology of circular minichromosomes was fixed *in vivo* by quickly mixing the liquid cultures with one cold volume (–20°C) of ETol solution (Ethanol 95%, 28 mM Toluene, 20 mM Tris-HCl pH 8.8, 5 mM EDTA) (Diaz-Ingelmo *et al.*, 2015). To measure cellular DNA content (1n, 2n), about 10<sup>6</sup> of ETol fixed cells were washed with saline-sodium citrate (SSC) buffer, incubated for 1 h at 37°C in SSC containing 0.1 mg/mL RNase-A and again incubated for 1 h at 50°C in SSC containing 1 mg/mL Proteinase K. Cell samples in 1 mL SSC were sonicated for two 30 sec cycles at 4C and incubated at 25°C for 1h in presence of 3 mg/mL propidium iodide prior flow cytometry reading on a Gallios (Beckman Coulter) cell analyzer. To extract total DNA, ETol fixed cells from 25 ml cultures were sedimented, washed twice with TE, resuspended in 400μl of TE, and transferred to a 1.5-ml microfuge tube containing 400μl of phenol and 400μl of acid-washed glass beads (425–600 μm, Sigma). Mechanic lysis of > 80% cells was achieved by shaking the tubes in a FastPrep® apparatus for 10 sec at power 5. The aqueous phase of the cell lysates was collected, extracted with chloroform, precipitated with ethanol, and dissolved in 100 μl of TE containing RNase-A. Following 10-min incubation at 37°C, ammonium acetate was added to 0.5 M and DNA was precipitated with ethanol. Each DNA sample was dissolved in 40 μl of TE prior gel electrophoresis.

### DNA electrophoresis for topology analyses

Lk distributions of control plasmid YEp24 were examined with 1D-electrophoreses carried out in 0.8% agarose gels in TBE buffer (89 mM Tris-borate, 2 mM EDTA) plus 0.2 μg/ml of chloroquine and run at 50V for 14 h. Lk distribution of minichromosomes YEp13, YRp21, and YCp50 were examined with 2D-electrophoreses carried out in 0.6% agarose gels (20 × 20 cm) in TBE buffer plus 0.6 μg/ml of chloroquine in the first dimension (30V for 36 h) and in TBE buffer plus 3 μg/ml of chloroquine in the second dimension (80V for 4 h). 2D electrophoreses of YRp3, YRp4, YRp5, and 2-micron circles were carried out in 0.8% agarose gels (20 × 20 cm)

in TBE buffer plus 0.6 μg/ml of chloroquine in the first dimension (50V for 14 h) and TBE buffer plus 3 μg/ml of chloroquine in the second dimension (60V for 6 h).

To examine the DNA knots formed in the minichromosomes, DNA samples were nicked with endonuclease BstNBI (NEB). 2D-electrophoreses of nicked DNA of YRp3, YRp4, and YRp5 circles were carried out in a 0.9% agarose gel (20x20 cm) in TBE buffer at 33V for 40 h in the first dimension and at 150V for 3 h in the second dimension. 2D-electrophoreses of nicked DNA of 2-micron and YCp50 circles were carried out in a 0.6% agarose in TBE buffer at 25V for 40 h in the first dimension and at 125V for 4 h in the second dimension. 2D-electrophoreses of nicked DNA of YEp13 and YRp21 circles were carried out in a 0.4% agarose in TBE buffer at 25V for 40 h in the first dimension and at 125V for 4 h in the second dimension.

All 2D-gels were blot-transferred to positively charged nylon membranes (Hybond-N<sup>+</sup>, Amersham Biosciences). Blots were hybridized with minichromosome DNA probes labeled with AlkPhos Direct (GE Healthcare®). Probe signals were visualized following incubation with CDP-Star detection reagent (GE Healthcare®) for 10 min at room temperature and recorded on X-ray films. DNA knot probability ( $P^{Kn}$ ) was calculated as described previously (Valdes *et al.*, 2018) by quantifying non-saturated signals obtained with serial dilutions of DNA knot samples or with different exposure periods, using the ImageJ software.  $P^{Kn}$  values are the relative abundance of total knot populations with respect to the total amount of unknotted and knotted DNA circles.

**Expanded View** for this article is available online.

### Acknowledgements

We would like to thank the laboratories of Kim Nasmyth, Jordi Torres, and Luis Aragón for sharing yeast strains. We would also like to thank Martí Aldea, David Moreno, and Jonathan Baxter for their insightful input and discussion. This research was supported by the Plan Estatal de Investigación Científica y Técnica of Spain, with grants BFU2015-67007-P and PID2019-109482GB-I00 to J.R.; and research fellowships BES-2016-077806 to S.D., BES-2012-061167 to J.S., and BES-2015-071597 to A.V.

### Author contributions

Experiments: JR, SD, JS, BM-G, AV; Data analysis: JR, SD; Manuscript writing: JR, SD, AV.

### Conflict of interest

The authors declare that they have no conflict of interest.

## References

- Abramo K, Valton AL, Venev SV, Ozadam H, Fox AN, Dekker J (2019) A chromosome folding intermediate at the condensin-to-cohesin transition during telophase. *Nat Cell Biol* 21: 1393–1402
- Aragon L (2018) The Smc5/6 Complex: New and Old Functions of the Enigmatic Long-Distance Relative. *Annu Rev Genet* 52: 89–107
- Arsuaga J, Vazquez M, Trigueros S, Summers D, Roca J (2002) Knotting probability of DNA molecules confined in restricted volumes: DNA knotting in phage capsids. *Proc Natl Acad Sci USA* 99: 5373–5377

- Bahng S, Hayama R, Marians KJ (2016) MukB-mediated Catenation of DNA Is ATP and MukEF Independent. *J Biol Chem* 291: 23999–24008
- Baxter J, Sen N, Martinez VL, De Carandini ME, Schwartzman JB, Diffley JF, Aragon L (2011) Positive supercoiling of mitotic DNA drives decatenation by topoisomerase II in eukaryotes. *Science* 331: 1328–1332
- Bhalla N, Biggins S, Murray AW (2002) Mutation of YCS4, a budding yeast condensin subunit, affects mitotic and nonmitotic chromosome behavior. *Mol Biol Cell* 13: 632–645
- Bhat MA, Philp AV, Glover DM, Bellen HJ (1996) Chromatid segregation at anaphase requires the barren product, a novel chromosome-associated protein that interacts with Topoisomerase II. *Cell* 87: 1103–1114
- Canela A, Maman Y, Jung S, Wong N, Callen E, Day A, Kieffer-Kwon KR, Pekowska A, Zhang H, Rao SSP et al (2017) Genome Organization Drives Chromosome Fragility. *Cell* 170(507–521): e18
- Charbin A, Bouchoux C, Uhlmann F (2014) Condensin aids sister chromatid decatenation by topoisomerase II. *Nucleic Acids Res* 42: 340–348
- Corbett KD, Berger JM (2004) Structure, molecular mechanisms, and evolutionary relationships in DNA topoisomerases. *Annu Rev Biophys Biomol Struct* 33: 95–118
- Cuvier O, Hirano T (2003) A role of topoisomerase II in linking DNA replication to chromosome condensation. *J Cell Biol* 160: 645–655
- D'Ambrosio C, Kelly G, Shirahige K, Uhlmann F (2008a) Condensin-dependent rDNA decatenation introduces a temporal pattern to chromosome segregation. *Curr Biol* 18: 1084–1089
- D'Ambrosio C, Schmidt CK, Katou Y, Kelly G, Itoh T, Shirahige K, Uhlmann F (2008b) Identification of cis-acting sites for condensin loading onto budding yeast chromosomes. *Genes Dev* 22: 2215–2227
- D'Amours D, Stegmeier F, Amon A (2004) Cdc14 and condensin control the dissolution of cohesin-independent chromosome linkages at repeated DNA. *Cell* 117: 455–469
- Davidson IF, Bauer B, Goetz D, Tang W, Wutz G, Peters JM (2019) DNA loop extrusion by human cohesin. *Science* 366: 1338–1345
- Denker A, de Laat W (2016) The second decade of 3C technologies: detailed insights into nuclear organization. *Genes Dev* 30: 1357–1382
- Diaz-Ingelmo O, Martinez-Garcia B, Segura J, Valdes A, Roca J (2015) DNA Topology and Global Architecture of Point Centromeres. *Cell Rep* 13: 667–677
- Dorier J, Stasiak A (2009) Topological origins of chromosomal territories. *Nucleic Acids Res* 37: 6316–6322
- Eeftens JM, Bisht S, Kerssemakers J, Kschonsak M, Haering CH, Dekker C (2017) Real-time detection of condensin-driven DNA compaction reveals a multistep binding mechanism. *EMBO J* 36: 3448–3457
- Frank-Kamenetskii MD, Lukashin AV, Vologodskii AV (1975) Statistical mechanics and topology of polymer chains. *Nature* 258: 398–402
- Freeman L, Aragon-Alcaide L, Strunnikov A (2000) The condensin complex governs chromosome condensation and mitotic transmission of rDNA. *J Cell Biol* 149: 811–824
- Frosi Y, Haering CH (2015) Control of chromosome interactions by condensin complexes. *Curr Opin Cell Biol* 34: 94–100
- Fudenberg G, Imakaev M, Lu C, Goloborodko A, Abdennur N, Mirny LA (2016) Formation of Chromosomal Domains by Loop Extrusion. *Cell Rep* 15: 2038–2049
- Ganji M, Shaltiel IA, Bisht S, Kim E, Kalichava A, Haering CH, Dekker C (2018) Real-time imaging of DNA loop extrusion by condensin. *Science* 360: 102–105
- Glynn EF, Megee PC, Yu HG, Mistrot C, Unal E, Koshland DE, DeRisi JL, Gerton JL (2004) Genome-wide mapping of the cohesin complex in the yeast *Saccharomyces cerevisiae*. *PLoS Biol* 2: E259
- Goloborodko A, Imakaev MV, Marko JF, Mirny L (2016a) Compaction and segregation of sister chromatids via active loop extrusion. *Elife* 5
- Goloborodko A, Marko JF, Mirny LA (2016b) Chromosome Compaction by Active Loop Extrusion. *Biophys J* 110: 2162–2168
- Hanai R, Roca J (1999) Two-dimensional agarose-gel electrophoresis of DNA topoisomers. *Methods Mol Biol* 94: 19–27
- Hassler M, Shaltiel IA, Haering CH (2018) Towards a Unified Model of SMC Complex Function. *Curr Biol* 28: R1266–R1281
- Hirano T (2012) Condensins: universal organizers of chromosomes with diverse functions. *Genes Dev* 26: 1659–1678
- Hirano T, Kobayashi R, Hirano M (1997) Condensins, chromosome condensation protein complexes containing XCAP-C, XCAP-E and a *Xenopus* homolog of the *Drosophila* Barren protein. *Cell* 89: 511–521
- Hirota T, Gerlich D, Koch B, Ellenberg J, Peters JM (2004) Distinct functions of condensin I and II in mitotic chromosome assembly. *J Cell Sci* 117: 6435–6445
- Hsieh T (1983) Knotting of the circular duplex DNA by type II DNA topoisomerase from *Drosophila melanogaster*. *J Biol Chem* 258: 8413–8420
- Kanno T, Berta DG, Sjogren C (2015) The Smc5/6 Complex Is an ATP-Dependent Intermolecular DNA Linker. *Cell Rep* 12: 1471–1482
- Kim Y, Shi Z, Zhang H, Finkelstein IJ, Yu H (2019) Human cohesin compacts DNA by loop extrusion. *Science* 366: 1345–1349
- Kimura K, Rybenkov VV, Crisona NJ, Hirano T, Cozzarelli NR (1999) 13S condensin actively reconfigures DNA by introducing global positive writhe: implications for chromosome condensation. *Cell* 98: 239–248
- Lavoie BD, Hogan E, Koshland D (2002) In vivo dissection of the chromosome condensation machinery: reversibility of condensation distinguishes contributions of condensin and cohesin. *J Cell Biol* 156: 805–815
- Lazar-Stefanita L, Scolari VF, Mercy G, Muller H, Guerin TM, Thierry A, Mozziconacci J, Koszul R (2017) Cohesins and condensins orchestrate the 4D dynamics of yeast chromosomes during the cell cycle. *EMBO J* 36: 2684–2697
- Lieberman-Aiden E, van Berkum NL, Williams L, Imakaev M, Ragoczy T, Telling A, Amit I, Lajoie BR, Sabo PJ, Dorschner MO et al (2009) Comprehensive mapping of long-range interactions reveals folding principles of the human genome. *Science* 326: 289–293
- Losada A, Hirano T (2001) Intermolecular DNA interactions stimulated by the cohesin complex in vitro: implications for sister chromatid cohesion. *Curr Biol* 11: 268–272
- Maeshima K, Laemmli UK (2003) A two-step scaffolding model for mitotic chromosome assembly. *Dev Cell* 4: 467–480
- Martinez-Garcia B, Fernandez X, Diaz-Ingelmo O, Rodriguez-Campos A, Manichanh C, Roca J (2014) Topoisomerase II minimizes DNA entanglements by proofreading DNA topology after DNA strand passage. *Nucleic Acids Res* 42: 1821–1830
- Michaelis C, Ciosk R, Nasmyth K (1997) Cohesins: chromosomal proteins that prevent premature separation of sister chromatids. *Cell* 91: 35–45
- Micheletti C, Marenduzzo D, Orlandini E, Sumners DW (2008) Simulations of knotting in confined circular DNA. *Biophys J* 95: 3591–3599
- Mirny LA (2011) The fractal globule as a model of chromatin architecture in the cell. *Chromosome Res* 19: 37–51
- Nagasaka K, Hossain MJ, Roberti MJ, Ellenberg J, Hirota T (2016) Sister chromatid resolution is an intrinsic part of chromosome organization in prophase. *Nat Cell Biol* 18: 692–699
- Najafi S, Potestio R (2015) Two Adhesive Sites Can Enhance the Knotting Probability of DNA. *PLoS One* 10: e0132132
- Nasmyth K, Haering CH (2009) Cohesin: its roles and mechanisms. *Annu Rev Genet* 43: 525–558

- Nishide K, Hirano T (2014) Overlapping and non-overlapping functions of condensins I and II in neural stem cell divisions. *PLoS Genet* 10: e1004847
- Nitiss JL (2009) DNA topoisomerase II and its growing repertoire of biological functions. *Nat Rev Cancer* 9: 327–337
- Nitiss JL, Wang JC (1996) Mechanisms of cell killing by drugs that trap covalent complexes between DNA topoisomerases and DNA. *Mol Pharmacol* 50: 1095–1102
- Onn I, Heidinger-Pauli JM, Guacci V, Unal E, Koshland DE (2008) Sister chromatid cohesion: a simple concept with a complex reality. *Annu Rev Cell Dev Biol* 24: 105–129
- Ono T, Losada A, Hirano M, Myers MP, Neuwald AF, Hirano T (2003) Differential contributions of condensin I and condensin II to mitotic chromosome architecture in vertebrate cells. *Cell* 115: 109–121
- Orlandini E, Marenduzzo D, Michieletto D (2019) Synergy of topoisomerase and structural-maintenance-of-chromosomes proteins creates a universal pathway to simplify genome topology. *Proc Natl Acad Sci USA* 116: 8149–8154
- Paul MR, Hochwagen A, Ercan S (2019) Condensin action and compaction. *Curr Genet* 65: 407–415
- Paul MR, Markowitz TE, Hochwagen A, Ercan S (2018) Condensin Depletion Causes Genome Decompaction Without Altering the Level of Global Gene Expression in *Saccharomyces cerevisiae*. *Genetics* 210: 331–344
- Petrushenko ZM, Lai CH, Rai R, Rybenkov VV (2006) DNA reshaping by MukB. Right-handed knotting, left-handed supercoiling. *J Biol Chem* 281: 4606–4615
- Piskadlo E, Tavares A, Oliveira RA (2017) Metaphase chromosome structure is dynamically maintained by condensin I-directed DNA (de)catenation. *Elife* 6
- Portugal J, Rodriguez-Campos A (1996) T7 RNA polymerase cannot transcribe through a highly knotted DNA template. *Nucleic Acids Res* 24: 4890–4894
- Racko D, Benedetti F, Goundaroulis D, Stasiak A (2018) Chromatin Loop Extrusion and Chromatin Unknotting. *Polymers* Basel 10
- Renshaw MJ, Ward JJ, Kanemaki M, Natsume K, Nedelec FJ, Tanaka TU (2010) Condensins promote chromosome recoiling during early anaphase to complete sister chromatid separation. *Dev Cell* 19: 232–244
- Roca J, Berger JM, Wang JC (1993) On the simultaneous binding of eukaryotic DNA topoisomerase II to a pair of double-stranded DNA helices. *J Biol Chem* 268: 14250–14255
- Rodriguez-Campos A (1996) DNA knotting abolishes in vitro chromatin assembly. *J Biol Chem* 271: 14150–14155
- Rosin LF, Nguyen SC, Joyce EF (2018) Condensin II drives large-scale folding and spatial partitioning of interphase chromosomes in *Drosophila* nuclei. *PLoS Genet* 14: e1007393
- Rothstein R (1991) Targeting, disruption, replacement, and allele rescue: integrative DNA transformation in yeast. *Methods Enzymol* 194: 281–301
- Rowley MJ, Lyu X, Rana V, Ando-Kuri M, Karns R, Bosco G, Corces VG (2019) Condensin II Counteracts Cohesin and RNA Polymerase II in the Establishment of 3D Chromatin Organization. *Cell Rep* 26(2890–2903): e3
- Rybenkov VV, Cozzarelli NR, Vologodskii AV (1993) Probability of DNA knotting and the effective diameter of the DNA double helix. *Proc Natl Acad Sci USA* 90: 5307–5311
- Rybenkov VV, Ullsperger C, Vologodskii AV, Cozzarelli NR (1997) Simplification of DNA topology below equilibrium values by type II topoisomerases. *Science* 277: 690–693
- Sarnorn AL, Rao SS, Huang SC, Durand NC, Huntley MH, Jewett AI, Bochkov ID, Chinnappan D, Cutkosky A, Li J et al (2015) Chromatin extrusion explains key features of loop and domain formation in wild-type and engineered genomes. *Proceedings of the National Academy of Sciences* 112 (47): E6456–E6465.
- Schmitt AD, Hu M, Ren B (2016) Genome-wide mapping and analysis of chromosome architecture. *Nat Rev Mol Cell Biol* 17: 743–755
- Segura J, Joshi RS, Diaz-Ingelmo O, Valdes A, Dyson S, Martinez-Garcia B, Roca J (2018) Intracellular nucleosomes constrain a DNA linking number difference of -1.26 that reconciles the Lk paradox. *Nat Commun* 9: 3989
- Sen N, Leonard J, Torres R, Garcia-Luis J, Palou-Marin G, Aragon L (2016) Physical Proximity of Sister Chromatids Promotes Top2-Dependent Intertwining. *Mol Cell* 64: 134–147
- Shaw SY, Wang JC (1993) Knotting of a DNA chain during ring closure. *Science* 260: 533–536
- Siebert JT, Kivel AN, Atkinson LP, Stevens TJ, Laue ED, Virnau P (2017) Are There Knots in Chromosomes? *Polymers* 9(12): 317.
- Stevens TJ, Lando D, Basu S, Atkinson LP, Cao Y, Lee SF, Leeb M, Wohlfahrt KJ, Boucher W, O'Shaughnessy-Kirwan A et al (2017) 3D structures of individual mammalian genomes studied by single-cell Hi-C. *Nature* 544: 59–64
- Strunnikov AV, Hogan E, Koshland D (1995) SMC2, a *Saccharomyces cerevisiae* gene essential for chromosome segregation and condensation, defines a subgroup within the SMC family. *Genes Dev* 9: 587–599
- Sulkowska JJ, Niewieczczal S, Jarmolinska AI, Siebert JT, Virnau P, Niemyska W (2018) KnotGenome: a server to analyze entanglements of chromosomes. *Nucleic Acids Res* 46: W17–W24
- Terakawa T, Bisht S, Eeftens JM, Dekker C, Haering CH, Greene EC (2017) The condensin complex is a mechanochemical motor that translocates along DNA. *Science* 358: 672–676
- Thomson NH, Santos S, Mitchenall LA, Stuchinskaya T, Taylor JA, Maxwell A (2014) DNA G-segment bending is not the sole determinant of topology simplification by type II DNA topoisomerases. *Sci Rep* 4: 6158
- Torres-Rosell J, Machin F, Farmer S, Jarmuz A, Eydmann T, Dalgaard JZ, Aragon L (2005) SMC5 and SMC6 genes are required for the segregation of repetitive chromosome regions. *Nat Cell Biol* 7: 412–419
- Trigueros S, Arsuaga J, Vazquez ME, Summers DW, Roca J (2001) Novel display of knotted DNA molecules by two-dimensional gel electrophoresis. *Nucleic Acids Res* 29: E67–E77
- Trigueros S, Roca J (2001) Circular minichromosomes become highly recombinogenic in topoisomerase-deficient yeast cells. *J Biol Chem* 276: 2243–2248
- Uhlmann F (2016) SMC complexes: from DNA to chromosomes. *Nat Rev Mol Cell Biol* 17: 399–412
- Uuskula-Reimand L, Hou H, Samavarchi-Tehrani P, Rudan MV, Liang M, Medina-Rivera A, Mohammed H, Schmidt D, Schwalie P, Young EJ et al (2016) Topoisomerase II beta interacts with cohesin and CTCF at topological domain borders. *Genome Biol* 17: 182
- Valdes A, Coronel L, Martinez-Garcia B, Segura J, Dyson S, Diaz-Ingelmo O, Micheletti C, Roca J (2019) Transcriptional supercoiling boosts topoisomerase II-mediated knotting of intracellular DNA. *Nucleic Acids Res*
- Valdes A, Segura J, Dyson S, Martinez-Garcia B, Roca J (2018) DNA knots occur in intracellular chromatin. *Nucleic Acids Res* 46: 650–660
- Vologodskii A (2016) Type II topoisomerases: Experimental studies, theoretical models, and logic: Reply to comments on "Disentangling DNA molecules". *Phys Life Rev* 18: 165–167
- Walther N, Hossain MJ, Politi AZ, Koch B, Kueblbeck M, Odegard-Fougner O, Lampe M, Ellenberg J (2018) A quantitative map of human Condensins provides new insights into mitotic chromosome architecture. *J Cell Biol* 217: 2309–2328

Wang BD, Eyre D, Basrai M, Lichten M, Strunnikov A (2005) Condensin binding at distinct and specific chromosomal sites in the *Saccharomyces cerevisiae* genome. *Mol Cell Biol* 25: 7216–7225

Wang JC (1998) Moving one DNA double helix through another by a type II DNA topoisomerase: the story of a simple molecular machine. *Q Rev Biophys* 31: 107–144

Wasserman SA, Cozzarelli NR (1991) Supercoiled DNA-directed knotting by T4 topoisomerase. *J Biol Chem* 266: 20567–20573

Yatskevich S, Rhodes J, Nasmyth K (2019) Organization of Chromosomal DNA by SMC Complexes. *Annu Rev Genet* 53: 445–482

Zhang H, Emerson DJ, Gilgenast TG, Titus KR, Lan Y, Huang P, Zhang D, Wang H, Keller CA, Giardine B et al (2019) Chromatin structure dynamics during the mitosis-to-G1 phase transition. *Nature* 576: 158–162



**License:** This is an open access article under the terms of the Creative Commons Attribution 4.0 License, which permits use, distribution and reproduction in any medium, provided the original work is properly cited.

## Expanded View Figures

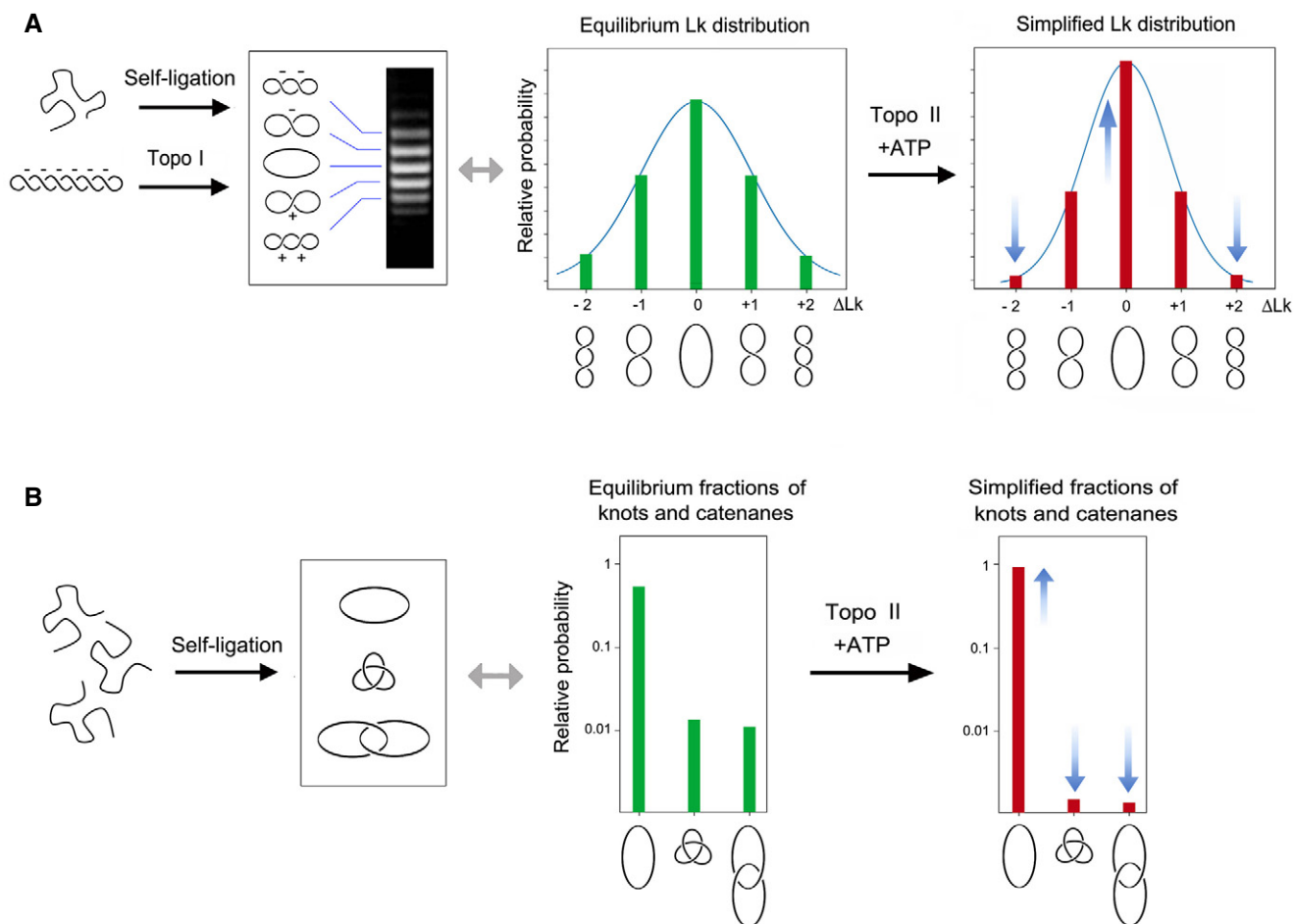


**Figure EV1. Equilibrium DNA topology and its simplification by Topo II.**

- A Either the self ligation of a linear DNA duplex into a covalently closed ring or the relaxation of a DNA plasmid with a type-1B topoisomerase (topo I) produce identical equilibrium distributions of Lk topoisomers, which reflect the thermal fluctuations (twisting and bending) of DNA molecules in free solution. ATP-dependent DNA passage catalyzed by topo II simplifies (i.e., reduces the variance, narrows) the equilibrium distribution of Lk topoisomers.  $\Delta Lk$  values indicate the Lk difference relative to the distribution center (Lk = 0).
- B Circularization of linear DNA molecules in free solution can also produce knotted and/or catenated DNA rings. Knotting probability increases with DNA length, whereas catenane probability increases with DNA concentration. As in the case of the Lk distribution, the knotting and catenation probability reflect the equilibrium topology of DNA in free solution. ATP-dependent DNA passage catalyzed by topo II markedly reduces (i.e., simplifies) the equilibrium fractions of knotted and catenated forms.

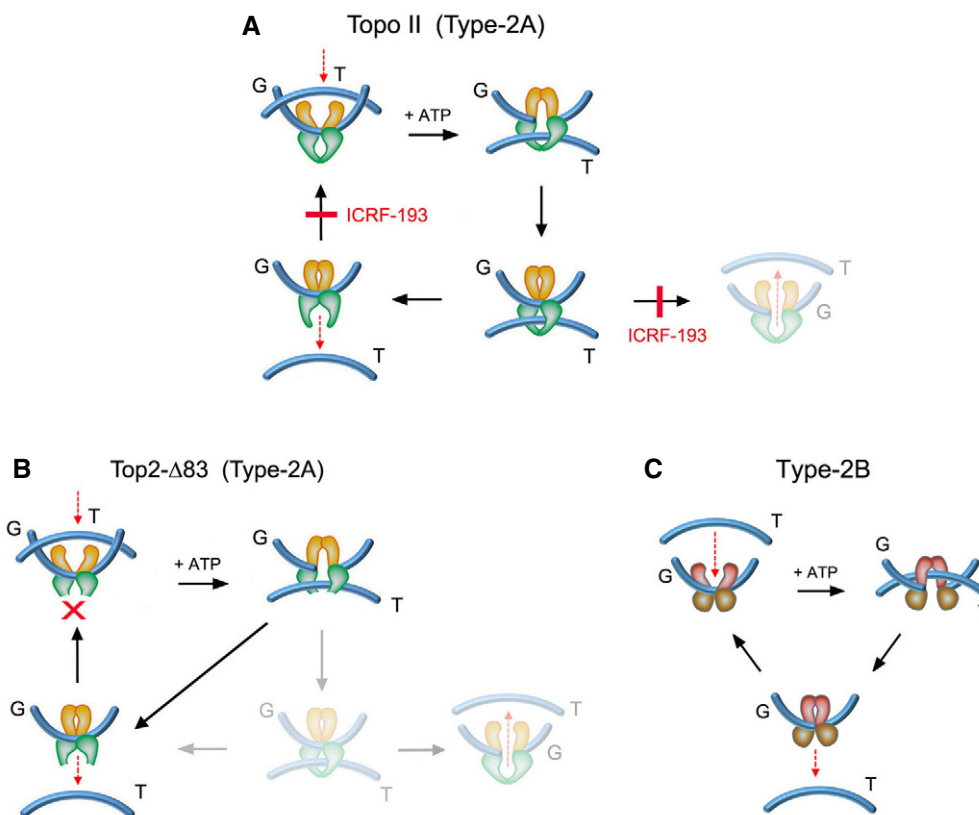


**Figure EV2. Conditions that preclude topo II capacity to simplify DNA topology.**

- A The topo II inhibitor ICRF-193 impedes the reopening of the N-gate once the T-segment has been captured and passed across the G-segment. ICRF-193 blocks thereby the enzyme turnover and the plausible backtracking of the T-segment across the G-segment. When topo II activity is quenched with ICRF-193, the last DNA-passage event conducted by the enzyme does not simplify the equilibrium DNA topology.
- B The topo II construct top2- $\Delta$ 83, in which the C-gate has been deleted, is able to perform DNA passage and the T-segment cannot backtrack since it is freed upon crossing the G-segment. This truncated enzyme can relax and unlink DNA molecules but has lost the capacity to simplify the equilibrium DNA topology.
- C Type-2B topoisomerases are mechanically similar to type-2A topoisomerases (topo II). The T-segment is captured by the N-gate and is passed across the bended G-segment at the DNA-gate. However, type-2B topoisomerases do not have a C-gate, so the passed T-segment is naturally freed upon crossing the G-segment. As in the case of top2- $\Delta$ 83, type-2B topoisomerases relax and unlink DNA molecules but do not simplify equilibrium DNA topology.

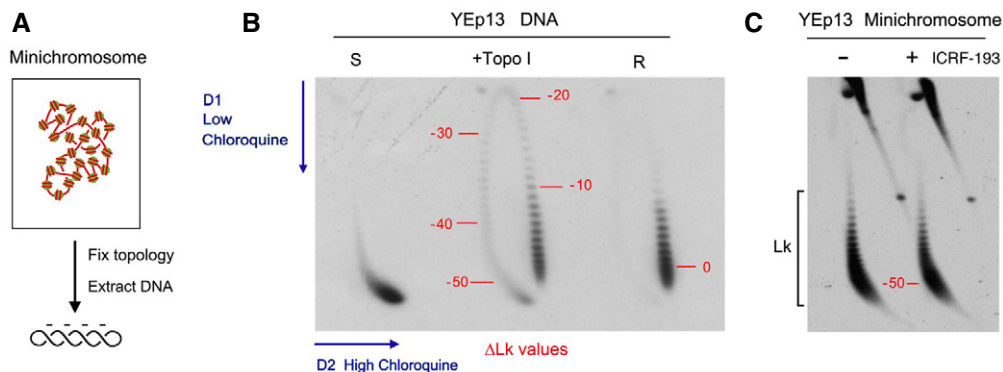


**Figure EV3.**



**Figure EV3. 2D gel electrophoresis of the DNA linking number distribution of circular minichromosomes.**

- A DNA molecules extracted from yeast circular minichromosomes are negatively supercoiled since each nucleosome constrains about one negative supercoil ( $\Delta Lk \approx -1$ ).
- B 2D gel electrophoresis of covalently closed DNA circles, in which the first and second gel dimensions are run in the presence of low and high concentrations of chloroquine, respectively, allow the Lk distribution of DNA topoisomers to be resolved along an arch, in which Lk values increase clockwise. The 2D gel shows highly negatively supercoiled (S), partially relaxed (+topo I), and fully relaxed (R) forms of the YEp13 plasmid. Numbers in red indicate approximate  $\Delta Lk$  values relative to the center of the relaxed (R) Lk distribution ( $\Delta Lk = 0$ ).
- C 2D gel electrophoresis of DNA of the YEp13 minichromosome (as in Fig 2C). Comparison of the gels in (B and C) indicates that DNA in the YEp13 minichromosome is negatively supercoiled and has  $\Delta Lk$  close to  $-50$ . This value is consistent with the plausible number of nucleosomes assembled in YEp13 (10.7 Kb). However, note that since the outline of Lk distributions can vary in separate 2D gels (i.e., due to differences in tank dimensions, power supply and temperature during electrophoresis), only DNA samples that ran in the same gel (side by side) can be accurately compared.

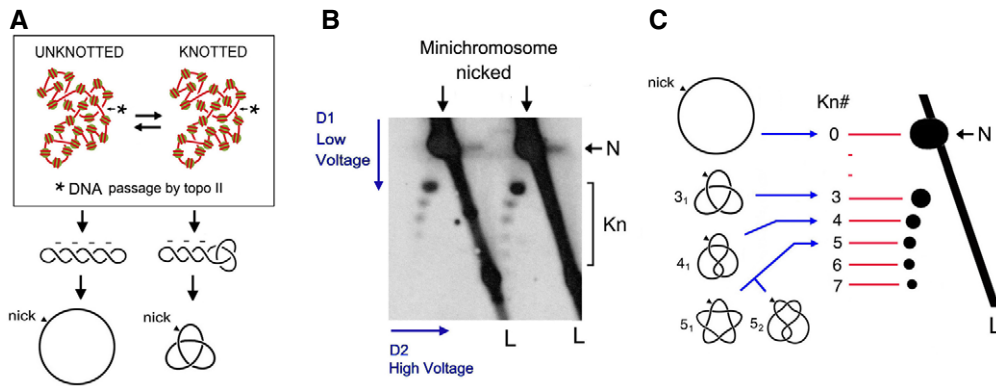


**Figure EV4. 2D gel electrophoresis of DNA knots formed in yeast circular minichromosomes.**

- A DNA molecules extracted from yeast minichromosomes might contain knots due to the knotting-unknotting activity of intracellular topo II. Knotted and unknotted molecules are hard to distinguish when DNA is supercoiled because all of them present similar compaction. Upon nicking the DNA, supercoiling is dissipated and knotted molecules remain more compact than unknotted ones.
- B 2D gel electrophoresis of nicked DNA of the YEp13 minichromosome (as in Fig 2C). The first and second gel-dimensions run at low and high voltage, respectively. In the first dimension, knotted molecules (Kn) are more compact and so move faster than unknotted ones (N). In the second gel-dimension, knotted molecules are retarded from the diagonal of linear DNA fragments (L), which produces a strong signal due to genomic DNA present in the samples.
- C Identification of DNA knot populations according to the irreducible number of DNA crossings of each knot (Kn#). From the position of the unknotted circle that has zero crossings (0), a ladder of knot populations of increasing complexity begins with the knot of three crossings ( $3_1$ ), followed by the knot with four crossings ( $4_1$ ), two knots with five crossings ( $5_1$  and  $5_2$ ), and so on.

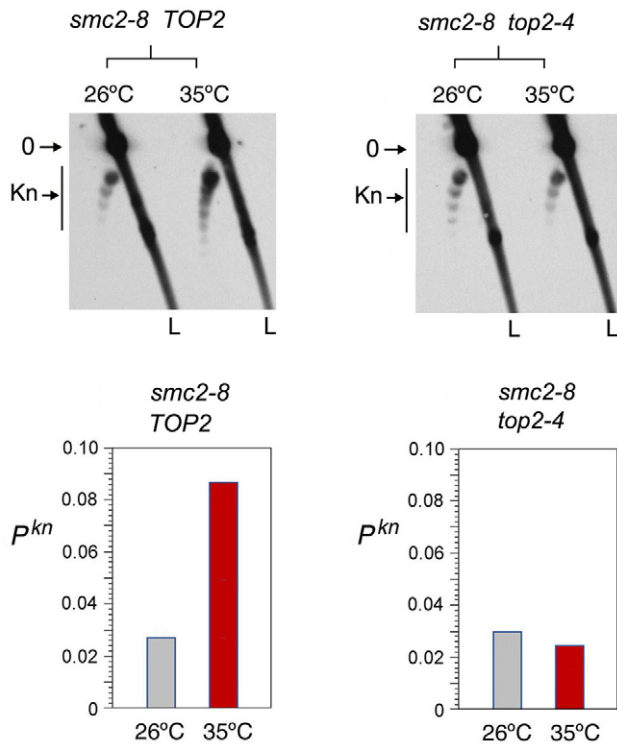


**Figure EV5. Topo II dependence of knot formation upon inactivation of condensin.**

The *smc2-8* mutation was introduced by gene replacement in yeast strains JCW25 (*TOP2*) and JCW26 (*top2-4*). The 2D gel electrophoresis shows the knotted forms of the minichromosome YEp13 in the resulting *smc2-8 TOP2* and *smc2-8 top2-4* mutants sampled at 26°C and after shifting the cell cultures to 35°C for 60 min. Gel signals: 0, unknotted DNA circles; Kn, knotted forms. L, linear DNA fragments. Graphs:  $p^{kn}$  of YEp13 before and after inactivation of the thermo-sensitive alleles.

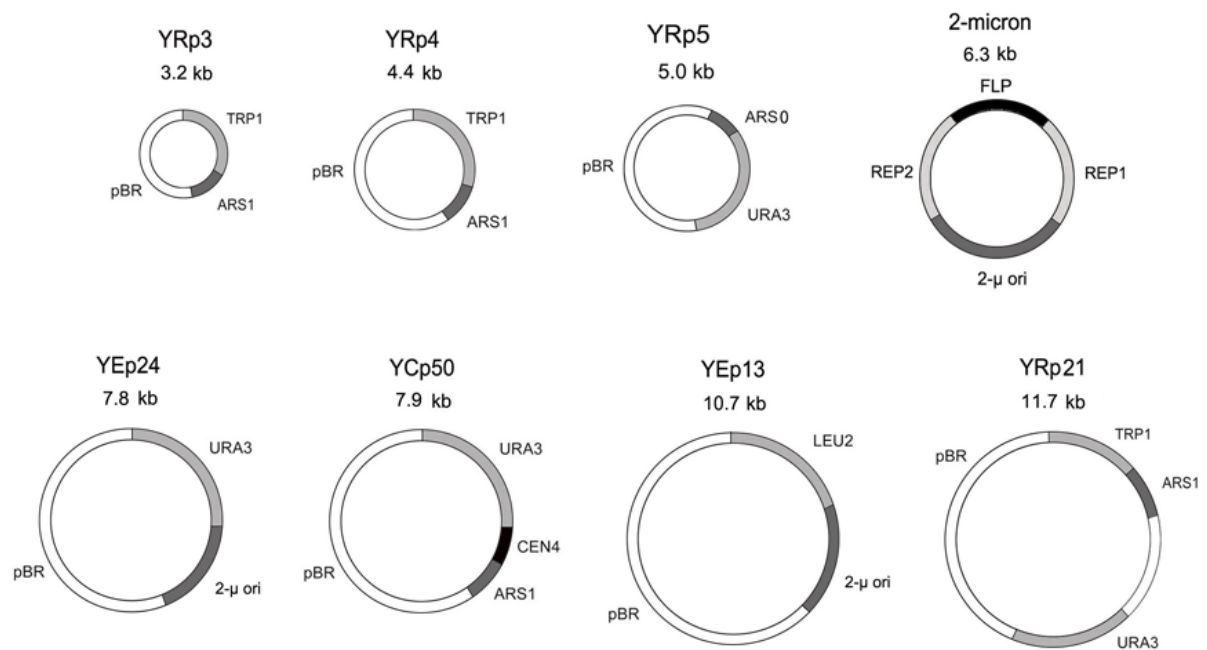
# **Condensin minimizes topoisomerase II-mediated entanglements of DNA *in vivo***

Sílvia Dyson, Joana Segura, Belén Martínez-García, Antonio Valdés, and Joaquim Roca\*

## **Appendix**

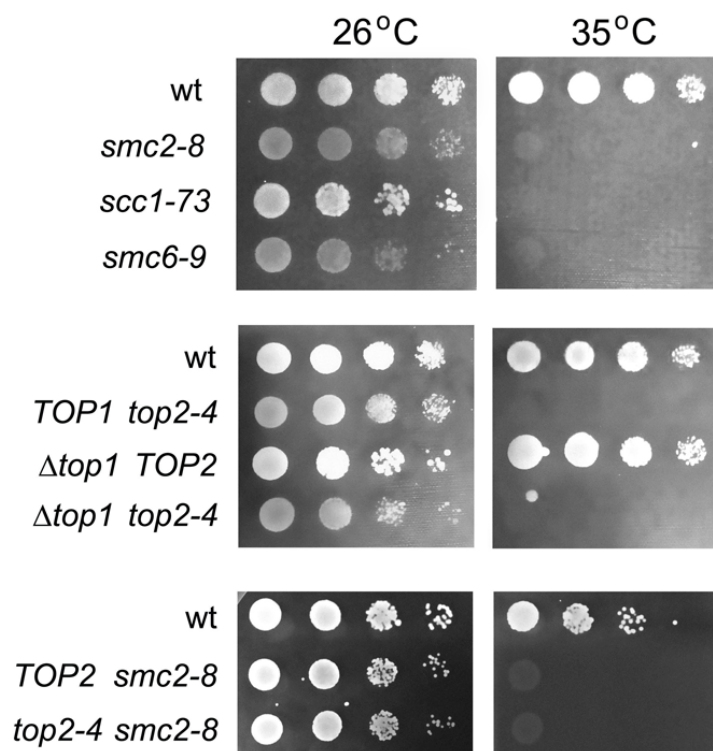
**Figure S1. Plasmids and minichromosomes analyzed in the study.**

**Figure S2. Drop assays of yeast strains used in the study.**



**Appendix Figure S1. Plasmids and minichromosomes analyzed in the study.**

Minichromosomes containing pBR sequences were amplified as bacterial plasmids in *Escherichia coli* and used to transform *Saccharomyces cerevisiae*. The 2-micron plasmid was endogenous in all the yeast strains used. Minichromosomes differed in size, replication origins (autonomous replication sequences (ARS) or 2-micron origin), presence of centromere (CEN), and selectable gene markers (TRP1, URA3, LEU2) as indicated.



**Appendix Figure S2. Drop assays of yeast strains used in the study.**

Yeast strains carrying thermo-sensitive mutations that inactivate SMC complexes and/or topoisomerase activities were grown to late-log phase at 26°C and spotted in 10-fold dilutions on YPD. Plates were incubated at 26°C or 35°C. *JCW25* was used as the wild-type (wt) control in all plates.



---

# General Discussion

---





**GENERAL DISCUSSION:**

Studies carried out in our laboratory provided the first evidence of DNA knot formation in eukaryotic cells (Valdes et al., 2018). These studies showed that intracellular DNA knots occur regardless of chromatin's structural or functional elements and also regardless of the stage of the cell cycle. The presence of knots only changed during DNA transcription in a topoisomerase II dependent manner (Valdes et al., 2019). These findings were not surprising considering the high concentration of DNA segments within chromatin fibers and the abundant topoisomerase II activity that can pass these segments through one another. However, the most striking observation was the nonlinear correlation found between the DNA knotting probability ( $P^{kn}$ ) and chromatin length. The results uncovered that in circular minichromosomes of up to about 5 Kb in size, the  $P^{kn}$  increased linearly, reaching a value of around 0.025. However, in minichromosomes above this size the slope of  $P^{kn}$  was abruptly reduced, such that in larger chromatin domains (5 to 12 Kb) the  $P^{kn}$  was maintained at around 0.03. This inflection of the  $P^{kn}$  value was in conflict with polymer simulations (Rybenkov et al., 1993) and DNA in vitro studies (Shaw & Wang, 1993), which demonstrated that the  $P^{kn}$  always increases proportionally to chain length.

Remarkably, short chromatin domains (i.e., minichromosomes of 2-5 Kb) presented a higher  $P^{kn}$  than naked DNA with the corresponding size (Figure 28). This difference is likely reflecting the flexibility that nucleosomes grant to linker DNA regions, which markedly increase the juxtaposition probability of the chromatinized DNA segments in comparison to naked DNA. By comparing the  $P^{kn}$  of in vivo chromatin with the one obtained via polymer simulations, we estimated that the nucleosomal fiber behaves like a chain with persistence length ( $P_L$ ) of about  $\approx 10$  nm and effective diameter ( $d_E$ )  $\approx 0$  nm. These values contrast with those of naked DNA which has a  $P_L = 50$  nm and an  $d_E = 5$  nm (Valdes et al., 2018).

The abrupt reduction of the chromatin's  $P^{kn}$  slope when the size of the minichromosomes surpassed 4-5 kb (about 25 nucleosomes) evidenced that some

mechanism was preventing knot formation from escalating. The goal of this thesis has been to find this mechanism.

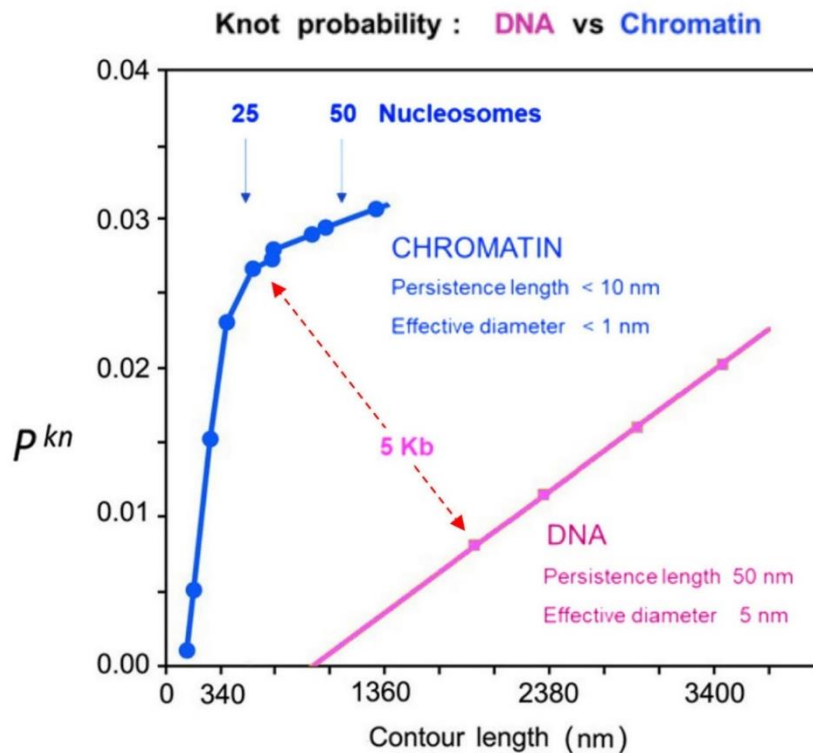


**Figure 28 – Chromatin vs naked DNA knotting probability.** Chromatin is much more flexible than naked DNA. As an example (red arrow), when comparing a DNA length of 5kb, the  $P^{kn}$  increases four times more in chromatinized DNA than in naked DNA. However, the  $P^{kn}$  of chromatin attenuates at a DNA length of about 25 nucleosomes, whereas naked DNA keeps increasing linearly with DNA length.

As explained in the introduction, it seems unlikely that a length-dependent transition in the conformation of nucleosomal fibers could be the mechanism that minimizes DNA knot formation. In the length scales where knot minimization occurs in vivo, nucleosomal fibers are folded quite irregularly forming heterogeneous clusters rather than a highly ordered structure (Hsieh et al., 2015; Ou et al., 2017).

Therefore, the purpose of the present thesis has been to test whether DNA supercoiling, the simplification activity of topoisomerase II and/or the loop extrusion activity of SMC complexes were responsible for minimizing the entanglement of DNA in vivo. The main findings of these studies are discussed below.

## 1. DNA supercoiling markedly increases DNA knotting probability in chromatin

Considering that DNA supercoiling increases the juxtaposition of intramolecular DNA segments, several studies had already tackled the idea that supercoiling had a direct connection with knot formation and resolution. On one hand, several *in vitro* experiments carried out with DNA plasmids had revealed that type-2A topoisomerases produce more knots in supercoiled plasmids than in relaxed ones (Wasserman & Cozzarelli, 1991; Roca et al., 1993). But on the other hand, computer simulations proposed that DNA supercoiling could tighten existing DNA knots and facilitate their removal by type-2A topoisomerases (Witz et al., 2011). Thus, there was no clear consensus on this matter. Moreover, nobody had tested the effect of supercoiling on knot formation in native chromatin, which is why it was the first objective of this thesis.

The Lk distributions of yeast minichromosomes containing DNA knots presented no evidence of unconstrained supercoiling that could possibly be promoting DNA knot formation or resolution *in vivo* (Valdés et al., 2018). However, changes in the DNA supercoiling *in vivo* are likely to be transient (i.e., quickly relaxed) and hence not captured when analyzing the Lk distributions. This is why, in a subsequent study, we used an experimental approach that accumulated positive ((+)S) and negative ((-)S) supercoils in minichromosomes *in vivo*, which allowed us to catch the effect of supercoiling on the  $P^{kn}$  (Figure 29) (Valdes et al., 2019).

Surprisingly, whereas (-)S did not alter the  $P^{kn}$  of the minichromosomes, (+)S produced a 25-fold increase in knot formation (Figure 29). Therefore, (+)S produced the opposite effect of minimizing the  $P^{kn}$ . One possible explanation for this robust increase in the  $P^{kn}$  was to consider that (+)S produces a strong compaction of the nucleosomal fibers. To test this notion, we asked Dr. Cristian Micheletti (our collaborators at SISSA, Trieste) to conduct the first computer simulation of DNA  $P^{kn}$  in nucleosomal fibers with increasing levels of compaction. The results showed that a 5-fold volume compaction, which is equivalent to reducing the radius of gyration of the nucleosomal fibers to 60%, would suffice to increase the  $P^{kn}$  by 25-fold (Valdes et al., 2019). Thus, the strong rise in knot

## General Discussion

formation is likely to result from the compaction effect that (+)S has on in vivo chromatin.

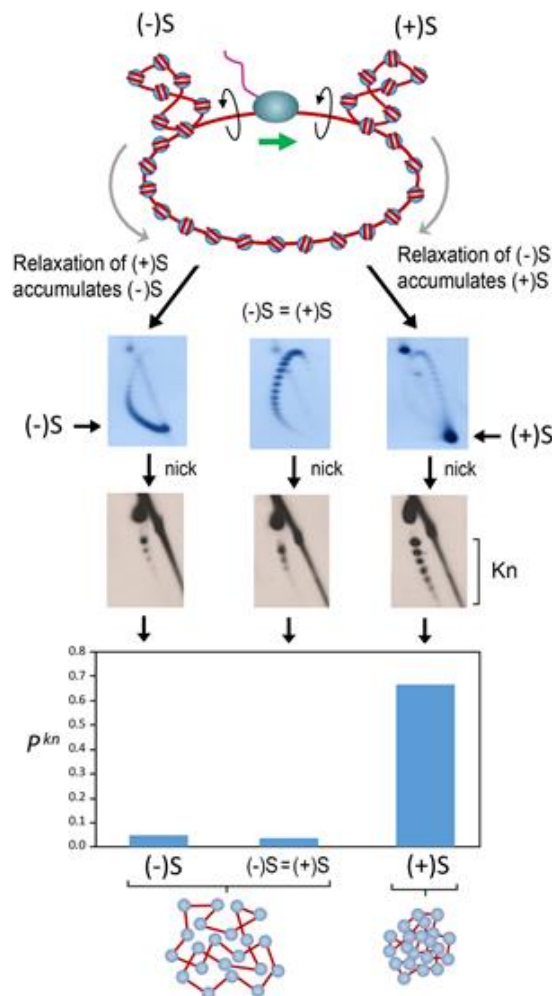


**Figure 29 – Supercoiling and DNA knotting.** Both (-)S or (+)S generated during DNA transcription can be accumulated in vivo by enforcing an unbalanced relaxation of (+)S or (-)S. Accumulation of (-)S and (+)S is shown in the 2D-gels of Lk topoisomers. Upon nicking the DNA, the relative abundance of DNA knots ( $P^{kn}$ ) was found to be 25-fold higher in (+)S than in (-)S DNA molecules. Computer simulations (balls and sticks) illustrate that a 5-fold volume compaction of the nucleosomal fibers can produce this large increase in the  $P^{kn}$ .

To explain why (-)S did not alter the  $P^{kn}$  in the same way as (+)S, a different level of chromatin compaction could be responsible. In fact, previous in vitro studies had shown that (-)S (DNA un-twisting) does not compact nucleosomal fibers to the same extent as (+)S (DNA over-twisting) (Bancaud et al., 2006; Lavelle et al., 2010). Moreover, in vivo studies had also indicated that, chromosomal domains with (+)S seem more compacted than the ones with (-)S (Naughton et al., 2013). The differential response that chromatin

conformation has to (+)S and (-)S was also inferred by our laboratory when we found that topoisomerase II relaxes (+)S faster than (-)S in vivo (Salceda et al., 2006; Fernández et al., 2014). Therefore, the differences in the  $P^{kn}$  obtained in this thesis further confirm that (+)S compacts intracellular chromatin to a much larger degree than (-)S.

## **2. Transient DNA knotting is common during transcriptional supercoiling of DNA**

The (+)S that we accumulated in yeast minichromosomes was generated through DNA transcription (Liu & Wang, 1987). Eukaryotic RNA polymerases transcribe DNA at rates of around 100 bp/s, which allows the DNA domain found in front of a polymerase to become over-twisted at a rate of around 10 turns/s (Dundr et al., 2002). Since yeast minichromosomes are circular domains, such (+)S is usually cancelled by the (-)S generated behind the RNA polymerase. For this reason, in order to accumulate (+)S in circular minichromosomes, we have to increase the relaxation rate of (-)S by expressing *E.coli* topoisomerase I in yeast (which is a type-1A topoisomerase that is only able to relax (-)S but not (+)S).

Contrary to circular minichromosomes, when (+)S is generated during gene transcription along the much larger and linear cellular chromosomes, twin domains with (+)S and (-)S cannot be cancelled (Nelson, 1999; Joshi et al., 2010). In this case, accumulation of (+)S is likely to occur when RNA polymerases run into barriers that block the twist diffusion of the double helix, or when RNA polymerases converge or run into a replication fork. In all these scenarios, the RNA polymerase would still be able to transcribe until (+)S reached levels comparable to those experimentally generated in the circular minichromosomes ( $\sigma > +0.05$ ) (Salceda et al., 2006). When these values are reached, it is likely that the (+)S DNA domains found in front the RNA polymerases become knotted to the same extent observed in the circular minichromosomes (Figure 30). However, the presence of these knots is likely to be ephemeral since they will only persist as long as the (+)S does. In normal conditions, the (+)S is rapidly relaxed by cellular topoisomerase

## General Discussion

I and/or topoisomerase II. Therefore, the knots produced will be resolved by topoisomerase II concomitantly to the relaxation of (+)S.

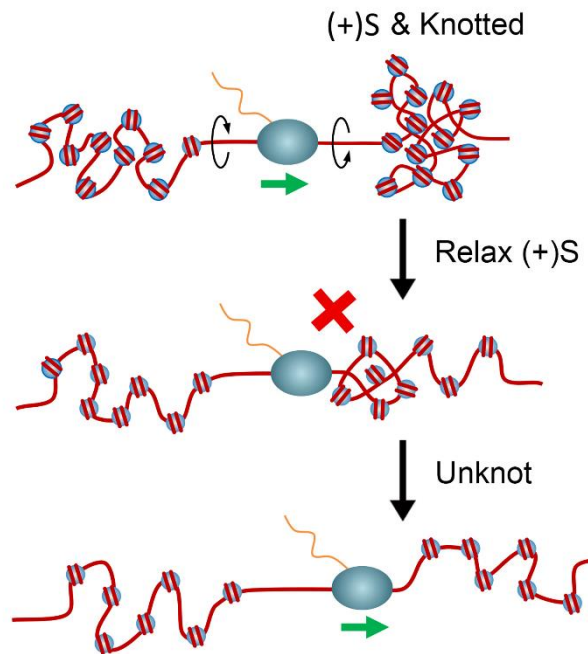


**Figure 30 – DNA knotting during gene transcription.** When (+)S increases during chromosomal DNA transcription, (+)S DNA is likely to become knotted to the same extent observed in circular minichromosomes. Then, progression of the transcribing RNA polymerases requires, not only the relaxation of (+)S by topoisomerase I or topoisomerase II, but also the concomitant removal of DNA knots by topoisomerase II.

However, if (+)S were relaxed but DNA knots persisted, *in vivo* RNA polymerases would likely be stalled when they ran into a knot. *In vitro* studies had already demonstrated that RNA polymerases are not able to transcribe in knotted DNA templates (Portugal & Rodriguez-Campos, 1996; Rodriguez-Campos, 1996). Remarkably, this scenario explains an intriguing observation made in our laboratory years ago. Our observations showed that when inactivating topoisomerase II during the transcription of long genes, RNA polymerases were stalled (Joshi et al., 2012). Strikingly, this stalling could not be rescued by solely relaxing the (+) S with topoisomerase I, however, it was rescued by topoisomerase II. This finding excluded the idea that the polymerases were stalled just by the action of (+)S. Now, with our current knowledge, we envision that the polymerases were stalled by the presence of DNA knots formed due to the accumulation

of (+)S. Since topoisomerase II is able to unknot the DNA, it was the only enzyme able to restore the transcription process (Figure 30).

### **3. Topoisomerase II activity alone does not minimize intracellular DNA knots**

As mentioned in the introduction, type-2A topoisomerases are able to produce steady-state fractions of catenates, knots and supercoil crossovers that are many times lower than the corresponding equilibrium fractions (Rybenkov et al., 1997).

However, the mechanism by which type-2A topoisomerases simplified the DNA's equilibrium topology was controversial for a long time (Stuchinskaya et al., 2009; Vologodskii, 2016). It wasn't until our laboratory studied in detail the passage of the DNA T-segment across the three gates of topoisomerase II that the simplification mechanism was uncovered (Martinez-Garcia et al., 2014). The results of this study indicated that after T-segment capture and passage, the topoisomerase challenges the release of the T-segment through the C-gate. This hindering allows either the completion or the cancellation (backtracking) of DNA transport. The exit of the T-segment through the C-gate is likely to be quick when the topoisomerase inverts DNA crossovers that are generated by topological stress. For example, in the case of catenates between newly replicated DNA duplexes or supercoils arising during DNA replication and transcription. However, the release of the T-segment by the C-gate may be delayed when the topoisomerase inverts juxtaposed DNA segments that are randomly produced during the DNA's topological equilibration. In this case, if the entrance gate (N-gate) re-opens before the exit gate (C-gate), the T-segment might backtrack and consequently cancel the DNA transport.

Remarkably, when the backtracking of the T-segment was prevented by blocking the N-gate or by keeping the C-gate open, the capacity of topoisomerase II to simplify the equilibrium topology of the DNA was abolished (Martinez-Garcia et al., 2014).

Interestingly, the role of the C-gate in the simplification mechanism is consistent with the observation that type-2B topoisomerases, which innately lack the C-gate domain, do not have the capacity to simplify the DNA's equilibrium topology (Thomson et al., 2014).

## General Discussion

For many years, it has been assumed that the intrinsic capacity of topoisomerase II to simplify the DNA equilibrium topology in vitro, was the mechanism that prevents indiscriminate entanglement of intracellular DNA. In this thesis we conducted the first experimental study to check this assumption. In order to target the simplification mechanism of intracellular topoisomerase II, two experimental approaches were used (Dyson et al., 2021).

Our first approach was to hinder the backtracking of the T-segment by blocking the N-gate of intracellular topoisomerase II with ICRF-193 (Figure 31A) (Roca et al., 1994; Classen et al., 2003). The results showed that the  $P^{kn}$  of the minichromosomes was not significantly altered (Figure 31C) (Dyson et al., 2021).

Our second approach was to impede any possible T-segment backtracking by expressing a truncated topoisomerase II (Top2-  $\Delta$ 83), in which the C-gate domain was removed (Figure 31B) (Martinez-Garcia et al., 2014). The results showed that the  $P^{kn}$  of the minichromosomes was not significantly altered by the activity of Top2- $\Delta$ 83 in vivo (Figure 31C) (Dyson et al., 2021).

Therefore, the in vitro capacity of topoisomerase II to simplify the DNA equilibrium topology was not minimizing the occurrence of DNA knots in vivo (Figure 31C). These results corroborate the knowledge that topoisomerase II does not perform in chromatinized DNA in the same way as in naked DNA (Salceda et al., 2006). Moreover, the topological equilibrium of chromatinized DNA in vivo is much more complex and variable than in naked DNA molecules in free solution (Stuchinskaya et al., 2009). We hypothesize that the C-gate of type-2A topoisomerases might have another role in vivo. The C-gate could provide further stability to the dimeric topoisomerase during DNA cleavage, or could play a structural role by keeping both the T-segment and G-segment entrapped together.



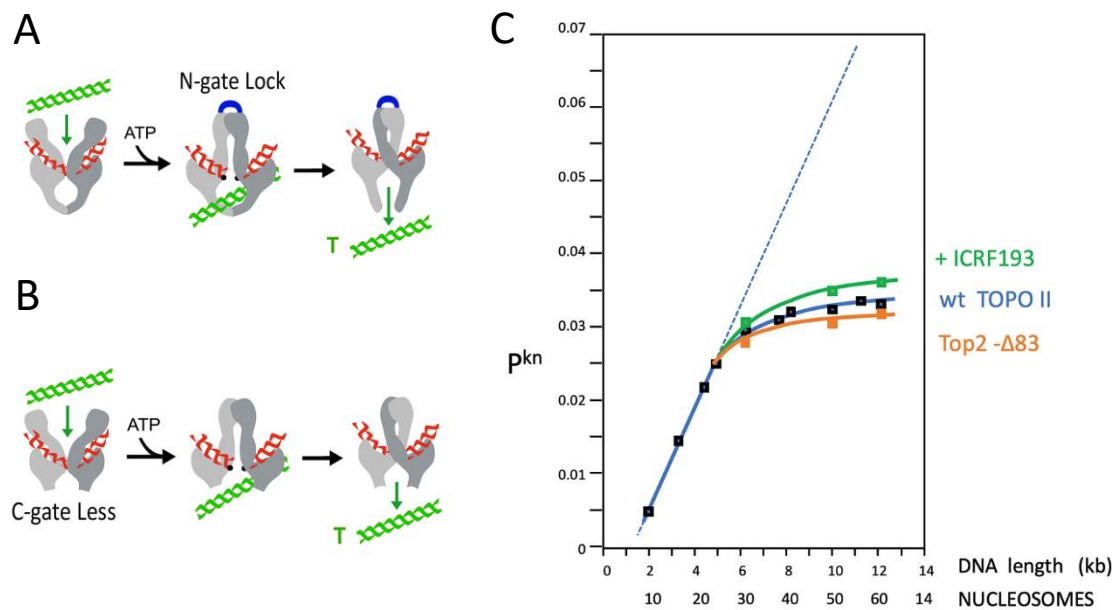


**Figure 31 – Topoisomerase II simplification activity.** (A) Locking the N-gate after T-segment entry allows topoisomerase II to complete DNA passage but precludes the simplification of the DNA equilibrium topology (B) Removal of the C-gate allows topoisomerase II to perform DNA passage but abolishes its capacity to simplify the equilibrium topology. (C) Comparison of the  $p^{kn}$  of in vivo chromatin in the presence of wildtype, C-gateless (Top2- $\Delta$ 83), and N-locked (+ ICRF193) topoisomerase II enzymes.

#### 4. Condensin is required to minimize DNA knotting in chromatin

Computer simulation studies have shown that DNA loop extrusion processes can robustly compact and at the same time disentangle entire chromosomes (Goloborodko, Marko, et al., 2016). Subsequent molecular dynamic simulations also indicated that DNA loop extrusion processes would tighten any intra- or inter-molecular DNA entanglement and enforce their removal by topoisomerase II (Racko et al., 2018; Orlandini et al., 2019). Consequently, the last objective of this thesis was to test whether the minimization of intracellular DNA knots depended on the activity of the DNA loop extruders (i.e., cohesin and condensin).

The results clearly show that, upon inactivation of condensin, knot formation in large circular minichromosomes (5 to 12 Kb) increases to levels that restore a linear correlation between  $p^{kn}$  and DNA length. In other words, condensin activity is responsible for the observed inflection in the  $p^{kn}$ . Remarkably, this effect occurs

irrespective of DNA sequence and is observed throughout the cell cycle. Therefore, the activity of condensin is necessary to minimize the  $P^{kn}$  of chromatin (Dyson et al., 2021). Surprisingly, inactivation of cohesin produced the opposite effect from condensin, as discussed further below.

### **5. Condensin mediated knot minimization supports that its DNA loop extrusion activity performs in vivo**

Whereas in vitro single-molecule studies have shown that condensin and cohesin are able to extrude DNA into loops (Ganji et al., 2018; Davidson et al., 2019; Kim et al., 2019), there is no definitive proof of this activity in vivo. Only some indirect evidence supports the loop extrusion activity of intracellular SMC complexes. For instance, it has been proposed that the TADs that were uncovered from analyzing the DNA-DNA contact matrices obtained during Hi-C analyses (Dixon et al., 2012), are the result of DNA loop extrusion processes conducted by cohesin (Sanborn et al., 2015; Fudenberg et al., 2016). Moreover, the different contacts of the Hi-C matrix, are likely to be loop extrusion processes stalled at different positions before the loop is anchored by cohesin at specific boundary sites. Regarding condensin, direct sign of its DNA loop extrusion activity in vivo is still missing.

Our findings, which show that condensin activity is necessary to minimize DNA knots, are consistent with computer simulations that demonstrated how loop extrusion processes can tighten DNA entanglements and enforce their removal by topoisomerase II (Goloborodko, Marko, et al., 2016; Racko et al., 2018; Orlandini et al., 2019). Thereby, our results strongly support that the loop extrusion activity of condensin does perform in vivo, however, we cannot discard that condensin may be using another mechanism to promote DNA knot removal.

## 6. Opposite effects of condensin and cohesin

In contrast to condensin, inactivation of cohesin did not increase knot formation but instead it produced a slight decrease in the  $P^{kn}$  (Figure 32) (Dyson et al., 2021). The opposite effects of condensin and cohesin were quite puzzling since both complexes are able to perform loop extrusion. We have two hypotheses to explain why condensin and cohesin behave differently when it comes to DNA knotting.

The first possibility relies on distinct kinetics or turnover of the loop extrusion activity of condensin and cohesin. As previously commented, cohesin is essential to establish TADs. Therefore, cohesin might only perform one or very few rounds of loop extrusion to generate structural loops within specific boundaries. In the case of vertebrates, these boundaries are determined by CTCF binding sites (Ong & Corces, 2014 ; Wendt et al., 2008). In yeast and drosophila, there are no CTCF sites, which means that other mechanisms might define such boundaries. Once these loops or TADs are stabilized, they would favor the DNA's intramolecular entanglement due to the increased juxtaposition of nearby DNA segments (Figure 32). This notion is backed by polymer simulations which show that bridging distant DNA sites to form a loop increases its  $P^{kn}$  (Najafi & Potestio, 2015). In contrast to cohesin, condensin might not produce long-lasting DNA loops with defined boundaries. Instead, condensin might perform continuous rounds of loop extrusion. This reiteration could allow condensin to scan the presence of DNA entanglements genome-wide and drag them until they are tightened and removed by topoisomerase II (Figure 32).

A second possibility could rely on a distinct cooperation of condensin and cohesin with topoisomerase II. Based on immunofluorescence and ChIP data, topoisomerase II often colocalizes with condensin and cohesin, however their collaborative role remains unknown. Some studies suggested that condensin physically interacts with topoisomerase II and stimulates its activity (Bhat et al., 1996; D'Ambrosio et al., 2008). However, other studies have denied a physical interaction between the two (Bhalla et al., 2002; Lavoie et al., 2002; Cuvier & Hirano, 2003). Likewise, a functional interaction of cohesin and topoisomerase II has been proposed because both complexes colocalize at DNA loop boundaries, but there is no evidence of a physical interaction (Uuskula-

## General Discussion

Reimand et al., 2016; Canela et al., 2017). Thus, it is plausible that condensin and cohesin interact differently with topoisomerase II to produce opposite DNA knotting and unknotting outcomes.

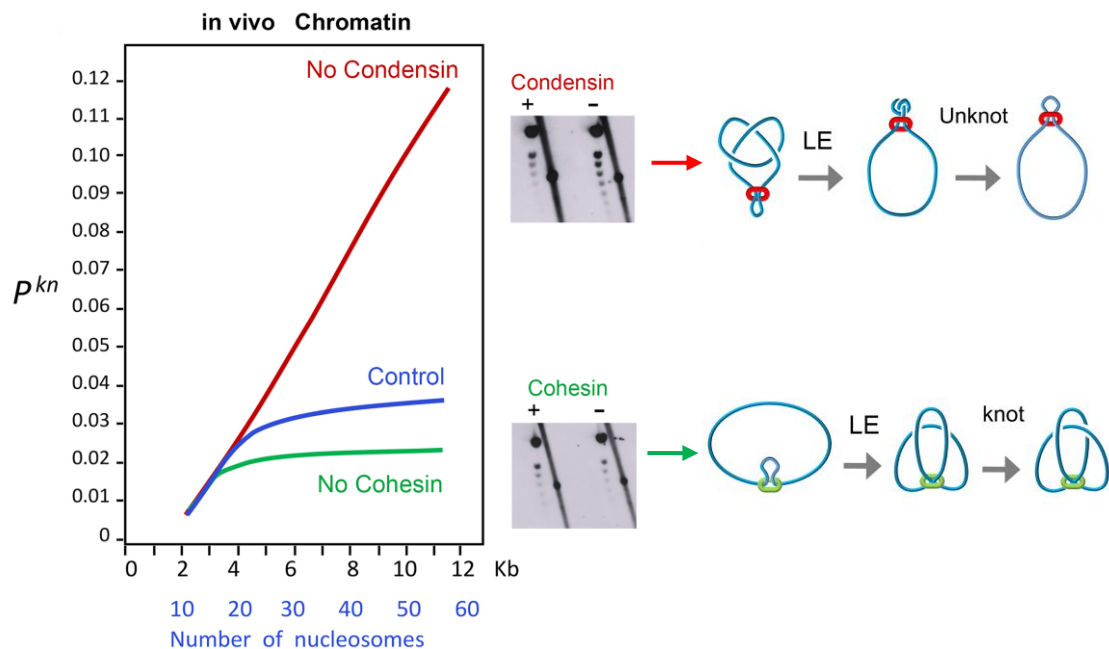


**Figure 32 – Opposite effects of condensin and cohesin on the  $P^{kn}$  of chromatin.** Inactivation of condensin increases the  $P^{kn}$  to levels that restore a linear correlation with DNA length, whereas inactivation of cohesin slightly reduces the  $P^{kn}$ . Representative 2D-gel electrophoreses of the knot formation are shown. Condensin’s loop extrusion activity displaces and constricts DNA knots outside the extruded loop. The tightening of the DNA knot crossovers promotes their dissolution (unknotting) by topoisomerase II. Cohesin’s loop extrusion can generate long-lasting loops, which could favor topoisomerase II-mediated intramolecular DNA entanglement.

## 7. Condensin’s loop extrusion activity might resolve sister chromatid interlinks

When DNA replication is completed and cells enter the G2 phase, the newly synthesized DNA molecules are highly interlinked (catenated) and also remain cohered by cohesin bridges all across the DNA molecule (Hirano, 2005; Farcas et al., 2011). However, experimental evidence shows that, even though sister chromatids are in very close proximity until anaphase by the effect of cohesin, sister chromatid interlinks (SCIs) are almost completely removed at the end of prophase via topoisomerase II (Nagasaka et

al., 2016). This is surprising because the topological equilibration of two huge DNA molecules that are in close proximity should favor their entanglement, not their resolution. In this regard, a crucial observation revealed that newly formed SCIs reappeared when condensin was inactivated during metaphase (Sen et al., 2016; Piskadlo et al., 2017). This observation indicated that condensin has an active role in disentangling sister chromatids throughout mitosis despite the close proximity of the DNA molecules which favors their interlinking (Figure 33).

To explain the active removal of SCIs, it had been proposed that condensin could be generating positive DNA supercoils to compact sister chromatids and that such (+)S would perhaps direct the activity of topoisomerase II towards the removal of SCIs (Baxter et al., 2011; Sen et al., 2016). However, subsequent *in vitro* studies showed that condensin does not compact DNA by inducing supercoiling (Eeftens et al., 2017). Additionally, our results clearly show that (+)S strongly promotes knot formation, not the opposite (Valdes et al., 2019). Accordingly, if condensin were generating (+)S, it would increase knot formation in mitotic chromatin and such increase is not observed. Consequently, our observations support that, like in the case of knots, the removal of SCIs is promoted via the loop extrusion activity of condensin. This inference is supported by *in silico* studies that show how DNA loop extrusion is sufficient to yield the compaction of mitotic chromosomes and disentanglement of their SCIs (Goloborodko, Imakaev, et al., 2016). Therefore, the loop extrusion activity of condensin may enforce topoisomerase II to remove both intra- and inter-molecular DNA entanglements (i.e., knots and SCIs) (Figure 33).

Remarkably, in both cases condensin activity somehow counteracts the effect of cohesin, which stimulates DNA knotting within TADs during interphase and also promotes the persistence of SCIs up until metaphase.

## **8. Short- and long-range DNA entanglements of intracellular chromatin**

When cells exit mitosis, individual chromosomes decondense as they maintain their territorial organization intact (Cremer & Cremer, 2001). Inside each territory, chromosomes are compartmentalized holding domains of active and inactive chromatin, which cluster together to form, respectively, euchromatic and heterochromatic compartments (Tavares-Cadete et al., 2020). Inside each domain, the DNA is folded into sub-domains or TADs. This overall organization has led to propose that chromatin has a similar behavior to a fractal globule (Baù et al., 2011; Mirny, 2011). One property of such fractal architecture is that it drastically reduces the topological complexity of intracellular DNA in long range-scales. Yet, as indicated by our results, topoisomerase II can still randomly pass neighboring DNA segments through one another and consequently produce knots within nucleosomal fibers in short-length scales. Then, it could be expected that, if DNA segments from different chromosome territories or chromatin domains come into close contact, topoisomerase II could also accidentally interlink them. Moreover, given enough time, these interface DNA entanglements would result in the complete intermixing of chromosomal territories and domains (Dorier & Stasiak, 2009). However, when looking the high-order organization of chromatin, such DNA entanglements are rarely found (Lieberman-Aiden et al., 2009; Stevens et al., 2017). Multi-contact 3C analyses show that chromatin domains from one chromosome can locally invade another territory or domain to some extent, without apparently becoming topologically linked (Branco et al., 2008; Tavares-Cadete et al., 2020).

We believe that the loop extrusion activity of condensin might also operate to remove these interface DNA entanglements, which are similar to SCIs (Figure 33). Therefore, we envision that the fractal architecture of chromatin along with the loop extrusion activity of condensin are the main operators that keep the genome untangled. Yet, the efficiency of these two operators might be lost in very short length scales (<5Kb). This would explain why the DNA's  $P^{kn}$  increases up to a length of about 25 nucleosomes and then tends to flatten for longer length scales.

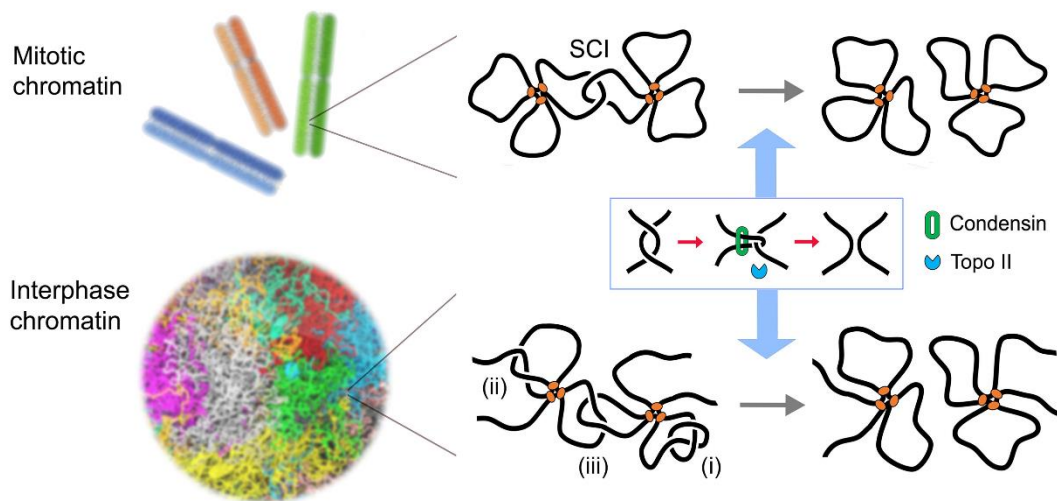


**Figure 33 – Plausible general role of condensin in minimizing DNA entanglements both in mitotic and interphase chromatin.** The loop extrusion activity of condensin might tighten SCIs and enforce their removal by topoisomerase II during mitotic prophase. Likewise, the loop extrusion activity of condensin might tighten and promote the removal of local DNA knots (i), and DNA interlinks produced within (ii) and across (iii) nearby chromatin domains in interphase chromatin.

## 9. Relevance of condensin in interphase

For many years, the most common and well-known function of condensin has been the compaction and individualization of sister chromatids during mitosis to facilitate their segregation (Strunnikov et al., 1995; Hirano et al., 1997). However, many studies have proven the presence of condensin in budding yeast along every chromosome throughout all the cell cycle (Lavoie et al., 2002; Wang et al., 2005; D’Ambrosio et al., 2008). Likewise, studies in metazoans, which contain two condensin complexes (condensin I and II) that associate with mitotic chromosomes at different stages (Ono et al., 2003; Gibcus et al., 2018; Walther et al., 2018b), show that condensin II is not only present during mitosis but also in interphase chromatin (Hirano, 2012).

Although the function of condensin in interphase remains unclear, its inactivation causes large-scale structural and functional alterations. In budding yeast inactivation of condensin provokes genome decompaction leading to a global decrease in close-range

## General Discussion

intra-chromosomal interactions (Paul et al., 2018). In *Drosophila*, inactivation of condensin II during interphase produces changes in the shape and level of intermixing, causing stronger chromosomal interactions between different chromosome territories (Rosin et al., 2018; Rowley et al., 2019). In mammals, depletion of condensin II displays hyper-clustering of pericentric heterochromatin and consequently provokes an increase of inter-chromosome associations, indicating that condensin II plays a critical role in establishing the nuclear architecture during interphase (Nishide & Hirano, 2014). A recent comparison of the nuclear architecture across the tree of life revealed that species having condensin II share a similar architecture type during interphase (Hoencamp et al., 2021). Additionally, condensin disruption is also found to alter a wide range of gene processes including transcriptional regulation, DNA repair and recombination (Frosi & Haering, 2015; Paul et al., 2019).

The studies mentioned above strongly suggest that, as in the case of cohesin, condensin also plays a structural role in organizing chromosome folding patterns during interphase. This role seems to prevent the disruption of chromosomal territories, which are unusually stable across different cell types (Rosin et al., 2018). In this respect, the results from this thesis indicate that what condensin may be doing in interphase is promoting the removal of DNA knots and links that topoisomerase II may accidentally produce during the topological equilibration of intracellular DNA. If such entanglements were not removed, they would affect critical processes such as the progression of RNA polymerases or the proper assembly of nucleosomes, as some *in vitro* studies have demonstrated (Portugal & Rodriguez-Campos, 1996; Rodriguez-Campos, 1996). Failing to remove these DNA entanglements would explain the diversity of structural and functional alterations that occur in interphase chromatin upon condensin inactivation.



## **10. An ancestral solution to the general problem of DNA entanglement**

During the establishment of the modern DNA world, one of the main challenges has been to keep DNA molecules properly organized within small volumes, as the cell genomes continuously increased in size and functional complexity. Today, we can see that the three cellular domains of life (Archaea, Bacteria and Eukarya) have developed a great variety of proteins and interaction modes to compact the DNA. However, a common trait in the three kingdoms is the presence of type-2 topoisomerases and SMC complexes. Type-2 topoisomerases conserve very similar structure and mechanistic properties in Archaea, Bacteria and Eukarya (Forterre et al., 2007). Similarly, SMCs are evolutionarily conserved multi-subunit protein complexes that present a very similar architecture in the three kingdoms (Hirano, 1998; Jessberger et al., 1998).

From the results of this thesis, it is tempting to speculate that some coordination between type-2 topoisomerases and SMC complexes might have originated in the last universal common ancestor and has been conserved throughout evolution to minimize DNA entanglements as genomes increased in size and complexity.

Lastly, in the same way that cells strive to minimize DNA entanglements, it is also plausible that DNA knot formation might have been exploited to stabilize specific chromatin conformations. Some studies have suggested that mitotic chromosomes are stabilized by the presence of specific DNA entanglements produced by topoisomerase II (Kawamura et al., 2010). Moreover, topoisomerase II activity has been found necessary in both formation and resolution of facultative heterochromatin (Miller et al., 2017). Future research will uncover whether DNA knots are just an inevitable outcome of topoisomerase II activity that needs to be minimized or whether DNA knot formation has deeper implications in the regulation of chromatin structure and functions.



---

# Conclusions

---



## CONCLUSIONS

1. DNA supercoiling does not bias topoisomerase II activity towards the removal of DNA knots. Positive supercoiling generated during gene transcription markedly increases DNA knot formation, whereas negative supercoiling does not significantly affect DNA knotting probability.
2. The different effects of positive and negative supercoiling on DNA knot formation indicate that transcriptional supercoiling produces a much larger degree of DNA compaction in front of RNA polymerases rather than behind them.
3. The intrinsic capacity of topoisomerase II to simplify the equilibrium topology of naked DNA in vitro does not affect the knotting probability of DNA in vivo. Therefore, this ability of topoisomerase II might not function in chromatinized DNA.
4. Inactivation of cohesin slightly decreases knot formation in intracellular chromatin. Therefore, cohesins are somewhat favouring DNA knotting, rather than minimizing it.
5. Inactivation of condensin markedly increases knot formation in vivo and restores the expected linear correlation between DNA knot formation and chromatin length throughout the entire cell cycle. Thereby, condensin is responsible for minimizing the overall entanglement of intracellular DNA.
6. The opposite effects of cohesin and condensin on DNA knot formation suggest different kinetics of their DNA loop extrusion activities and/or a different interplay with topoisomerase II.
7. Condensin's newly identified role in minimizing DNA entanglements throughout the entire cell cycle clarifies why condensin inactivation produces many dysfunctions both in interphase and mitotic chromatin.



---

# References

---





## REFERENCES

- Adrian, M., Heggeler-Bordier, B. ten, Wahli, W., Stasiak, A. Z., Stasiak, A., & Dubochet, J. (1990). Direct visualization of supercoiled DNA molecules in solution. *The EMBO Journal*, *9*(13), 4551–4554.
- Anderson, P., & Bauer, W. (1978). Supercoiling in closed circular DNA: dependence upon ion type and concentration. *Biochemistry*, *17*(4), 594–601.
- Antonin, W., & Neumann, H. (2016). Chromosome condensation and decondensation during mitosis. *Current Opinion in Cell Biology*, *40*, 15–22.
- Aragón, L. (2018). The Smc5/6 complex: New and old functions of the enigmatic long-distance relative. In *Annual Review of Genetics* (Vol. 52).
- Arsuaga, J., Vazquez, M., McGuirk, P., Trigueros, S., Sumners, D., & Roca, J. (2005). DNA knots reveal a chiral organization of DNA in phage capsids. *Proc Natl Acad Sci U S A*, *102*(26), 9165–9169.
- Arsuaga, J., Vazquez, M., Trigueros, S., Sumners, D., & Roca, J. (2002). Knotting probability of DNA molecules confined in restricted volumes: DNA knotting in phage capsids. *Proc Natl Acad Sci U S A*, *99*(8), 5373–5377.
- Bancaud, A., Conde e Silva, N., Barbi, M., Wagner, G., Allemand, J.-F., Mozziconacci, J., Lavelle, C., Croquette, V., Victor, J.-M., Prunell, A., & Viovy, J.-L. (2006a). Structural plasticity of single chromatin fibers revealed by torsional manipulation. *Nature Structural & Molecular Biology*, *13*(5), 444–450.
- Bancaud, A., Conde e Silva, N., Barbi, M., Wagner, G., Allemand, J., Mozziconacci, J., Lavelle, C., Croquette, V., Victor, J., Prunell, A., & Viovy, J. (2006b). Structural plasticity of single chromatin fibers revealed by torsional manipulation. *Nature Structural & Molecular Biology*, *13*(5), 444–450.
- Banigan, E., van den Berg, A., Brandão, H., Marko, J., & Mirny, L. (2020). Chromosome organization by one-sided and two-sided loop extrusion. *ELife*, *9*.
- Bates, A. D., & Maxwell, A. (2005). DNA topology. *Oxford University Press*, 198.
- Baù, D., Sanyal, A., Lajoie, B. R., Capriotti, E., Byron, M., Lawrence, J. B., Dekker, J., & Marti-Renom, M. A. (2011). The three-dimensional folding of the  $\alpha$ -globin gene domain reveals formation of chromatin globules. *Nature Structural & Molecular Biology*, *18*(1), 107.

## References

- Baxter, J., Sen, N., Martínez, V. L., De Carandini, M. E. M., Schwartzman, J. B., Diffley, J. F. X., & Aragón, L. (2011). Positive supercoiling of mitotic DNA drives decatenation by topoisomerase II in eukaryotes. *Science (New York, N.Y.)*, *331*(6022), 1328–1332.
- Belmont, A., Braunfeld, M., Sedat, J., & Agard, D. (1989). Large-scale chromatin structural domains within mitotic and interphase chromosomes in vivo and in vitro. *Chromosoma*, *98*(2), 129–143.
- Belmont, A., & Bruce, K. (1994). Visualization of G1 chromosomes: a folded, twisted, supercoiled chromonema model of interphase chromatid structure. *The Journal of Cell Biology*, *127*(2), 287–302.
- Bhalla, N., Biggins, S., & Murray, A. W. (2002). Mutation of YCS4, a Budding Yeast Condensin Subunit, Affects Mitotic and Nonmitotic Chromosome Behavior. *Molecular Biology of the Cell*, *13*(2), 632.
- Bhat, M. A., Philp, A. V., Glover, D. M., & Bellen, H. J. (1996). Chromatid segregation at anaphase requires the barren product, a novel chromosome-associated protein that interacts with topoisomerase II. *Cell*, *87*(6), 1103–1114.
- Bloom, K. S. (2008). Beyond the code: the mechanical properties of DNA as they relate to mitosis. *Chromosoma*, *117*(2), 103–110.
- Boles, T., White, J., & Cozzarelli, N. (1990). Structure of plectonemically supercoiled DNA. *Journal of Molecular Biology*, *213*(4), 931–951.
- Branco, M. R., Branco, T., Ramirez, F., & Pombo, A. (2008). Changes in chromosome organization during PHA-activation of resting human lymphocytes measured by cryo-FISH. *Chromosome Research* 2008 16:3, *16*(3), 413–426.
- Bronstein, I., Israel, Y., Kepten, E., Mai, S., Shav-Tal, Y., Barkai, E., & Garini, Y. (2009). Transient anomalous diffusion of telomeres in the nucleus of mammalian cells. *Physical Review Letters*, *103*(1).
- Buck, G. (1998). Four-thirds power law for knots and links. *Nature* 1998 392:6673, *392*(6673), 238–239.
- Buck, G. R., & Lynn Zechiedrich, E. (2004). DNA Disentangling by Type-2 Topoisomerases. *Journal of Molecular Biology*, *340*(5), 933–939.
- Burnier, Y., Dorier, J., & Stasiak, A. (2008). DNA supercoiling inhibits DNA knotting. *Nucleic Acids Research*, *36*(15), 4956.

- Canela, A., Maman, Y., Jung, S., Wong, N., Callen, E., Day, A., Kieffer-Kwon, K., Pekowska, A., Zhang, H., Rao, S., Huang, S., Mckinnon, P., Aplan, P., Pommier, Y., Aiden, E., Casellas, R., & Nussenzweig, A. (2017). Genome Organization Drives Chromosome Fragility. *Cell*, *170*(3), 507-521.e18.
- Champoux, J. J. (1990). 6 Mechanistic Aspects of Type-I Topoisomerases. *Cold Spring Harbor Monograph Archive*, *20*(0), 217–242.
- Champoux, J. J. (2001). DNA topoisomerases: structure, function, and mechanism. *Annu Rev Biochem*, *70*, 369–413.
- Chen, S. H., Chan, N. L., & Hsieh, T. S. (2013). New mechanistic and functional insights into DNA topoisomerases. *Annu Rev Biochem*, *82*, 139–170.
- Chirikjian, G. S. (2013). Framed curves and knotted DNA. *Biochemical Society Transactions*, *41*(2), 635–638.
- Classen, S., Olland, S., & Berger, J. M. (2003). Structure of the topoisomerase II ATPase region and its mechanism of inhibition by the chemotherapeutic agent ICRF-187. *Proceedings of the National Academy of Sciences of the United States of America*, *100*(19), 10629.
- Corbett, K., & Berger, J. (2003). Structure of the topoisomerase VI-B subunit: implications for type II topoisomerase mechanism and evolution. *The EMBO Journal*, *22*(1), 151–163.
- Coronel, L., Suma, A., & Micheletti, C. (2018). Dynamics of supercoiled DNA with complex knots: large-scale rearrangements and persistent multi-strand interlocking. *Nucleic Acids Research*, *46*(15), 7533.
- Cortés, F., Pastor, N., Mateos, S., & Domínguez, I. (2003). Roles of DNA topoisomerases in chromosome segregation and mitosis. *Mutation Research*, *543*(1), 59–66.
- Cremer, T., & Cremer, C. (2001). Chromosome territories, nuclear architecture and gene regulation in mammalian cells. *Nature Reviews Genetics* *2001* *2*:4, *2*(4), 292–301.
- Cuvier, O., & Hirano, T. (2003). A role of topoisomerase II in linking DNA replication to chromosome condensation. *The Journal of Cell Biology*, *160*(5), 645.
- D'Ambrosio, C., Schmidt, C. K., Katou, Y., Kelly, G., Itoh, T., Shirahige, K., & Uhlmann, F. (2008). Identification of cis-acting sites for condensin loading onto budding yeast chromosomes. *Genes and Development*, *22*(16), 2215–2227.

## References

- Davey, C. A., Sargent, D. F., Luger, K., Maeder, A. W., & Richmond, T. J. (2002). Solvent Mediated Interactions in the Structure of the Nucleosome Core Particle at 1.9 Å Resolution. *Journal of Molecular Biology*, *319*(5), 1097–1113.
- Davidson, I., Bauer, B., Goetz, D., Tang, W., Wutz, G., & Peters, J. (2019). DNA loop extrusion by human cohesin. *Science (New York, N.Y.)*, *366*(6471), 1338–1345.
- Davidson, I. F., Bauer, B., Goetz, D., Tang, W., Wutz, G., & Peters, J. M. (2019). DNA loop extrusion by human cohesin. *Science*, *366*(6471), 1338–1345.
- Davidson, I. F., & Peters, J. M. (2021). Genome folding through loop extrusion by SMC complexes. *Nature Reviews Molecular Cell Biology*, *0123456789*.
- Dekker, J., Rippe, K., Dekker, M., & Kleckner, N. (2002). Capturing chromosome conformation. *Science (New York, N.Y.)*, *295*(5558), 1306–1311.
- Depew, D. E., & Wang, J. C. (1975). Conformational fluctuations of DNA helix. *Proceedings of the National Academy of Sciences of the United States of America*, *72*(11), 4275.
- Dixon, J. R., Selvaraj, S., Yue, F., Kim, A., Li, Y., Shen, Y., Hu, M., Liu, J. S., & Ren, B. (2012). Topological Domains in Mammalian Genomes Identified by Analysis of Chromatin Interactions. *Nature*, *485*(7398), 376.
- Dixon, J., Selvaraj, S., Yue, F., Kim, A., Li, Y., Shen, Y., Hu, M., Liu, J., & Ren, B. (2012). Topological domains in mammalian genomes identified by analysis of chromatin interactions. *Nature*, *485*(7398), 376–380.
- Dorier, J., & Stasiak, A. (2009). Topological origins of chromosomal territories. *Nucleic Acids Research*, *37*(19), 6316.
- Dorigo, B., Schalch, T., Kulangara, A., Duda, S., Schroeder, R. R., & Richmond, T. J. (2004). Nucleosome arrays reveal the two-start organization of the chromatin fiber. *Science*, *306*(5701), 1571–1573.
- Dundr, M., Hoffmann-Rohrer, U., Hu, Q., Grummt, I., Rothblum, L. I., Phair, R. D., & Misteli, T. (2002). A Kinetic Framework for a Mammalian RNA Polymerase in Vivo. *Science*, *298*(5598), 1623–1626.
- Dyson, S., Segura, J., Martínez-García, B., Valdés, A., & Roca, J. (2021). Condensin minimizes topoisomerase II-mediated entanglements of DNA in vivo. *The EMBO Journal*, *40*(1).
- Eeftens, J. M., Bisht, S., Kerssemakers, J., Kschonsak, M., Haering, C. H., & Dekker, C.

- (2017). Real-time detection of condensin-driven DNA compaction reveals a multistep binding mechanism. *EMBO J*, *36*(23), 3448–3457.
- Eng, W., Pandit, S., & Sternglanz, R. (1989). Mapping of the active site tyrosine of eukaryotic DNA topoisomerase I. *The Journal of Biological Chemistry*, *264*(23), 13373–13376.
- Ernst, C., & Sumners, D. W. (1987). The growth of the number of prime knots. *Mathematical Proceedings of the Cambridge Philosophical Society*, *102*(2), 303–315.
- Farcas, A.-M., Uluocak, P., Helmhart, W., & Nasmyth, K. (2011). Cohesin's Concatenation of Sister DNAs Maintains Their Intertwining. *Molecular Cell*, *44*(1–3), 97.
- Fernández, X., Díaz-Ingelmo, O., Martínez-García, B., & Roca, J. (2014). Chromatin regulates DNA torsional energy via topoisomerase II-mediated relaxation of positive supercoils. *The EMBO Journal*, *33*(13), 1492.
- Fielden, S. D. P., Leigh, D. A., & Woltering, S. L. (2017). Molecular Knots. *Angewandte Chemie - International Edition*, *56*(37), 11166–11194.
- Forterre, P., Gribaldo, S., Gabelle, D., & Serre, M. C. (2007). Origin and evolution of DNA topoisomerases. *Biochimie*, *89*(4), 427–446.
- Frank-Kamenetskii, M. D. (1997). Biophysics of the DNA molecule. *Physics Reports*, *288*(1–6), 13–60.
- Frank-Kamenetskii, M., Lukashin, A., & Vologodskii, A. (1975). Statistical mechanics and topology of polymer chains. *Nature*, *258*(5534), 398–402.
- Franklin, R. E., & Gosling, R. G. (1953). Molecular Configuration in Sodium Thymonucleate. *Nature* 1953 171:4356, *171*(4356), 740–741.
- Frosi, Y., & Haering, C. H. (2015). Control of chromosome interactions by condensin complexes. *Curr Opin Cell Biol*, *34*, 94–100.
- Fudenberg, G., Imakaev, M., Lu, C., Goloborodko, A., Abdennur, N., & Mirny, L. (2016). Formation of Chromosomal Domains by Loop Extrusion. *Cell Reports*, *15*(9), 2038–2049.
- Fuller, F. (1971). The writhing number of a space curve. *Proceedings of the National Academy of Sciences of the United States of America*, *68*(4), 815–819.
- Fuller, F. (1978). Decomposition of the linking number of a closed ribbon: A problem

## References

- from molecular biology. *Proceedings of the National Academy of Sciences of the United States of America*, 75(8), 3557–3561.
- Ganji, M., Shaltiel, I. A., Bisht, S., Kim, E., Kalichava, A., Haering, C. H., & Dekker, C. (2018). Real-time imaging of DNA loop extrusion by condensin. *Science*, 360(6384), 102–105.
- Gellert, M., Mizuuchi, K., O’Dea, M. H., & Nash, H. A. (1976). DNA gyrase: an enzyme that introduces superhelical turns into DNA. *Proc. Natl. Acad. Sci. USA*, 73(11), 3872–3876.
- Giaever, G. N., & Wang, J. C. (1988). Supercoiling of intracellular DNA can occur in eukaryotic cells. *Cell*, 55(5), 849–856.
- Gibcus, J. H., Samejima, K., Goloborodko, A., Samejima, I., Naumova, N., Nuebler, J., Kanemaki, M. T., Xie, L., Paulson, J. R., Earnshaw, W. C., Mirny, L. A., & Dekker, J. (2018). A pathway for mitotic chromosome formation. *Science*, 359(6376).
- Goloborodko, A., Imakaev, M. V, Marko, J. F., & Mirny, L. (2016). Compaction and segregation of sister chromatids via active loop extrusion. *Elife*, 5.
- Goloborodko, A., Marko, J. F., & Mirny, L. A. (2016). Chromosome Compaction by Active Loop Extrusion. *Biophysical Journal*, 110(10), 2162.
- Gray, H. B., Upholt, W. B., & Vinograd, J. (1971). A buoyant method for the determination of the superhelix density of closed circular DNA. *Journal of Molecular Biology*, 62(1), 1–19.
- Grigoryev, S. A., Bascom, G., Buckwalter, J. M., Schubert, M. B., Woodcock, C. L., & Schlick, T. (2016). Hierarchical looping of zigzag nucleosome chains in metaphase chromosomes. *Proc Natl Acad Sci U S A*, 113(5), 1238–1243.
- Hagerman, P. J. (1988). Flexibility of DNA. *Annu Rev Biophys Biophys Chem*, 17, 265–286.
- Hanai, R., & Roca, J. (1999). Two-dimensional agarose-gel electrophoresis of DNA topoisomers. *Methods Mol Biol*, 94, 19–27.
- Hassler, M., Shaltiel, I. A., & Haering, C. H. (2018). Towards a Unified Model of SMC Complex Function. *Curr Biol*, 28(21), R1266–R1281.
- Heinemann, U., & Roske, Y. (2020). Symmetry in Nucleic-Acid Double Helices. *Symmetry 2020, Vol. 12, Page 737, 12(5), 737*.
- Hirano, T. (1998). SMC protein complexes and higher-order chromosome dynamics.

- Current Opinion in Cell Biology*, 10(3), 317–322.
- Hirano, T. (2005). SMC proteins and chromosome mechanics: from bacteria to humans. *Philosophical Transactions of the Royal Society B: Biological Sciences*, 360(1455), 507–514.
- Hirano, T. (2012a). Condensins: universal organizers of chromosomes with diverse functions. *Genes Dev*, 26(15), 1659–1678.
- Hirano, T. (2012b). Condensins: Universal organizers of chromosomes with diverse functions. *Genes and Development*, 26(15), 1659–1678.
- Hirano, T., Kobayashi, R., & Hirano, M. (1997). Condensins, Chromosome Condensation Protein Complexes Containing XCAP-C, XCAP-E and a Xenopus Homolog of the Drosophila Barren Protein. *Cell*, 89(4), 511–521.
- Hoencamp, C., Dudchenko, O., Elbatsh, A. M. O., Brahmachari, S., Raaijmakers, J. A., Schaik, T. van, Cacciatore, Á. S., Contessoto, V. G., Heesbeen, R. G. H. P. van, Broek, B. van den, Mhaskar, A. N., Teunissen, H., Hilaire, B. G. S., Weisz, D., Omer, A. D., Pham, M., Colaric, Z., Yang, Z., Rao, S. S. P., ... Rowland, B. D. (2021). 3D genomics across the tree of life reveals condensin II as a determinant of architecture type. *Science*, 372(6545), 984–989.
- Hsieh, T.-H. S., Weiner, A., Lajoie, B., Dekker, J., Friedman, N., & Rando, O. J. (2015). Mapping nucleosome resolution chromosome folding in yeast by Micro-C. *Cell*, 162(1), 108.
- Hsieh, T.-S. (1990). 7 Mechanistic Aspects of Type-II DNA Topoisomerases. *Cold Spring Harbor Monograph Archive*, 20(0), 243–263.
- Hsieh, T. (1983). Knotting of the circular duplex DNA by type II DNA topoisomerase from *Drosophila melanogaster*. *J Biol Chem*, 258(13), 8413–8420.
- Ishii, S., Murakami, T., & Shishido, K. (1991). Gyrase inhibitors increase the content of knotted DNA species of plasmid pBR322 in *Escherichia coli*. *J Bacteriol*, 173(17), 5551–5553.
- Jessberger, R., Frei, C., & Gasser, S. M. (1998). Chromosome dynamics: the SMC protein family. *Current Opinion in Genetics & Development*, 8(2), 254–259.
- Jin, F., Li, Y., Dixon, J., Selvaraj, S., Ye, Z., Lee, A., Yen, C., Schmitt, A., Espinoza, C., & Ren, B. (2013). A high-resolution map of the three-dimensional chromatin interactome in human cells. *Nature*, 503(7475), 290–294.

## References

- Joshi, R. S., Piña, B., & Roca, J. (2010). Positional dependence of transcriptional inhibition by DNA torsional stress in yeast chromosomes. *The EMBO Journal*, 29(4), 740–748.
- Joshi, R. S., Piña, B., & Roca, J. (2012). Topoisomerase II is required for the production of long Pol II gene transcripts in yeast. *Nucleic Acids Research*, 40(16), 7907.
- Kampranis, S. C., Bates, A. D., & Maxwell, A. (1999). A model for the mechanism of strand passage by DNA gyrase. *Proceedings of the National Academy of Sciences of the United States of America*, 96(15), 8414.
- Kawamura, R., Pope, L. H., Christensen, M. O., Sun, M., Terekhova, K., Boege, F., Mielke, C., Andersen, A. H., & Marko, J. F. (2010). Mitotic chromosomes are constrained by topoisomerase II-sensitive DNA entanglements. *The Journal of Cell Biology*, 188(5), 653.
- Kim, R. A., & Wang, J. C. (1992). Identification of the yeast TOP3 gene product as a single strand-specific DNA topoisomerase. *Journal of Biological Chemistry*, 267(24), 17178–17185.
- Kim, Y., Shi, Z., Zhang, H., Finkelstein, I. J., & Yu, H. (2019). Human cohesin compacts DNA by loop extrusion. *Science*, 366(6471), 1345–1349.
- Kimura, K., Rybenkov, V. V., Crisona, N. J., Hirano, T., & Cozzarelli, N. R. (1999). 13S condensin actively reconfigures DNA by introducing global positive writhe: Implications for chromosome condensation. *Cell*, 98(2), 239–248.
- Klenin, K., Vologodskii, A., Anshelevich, V., Dykhne, A., & Frank-Kamenetskii, M. (1988). Effect of excluded volume on topological properties of circular DNA. *J Biomol Struct Dyn*, 5(6), 1173–1185.
- Lavelle, C. (2014). Pack, unpack, bend, twist, pull, push: the physical side of gene expression. *Current Opinion in Genetics & Development*, 25(1), 74–84.
- Lavelle, C., Victor, J. M., & Zlatanova, J. (2010). Chromatin fiber dynamics under tension and torsion. *Int J Mol Sci*, 11(4), 1557–1579.
- Lavoie, B. D., Hogan, E., & Koshland, D. (2002a). In vivo dissection of the chromosome condensation machinery: reversibility of condensation distinguishes contributions of condensin and cohesin. *J Cell Biol*, 156(5), 805–815.
- Lavoie, B. D., Hogan, E., & Koshland, D. (2002b). In vivo dissection of the chromosome condensation machinery: Reversibility of condensation distinguishes



- contributions of condensin and cohesin. *Journal of Cell Biology*, 156(5), 805–815.
- Levene, S. D., & Tsen, H. (1999). Analysis of DNA Knots and Catenanes by Agarose-Gel Electrophoresis. *Methods in Molecular Biology (Clifton, N.J.)*, 94, 75–85.
- Li, G., & Zhu, P. (2015). Structure and organization of chromatin fiber in the nucleus. *FEBS Letters*, 589(20 Pt A), 2893–2904.
- Lieberman-Aiden, E., van Berkum, N. L., Williams, L., Imakaev, M., Ragozy, T., Telling, A., Amit, I., Lajoie, B. R., Sabo, P. J., Dorschner, M. O., Sandstrom, R., Bernstein, B., Bender, M. A., Groudine, M., Gnirke, A., Stamatoyannopoulos, J., Mirny, L. A., Lander, E. S., & Dekker, J. (2009). Comprehensive mapping of long-range interactions reveals folding principles of the human genome. *Science*, 326(5950), 289–293.
- Lieberman-Aiden, E., van Berkum, N., Williams, L., Imakaev, M., Ragozy, T., Telling, A., Amit, I., Lajoie, B., Sabo, P., Dorschner, M., Sandstrom, R., B, B., MA, B., Groudine, M., Gnirke, A., Stamatoyannopoulos, J., Mirny, L., Lander, E., & Dekker, J. (2009). Comprehensive mapping of long-range interactions reveals folding principles of the human genome. *Science (New York, N.Y.)*, 326(5950), 289–293.
- Liu, L. F., Davis, J. L., & Calendar, R. (1981). Novel topologically knotted DNA from bacteriophage P4 capsids: studies with DNA topoisomerases. *Nucleic Acids Research*, 9(16), 3979.
- Liu, L. F., Perkocha, L., Calendar, R., & Wang, J. C. (1981). Knotted DNA from bacteriophage capsids. *Proceedings of the National Academy of Sciences of the United States of America*, 78(9), 5498.
- Liu, L. F., & Wang, J. C. (1987). Supercoiling of the DNA template during transcription. *Proc Natl Acad Sci U S A*, 84(20), 7024–7027.
- Luger, K., Mäder, A., Richmond, R., Sargent, D., & Richmond, T. (1997). Crystal structure of the nucleosome core particle at 2.8 Å resolution. *Nature*, 389(6648), 251–260.
- Lynn, E. Z., & Crisona, N. J. (1999). Coating DNA with RecA Protein to Distinguish DNA Path by Electron Microscopy. *Methods in Molecular Biology (Clifton, N.J.)*, 94, 99–107.
- Lynn, R., Bjornsti, M., Caron, P., & Wang, J. (1989). Peptide sequencing and site-directed mutagenesis identify tyrosine-727 as the active site tyrosine of

## References

- Saccharomyces cerevisiae* DNA topoisomerase I. *Proceedings of the National Academy of Sciences of the United States of America*, 86(10), 3559–3563.
- Maeshima, K., Rogge, R., Tamura, S., Joti, Y., Hikima, T., Szerlong, H., Krause, C., Herman, J., Seidel, E., DeLuca, J., Ishikawa, T., & Hansen, J. C. (2016). Nucleosomal arrays self-assemble into supramolecular globular structures lacking 30-nm fibers. *Embo J*, 35(10), 1115–1132.
- Marko, A., Denysenkov, V., Margraf, D., Cekan, P., Schiemann, O., Sigurdsson, S. T., & Prisner, T. F. (2011). Conformational Flexibility of DNA. *Journal of the American Chemical Society*, 133(34), 13375–13379.
- Marko, J. F., & Siggia, E. D. (1995). Statistical mechanics of supercoiled DNA. *Physical Review E*, 52(3), 2912.
- Martinez-Garcia, B., Fernandez, X., Diaz-Ingelmo, O., Rodriguez-Campos, A., Manichanh, C., & Roca, J. (2014). Topoisomerase II minimizes DNA entanglements by proofreading DNA topology after DNA strand passage. *Nucleic Acids Res*, 42(3), 1821–1830.
- McCoubrey, W. K., & Champoux, J. J. (1986). The role of single-strand breaks in the catenation reaction catalyzed by the rat type I topoisomerase. *Journal of Biological Chemistry*, 261(11), 5130–5137.
- McKie, S. J., Neuman, K. C., & Maxwell, A. (2021). DNA topoisomerases: Advances in understanding of cellular roles and multi-protein complexes via structure-function analysis. *BioEssays*, 43(4), 2000286.
- Micheletti, C., Marenduzzo, D., Orlandini, E., & Sumners, D. W. (2008). Simulations of knotting in confined circular DNA. *Biophys J*, 95(8), 3591–3599.
- Michieletto, D., Marenduzzo, D., Orlandini, E., & Turner, M. S. (2017). Ring Polymers: Threadings, Knot Electrophoresis and Topological Glasses. *Polymers*, 9(8).
- Miller, E. L., Hargreaves, D. C., Kadoch, C., Chang, C.-Y., Calarco, J. P., Hodges, C., Buenrostro, J. D., Cui, K., Greenleaf, W. J., Zhao, K., & Crabtree, G. R. (2017). TOP2 synergizes with BAF chromatin remodeling for both resolution and formation of facultative heterochromatin. *Nature Structural & Molecular Biology*, 24(4), 344.
- Mirkin, S. M. (2001). DNA Topology : Fundamentals. *Life Sciences*, 123(c), 1–11.
- Mirny, L. A. (2011). The fractal globule as a model of chromatin architecture in the cell. *Chromosome Res*, 19(1), 37–51.

- Nagasaka, K., Hossain, M. J., Roberti, M. J., Ellenberg, J., & Hirota, T. (2016). Sister chromatid resolution is an intrinsic part of chromosome organization in prophase. *Nature Cell Biology*, *18*(6), 692–699.
- Najafi, S., & Potestio, R. (2015). Two Adhesive Sites Can Enhance the Knotting Probability of DNA. *PLoS One*, *10*(7), e0132132.
- Nasmyth, K., & Haering, C. H. (2009). Cohesin: its roles and mechanisms. *Annu Rev Genet*, *43*, 525–558.
- Naughton, C., Avlonitis, N., Corless, S., Prendergast, J. G., Mati, I. K., Eijk, P. P., Cockroft, S. L., Bradley, M., Ylstra, B., & Gilbert, N. (2013). Transcription forms and remodels supercoiling domains unfolding large-scale chromatin structures. *Nature Structural & Molecular Biology*, *20*(3), 387–395.
- Nelson, P. (1999). Transport of torsional stress in DNA. *Proc Natl Acad Sci U S A*, *96*(25), 14342–14347.
- Nielsen, C. F., Zhang, T., Barisic, M., Kalitsis, P., & Hudson, D. F. (2020). Topoisomerase II $\alpha$  is essential for maintenance of mitotic chromosome structure. *Proceedings of the National Academy of Sciences*, *117*(22), 12131–12142.
- Nishide, K., & Hirano, T. (2014). Overlapping and non-overlapping functions of condensins I and II in neural stem cell divisions. *PLoS Genet*, *10*(12), e1004847.
- Nitiss, J. (2009). DNA topoisomerase II and its growing repertoire of biological functions. *Nature Reviews. Cancer*, *9*(5), 327–337.
- Olavarrieta, L., Martinez-Robles, M. L., Sogo, J. M., Stasiak, A., Hernandez, P., Krimer, D. B., & Schwartzman, J. B. (2002). Supercoiling, knotting and replication fork reversal in partially replicated plasmids. *Nucleic Acids Res*, *30*(3), 656–666.
- Ong, C.-T., & Corces, V. G. (2014). CTCF: An Architectural Protein Bridging Genome Topology and Function. *Nature Reviews. Genetics*, *15*(4), 234.
- Onn, I., Heidinger-Pauli, J. M., Guacci, V., Unal, E., & Koshland, D. E. (2008). Sister chromatid cohesion: a simple concept with a complex reality. *Annu Rev Cell Dev Biol*, *24*, 105–129.
- Ono, T., Losada, A., Hirano, M., Myers, M. P., Neuwald, A. F., & Hirano, T. (2003). Differential contributions of condensin I and condensin II to mitotic chromosome architecture in vertebrate cells. *Cell*, *115*(1), 109–121.
- Orlandini, E., Marenduzzo, D., & Michieletto, D. (2019a). Synergy of topoisomerase and

## References

- structural-maintenance-of-chromosomes proteins creates a universal pathway to simplify genome topology. *Proceedings of the National Academy of Sciences of the United States of America*, *116*(17), 8149–8154.
- Orlandini, E., Marenduzzo, D., & Michieletto, D. (2019b). Synergy of topoisomerase and structural-maintenance-of-chromosomes proteins creates a universal pathway to simplify genome topology. *Proc Natl Acad Sci U S A*, *116*(17), 8149–8154.
- Ou, H. D., Phan, S., Deerinck, T. J., Thor, A., Ellisman, M. H., & O’Shea, C. C. (2017). ChromEMT: Visualizing 3D chromatin structure and compaction in interphase and mitotic cells. *Science (New York, N.Y.)*, *357*(6349), 25.
- Paul, M. R., Hochwagen, A., & Ercan, S. (2019). Condensin action and compaction. *Curr Genet*, *65*(2), 407–415.
- Paul, M. R., Markowitz, T. E., Hochwagen, A., & Ercan, S. (2018). Condensin Depletion Causes Genome Decompaction Without Altering the Level of Global Gene Expression in *Saccharomyces cerevisiae*. *Genetics*, *210*(1), 331–344.
- Peck, L., & Wang, J. (1981). Sequence dependence of the helical repeat of DNA in solution. *Nature*, *292*(5821), 375–378.
- Peters, J. P., & Maher, L. J. (2010). DNA curvature and flexibility in vitro and in vivo. In *Quarterly Reviews of Biophysics* (Vol. 43, Issue 01).
- Piskadlo, E., Tavares, A., & Oliveira, R. A. (2017). Metaphase chromosome structure is dynamically maintained by condensin I-directed DNA (de)catenation. *Elife*, *6*.
- Podtelezhnikov, A., Cozzarelli, N., & Vologodskii, A. (1999). Equilibrium distributions of topological states in circular DNA: interplay of supercoiling and knotting. *Proceedings of the National Academy of Sciences of the United States of America*, *96*(23), 12974–12979.
- Portugal, J., & Rodriguez-Campos, A. (1996). T7 RNA polymerase cannot transcribe through a highly knotted DNA template. *Nucleic Acids Res*, *24*(24), 4890–4894.
- Post, C. B., & Zimm, B. H. (1980). DNA condensation and how it relates to phase equilibrium in solution. *Biophysical Journal*, *32*(1), 448–450.
- Racko, D., Benedetti, F., Goundaroulis, D., & Stasiak, A. (2018a). Chromatin loop extrusion and chromatin unknotting. *Polymers*, *10*(10), 1–11.
- Racko, D., Benedetti, F., Goundaroulis, D., & Stasiak, A. (2018b). Chromatin Loop

- Extrusion and Chromatin Unknotting. *Polymers (Basel)*, 10(10).
- Ricci, M. A., Manzo, C., García-Parajo, M. F., Lakadamyali, M., & Cosma, M. P. (2015). Chromatin Fibers Are Formed by Heterogeneous Groups of Nucleosomes In Vivo. *Cell*, 160(6), 1145–1158.
- Richmond, T., Finch, J., Rushton, B., Rhodes, D., & Klug, A. (1984). Structure of the nucleosome core particle at 7 Å resolution. *Nature*, 311(5986), 532–537.
- Robinson, P., Fairall, L., Huynh, V., & Rhodes, D. (2006). EM measurements define the dimensions of the “30-nm” chromatin fiber: evidence for a compact, interdigitated structure. *Proceedings of the National Academy of Sciences of the United States of America*, 103(17), 6506–6511.
- Roca, J. (2009). Two-dimensional agarose gel electrophoresis of DNA topoisomers. *Methods in Molecular Biology (Clifton, N.J.)*, 582, 27–37.
- Roca, J. (2011a). The torsional state of DNA within the chromosome. *Chromosoma*, 120(4), 323–334.
- Roca, J. (2011b). The torsional state of DNA within the chromosome. *Chromosoma*, 120(4), 323–334.
- Roca, J., Berger, J. M., Harrison, S. S., & Wang, J. C. (1996). DNA transport by a type II topoisomerase: direct evidence for a two-gate mechanism. *Proceedings of the National Academy of Sciences of the United States of America*, 93(9), 4057–4062.
- Roca, J., Berger, J. M., & Wang, J. C. (1993). On the simultaneous binding of eukaryotic DNA topoisomerase II to a pair of double-stranded DNA helices. *J Biol Chem*, 268(19), 14250–14255.
- Roca, J., Ishida, R., Berger, J. M., Andoh, T., & Wang, J. C. (1994). Antitumor bisdioxopiperazines inhibit yeast DNA topoisomerase II by trapping the enzyme in the form of a closed protein clamp. *Proceedings of the National Academy of Sciences of the United States of America*, 91(5), 1781–1785.
- Roca, J., & Wang, J. (1992). The capture of a DNA double helix by an ATP-dependent protein clamp: a key step in DNA transport by type II DNA topoisomerases. *Cell*, 71(5), 833–840.
- Roca, J., & Wang, J. C. (1994). DNA transport by a type II DNA topoisomerase: Evidence in favor of a two-gate mechanism. *Cell*, 77(4), 609–616.
- Rodríguez-Campos, A. (1996). DNA knotting abolishes in vitro chromatin assembly. *J*

## References

- Biol Chem*, 271(24), 14150–14155.
- Rosin, L. F., Nguyen, S. C., & Joyce, E. F. (2018). Condensin II drives large-scale folding and spatial partitioning of interphase chromosomes in *Drosophila* nuclei. *PLoS Genet*, 14(7), e1007393.
- Rowley, M. J., Lyu, X., Rana, V., Ando-Kuri, M., Karns, R., Bosco, G., & Corces, V. G. (2019). Condensin II Counteracts Cohesin and RNA Polymerase II in the Establishment of 3D Chromatin Organization. *Cell Rep*, 26(11), 2890–2903 e3.
- Rybenkov, V. V., Cozzarelli, N. R., & Vologodskii, A. V. (1993). Probability of DNA knotting and the effective diameter of the DNA double helix. *Proceedings of the National Academy of Sciences of the United States of America*, 90(11), 5307.
- Rybenkov, V. V., Ullsperger, C., Vologodskii, A. V., & Cozzarelli, N. R. (1997). Simplification of DNA topology below equilibrium values by type II topoisomerases. *Science*, 277(5326), 690–693.
- Salceda, J., Fernández, X., & Roca, J. (2006). Topoisomerase II, not topoisomerase I, is the proficient relaxase of nucleosomal DNA. *The EMBO Journal*, 25(11), 2575–2583.
- Sanborn, A. L., Rao, S. S., Huang, S. C., Durand, N. C., Huntley, M. H., Jewett, A. I., Bochkov, I. D., Chinnappan, D., Cutkosky, A., Li, J., Geeting, K. P., Gnirke, A., Melnikov, A., McKenna, D., Stamenova, E. K., Lander, E. S., & Aiden, E. L. (2015). Chromatin extrusion explains key features of loop and domain formation in wild-type and engineered genomes. *Proc Natl Acad Sci U S A*, 112(47), E6456–65.
- Segura, J., Joshi, R. S., Diaz-Ingelmo, O., Valdes, A., Dyson, S., Martinez-Garcia, B., & Roca, J. (2018). Intracellular nucleosomes constrain a DNA linking number difference of -1.26 that reconciles the Lk paradox. *Nat Commun*, 9(1), 3989.
- Sen, N., Leonard, J., Torres, R., Garcia-Luis, J., Palou-Marin, G., & Aragón, L. (2016a). Physical Proximity of Sister Chromatids Promotes Top2-Dependent Intertwining. *Molecular Cell*, 64(1), 134–147.
- Sen, N., Leonard, J., Torres, R., Garcia-Luis, J., Palou-Marin, G., & Aragón, L. (2016b). Physical Proximity of Sister Chromatids Promotes Top2-Dependent Intertwining. *Molecular Cell*, 64(1), 134–147.
- Shaw, S., & Wang, J. (1993). Knotting of a DNA chain during ring closure. *Science*, 260(5107), 533–536.

- Shaw, S. Y., & Wang, J. C. (1997). Chirality of DNA trefoils: Implications in intramolecular synapsis of distant DNA segments. *Proceedings of the National Academy of Sciences of the United States of America*, *94*(5), 1692.
- Shishido, K., Komiyama, N., & Ikawa, S. (1987). Increased production of a knotted form of plasmid pBR322 DNA in *Escherichia coli* DNA topoisomerase mutants. *J Mol Biol*, *195*(1), 215–218.
- Shuman, S., & Moss, B. (1987). Identification of a vaccinia virus gene encoding a type I DNA topoisomerase. *Proceedings of the National Academy of Sciences of the United States of America*, *84*(21), 7478–7482.
- Simonis, M., Klous, P., Splinter, E., Moshkin, Y., Willemsen, R., de Wit, E., van Steensel, B., & de Laat, W. (2006). Nuclear organization of active and inactive chromatin domains uncovered by chromosome conformation capture–on-chip (4C). *Nature Genetics* *2006 38:11*, *38*(11), 1348–1354.
- Sogo, J. M., Stasiak, A., Martinez-Robles, M. L., Krimer, D. B., Hernandez, P., & Schwartzman, J. B. (1999). Formation of knots in partially replicated DNA molecules. *J Mol Biol*, *286*(3), 637–643.
- Song, F., Chen, P., Sun, D., Wang, M., Dong, L., Liang, D., Xu, R. M., Zhu, P., & Li, G. (2014). Cryo-EM study of the chromatin fiber reveals a double helix twisted by tetranucleosomal units. *Science*, *344*(6182), 376–380.
- Stasiak, A., Katritch, V., Bednar, J., Michoud, D., & Dubochet, J. (1996). Electrophoretic mobility of DNA knots [letter]. *Nature*, *384*(6605), 122.
- Stevens, T. J., Lando, D., Basu, S., Atkinson, L. P., Cao, Y., Lee, S. F., Leeb, M., Wohlfahrt, K. J., Boucher, W., O’Shaughnessy-Kirwan, A., Cramard, J., Faure, A. J., Ralser, M., Blanco, E., Morey, L., Sanso, M., Palayret, M. G. S., Lehner, B., Di Croce, L., ... Laue, E. D. (2017). 3D structures of individual mammalian genomes studied by single-cell Hi-C. *Nature*, *544*(7648), 59–64.
- Strunnikov, A. V., Hogan, E., & Koshland, D. (1995). SMC2, a *Saccharomyces cerevisiae* gene essential for chromosome segregation and condensation, defines a subgroup within the SMC family. *Genes and Development*, *9*(5), 587–599.
- Stuchinskaya, T., Mitchenall, L. A., Schoeffler, A. J., Corbett, K. D., Berger, J. M., Bates, A. D., & Maxwell, A. (2009). How Do Type II Topoisomerases Use ATP Hydrolysis to Simplify DNA Topology beyond Equilibrium? Investigating the Relaxation

## References

- Reaction of Nonsupercoiling Type II Topoisomerases. *Journal of Molecular Biology*, 385(5), 1397–1408.
- Tavares-Cadete, F., Norouzi, D., Dekker, B., Liu, Y., & Dekker, J. (2020). Multi-contact 3C reveals that the human genome during interphase is largely not entangled. *Nature Structural & Molecular Biology*, 27(12), 1105.
- Travers, A., & Muskhelishvili, G. (2015). DNA structure and function. *The FEBS Journal*, 282(12), 2279–2295.
- Trigueros, S., Arsuaga, J., Vazquez, M. E., Summers, D. W., & Roca, J. (2001). Novel display of knotted DNA molecules by two-dimensional gel electrophoresis. *Nucleic Acids Res*, 29(13), E67-7.
- Trigueros, S., Salceda, J., Bermudez, I., Fernandez, X., & Roca, J. (2004). Asymmetric removal of supercoils suggests how topoisomerase II simplifies DNA topology. *J Mol Biol*, 335(3), 723–731.
- Uhlmann, F. (2016). SMC complexes: from DNA to chromosomes. *Nat Rev Mol Cell Biol*, 17(7), 399–412.
- Uuskula-Reimand, L., Hou, H., Samavarchi-Tehrani, P., Rudan, M. V., Liang, M., Medina-Rivera, A., Mohammed, H., Schmidt, D., Schwalie, P., Young, E. J., Reimand, J., Hadjur, S., Gingras, A. C., & Wilson, M. D. (2016). Topoisomerase II beta interacts with cohesin and CTCF at topological domain borders. *Genome Biol*, 17(1), 182.
- Valdes, A., Coronel, L., Martinez-Garcia, B., Segura, J., Dyson, S., Diaz-Ingelmo, O., Micheletti, C., & Roca, J. (2019). Transcriptional supercoiling boosts topoisomerase II-mediated knotting of intracellular DNA. *Nucleic Acids Res*.
- Valdés, A., Martínez-García, B., Segura, J., Dyson, S., Díaz-Ingelmo, O., & Roca, J. (2019). Quantitative disclosure of DNA knot chirality by high-resolution 2D-gel electrophoresis. *Nucleic Acids Research*, 47(5), e29.
- Valdes, A., Segura, J., Dyson, S., Martinez-Garcia, B., & Roca, J. (2018). DNA knots occur in intracellular chromatin. *Nucleic Acids Res*, 46(2), 650–660.
- Vinograd, J., Lebowitz, J., Radloff, R., Watson, R., & Laipis, P. (1965). The twisted circular form of polyoma viral DNA. *Proceedings of the National Academy of Sciences of the United States of America*, 53(5), 1104–1111.
- Vologodskii, A. (2016). Disentangling DNA molecules. *Phys Life Rev*, 18, 118–134.
- Vologodskii, a. V., Zhang, W., Rybenkov, V. V., Podtelezhnikov, a. a., Subramanian, D.,



- Griffith, J. D., & Cozzarelli, N. R. (2001). Mechanism of topology simplification by type II DNA topoisomerases. *Proceedings of the National Academy of Sciences*, *98*(6), 3045–3049.
- Vrielynck, N., Chambon, A., Vezon, D., Pereira, L., Chelysheva, L., De Muyt, A., Mézard, C., Mayer, C., & Grelon, M. (2016). A DNA topoisomerase VI-like complex initiates meiotic recombination. *Science (New York, N.Y.)*, *351*(6276), 939–943.
- Wallis, J., Chrebet, G., Brodsky, G., Rolfe, M., & Rothstein, R. (1989). A hyper-recombination mutation in *S. cerevisiae* identifies a novel eukaryotic topoisomerase. *Cell*, *58*(2), 409–419.
- Walther, N., Hossain, M. J., Politi, A. Z., Koch, B., Kueblbeck, M., Ødegård-Fougner, Ø., Lampe, M., & Ellenberg, J. (2018). A quantitative map of human Condensins provides new insights into mitotic chromosome architecture. *Journal of Cell Biology*, *217*(7), 2309–2328.
- Wang, B.-D., Eyre, D., Basrai, M., Lichten, M., & Strunnikov, A. (2005). Condensin Binding at Distinct and Specific Chromosomal Sites in the *Saccharomyces cerevisiae* Genome. *Molecular and Cellular Biology*, *25*(16), 7216–7225.
- Wang, J. (1971). Interaction between DNA and an *Escherichia coli* protein omega. *Journal of Molecular Biology*, *55*(3).
- Wang, J. (1996). DNA topoisomerases. *Annual Review of Biochemistry*, *65*, 635–692.
- Wang, J. C. (1979). Helical repeat of DNA in solution. *Proceedings of the National Academy of Sciences of the United States of America*, *76*(1), 200–203.
- Wang, J. C. (1998). Moving one DNA double helix through another by a type II DNA topoisomerase: the story of a simple molecular machine. *Quarterly Reviews of Biophysics*, *31*(02), 107–144.
- Wang, J. C. (2002). Cellular roles of DNA topoisomerases: a molecular perspective. *Nat Rev Mol Cell Biol*, *3*(6), 430–440.
- Wang, X., Le, T., Lajoie, B., Dekker, J., Laub, M., & Rudner, D. (2015). Condensin promotes the juxtaposition of DNA flanking its loading site in *Bacillus subtilis*. *Genes & Development*, *29*(15), 1661–1675.
- Wasserman, S. A., & Cozzarelli, N. R. (1991). Supercoiled DNA-directed knotting by T4 topoisomerase. *J Biol Chem*, *266*(30), 20567–20573.
- Wasserman, S., Dungan, J., & Cozzarelli, N. (1985). Discovery of a predicted DNA knot

## References

- substantiates a model for site-specific recombination. *Science*, 229(4709), 171–174.
- Watson, J. D., & Crick, F. H. (1953). Molecular structure of nucleic acids; a structure for deoxyribose nucleic acid. *Nature*, 171(4356), 737–738.
- Wendorff, T., & Berger, J. (2018). Topoisomerase VI senses and exploits both DNA crossings and bends to facilitate strand passage. *ELife*, 7.
- Wendt, K. S., Yoshida, K., Itoh, T., Bando, M., Koch, B., Schirghuber, E., Tsutsumi, S., Nagae, G., Ishihara, K., Mishiro, T., Yahata, K., Imamoto, F., Aburatani, H., Nakao, M., Imamoto, N., Maeshima, K., Shirahige, K., & Peters, J. M. (2008). Cohesin mediates transcriptional insulation by CCCTC-binding factor. *Nature*, 451(7180), 796–801.
- White, J. H. (1969). Self-Linking and the Gauss Integral in Higher Dimensions. *American Journal of Mathematics*, 91(3), 693.
- Wiggins, P. A., Cheveralls, K. C., Martin, J. S., Lintner, R., & Kondev, J. (2010). Strong intranucleoid interactions organize the Escherichia coli chromosome into a nucleoid filament. *Proceedings of the National Academy of Sciences of the United States of America*, 107(11), 4991.
- Witz, G., Dietler, G., & Stasiak, A. (2011). Tightening of DNA knots by supercoiling facilitates their unknotting by type II DNA topoisomerases. *Proceedings of the National Academy of Sciences of the United States of America*, 108(9), 3608.
- Yatskevich, S., Rhodes, J., & Nasmyth, K. (2019). Organization of Chromosomal DNA by SMC Complexes. *Annu Rev Genet*, 53, 445–482.
- Zhang, H., Emerson, D. J., Gilgenast, T. G., Titus, K. R., Lan, Y., Huang, P., Zhang, D., Wang, H., Keller, C. A., Giardine, B., Hardison, R. C., Phillips-Cremins, J. E., & Blobel, G. A. (2019). Chromatin structure dynamics during the mitosis-to-G1 phase transition. *Nature*, 576(7785), 158–162.
- Zhou, B., & Bai, Y. (2019). Chromatin structures condensed by linker histones. *Essays in Biochemistry*, 63(1), 75–87.



